# SILICON-BASED ORGANIC AND INORGANIC POLYMERS

by

Maria Spinu

Dissertation submitted to the Faculty of the

Virginia Polytechnic Institute and State University in partial fulfillment of the

requirements for the degree of

Doctor of philosophy

in

Chemistry

Approved by

J. E. McGrath, Chairman

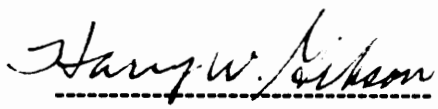

H. W. Gibson

H. M. McNair

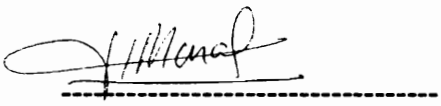

H. Marand

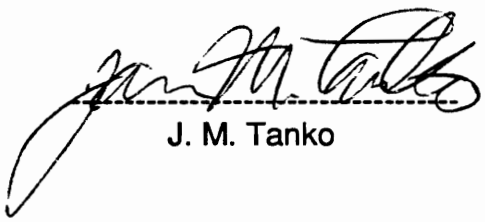

J. M. Tanko

October, 1990

Blacksburg, Virginia

# SILICON-BASED ORGANIC AND INORGANIC POLYMERS

by

Maria Spinu

James E. McGrath, Committee Chairperson

Department of Chemistry

(ABSTRACT)

The range of polymeric materials containing the Si-O bond spans from the three-dimensional inorganic networks of silica ($SiO_2$), to linear high molecular weight polysiloxanes which display properties of both organic and inorganic materials.

Part 1 of this dissertation describes the synthesis of three-dimensional inorganic $SiO_2$ networks and organic-inorganic hybrid networks using a low temperature solution technique known as *the sol-gel process* . During this process, hydrolysis and subsequent condensation of inorganic alkoxides (most often tetraethylorthosilicate, TEOS) in the presence of catalysts leads to the formation of three-dimensional $SiO_2$ networks. However, the strong acid or base catalysts typically employed in sol-gel reactions would also cause undesirable degradation of many organic modifiers, especially at higher temperatures required for the drying of the gels.

A catalyst-free sol-gel process, based on tetramethylorthosilicate (TMOS), the most reactive silicon tetraalkoxide in the series, was developed. The catalyst-free route provides an optimum reaction environment for the synthesis of organic-inorganic materials through copolymerization reactions. This concept willl be exemplified by two organic-inorganic systems in which TMOS was used as the inorganic component while poly(dimethylsiloxane) and polyimide oligomers respectively, were employed as the organic component. The effect of such modifications on the surface and bulk properties of the inorganic $SiO_2$ networks was also investigated.

Part 2 of this dissertation describes specific aspects associated with the synthesis of amine containing polysiloxane oligomers. A new molecular design which allows for independent control of molecular weight and amine functionalities was developed. The new synthesis involves anionic ring opening equilibrium copolymerization of the cyclic siloxane tetramer $D_4$ with a new cyclic siloxane monomer containing amine functionalities as pendant groups on silicon atoms. The effect of the bulky substituent {-$CH_2CH(CH_3)CH_2NHCH_2CH_2NH_2$} of the silicon atom on the position of thermodynamic equilibrium, and the extent of molecular weight and composition control in the linear polysiloxane oligomers was studied.

## *ACKNOWLEDGEMENTS*----------

In any educational endeavor of this nature there are many people to acknowledge for their influence, guidance and support. A special mention of my personal thanks must go to Dr. Judy Riffle who was instrumental in my decision to begin doctoral studies at Virginia Tech. Greatful appreciation is expressed to my advisor and committee chair, Dr. James E. McGrath, not only for his professional guidance, but also for the personal support and encouragement which he unselfishly gave. I also extend my deepest appreciation to my doctoral advisory committee members, Dr. Harry W. Gibson, Dr. Herve Marand, Dr. Harold H. McNair, and Dr. James M. Tanko for their guidance and support of my doctoral work and for giving their time and insights to the value of my graduate education.

There are many whom I am indebted to for creating a forum for discussions, these include Dr. Guru Sinai-Zingde, Dr. Akhil Verma, Dr. Ramji Srinivasan, Dr. Mia Siochi, Dr. Joe DeSimone, Mr. Niranjan Patel, Mr. Carrington Smith, Mr. Tom Glass, Mr. Steve McCartney, to name a few. I would also like to thank Mr. Toni Brennan in Prof. Wilkes' lab for sharing with me some of the *not so good times* on the sol-gel project. To all the others who made my graduate school years an enjoyable experience, my sincere thanks. Special appreciation goes to Mrs. Bonnie Johnson for her tireless help and kind assistance, and for keeping things running smoothly.

For friendship and understanding, for faith and encouragement, I owe my deepest thanks to my long time friend and sister, Cindy. Most importantly, to my daughter, Oana Monica, and my husband Ionel who in their own way have contributed immensly to the successful completion of the program. Last but not least I owe my strength and determination to my mother, Ruxandra, for her incredible courrage and unselfish sacrifice in raising five children and giving each and everyone of us the opportunity to a good start in our education. From there on it was up to each of us to follow our call. Without her vision I could have missed on the joy of learning.

dedicated with love to my mother and my daughter

to my mother,
for her unselfish giving

to my daughter
for being my friend, as well as my daughter,
for sharing the good times,
and not complaining about the many evening and weekends
she spent alone

*TABLE OF CONTENTS*----------

***PART 1***

## *LIST OF FIGURES*

*FIGURE NO.* *PAGE*

*PART 1*

## *LIST OF SCHEMES*----------

*SCHEME NO.* *PAGE*

*PART 1*

## *LIST OF TABLES*----------

*TABLE NO.* *PAGE*

*PART 1*

*PART 2*

# PART 1

# Synthesis and Characterization of Organic-Inorganic Polymer Networks via Sol-Gel Chemistry

# *CHAPTER I*

# *INTRODUCTION*

For the last few decades polymeric materials have been extensively used in almost every aspect of human life. New polymers with improved properties are being created each year. Although each homopolymer has its individual features, the most versatile way of creating new materials is through combination of homopolymers. This can be achieved by either blending or copolymerization. Hundreds of such systems have been developed and many have been commercially applied. However, among all of these, organic compounds are usually the major ingredient and the example of combining them with inorganic compounds are uncommon, except for fillers.

Silica glass, a highly crosslinked, defect containing $SiO_2$ network is a very representative material in the inorganic field and it is well known for its good optical properties, high hardness and modulus, and its outstanding thermal and dimensional stability unobtainable with any of the known organic systems. On the other hand, the flexible organic chemistry allows for a remarkable variety in molecular and properties design of the organic polymers. Combination of organic and inorganic materials, at the molecular level, through chemical reactions, appears as a very attractive approach for generating new materials which would bring together the best of both the inorganic and the organic worlds.

Traditionally, solid melting techniques are used in melting silica powder ($SiO_2$) into a viscous liquid under very high temperature (>1400°C), to make glass or ceramics. Temperatures of this magnitude would degrade any organic component and therefore rule out any successful attempt for combining organic and inorganic materials. The conventional melting method has been substituted in part by a new technique which has, as the most significant feature, the ability to

generate glasses at lower temperatures. This new technology known as the **sol-gel process** refers to the evolution of a network glass from solution. During this process hydrolysis and subsequent condensation of organic or inorganic alkoxides leads to the formation of three dimensional networks. The advantages are several-fold. The new method leads to homogeneous products because of the fact that the precursor materials are liquids, allowing "miscibility" at the molecular level. Also materials with higher purity can be achieved because it is possible to distill the starting monomers. However, the most important advantage of this process is the use of low temperature operation to acquire the gels. The result is an exciting new area of research for producing organic-inorganic materials by copolymerization techniques.

The initial objective of the present research was to select an inorganic sol-gel system which could provide the best environment for further modification with organic components. Traditionally, tetraethylorthosilicate (TEOS) is the most commonly used starting alkoxide for the silicon based sol-gel reactions. However, the strong acid or base catalysts typically utilized to hydrolyze TEOS would also cause undesirable degradation of many organic modifiers, especially at higher temperatures required for the drying of the gels. Thus, a relatively neutral reaction environment is required for many of the organically modified systems. In order to eliminate the need for a reaction catalyst, tetramethylorthosilicate (TMOS), the most reactive tetraalkoxysilane in the series, was used as the inorganic starting alkoxide. The inorganic sol-gel system based on TMOS was initially investigated in order to demonstrate that this starting alkoxide can provide a catalyst-free route for the generation of $SiO_2$ networks. The hydrolysis and condensation of TMOS, in the absence of catalyst, were investigated under a variety of reaction conditions in order to determine the most important parameters affecting the reaction rate and conversion and to understand the growth mechanism (known to be important for the resulting microstructure) under catalyst free conditions.

In addition, synthesis of organic oligomers of controlled molecular weight and functionality, and their subsequent hydrolysis and co-condensation reactions with inorganic alkoxides to generate organic-inorganic hybrid networks, were investigated. The first organic-inorganic system which will be discussed will refer to the incorporation of an elastomeric type modifier into the sol-gel glasses. Hence, reactive poly(dimethylsiloxane) (PSX) oligomers were synthesized through a two-step reaction. In the initial step, vinyl terminated PSX oligomers of controlled molecular weight were prepared by anionic ring opening polymerization of octamethylcyclotetrasiloxane ($D_4$), using 1,3-divinyltetramethyldisiloxane as the chain transfer agent or end capper. Next, methoxy functionalized oligomers were produced by a hydrosilation reaction at the terminal vinyl double bonds, using methoxysilanes as the hydrosilating agents. A second organic-inorganic system which will be discussed refers to the incorporation of a glassy component (below the $T_g$) in a sol-gel inorganic network. Polyimide (PI) oligomers were selected for this study as the organic "glassy" modifiers. Initially, amine terminated, fully imidized polyimide oligomers of controlled molecular weight were synthesized by solution imidization techniques. Quantitative conversion of amine terminal groups to nadimide endgroups and further hydrosilation at the nadimide double bond with methoxysilanes as the hydrosilating agent, allowed for the synthesis of methoxy functionalized polyimide oligomers. The above reactive oligomers were copolymerized with inorganic alkoxides (TMOS) to generate organic-inorganic three-dimensional networks. The chemistry of the copolymerization was investigated for the two organic-inorganic systems and selective characterization was carried out.

In the forthcoming Chapter 2 Literature Review, the chemistry and supramolecular structure in silicon based sol-gel systems will be discussed in detail. The experimental and analytical techniques utilized in this work are outlined in Chapter 3. Synthesis of reactive PSX and PI oligomers and their subsequent copolymerization with inorganic alkoxides will be discussed in

Chapter 4 which details the experimental results, followed by conclusions and suggested future studies.

*CHAPTER 2*

*LITERATURE REVIEW*----------

# *CHAPTER 2*

# *LITERATURE REVIEW*----------

## *2.1. INTRODUCTION TO THE SOL-GEL PROCESS*

In the general sense, any process during which a solution or "sol" becomes an insoluble three-dimensional network or "gel" can be defined as a sol-gel process. Sol-gel technology, well known to ceramic engineers, refers to a low temperature technique for preparing single-component or multicomponent oxide glasses. The process involves the hydrolysis and condensation of a solution of inorganic alkoxides, inorganic/organic alkoxides or other inorganic or organic compounds. For example, synthetic silicates (I), prepared by sol-gel processing of alkoxysilanes (equation 1), allow for the generation of amorphous materials that are precursors for high purity glasses, ceramics, coatings and fibers.

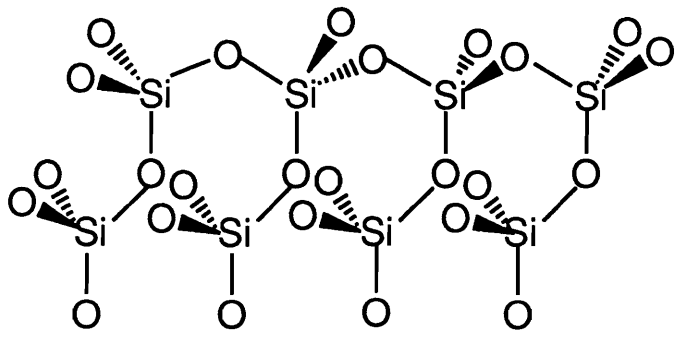

I

$$nSi(OR)_4 + 2nH_2O \xrightarrow{\text{catalyst}} (SiO_2)_n + 4nROH \qquad (1)$$

The generation of such three-dimensional networks through sol-gel processes comprises two main aspects: (a) the chemistry of the process in homogeneous solutions and (b) the post-gelation physico-chemical transformations.

(a) The initial chemistry takes place in homogeneous solutions, usually by the use of a mutual solvent since $Si(OR)_4$ and $H_2O$ are immiscible. The rate of reaction is significantly affected by the presence of catalyst. In general, the reaction occurs in two stages, hydrolysis, according to equation (2) and condensation, according to equations (3) and (4) below [1]:

$$\left.\begin{aligned} Si(OR)_4 + H_2O &\rightleftharpoons HOSi(OR)_3 + ROH \\ HOSi(OR)_3 + H_2O &\rightleftharpoons (HO)_2Si(OR)_2 + ROH \\ (HO)_2Si(OR)_2 + H_2O &\rightleftharpoons (HO)_3Si(OR) + ROH \\ (HO)_3Si(OR) + H_2O &\rightleftharpoons (HO)_4Si + ROH \end{aligned}\right\} \quad (2)$$

$$\equiv Si-OR + HO\cdot Si\equiv \longrightarrow \equiv Si-O-Si\equiv + ROH \quad (3)$$

$$\equiv Si-OH + HO\cdot Si\equiv \longrightarrow \equiv Si-O-Si\equiv + H_2O \quad (4)$$

The above reactions which can take place in a very complex sequence demonstrate that the sol-gel process from an alkoxysilane to a three dimensional oxide network is not a simple one, but many different intermediates are possible. Furthermore, it is very difficult to separate hydrolysis from condensation reactions in such systems. This means that in most cases reactions according to equations (3) and (4) will start very soon after equation (2) and, if the degree of polymerization has reached a sufficient state, gelation occurs due to the formation of three-dimensional insoluble networks. For this reason, many studies deal with both hydrolysis and condensation. The particular alkoxide, the solvent, the catalyst and the gelation temperature can all be changed. These changes can drastically affect the gelation time as well as the properties of the gel.

(b) In addition to the complex chemical reactions taking place in homogeneous solutions, physical transformations during the post-gelation process can also affect the material properties. The two stages of the sol-gel formation are interconnected and their combined effect is very complicated. The sequence of structural changes occuring during the sol-gel process is schematically

illustrated in ***Figure 1.1*** [1]. The key processes here are the sol-to-gel conversion, the gel-to-glass transformation, and the densification process.

## *2.2. HISTORIC PERSPECTIVE*

The first, although incidental, observation of a sol-gel process dates back to 1846 [2]. It covered the hydrolysis and polycondensation of tetraethylorthosilicate, $Si(OC_2H_5)_4$, under humidity conditions, leading to silica gel. Ebelman described that clear monolithic products with a hardness able to scratch glass were obtained after some months storage at room temperature. *This means that basic principles of the sol-gel process were discovered about 145 years ago.* About fifty years ago two german scientists (Geffcken and Berger) prepared single oxide coatings and patented the sol-gel technology in 1939 [3]. In the next thirty years, the progress in the sol-gel field was relatively limited. This was mainly due to the relatively high cost of the metal alkoxides starting materials and the difficulties encountered in making monolithic objects.

A new stage in the development of the sol-gel technology began in the late sixties. The basic principles of the chemical reactions and process technology for coatings were known when in 1969 Dislich and Hinz elaborated the chemical basis for the preparation of multicomponent oxides. Patent applications were filed in 1969 [4] and the details of the process were published in 1971 [5]. Since 1971 it has been known that any type of multicomponent oxide can be synthesized by the sol-gel process using the alkoxides of various elements. The sol-gel process has been proven useful and reliable in laboratory. Its chemistry has been shown to be extremely variable and complex. Roughly speaking, this chemical process opens the door to nearly everything, equally to glasses, glass-ceramics or crystalline systems. However, only if the parameters which govern the individual steps are well established and controllable, will the chemical multitude be followed by a multitude of products and applications.

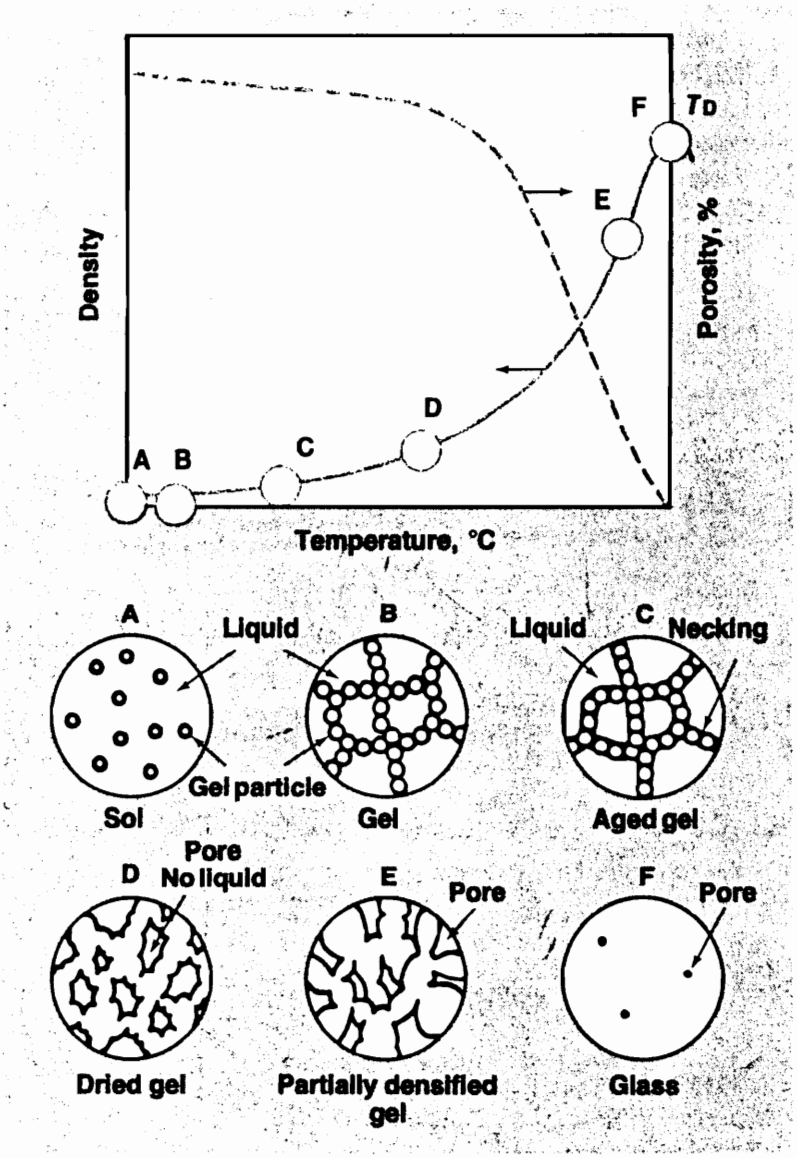


***Figure 1.1.*** Sequence of structural changes during gelation, drying, and densification of sol-gel derived glasses [1].

### *2.3. MECHANISM OF SOL-GEL REACTIONS*

Although several metallic elements such as aluminum, titanium, boron and sodium have been used in the sol-gel process [6-10], the one that has been most extensively studied is silicon. The main reason is that silicon alkoxides have the slowest rate of reaction among all the metal alkoxides commercially available [9,10] and this greatly enables one to control the reaction and to study its kinetic and mechanistic details. The present literature review is exclusively concerned with silicon based sol-gel systems. The mechanism of hydrolysis and condensation of alkoxysilanes is very difficult to study because it is almost impossible to separate hydrolysis from condensation. For this reason, a large number of studies in the literature deal with both, hydrolysis and condensation. The mechanistic studies become even more complicated when dealing with multifunctional alkoxides used in sol-gel reactions. Under these conditions a complex sequence of hydrolysis and condensation reactions (equations 2 through 4) lead to insoluble three-dimensional networks.

#### *2.3.1. HYDROLYSIS REACTIONS*

The interest in the mechanism of hydrolysis of organosilanes has increased parallel to the evaluation of mechanistic considerations in modern organic chemistry. To the extent that models for the reaction at the C-O bond were developed, investigations were carried out to prove how these models are transferable to the Si-O bond. As a general feature, in the hydrolysis of organosilanes the Si-O bond is apparently cleaved in the vast majority of cases. This was demonstrated by the configuration of the reaction product obtained in the hydrolysis of optically active compounds [11]. Direct proof for cleavage of the Si-O bond was obtained when tetraethoxysilane was hydrolyzed using $H_2{}^{18}O$, which proceeds in neutral medium, as well as in the presence of acid or base, to give ordinary alcohol [12], according to equation (5) below:

$$\equiv Si-O-C_2H_5 \; + \; H_2{}^{18}O \longrightarrow \equiv Si-{}^{18}OH \; + \; C_2H_5\text{-}OH \qquad (5)$$

Investigating alkoxysilane reactions is difficult. A myriad of reactions are occuring simultaneously. For example, hydrolysis of alkyltrialkoxysilanes in water is thought to proceed stepwise through alkyldialkoxysilanols and alkylalkoxysilanediols to give alkylsilanetriols [12,13]. These species may condense with themselves to form a variety of siloxane oligomers [12]. Monitoring a single reaction of alkyltrialkoxysilane, i.e., the first hydrolysis step, which is not obscured by further hydrolysis and condensation reactions has discouraged mechanistic investigations using multifunctional alkoxysilanes. In general, silicon compounds with only one reactive alkoxy or aryloxy group in mixed aqueous-organic solvents have been used in hydrolysis studies [12].

#### *2.3.1.1. Base-catalysed hydrolysis*

A better understanding of the chemistry of alkoxysilanes in aqueous solutions, especially the nature of the transition states, was possible by the examination of the steric and inductive effects of the alkyl group on the rates of hydrolysis and condensation reactions of alkyltrialkoxysilanes. The rate constants for a series of alkyl *tris*-(2-methoxyethoxy)silanes were used to define a modified Taft equation, $\log(k^{OH}/k_0)=\rho^*\sigma^*+sE_s$ [14] where $k_0$ is the hydroxide ion catalyzed rate of hydrolysis for methyl *tris*-(2-methoxyethoxy)silane, chosen as the reference; $\sigma^*$ is the Taft polar substituent constant and $E_s$ is the Taft steric substituent constant. The values of $\rho^*$ and $s$ were obtained for the best linear least-squares fit for the above equation. The values of $\rho^*$ and $s$ are often used to qualitatively describe changes in structure and charge distribution as the reaction proceeds along the reaction coordinate from reactants to transition state [14]. Such studies on alkyltrialkoxysilanes [15] contributed to further verify the reaction mechanism proposed by McNeil et al. [13] for the first step of hydrolysis. A moderately large value was found for $\rho^*$ ($\rho^*$=2.48), suggesting that the transition state during the hydrolysis reaction is stabilized more than the reactants by electron withdrawing groups attached to silicon. This implies considerable *negative* charge on the silicon. In addition, the moderately large $s$ ($s$ = 1.67) suggests that the

transition state is more sterically crowded than the reactants [16]. These data are consistent with a bimolecular displacement reaction ($S_N2^{**}$-Si or $S_N2^{*}$-Si) with a pentacoordinate intermediate. $S_N2^{**}$-Si is rate determining formation ($k_{-1} < k_2$) and $S_N2^{*}$-Si is rate determining breakdown ($k_{-1} > k_2$) of the pentacoordinate intermediate, as showm in ***Scheme 1.1,*** [13]. According to this mechanism, negative charge development on silicon in the transition state (T.S.1 or T.S.2) should be considerable, therefore consistent with a large positive $\rho^*$. Electron withdrawing alkyl groups will therefore stabilize the developing negative charge and should lower the energy of the transition state. Consequently, a significant increase in the observed rate of hydrolysis should occur as the alkyl group becomes more electron withdrawing. Experimentally, hydrolysis of chloromethyl tris-(2-methoxyethoxy) silane was observed to be 1600 times faster than n-propyl substituted silane [15].

In addition, the proposed mechanism suggests that the crowding around the silicon should increase significantly as the reaction proceeds from the reactants to transition state, consistent with the relatively large s value observed. If the transition state T.S.1 is the highest energy point along the reaction coordinate, there should be considerable bond formation between the incoming hydroxyde anion and silicon. The bond order between the silicon and oxygen of the leaving group remains essentially unchanged, at one. The high negative charge density on silicon and oxygen of the nucleophile should produce a tight transition state structure [15]. As the number of substituents surrounding the central atom increases, so should the steric crowding. Similar arguments can be made if the transition state T.S.2 is the highest energy point along the reaction coordinate.

***Scheme 1.1***. Proposed mechanism for base-catalyzed hydrolysis of alkyltrialkoxysilanes [13].

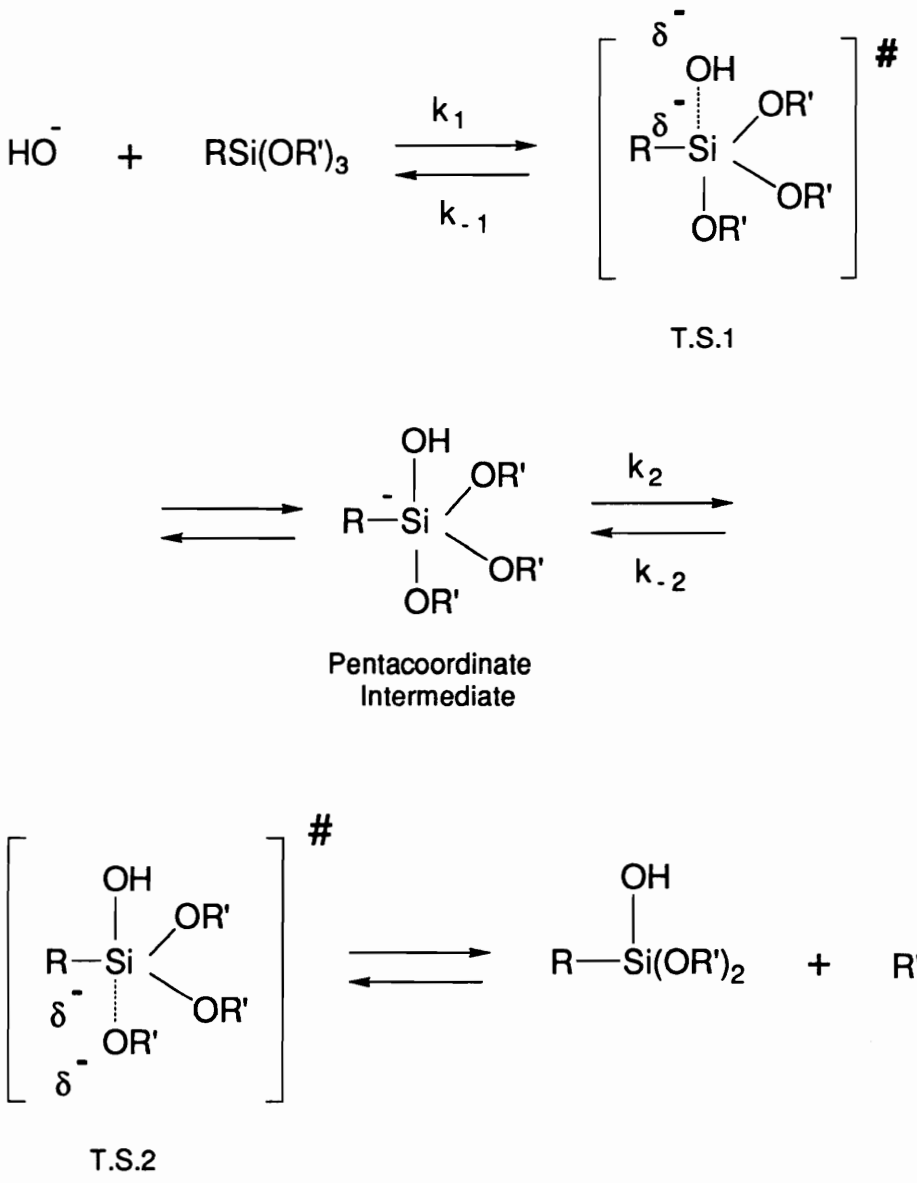

This model for hydrolysis reaction has been accepted because hypervalent silicon intermediates have been previously observed [17] in many other chemical reactions. In the alternative $S_N$-2 type bimolecular displacement mechanism without a pentacoordinate intermediate, a looser transition state would result. The steric effects of the alkyl groups bonded to silicon should, therefore, be considerably less than those associated with the mechanism given in Scheme 1.1. The relatively large value found for s [15] seems to better describe the mechanism given in Scheme 1.1 rather than a $S_N2$-type mechanism. In addition, $S_N2$-type mechanism generally gives a small negative $\rho^*$ value, which is inconsistent with the large positive $\rho^*$ values measured for base-catalyzed hydrolysis.

### *2.3.1.2. Acid-catalysed hydrolysis*

For acid catalyzed hydrolysis two different models have been proposed for the intermediate state. One model [18] assumes that the replacement of an alkoxy group by a hydroxyl follows the dissociation of the alkoxysilane, equation 6:

$$\equiv Si-OR + H_2O \longrightarrow \equiv Si^{+} + {}^{-}OR + H_2O \longrightarrow \equiv Si-OR + ROH \qquad (6)$$

The formation of a trivalent siliconium ion would be the limiting step of the hydrolysis process. Siliconium ions, however, may be at considerably higher energy with respect to starting materials. Detailed work to prove the siliconium ion formation has been carried out by Sommer et al. [19, 20] with optically active compounds. The hydrolysis of $R_1R_2R_3Si^*OR$ in acetone did not lead to racemization, indicating that no siliconium ion was present. This conclusion checks with the results of Swain [21].

The other model assumes that the hydrolysis is caused by the nucleophilic attack of a water molecule on a protonated alkoxide species or an electrophilic attack of a hydronium ion on a basic

alkoxide group. The two proposed mechanisms are described by ***Scheme 1.2*** [13] and ***Scheme 1.3*** [22], respectively. In the nucleophilic mechanism, Scheme 1.2, the proton is attracted by the oxygen atom of the OR group resulting in a shift of the electron cloud of the Si-O bond towards oxygen. As a result, the positive charge of the silicon atom increases and a water molecule can now attack the silicon atom. In the electrophilic reaction mechanism, Scheme 1.3, a protonated water molecule is attracted to the oxygen atoms in the basic, alkoxide group. In the proposed activated complex, partial bonds form between the protons and the oxygen atoms in the alkoxides, and between the water oxygen and the silicon. Meantime, the original bonds weaken. One set of partial bonds will strengthen fastest, forming the alcohol molecule and the silanol group. The extra proton is given up to another water molecule to complete the reaction in a second fast step.

The study of the steric and inductive effects of the alkyl groups on the rate of hydrolysis of alkyltrialkoxysilanes further contributed to the elucidation of hydrolysis mechanism under acidic conditions [15]. The values of previously defined parameters $\rho^*$ and $s$ of 1.39 and 1.06 respectively, agree with a mechanism for acid-catalyzed hydrolysis consisting of a rapid equilibrium protonation of the substrate, followed by a bimolecular $S_N2$-type displacement of the leaving group by water. The small, positive value of $\rho^*$ suggests a small increase of negative charge on silicon [14]. The positive $\rho^*$ also suggests the unlikelihood of a mechanism which proceeds through a siliconium ion intermediate. The smaller $s$ value implies a less crowded transition state for the acid catalyzed reaction when compared to the base-catalyzed reaction. Although several factors may influence the sensitivity of the steric parameters, such as solvation, the smaller value of $s$ is at least consistent with a change in mechanism from a bimolecular displacement with a pentacoordinate intermediate to a mechanism that has more $S_N2$-type character [13].

***Scheme 1.2.*** Nucleophilic mechanism for acid-catalyzed hydrolysis of alkyltrialkoxysilanes [13].

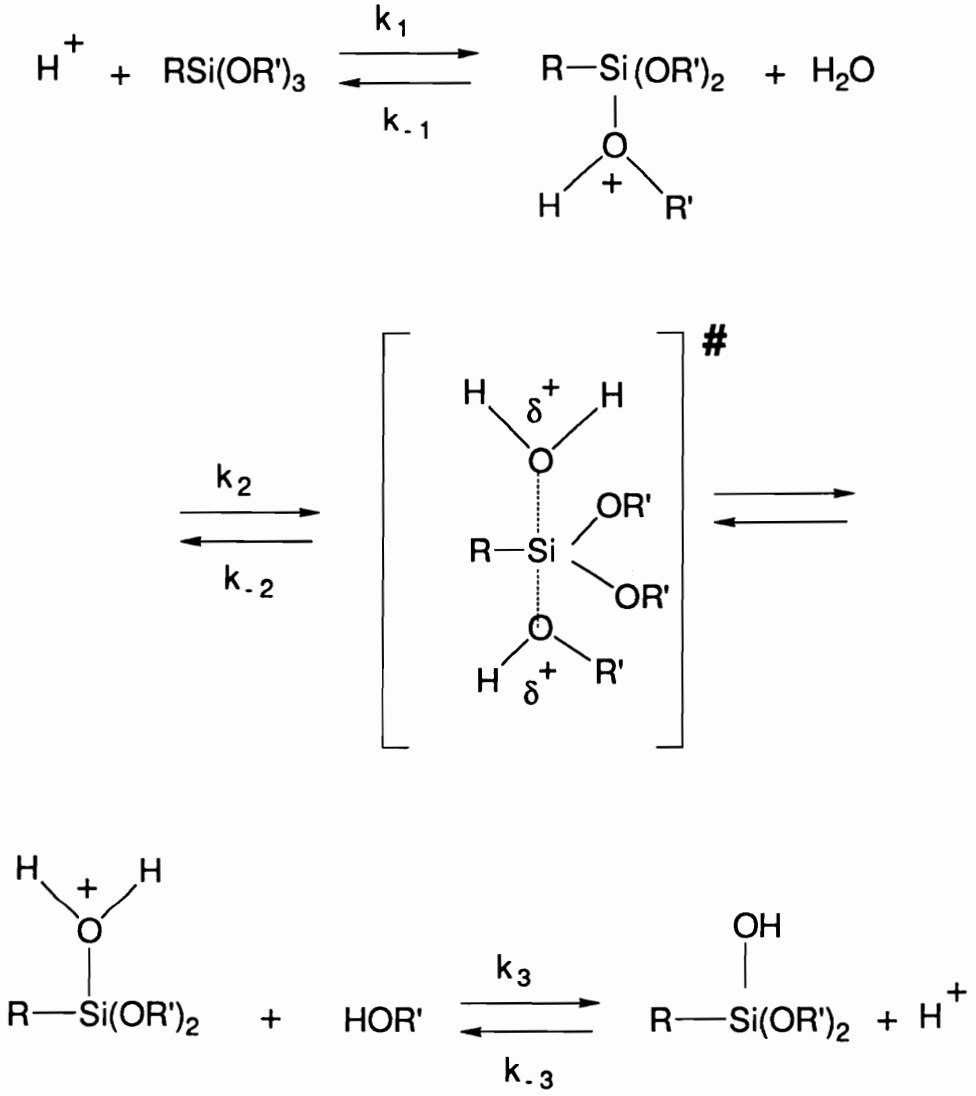

***Scheme 1.3***. Electrophilic mechanism for acid-catalyzed hydrolysis of alkoxysilanes [23].

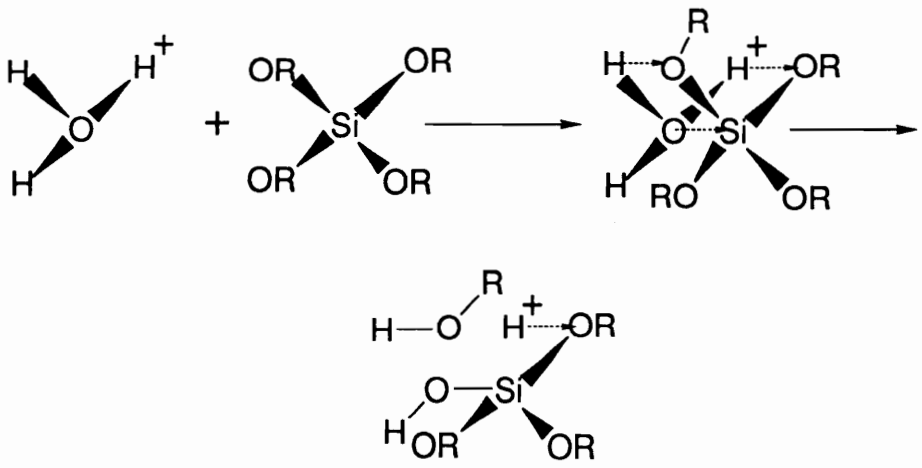

Kinetic studies are also useful in elucidating reaction mechanism. Kinetic measurements by Aelion et al. [23] on the acid catalyzed hydrolysis of ethyl silicate indicated a third order for the overall reaction. This can be fitted into the kinetic schemes of two subsequent second order reactions, namely, either the formation of the conjugate acid from the addition of a proton to the ester oxygen and subsequent hydrolysis with a molecule of water, Scheme 1.2, or the formation of an oxonium ion followed by its reaction with the ester, Scheme 1.3. The study of reaction kinetics on alkoxysilanes is complicated by the difference in the rate of reaction of the alkoxy groups. Hence, for more reliable data, the simplest alkoxysilane, monomethoxytrimethylsilane, was used by Leyden et al. to determine the reaction order [24]. These authors found the reaction to be first order in both silane and water concentrations. Enthalpies of hydrolysis have also been reported. To avoid complications by the superposition of additional heats of consecutive processes such as sol and gel formation, trimethylethoxysilane was used by Tiller et al. [25] to determine the enthalpy of hydrolysis for the reaction:

$$(CH_3)_3Si-OC_2H_5 \quad + \quad H_2O \xrightarrow{HCl} \quad (CH_3)_3Si-OH \quad + \quad C_2H_5OH \qquad (7)$$

The enthalpy of hydrolysis was found to be $(\Delta_R H_h)_{295°K} = -(6.2 \pm 0.3)$ KJ/mol, for 100% conversion and no detectable condensation reactions within the duration of the measurement.

### *2.3.1.3. Neutral hydrolysis*

The prefered mechanism of hydrolysis under neutral conditions can be schematically represented by the sequence of reactions described in ***Scheme 1.4*** [12]. Much less experimental data are available for these reaction conditions.

***Scheme 1.4.*** Proposed mechanism for hydrolysis of alkoxysilanes in neutral medium [12].

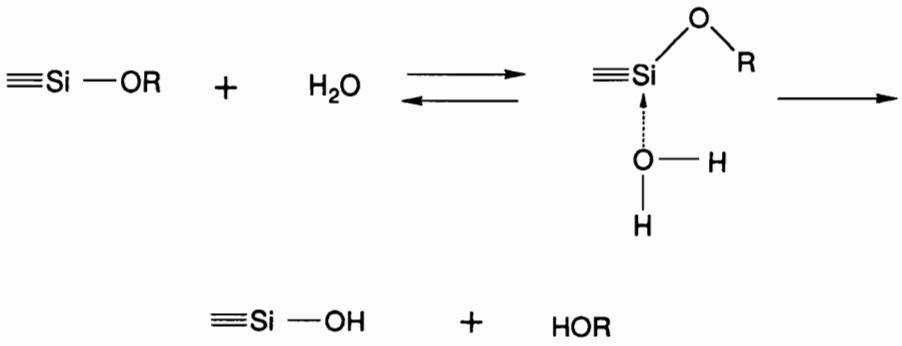

*2.3.2. CONDENSATION REACTIONS*

The mechanism of silanol condensation reaction is of considerable interest because of the absence of any exact analog in carbon chemistry. In the context of a sol-gel process, the condensation reaction has two different levels of complexity. Firstly, it is of interest to understand the mechanism of condensation in the absence of polymerization reactions. Information about this mechanism were obtained in early studies using monofunctional silanols which give a simple one-step reaction:

$$2\ R_3Si-OH \longrightarrow R_3Si-O-SiR_3 + H_2O \qquad (8)$$

and it was observed to be catalyzed by both acids and bases [26]. Secondly, for multifunctional alkoxides, condensation-polymerization reactions take place resulting in a continuous growth of the molecular weight and ultimately to the formation of an insoluble three-dimensional network. Many times, the study of condensation reactions was carried out using multifunctional alkoxides and much more information is available for these conditions. In sol-gel processes the need for understanding the molecular mechanism of condensation reactions was combined with the interest in elucidating the pathways for molecular growth in silica sol-gel polymerization. The apparently simple chemistry has been very difficult to understand since the nature of silica-gel obtained is known to be very sensitive to the precise reaction conditions employed [1]. In general, the rate of condensation-polymerization of multifunctional alkoxides and formation of silica gel is at a minimum at around pH 2. It has been assumed that since this is the isoelectric point of silica, the catalyst below pH 2 is the $H^+$ ion which forms an active cationic complex while above pH 2, the $OH^-$ ion is the catalyst and active anionic silica is generated under these conditions [27].

### *2.3.2.1. Base-catalyzed condensation*

The base-catalyzed route predominates during condensation-polymerization of silanols and silica gel formation at pH values above 2-3 [27] . Under these conditions the hydronium ion is believed to be the reaction catalyst. Early studies by Grubb [26] of the condensation of silanols in methyl alcohol under the influence of bases, indicated that the condensation rate was proportional to the catalyst concentration and independent of the nature of the cation. Based on these observations it was assumed that the active condensation centers were the free anions. Under these conditions, the condensation mechanism was proposed to occur according to **Scheme 1.5** [12]. The limiting step was considered to be the reaction of the anion with the silanol. Such reaction was proposed to occur by a rearward attack mechanism in which an electron donor molecule approaches the backside of the central atom undergoing displacement of one of its substituents, according to a $S_N2$-Si type mechanism.

Further insight into the mechanism of silanol condensation was achieved by the use of alkylsilanols which allow the investigation of the steric and inductive effects on the reaction rate [15]. However, the condensation reactions are still not as well understood as the hydrolysis. The lack of quantitative rate data on the condensation of alkylsilanols in aqueous solutions for example, arises because of the difficulty in monitoring the individual condensation reactions. Pohl and Osterholtz [29] developed $^{13}C$ and $^{29}Si$ NMR spectroscopic methods capable of measuring individual condensation reaction rates for alkylsilanetriols. Kinetic measurements indicated that the deuteroxide anion catalyzed condensations are second order in silanetriol and first order in deuteroxide anion. These facts are consistent with the mechanism proposed by Pohl [29] - **Scheme 1.6.** In this mechanism, the reversible reaction of silanetriol with deuteroxide anion is assumed to be rapid, leading to an equilibrium concentration of silanolate anion, the concentration of which is proportional to the deuteroxide anion and silanetriol concentration:

***Scheme 1.5.*** Proposed mechanism for base-catalyzed silanol condensation [28].

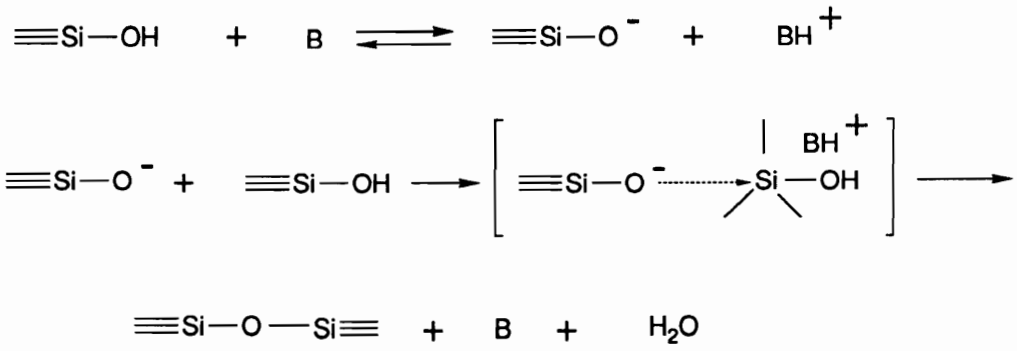


where B = base

***Scheme 1.6.*** Proposed mechanism for base-catalyzed condensation of silanetriol [29].

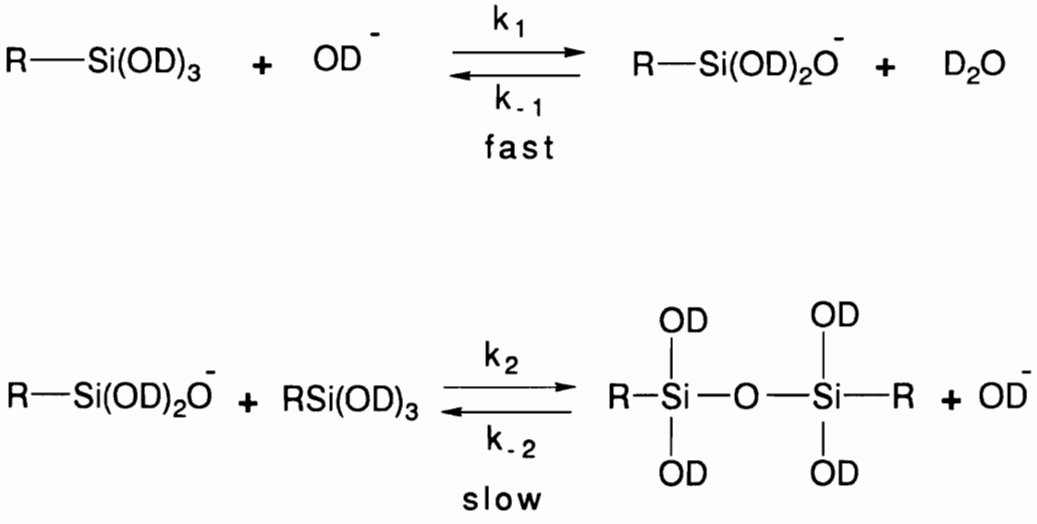

$$RSi(OD)_2O^- = k_1/k_{-1}[RSi(OD)_3][OD^-] \quad (9)$$

The slower second step gives the observed deuteroxide anion catalyzed rate of condensation of silanetriol to the dialkyltetrahydroxydisiloxane. The further condensation of silanetriol with dialkyltetrahydroxydisiloxane was not observed at short reaction time. This slower rate of condensation of silanetriol with dialkyltetrahydroxydisiloxane may be due to the increase of steric hindrance around the silicone in the disiloxane. Nucleophilic displacements at silicon are known to be significantly susceptible to steric hindrance [28]. The kinetic data and the mechanism proposed by Pohl [29] and described in Scheme 1.6 are consistent with both $S_N2$-type mechanism proposed by Grubb [26] and $S_N2^{**}$-Si or $S_N2^{*}$-Si mechanisms proposed by Swain [21], and does not distinguish between them.

Other investigators found that the influence of the base catalyst is very complex and it is not independent of the nature of the cation. For example, it was found that the condensation of 1,4-bis(dimethylhydroxysilyl) benzene in toluene, in the presence of KOH is 0.5 order in catalyst concentration [30]. It was postulated [30] that the 0.5 order in catalyst was due to the fact that the active condensation centers in a medium with low polarity (i. e. toluene) were the ion pairs of the potasium silanolate, which are found as the associates:

$$(\equiv SiOK)_2 \longrightarrow 2\ \equiv SiO^-,\ K^+ \quad (10)$$

On the other hand, the condensation of 1,1,3,3-tetramethyldihydroxydisiloxane in the presence of a sodium alkyl sulfonate was found to be proportional to the square of the concentration of catalyst [30]. To explain that, it was proposed that the salts are bipolar compounds that form ion pairs in solution [31], as shown in **Scheme 1.7**.

More recent investigations also agree with the fact that there are reasons to suspect that the nature of the base chosen will affect the silica condensation rate. First, Iler [27] has shown that the

***Scheme 1.7.*** Proposed mechanism for silanol condensation in the presence of neutral salts [31].

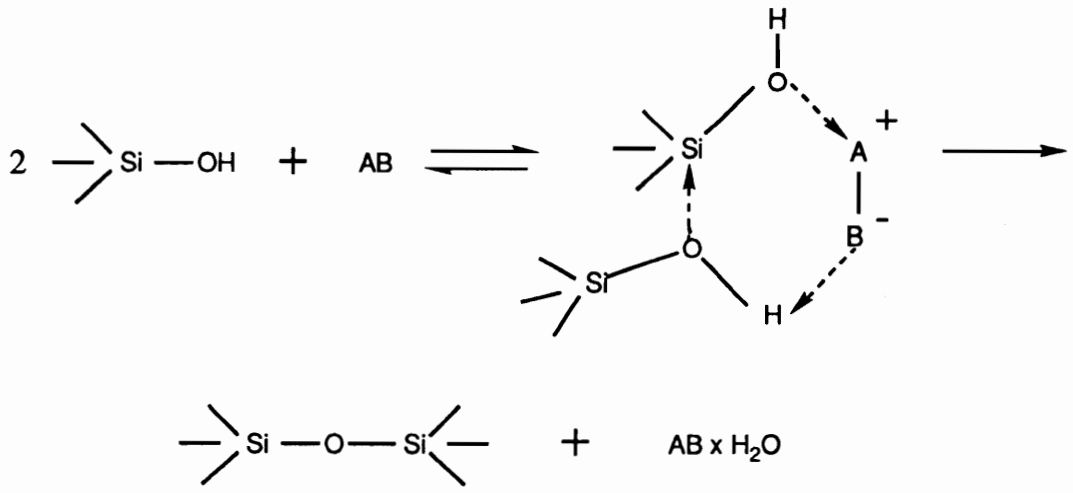

choice of base affects the dissolution rate of silica; this suggests that the cation possesses a catalytic role. Second, it is well known that the cations adsorb onto silica surfaces and large silicate anions [32]. Third, Kelts et al. [33] have reported that the use of NaOH instead of the more conventional $NH_4OH$ results in slower condensation of silica and a more complete conversion of TMOS reactant. Finally, it is known that in zeolite synthesis, which involves condensation of ionized silicate groups, the choice of the base exerts a dramatic influence on the structure of the product [34]. A recent study of the influence of alkali metal hydroxides on silica condensation rate [35] does confirm the effect of cations on the dynamics of Si exchange and this influence is attributed to the formation of cation-anion pairs. The selectivity of condensation involving large silicate fragments versus condensation involving small silicates will in turn influence the compactness of the resulting structure. Large alkali cations pair more efficiently with large silicate oligomers because of the large polarizability of such cations, which permits them to interact with distributed charges on rigid cage-like silicate anions. Thus, it is expected that condensation kinetics are influenced by the size of silicate fragment. In conclusion, in spite of a large number of studies on the silanol condensation, this is still poorly understood because of the complexity of factors which can influence the reaction.

Theoretical studies were also carried out [36] to help in understanding the mechanism of silanol polymerization reaction, under anionic conditions, according to equation (11) below:

$$2\,Si(OH)_4 \longrightarrow (HO)_3Si{-}O{-}Si(OH)_3 + H_2O \qquad (11)$$

The overall enthalpy of reaction for this process was calculated to be -14.8 kcal/mol, a value consistent with the experimental activation enthalpy of 15 kcal/mol for the condensation reaction in aqueous phase [27]. At pH higher than 2 the hydroxide ion can react in two ways:

***(1)*** Attack of hydroxide onto silicic acid produces a stable siliconate with formula $Si(OH)_5^-$. The calculations indicate that no barrier exists to the formation of this siliconate, and the enthalpy of

this reaction is predicted to be -37.7 kcal/mol (using the experimental value for the heat of formation of hydroxide ion) [36]. The hypervalent siliconate formed by addition of hydroxide can continue to react. Attack of this siliconate onto another silicic acid molecule results in a larger siliconate with formula $Si_2(OH)_9^-$:

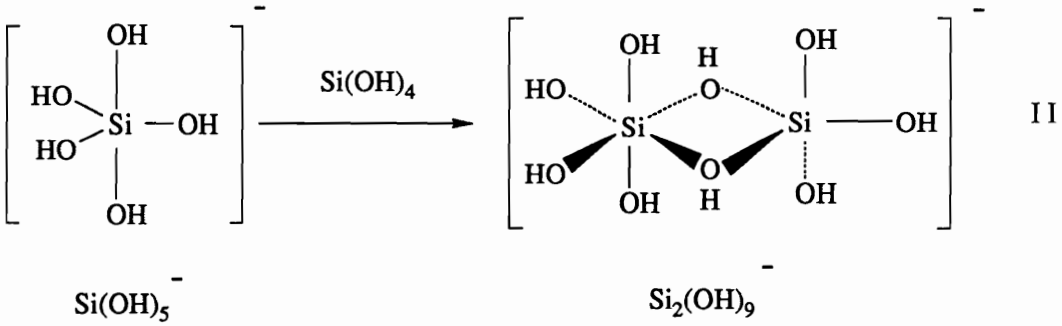


II

Again, the results of the calculations indicate that this reaction is exothermic, with a heat of reaction of -8.3 kcal/mol and no barrier exists to the formation of the larger siliconate [36]. This same process can continue indefinitely, forming a network of hydrated silica. The pentacoordinated end of the siliconate can attack another silicic acid molecule to continue the chain growth, resulting in another pentacoordinate silicon at the end of the chain. In order to form the required siloxane bond in the final silica product, water must be eliminated from these siliconate intermediates. Elimination of water with minimum energy consumption was considered to be the key to formation of the siloxane bond. The calculated activation enthalpies for this process are however much larger than the experimental values. This may be due to overpredicting the activation enthalpy when simple Modified Neglect of Diatomic Overlap (MNDO) method is used [36], or due to the possibility that water elimination is not the rate determining step for the overall condensation process.

*(2)* Another possible reaction of the hydroxide anion is abstraction of a proton from the silicic acid in a normal acid-base type reaction to produce water and the $Si(OH)_3O^-$ ion [36]. The

activation enthalpy for this reaction is only 11.9 kcal/mol, while there is no barrier to simple addition of hydroxide to silicic acid to form the pentavalent coordinate. The $Si(OH)_3O^-$ ion can, in turn, add exothermically to silicic acid to form a larger siliconate anion, $Si_2(OH)_7O^-$ according to equation 12 below:

$$Si(OH)_3O^- + Si(OH)_4 \longrightarrow Si_2(OH)_7O^- \qquad (12)$$

The proposed structure for this type of intermediate is given below:

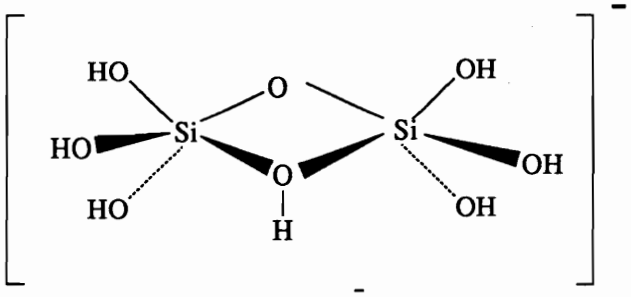


III

$Si_2(OH)_7O^-$

The process can continue to form larger species, as previously discussed. In any case, it is supposed that when silicon becomes coordinated with five or six oxygen atoms all the silicon-oxygen bonds are weakend so that rearrangements (required for the elimination of water with minimum energy) can occur. This has been considered in great detail by Strelko [37] who proposed a complex equation for the pH range from 2 to 10. The equation predicts a maximum in the rate of polymerization somewhere in the mid pH-range.

In conclusion, theoretical studies suggest that pentacoordinate silicon anions appear to be quite important in these systems because of the ease of addition of these anions to tetrahedral silicon compounds. Theoretical calculations support these siliconate structures as possible chain-carriers in anionic silanol polymerization. One of the major key to understanding the polymerization process lies in determining how and when water can be eliminated as the

polymerization proceeds. Whether the rate-determining step is the water elimination or addition and rearrangement of siliconates is not yet known. However, the importance of hypervalent siliconates in anionic polymerization is widely accepted [36].

### *2.3.2.2. Acid-catalysed condensation*

Grubb et al. [26] and Leyden et al. [24] found that under acidic conditions the silanol condensation reaction is bimolecular and that its rate is sensitive to steric factors. Reactions of this type occur in conventional carbon chemistry usually by a mechanism of rearward attack in which an electon donor molecule approaches the backside of the central atom undergoing displacement of one of its substituents. Such reactions follow a bimolecular rate law, $S_N2$-type mechanism, and their rates are sensitive to steric factors. Grubb proposed therefore that silanol condensation occurs in an analogous manner . For example the condensation of trimethylsilanol in methanol, under acid conditions may occur according to ***Scheme 1.8*** [26]. The proton is attracted by the oxygen atom in the silanol group resulting in a shift of the electron cloud of the Si-O bond towards oxygen. As a result, the positive charge of the silicon atom increases and a silanol group can now attack the silicon atom. All the protonated species are assumed to be in non-rate determining equilibrium [26]. The concentration of $(CH_3)_3SiOH_2^+$ is proportional to the acid concentration and thus the rate is first order in acid.

Kinetic measurements carried out by Pohl et al. [29] are consistent with the mechanism described in ***Scheme 1.9*** for deuterium ion catalyzed condensation reactions. For example the reactions are second order in silanetriol and first order in deuterium ion. All the protonated species are assumed to be in non-rate determining equilibrium. The results reported by Pohl are consistent with $S_N2$**-Si, $S_N2$*-Si or $S_N2$ -Si mechanisms [29].

***Scheme 1.8***. Proposed mechanism for acid-catalyzed silanol condensation reaction [26].

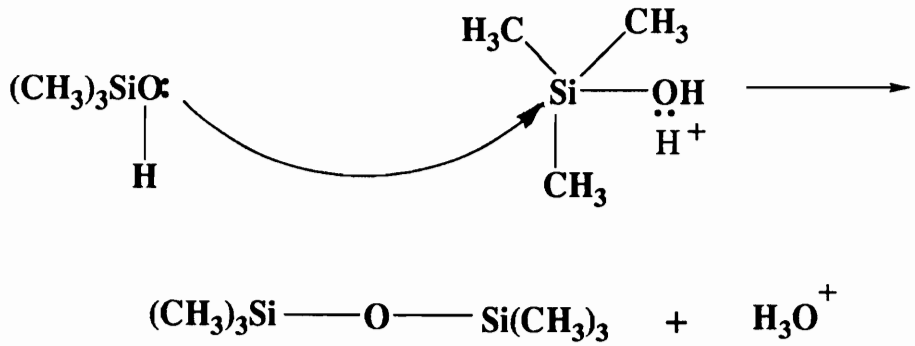

***Scheme 1.9.*** Proposed mechanism for hydronium ion catalyzed condensation of alkyltrihydroxysilane [29].

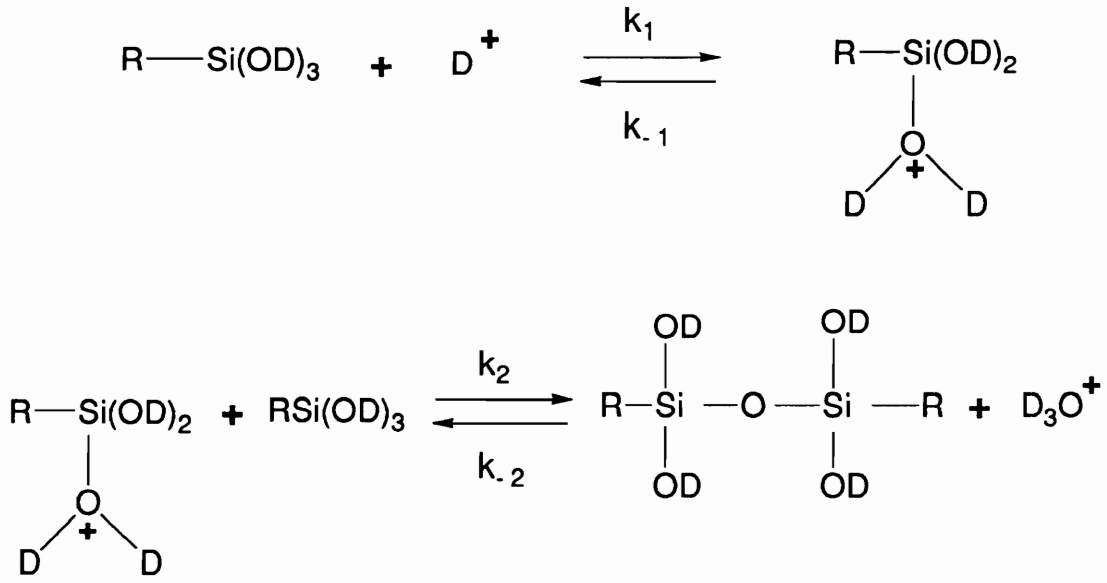

At very low pH, below pH 2, the rate of disappearance of monomer was found to be a third order reaction. The order of the reaction has been explained by Okkerse [38] on the basis that silicon increases its coordination number to 6, as a three-silicon intermediate is formed below pH 2:

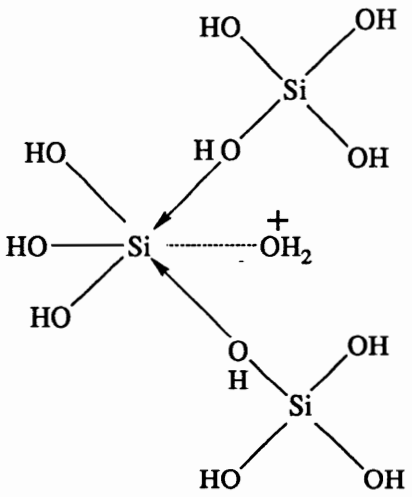


IV

*2.3.3. THE EQUILIBRIUM STATE OF SILANOLS IN ALCOHOLS*

As previously mentioned, sol-gel processes are usually complex, with a number of reactions occuring competitively. Hydrolysis and condensation reactions are the most important and they have been discussed so far. However, the silanol formation is a reversible reaction; when the reaction is carried out in alcohols (as is the case most often), silanols can react with the solvents through esterification reactions. Under these conditions, the following functional group reactions may be written [39]:

$$\equiv Si-OR + H_2O \underset{kE}{\overset{kH}{\rightleftharpoons}} \equiv Si-OH + ROH \quad (13)$$

$$\equiv Si-OR + OH-Si\equiv \xrightarrow{kA} \equiv Si-O-Si\equiv + ROH \quad (14)$$

$$\equiv Si-OH + OH-Si\equiv \xrightarrow{kW} \equiv Si-O-Si\equiv + H_2O \quad (15)$$

where $k_H$ is the hydrolysis rate constant, $k_E$ the esterification rate constant, $k_A$ the alcohol-forming condensation rate constant, and $k_W$ the water-forming condensation rate constant. The reesterification reactions are most significant under acid-catalyzed conditions. In a constant acid concentration these reaction rates are first order in each functional group concentration [28]. Assuming that the reaction rate is independent of the degree of substitution or polymerization of Si, the values of the reaction rate constants were experimentally determined for a sol-gel reaction based on TEOS, at low pH values. Such values are given in ***Table 1.1.*** According to these values, the esterification rate constants are more significant at higher acid concentration. The larger values for $k_E$ mean that the effect of esterification on the overall reaction increases with the increase of acid concentration. On the other hand, when compared with hydrolysis rate constant, the esterification rate constant is considerable even though it has a small absolute value at low acid concentration. Therefore, the esterification reactions should be taken into consideration in an alcoholic solvent system at higher acid concentration. The above data also show that the water-forming condensation rate is much larger than the alcohol forming condensation rate and that the condensation rate increases with the increase of the pH value.

### *2.4. INORGANIC SOL-GEL SYSTEMS*

The sol-gel process has been extensively investigated in the last twenty five years. The silicon-based sol-gel systems have been most extensively investigated due to the fact that the silicon alkoxides have the slowest reaction rate among all the metal alkoxides commercially available,

***Table 1.1*** Rate constants in l/mol-h for reactions (13) through (15) [39].

| Sample | Rxn. pH | kH | kE | kW | kA |
|---|---|---|---|---|---|
| s-1 | 0.9 | 9.6 | 1.6 | 0.48 | 0.09 |
| s-2 | 1.9 | 1.23 | 0.35 | 0.69 | 0.16 |
| s-3 | 3.0 | 0.082 | 0.014 | 1.3 | 0.32 |

where $k_H$, $k_E$, $k_W$, and $k_A$ are rate constants of hydrolysis, esterification, water-forming condensation and alcohol -forming condensation, respectively.

allowing to study the kinetic and mechanistic aspects in more details. Although the ultimate goal of this study is to synthesize organic modified sol-gel networks, a review on pure inorganic systems is important in establishing some basic understanding of the sol-gel reactions.

### *2.4.1. REACTION PARAMETERS*

The whole process of making a glass through the sol-gel route can be divided into three stages: (1) solution (sol), (2) gel, and (3) glass. The structure and properties of alkoxy-derived silicon gels vary widely, depending upon the physical and chemical parameters involved during the initial solution reaction. The molecular topology developed in the solution stage has a direct influence on the gelation process and the final structure of the gel. Although the drying and sintering procedures will also affect the final properties of the glass, it is the reaction variables involved in the solution stage that determines the structure of the materials. Knowledge with regard to the structural evolution during gel formation has rapidly increased over the past few years [40,41]. In this section, the effect of the following reaction conditions on the kinetics and properties of the silicon alkoxide derived gels will be reviewed and discussed:

1. Catalyst and pH value of the solution
2. Type of alkoxide
3. Water content
4. Silicon alkoxide concentration
5. Temperature
6. Type of solvent
7. Pressure

### *2.4.1.1. The effect of catalyst and pH value*

Both acids and bases have been used as catalysts for the reaction of silicon alkoxides in the sol-gel process. Both hydrolysis and condensation reactions are strongly affected by the presence of a catalyst. The effect of catalysts in the sol-gel reactions is two-fold: it affects the reaction rate of each of the two elementary steps (hydrolysis and condensation) as well as their relative rates. In general the reaction rate increases for both hydrolysis and condensation when either acid or base catalysts are used. However, the same catalyst may influence differently the two reactions. Hydrolysis reactions only require diffusion of relatively mobile water in the medium, whereas polymerization reactions require diffusion of larger and much slower organosilane molecules. As a result, the addition of catalyst affects the relative rates of hydrolysis and condensation, which will in turn, affect the topology of the developing chains and the microstructure of the resulting three-dimensional networks. The effect of catalyst on the microstructure of the gel will be detailed in sections 2.5 and 2.6 when the sol-to-gel and gel-to-glass transformations will be discussed.

In order to better understand the complex effect of catalysts, hydrolysis and condensation reactions were often studied on model compounds. For example kinetic measurements for the first *hydrolysis* step of gama-glycidoxypropyltrimethoxysilane indicated that a minimum reaction rate was achieved around pH 7, while a minimum in *condensation* rate was observed around pH 4.5, as shown in***Figure 1.2*** [29]. The hydrolysis appears to be both hydroxide anion and hydronium ion catalyzed since the slopes of the plot at pH above and below the rate minimum around pH 7.0 are drawn to be +1 and -1 respectively (Figure 1.2a). Similarly, the condensation reaction seems to be catalyzed by both hydroxyde and hydronium ions since the slopes of the plot at pH above and below the rate minimum around pH 4.5 are found to be +1 and -1 respectively (Figure 1.2b).

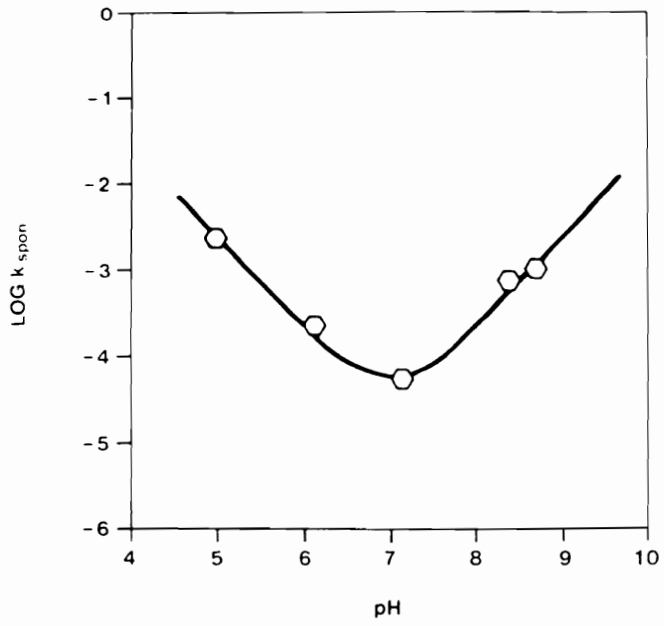


*(a)*

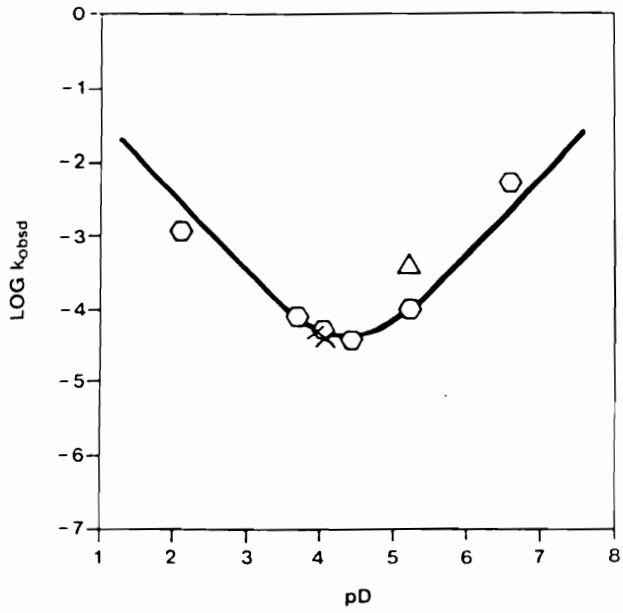


*(b)*

***Figure 1.2.*** Reaction rate dependence on pH [29]: ***(a)*** The first hydrolysis step of γ-glycidoxypropyltrimethoxysilane and, ***(b)*** The condensation of γ-glycidoxypropyl - trimethoxysilane to bis-(γ-glycidoxypropyl) tetrahydroxydisiloxane.

Yamane et al. [42] showed that in tetramethoxysilane (TMOS) solutions, a rapid hydrolysis occurs under acidic conditions, while a lower hydrolysis rate is observed under basic conditions. This was also confirmed by Brinker et al. [43] for tetraethoxysilane (TEOS). In addition, in the acid-catalyzed hydrolysis of the silicon tetraalkoxides the reactivity decreases as the number of OR groups on the silicon decreases with progression of hydrolysis. Under these conditions the probability of formation of $Si(OH)_4$ from $Si(OR)_4$ is small and the condensation reaction starts before the complete hydrolysis of $Si(OR)_4$ to $Si(OH)_4$ [44]. On the other hand, under basic conditions the reactivity increases as the number of OR groups on the silicon decreases, with progression of hydrolysis. The result is the formation of $Si(OH)_4$ while some silicon alkoxide molecules tend to remain nonhydrolyzed. The net result is that in the acid-catalyzed reactions, silicon alkoxide molecules with nonhydrolyzed alkoxy groups polymerize with each other producing polymers with low degree of crosslinking while in the base-catalyzed solutions $Si(OH)_4$ molecules participate in polycondensation reactions, producing highly crosslinked polymers [45].

It has also been shown that the structure of the acid used as catalyst affects the gelation behavior. The gelling time was observed to increase in the order

$$HCl < HNO_3 < H_2SO_4 < CH_3COOH \quad (16)$$

while the pH of the starting solutions decreased in the order

$$CH_3COOH > HNO_3 > H_2SO_4 > HCl \quad (17)$$

the same order as in the $pK_a$ of the acid. Pope and Mackenzie suggested that the variation in the gelation time and the porosity of the dried gels with the kind of acid cannot be explained by the pH of the starting solution alone, but has to be explained by the differences in the role of anions such as $Cl^-$, $F^-$ and $CH_3COO^-$ [46]. So far, the fluoride anion has turned out to be the most effective catalyst in accelerating the gelation process [47]. Even fluoride concentrations as small as about

$5 \times 10^{-5}$ M have a marked effect on the gelation time ($t_{gel}$), and the concentration of $10^{-3}$ M NaF reduces $t_{gel}$ from 33 hrs ($TMOS:H_2O:CH_3OH$ = 1.0:4.0:4.0, no NaF) to several minutes. The effect is also observed at lower pH value where the rate of hydrolysis is known to be much faster.

The addition of $F^-$ affects not only the reaction rate but also the microstructure. The mechanical properties of an HF catalyzed gel, such as the high porosity and low bulk density, appear to be similar to base-catalyzed reactions in which the hydrolysis proceeds via the nucleophilic substitution mechanism of $OH^-$ for $OR^-$ groups. Iler [ 27] postulated that the effectiveness of $F^-$ in the polymerization reaction is due to its smaller ionic radius versus that of hydroxyl and that the $F^-$ performs the same function of temporarily increasing the coordination number of silicon. The displacement reaction at silicon, induced by $F^-$, may thus be facilitated by its ability to form five-coordinate transition state, utilizing its d-orbitals, ***Scheme 1.10*** [47]. This leads to more electrophilic silicon species which can react faster with additional silanol groups, resulting in an acceleration of the rate of polymerization.

If acid and base catalysts had equivalent catalytic effect it would be easier to compare the results using a parameter such as pH. In general the acid catalyzed solutions undergo more complete hydrolysis than base catalyzed reactions, even though the rate of hydrolysis with respect to the rate of condensation is slower. With acid catalysts, hydrolysis is also reversible, so some reesterification occurs. The base catalyzed solutions, on the other hand, do not undergo complete hydrolysis. The rate of hydrolysis may be faster than the rate of condensation, but the strong crosslinking during polymerization makes elimination of alkoxy and hydroxy groups within clusters difficult [48]. Therefore, while the addition of catalysts generaly increases the overall reaction rate, the type of catalyst utilized will have a strong effect on the developed microstructure.

***Scheme 1.10***. Proposed mechanism for $F^-$ induced displacement reaction at silicon [47].

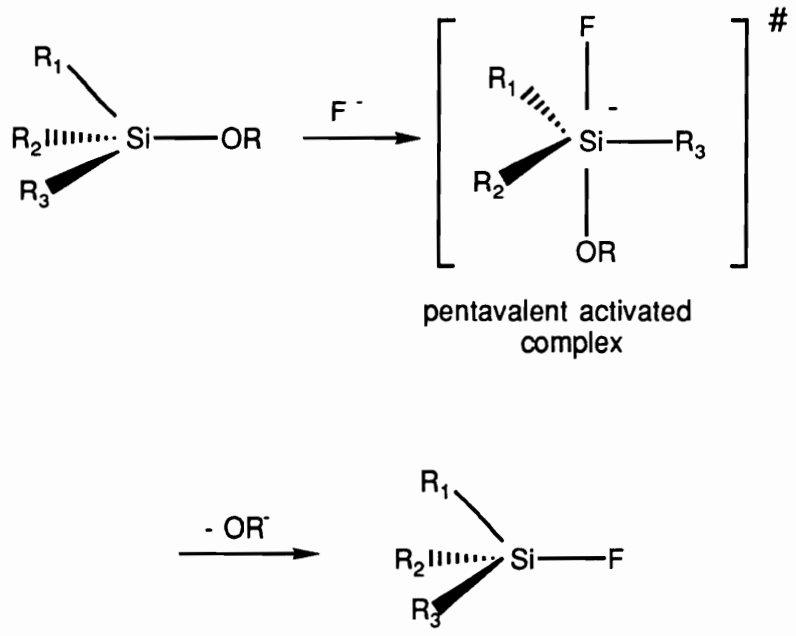

### *2.4.1.2. Type of alkoxide*

The influence of alkyl radicals on the hydrolysis rate of tetraalkoxysilanes, $Si(OR)_4$, was firstly investigated by Aelion et al. [22]. They showed that the rate constant of the proton catalyzed hydrolysis decreases significantly with increasing chain length of R. In the series of aliphatic silicic acid esters, the methyl and ethyl esters (TMOS and TEOS, respectively) are most susceptible to hydrolysis. Colby et al. measured the "apparent" activation energies for the polymerization of TEOS and TMOS [49], from the temperature dependence of these processes. For the overall reaction of TEOS, the "apparent" activation energy, E*, was found to be 14.6 and 13.2 kcal/mol for HF and HCl catalysts, respectively. For TMOS the "apparent" activation energy, E*, was found to be 9.5 and 11.8 kcal/mol for HF and HCl respectively. The magnitudes of E* do not appear to be associated with Si-O bond energies but rather to the transport of condensing species. The authors concluded that the higher values of E* for TEOS are possibly due to the difference in molecular volume and geometry between TEOS and TMOS.

The sensitivity to hydrolysis falls with the increasing number of carbon atoms [22, 50] and with the increasing branching of the hydrocarbon residue [50]. Thus, for example, it falls to a very pronounced extent in the sequence:

$$\equiv Si-O-n\text{-}C_4H_9 \;>\; \equiv Si-O-s\text{-}C_4H_9 \;>\; \equiv Si-O-t\text{-}C_4H_9 \qquad (18)$$

Silicic acid esters of phenols are already less sensitive to hydrolysis than the esters of the lower aliphatic alcohols. The resistance to hydrolysis can be increased considerably by the introduction of ethyl groups into the benzene ring in the 2,6 positions [50]:

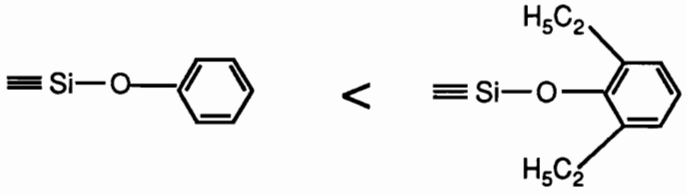


(19)

On passing from silicic acid esters of phenols to those of o-hydroxybiphenyl and 2,2'-dihydroxy-biphenyl, the resistance to hydrolysis increases in the sequence [50]:

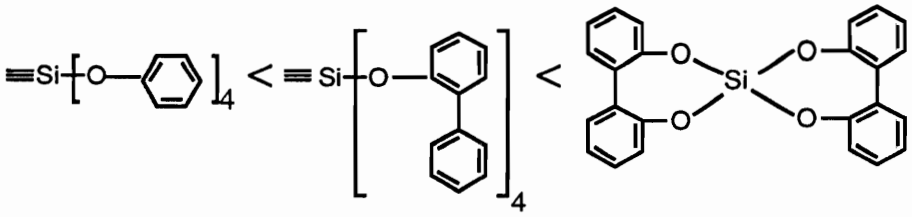

(20)

Another aspect of the effect of the R group can be attributed to the nature of the leaving group. Pohl [15] found that the relative rate of hydrolysis of alkyltrimethoxy, triethoxy and tris (2-methoxy-ethoxy) silanes were 1.0, 0.19 and 0.10, respectively, and he attributed this difference to the leaving group effect.

### *2.4.1.3. The effect of water content*

Konrad was the first to systematically investigate the role of water in its reaction with alkoxysilanes, in 1929 [51]. He carried out the hydrolysis of $Si(OCH_3)_4$ with addition of less than stoichiometric amount of water in varying amounts and concluded that hydrolysis is accompanied by condensation and that the water generated can further react. Water concentration is thus one of the most important parameters in determining the chemical intermediates, morphology and size distribution in sol-gel systems. Unlike other parameters (e.g. pressure, temperature, solvents, etc.) water is directly involved in the chemical reactions that form the molecular structure. The chemical requirement of water falls between 2 and 4 mole for a complete hydrolysis of $Si(OR)_4$. Formation of silicic acid monomer, $Si(OH)_4$, requires 4 mol of water/mol of $Si(OR)_4$, equation (21). However, this precludes any polymerization between species, and thus requires an infinite separation of the hydrolyzed species [52]:

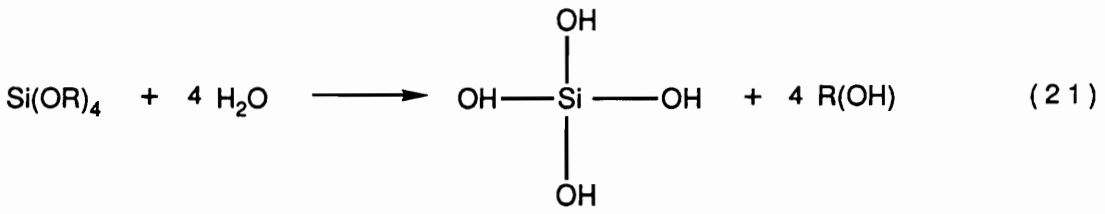


On the other hand, the chemical requirement of water would be 2 mol of water/mol $Si(OR)_4$ if an infinite polymerization takes place, equation (22):

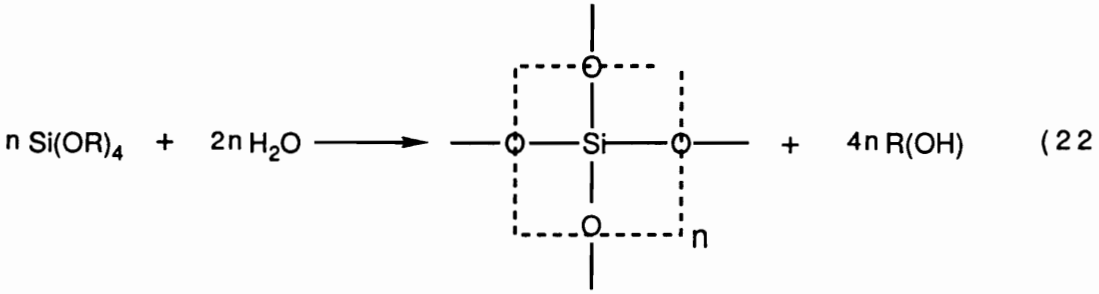


Reality falls between these two extreme cases, but it is much closer to the latter, since the molecular weights of these polycondensed materials are often in the thousands. The water requirement, from a purely chemical point of view, becomes slightly in excess of 2 mol, but its actual effect goes much beyond 4 mol of water [53]. The effect of water was for example investigated during the hydrolysis-condensation reactions for TMOS solutions having water contents of 1.5 and 4.0 in $[H_2O]/[TMOS]$, [44]. For these conditions it was found that alkoxyl groups rapidly disappear at higher water contents, whereas they remain until gelation at lower water contents. It was also shown that the solution of higher water content is characterized by a higher intensity of the Raman band corresponding to Si-O-Si vibration in the three-dimensionally developed silica structure. In general the amount of water used in hydrolysis of alkoxysilanes can affect:

(1) the rate of hydrolysis reaction [44,54,55]; Increased water levels increase the rate of hydrolysis under both acid and base-catalyzed conditions and tend to inhibit condensation, so the resulting products are more highly crosslinked.

(2) the equilibrium state; By Le Chatelier's principle, water promotes hydrolysis and impedes condensation. More water will drive the hydrolysis further before any significant condensation takes place. Also adding more water will suppress the reesterification and drive the hydrolysis toward completion. Conversly, when water concentration is reduced, silicate monomers may start to condense before they are fully hydrolyzed resulting in less dense polymers. Additionally, at low water content the reesterification reactions are favored [54,55,56].

(3) the system's dilution and gel microstructure; Strawbridge et al. [53] carried out an intensive study on the effect of [$H_2O$]/[TEOS] ratio on the structure of gels derived from an acid catalyzed system. At low water content, [$H_2O$]/TMOS]=2, or at high water content, [$H_2O$]/TMOS] = 25 or 50, low density gels are found due to (a) incomplete hydrolysis at low initial water content or (b) cyclization and particle formation for highly diluted solutions using high water contents. In case (a) the free volume is located around the chains whereas in case (b) larger interstices caused by packing of spheres would account for the free volume. The higher density gels occur at intermediate water content where complete hydrolysis is expected and gelation would occur by the entanglement of the linear species to give very small overlap clusters as suggested by Brinker et al. [40]. At the molecular level, water content largely determines the nature of the terminal bonds, and thus their activity with respect to condensation reactions and molecular size increase. A significant molecular size expansion occurs during the concentrating of solutions containing active polymers, e.g. having OH terminal bonds. No significant change occurs in the molecular make-up of polymers produced in alcohol with a limited amount of water [52].

#### *2.4.1.4. Effect of temperature*

Most chemical reactions, especially those occuring in liquid solutions, are dependent on temperature. Surprisingly, they are very few studies on the effect of temperature on the sol-gel process. In a sol-gel reaction carried out in a sealed container, the gelling time is given by:

$$1/t_{gel} = A \exp(-E^*/RT) \quad (23)$$

where $t_{gel}$ is the gelling time, A is the usual Arrhenius constant and E* is an "apparent" activation energy [57]. Limited studies on the effect of temperature on the gelation of silica have been reported [49, 58-63]. The general observation is that increasing temperature results in an increased reaction rate and shorter gelation times. For example, large differences in gelation rates were observed in a TEOS system as the temperature was increased from 25 to 50 and 70°C. The gelation times were: 9.2, 1.25 and 0.30 hrs for HF catalyzed systems and 380, 70, and 20 hrs for HCl [49]. Seven days of reaction at 20°C has approximatelly the same effect as 24 hrs at 60°C. Similarly, Bechtold et al. [58] have studied the formation of silica gels at 4, 24, and 60°C and found that the gelation times were highly dependent on temperature. This effect is more pronounced at higher solution concentrations and at higher $H_2O/Si(OC_2H_5)_4$ ratios. One of the reasons for these temperature effects is that the dehydration-polycondensation reaction between silanols on the surface of the sol particles is accelerated as the temperature is increased. Another reason is the increased rate of particle collision at higher temperatures. Higher particle collision rates imply higher rates of bond formation through dehydration-polycondensation [57].

In addition to the effect on the reaction rate, the temperature has a strong effect on the gel microstructure, ex. bulk densities. Yamane et al. [59] reported that the pore size distribution for silica gels is dependent on the gelation temperature, as summarized in ***Table 1.2*** for a TMOS based system.

#### *2.4.1.5. Effect of silicon alkoxide content*

In general, all other factors being equal, the concentration of the reaction mixture during the sol-gel process plays an important role. However, the effect of concentration of reacting species during the sol-gel process is interconnected with other variables in the system. For example,

***Table 1.2:*** Effect of gelling temperature on the bulk density of gels prepared by the hydrolysis-condensation of TMOS [59]

| Sample* | A | B | C | D |
|---|---|---|---|---|
| Gelling temp (°C) | 54 | 65 | 68 | 70 |
| Bulk Density g/cm3 | 1.46 | 1.13 | 1.02 | 0.98 |

* TMOS : MeOH : $H_2O$ = 1.0 : 4.6 : 4.0

under limited water hydrolysis, the increase in the solution concentration was observed to make very little difference in the molecular size distribution, as indicated by size exclusion chromatography (SEC) [52]. It is believed that under these conditions, the increase in the concentration can not lead to chemical reactions, due to the limited availability of reacting species (silanols). However, under the reaction conditions when reactive silanol groups are available, a ten-fold increase in the relative molecular weight was observed when a 1% eq. $SiO_2$ was concentrated to 5% eq. $SiO_2$ concentration.

Alcohols are most often used as solvents for both metal alkoxide and water in the sol-gel method. When the sol-gel reactions are carried out in alcohol, the effect of concentration of the solution is a complex one. Increasing the alcohol content can affect both hydrolysis and condensation.

(1) Since alcohols are hydrolysis products from silicon alkoxides, an increase in the alcohol content may promote esterification, the reverse of hydrolysis, resulting in a decrease in the hydrolysis rate [44]. This effect would be in addition to the general diluting of the reacting species as more alcohol is utilized as the reaction media.

(2) An increase in alcohol content is believed to reduce the probability of mutual collisions of hydrolyzed alkoxide molecules [52] resulting in a decrease in polymerization rate. To explain this behavior, Yoldas proposed, based on $^{29}Si$ NMR and SEC data, that molecular size expansion occurs initially by a smooth "growth" process, and in later stage by a "recombination" process. The recombination process takes place between high molecular weight species and generates a bimodal size distribution.

### *2.4.1.6. Effect of solvents and additives*

A systematic study of the effect of solvent on the formation of $SiO_2$ gel was carried out by Mackenzie [52], and Artaki et al. [64]. As discussed in previous sections (Section 2.3), the sol-gel reactions proceed, in general, through nucleophilic mechanisms. It is well known that hydrogen bonding as well as electrostatic interactions between the solvent and the nucleophile are of fundamental importance in bimolecular nucleophilic substitutions. To understand the effect of reaction media on the reaction rates, each of these interactions must be examined separately. The solvents and additives usually employed for sol-gel processes can be broadly grouped into three categories [64]: (i) polar protic (water, methanol, formamide); (ii) dipolar aprotic (dimethyl formamide, acetonitrile); (iii) non-polar, aprotic (dioxane). *Highly polar protic solvents* can decrease the condensation rate by deactivating the nucleophile through hydrogen bonding interactions [65]. Moreover, due to their strong dipole moments, they can stabilize the negative charge localized on the reactants resulting in an increase in the activation energy, further decreasing the condensation rate [65]. *Dipolar aprotic solvents* can not deactivate the nucleophile (no hydrogen bonds), but they can stabilize the reactants with respect to the activated complex, slowing down the reaction to some extent [65]. *Non-polar aprotic solvents* lack the ability to interact both electrostatically and through hydrogen bonding to either the reactants or the activated complex. The condensation reactions are most efficient under these conditions [65].

Considerable research efforts have recently focused on the use of Drying Control Chemical Additives (DCCA) to control pore size distribution and drying stress during the formation of homogeneous gel monoliths. Formamide has been considered the organic additive of choice. The addition of formamide to silicon alkoxides resulted in a drastic reduction in the rate of hydrolysis and led to the formation of extensively branched gel networks of increased porosity

and reduced density [64]. Artaki et al. [66] attempted to explain these macroscopic differences by the modifications taking place at the molecular level.

Lower hydrolysis rates were observed in the reactions containing formamide ($k_H = 1.0 \times 10^{-6}$ and $1.6 \times 10^{-6}$ $s^{-1}$ for solutions with formamide and without formamide respectively). The 25% increase in the solution viscosity as a result of formamide addition, believed to play a major role in slowing the hydrolysis rates [66], can not be solely responsible for the rate decrease, even though the nucleophilic reactions are known to be sensitive to the mobility of the reacting species. Instead, these differences can be more easily accounted for if one considers the hydrogen-bonding abilities of formamide and methanol. Formamide is known to form stronger hydrogen bonds with (Si-OH) and (Si-OR) groups than methanol. This will decrease the availability of such centers for nucleophilic attack at silicon and, therefore, slow the hydrolysis rate [66]. Mechanistic investigations did indeed suggest that the formamide plays an active role in the hydrolysis and does not behave as an inert solvent. It is capable of hydrogen bonding through both nitrogen and oxygen atoms, acting as either a donor or an acceptor of hydrogen bond. The possibility that formamide chemically bonds to the silicon network [67] was also considered. However, no resonance signals were detected in $^{29}Si$ NMR to support this mechanism [66].

In spite of the reduction in hydrolysis rate, the gelation time was observed to decrease with formamide addition. This is the result of a slight increase of condensation rate and it is expected if one assumes a nucleophilic condensation reaction mechanism. The species which are most likely to deprotonate a silanol bond is the formamide, thus the nucleophilic attack by deprotonated silanols is enhanced and shorter gelation times are observed when formamide is added.

Avnir et al. [68] showed that the solvent may be an unnecessary ingredient and that the biphasic starting mixture can lead to similar transparent, homogeneous, monolithic porous gels. This is possible since the alcohol reaction by-product is usually the reaction solvent. For example, a ratio of TMOS:$H_2O$ of 1.0:4.0 was observed to become homogeneous after aprox. 15 min of stirring. At that point, sufficient $CH_3OH$ was generated through hydrolysis reactions to form a homogeneous solution. Preliminary evaluations seem to indicate that the pore structure of the resulting gel is not different from the sample in which solvent has been used [68].

#### *2.4.1.7. Effect of pressure*

The hydrolysis and condensation reactions during the sol-gel processes take place through bimolecular nucleophilic mechanisms. Such reactions are known to be dependent on the viscosity of the reaction media. To change viscosity, one can add chemical additives to the system [66] or vary temperature and/or pressure. When additives are introduced into the system they affect not only the viscosity but also several other factors, such as dielectric susceptibility, hydrogen bonding, and steric hindrance effects. These factors can not be separated and the analysis of the results is very difficult. The role of pressure on the polymerization kinetics of sol-gel process was investigated by Artaki et al. [69]. A range of pressures from 1 bar to 5 kbar was investigated. It was concluded that high pressures have a dramatic accelerating effect on the condensation rate, but do not alter the mechanism via which the polycondensation proceeds. The enhancement of the condensation rate is most pronounced above 3 kbar. For instance, it requires the monomer 110 hrs to be depleted to 20% of its original concentration at 1 bar and less than 10 hrs at 5 kbar. Qualitatively it was found that the polycondensation rate from monomer to dimer is enhanced by approximately 18% at 2 kbar, 100% at 3 kbar, 200% at 4 kbar, 350% at 4.5 kbar and 900% at 5 kbar.

Although other parameters produce similar accelerating effects, they generally inflict structural modifications in the polymer gel networks. For instance, the fast polymerization of the base-catalyzed reactions produces easily sintered gels of high porosity but low purity with respect to unreacted organic groups, while the slow acid-catalized process forms gels of relatively high purity but poor sintering properties [69]. The preliminary studies indicate that by using pressure as an additional experimental variable it might be feasible to accelerate the polymerization process without altering the structural properties of the resulting glass-precursor gels. Similar results were obtained by Zerda [70] who investigated a TMOS system at pressures from 1 to 2000 bar . He found that the hydrolysis rate increases with increasing pressure and rationalized that the pressure-induced increased mobilities of ions accelerate the hydrolysis reactions.

### *2.5. SOL TO GEL TRANSITIONS*

It is sometimes not recognized that there is a basic difference between gelation and coagulation or flocculation. Both involve colloidal particles linking together and forming three-dimensional networks. When a sol is gelled, it first becomes viscous and then develops rigidity. On the other hand, when a sol is coagulated a precipitate is formed. In a concentrated sol the precipitate may be too voluminous to separate and will remain as a thixotropic mass, but in a dilute sol the precipitate will settle out. The difference is shown in ***Figure 1.3*** [27]. The word "aggregation" is used for all the ways in which colloidal particles are linked together: gelling, coagulation or flocculation. *Gelling* describes the particle growth during which the particles are linked together in branched chains that fill the whole volume of sol, so that there is no increase in the concentration of silica in any macroscopic region in the medium. Instead, the overall medium becomes viscous and then is solidified by a coherent network of particles which, by capillary action retain the liquid [27]. The formation of the gel has usually been ascribed to the condensation of $Si(OH)_4$ into siloxane chains, then branching and crosslinking to form a three-dimensional

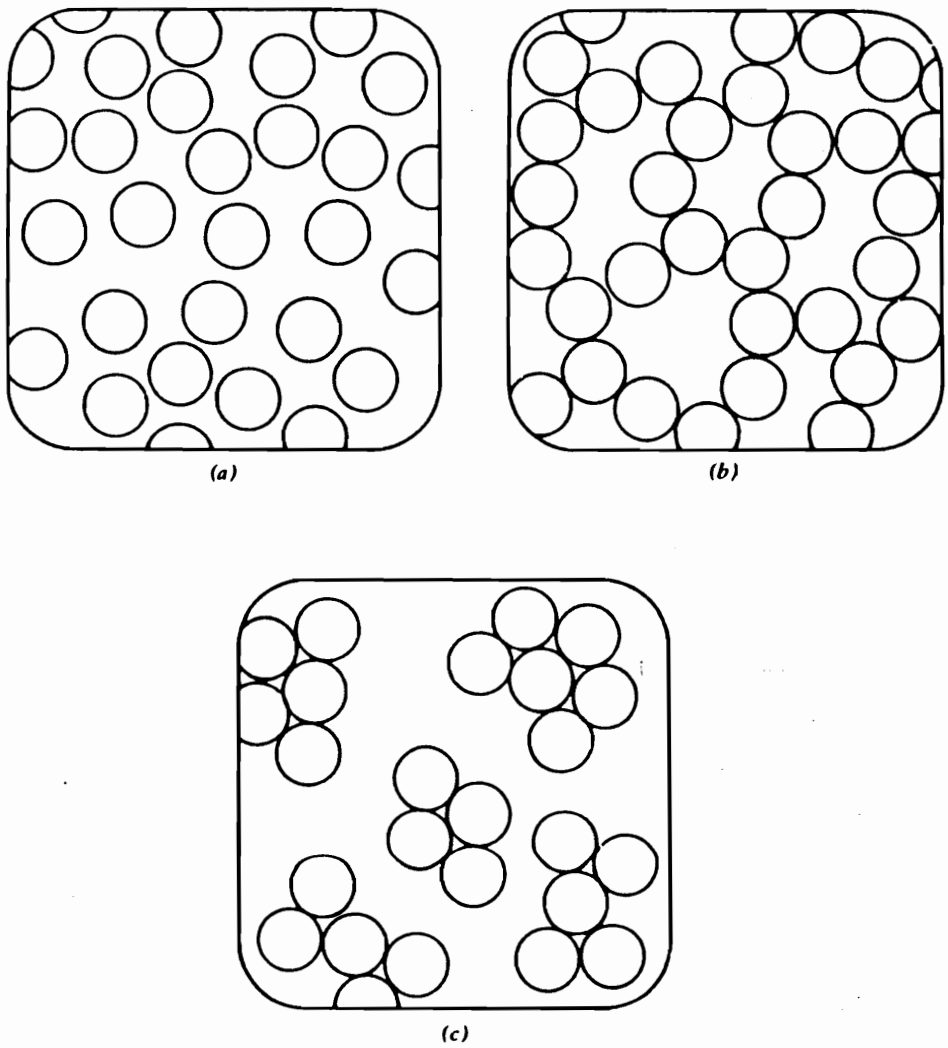


***Figure 1.3.*** Schematic representation of silica gel versus precipitate [27]; (a) sol; (b) gel, (c) flocculation and precipitation.

molecular network. Such a siloxane gel network might be obtained under conditions where depolymerization is least likely to occur so that the condensation is irreversible and siloxane bonds can not be hydrolyzed once they are formed. Owing to the insolubility of silica in the system (which is another way of saying that siloxane bonds are not readily broken) the condensation polymer of siloxane chains cannot undergo rearrangement into particles. ***Under these special conditions, perhaps, the polymerization of $Si(OH)_4$ might closely resemble the polymerization of a polyfunctional organic monomer and may follow the corresponding theories which have been developed in organic polymer chemistry [71].***

The solubility of silica in water is very dependent on the pH of the solution. This was found to be constant from pH 2 to 8, then increased rapidly at higher pH [27]. The pH range usually employed for sol-gel reactions is not considered to promote reversibility of bond formation to any considerable extent. The transformation of silica sols of relatively large discrete spherical particles of known uniform size into homogeneous gels suggest that most, if not all, silica gel networks may be made up of discrete particles rather than chains of individual $SiO_4$ tetrahedra. This building of the supramolecular structure will be discussed in the present and the following section.

As previously discussed, the chemistry of the sol-gel process is relatively simple and consists of hydrolysis and condensation of silicon tetraalkoxides. Still, there are many ways in which tetraalkoxysilane monomers can be polymerized. Branched siloxane polymers are obtained, followed by further growth and resulting in a microporous network that entraps the solvent and the reaction byproducts. The structure of the sol-gel materials is very much dependent on the chemistry at the early stages which is, in turn, dependent on the reaction conditions. In order to develop a reasonable model relating chemistry with microstructure, thus physical properties, the

structure of the sol-gel materials must be studied at several levels. ***At the molecular level*** it is important to know the development of the local chemistry around the silicon atom. Specifically, the kinetics of hydrolysis and condensation and the degree of branching are of central importance. This aspects associated with the sol-gel reactions in the initial solution stages have been discussed in the previous sections of this review. ***At the macromolecular level*** it is important to determine the structure of silica condensation polymers as a function of chemical reaction conditions. SAXS is the technique of choice for structure determination at the macromolecular level. At this level one is concerned with the structure of a single macromolecule and the concept of fractal geometry is very useful to describe the structure of silicates. These aspects will be discussed in the present section. ***A further level of structure*** relates to collective phenomena and the morphology of the bulk gel and dried solid. These aspects will be discussed in Section 2.6.

### *2.5.1. Analysis of sol-gel structures by x-ray scattering*

#### *2.5.1.1. Brief review of SAXS technique*

Small angle x-ray scattering (SAXS) from macromolecular solutions is of particular importance for developing models for the growth mechanisms during sol-gel reactions. This is the technique of choice for the determination of structure on the 10-1000Å scale. The present section will briefly review this technique and the type of information on the development of macromolecular chains during sol-gel reactions, provided by SAXS analysis. The principle of SAXS technique is based on Bragg's law which relates the peaks in the angle ($\theta$) dependence of the scattered x-ray intensity, I, to corresponding planes of spacing d in a crystal, equation (24), [72]:

$$1/d = 2/\lambda \sin(\theta/2) \qquad (24)$$

where $\lambda$ is the wavelength of the incident radiation. In amorphous systems, where distinct planes are not present, scattering may occur from correlated fluctuations of concentration or density. Scattering at an angle $\theta$ arises from fluctuations with the appropriate Fourier spatial frequency, K:

$$K = 4\pi/\lambda \sin(\theta/2) \qquad (25)$$

Comparing (24) and (25), scattering at angle $\theta$ is due to fluctuations whose characteristic length is $2\pi/K$. ***Figure 1.4*** shows a schematic small angle x-ray scattering curve from a dilute macromolecular solution [72]. Two lengths appear in this figure: R, the average radius of gyration of the macromolecule and **a**, the chemical length of the monomeric units. Typically R = 100Å and **a** = 1-2Å. Given the set of lengths ($K^{-1}$, R, **a**) it is convenient to divide the scattering curve in Figure 1.4 into several regions:

(I) At large scattering angles (K**a** =1) one probes distances comparable to chemical bonds. This region is called *Bragg scattering regime* and it is schematically represented in ***Figure 1.5a***. In this scheme the lines represent the spatial Fourier component of spacing $K^{-1}$ and **a** corresponds to the bond length. (II) *The Guinier regime* occurs when KR<1. ***Figure 1.5b*** shows a schematic picture of Guinier scattering for a polymer solution, the lines representing the spatial Fourier component of spacing $K^{-1}$ and R corresponding to the average radius of gyration. From the initial decay of I(K) one measures the Guinier radius, $R_g$, which in dilute solutions reduces to Z-average radius of gyration of the scatterers. In interacting or overlapped systems $R_g$ is a correlation length. For the sol-gel systems, the measurement of $R_g$ provides qualitative information on the degree of branching. (III) Finally, the regime in which $R >> K^{-1} >>$ **a** is called *Porod regime.* The Porod regime is shown schematically in ***Figure 1.6*** [72].

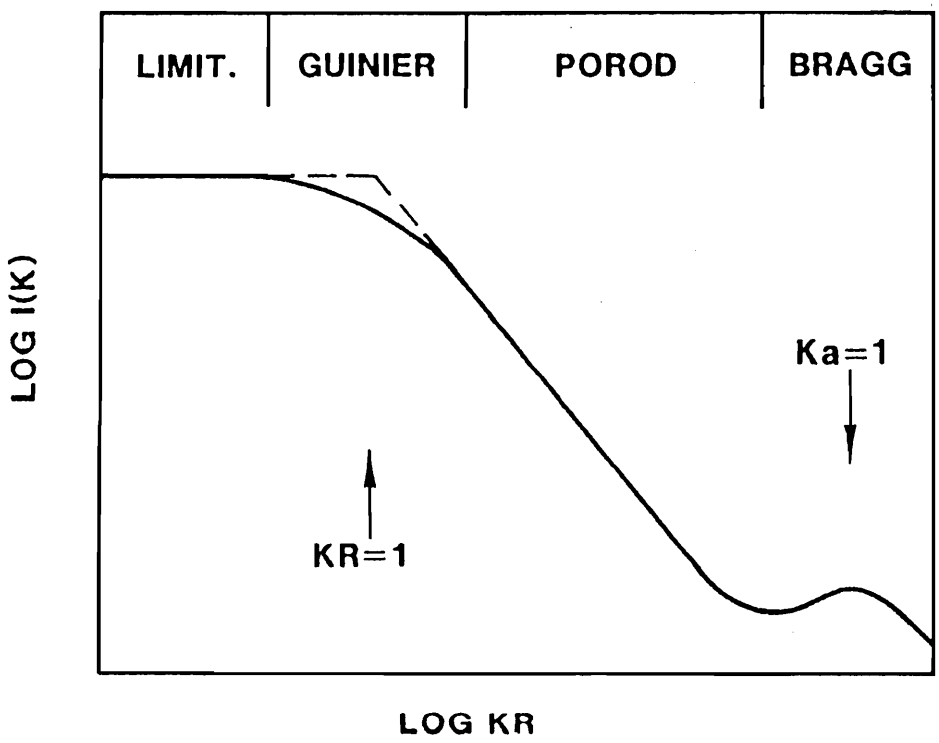


***Figure 1.4.*** Schematic small angle scattering curve from a dilute macromolecular solution [72].

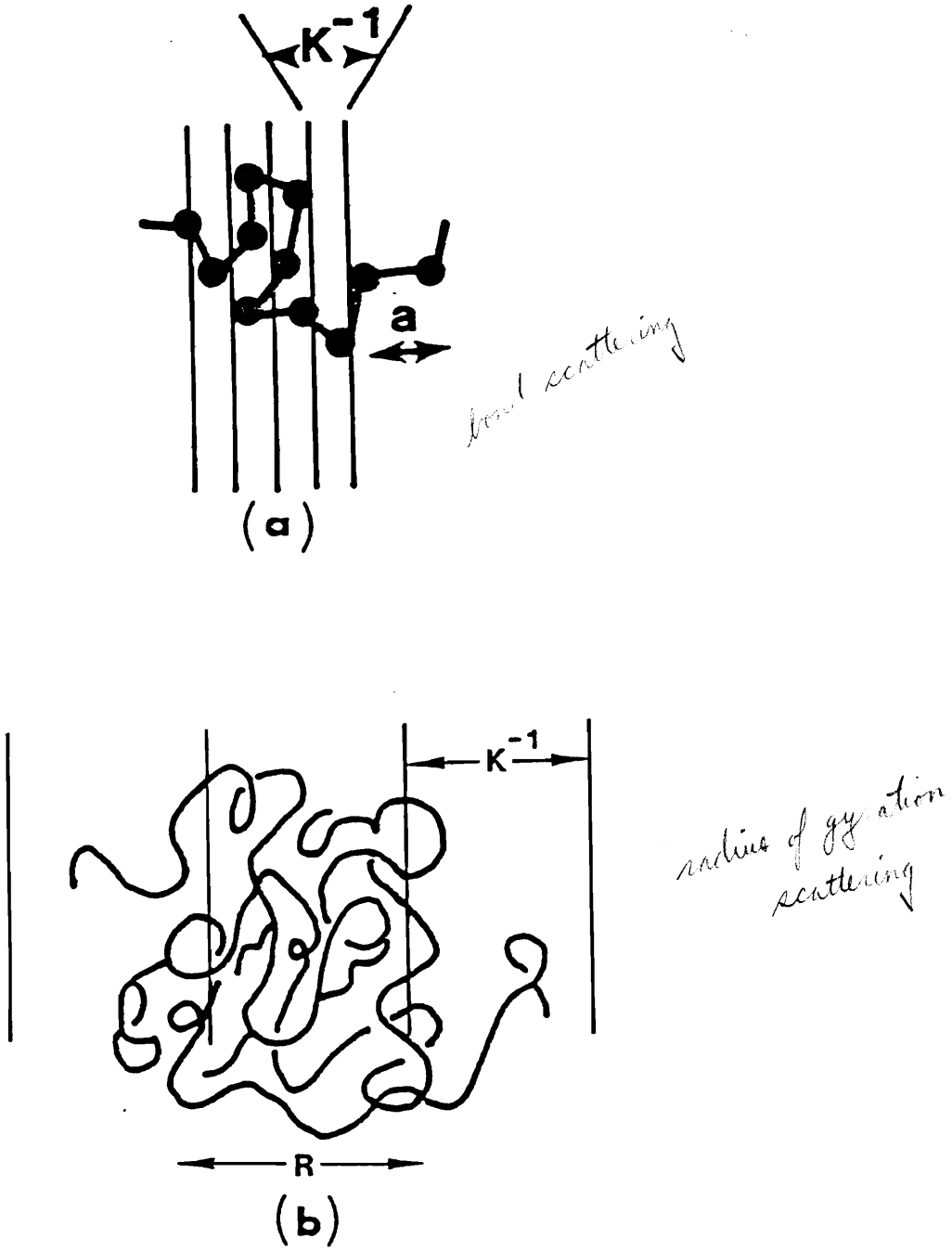


***Figure 1.5.*** Schematic representation of scattering in the Bragg (a) and Guinier (b) regimes [72]. **a** is the bond length and R is the radius of gyration.

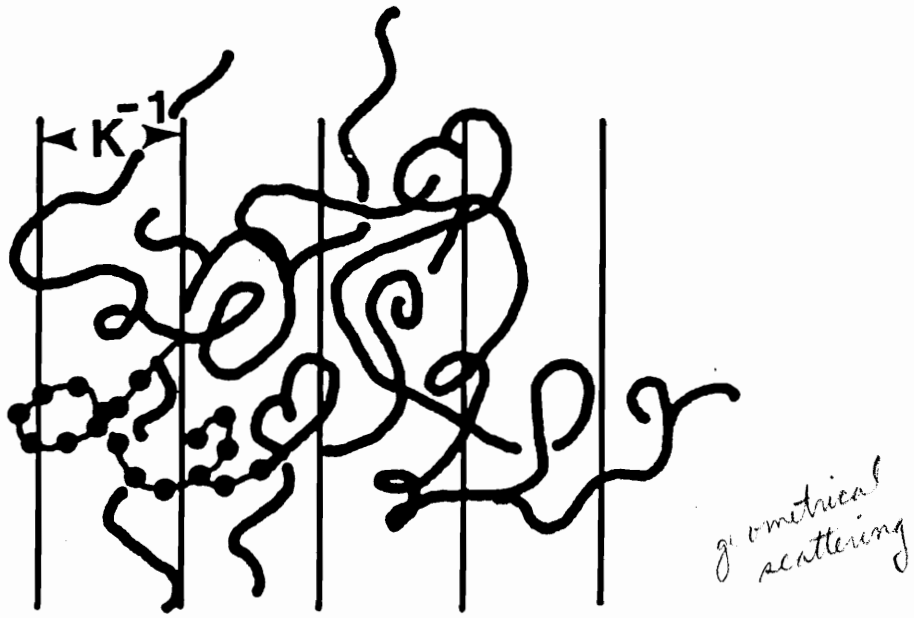


***Figure 1.6.*** Porod regime scattering. In this regime power-law decay is expected for I(K) [72].

Porod [73] showed that in this region the scattered intensity for systems with sharp boundaries decays as a power law. It turns out that power law decay is common for a wide variety of macromolecules and the exponent is sensitive to the geometry of the scatterers [74]. In the Porod regime the scattering curve contains no information which depends on **a**, Rg, or N (number average degree of polymerization). Only geometrical information remains so the power-law exponent must contain such information. Such systems obey the relationship: $N \sim R^D$, in which the power law exponent, D, is called the fractal dimension [75].

### *2.5.1.2. Analysis of sol-to-gel transitions by SAXS techniques*

SAXS can provide information on the size of the agglomerates and on the fractal dimensions of developing species in the sol-gel process, during the sol-to-gel transition [72, 76-78]. The slope in the Porod regime corresponds to the fractal dimension, D. The fractal dimension of the agglomerates can give some indication on the mechanism of gel formation. For a smooth particle with a smooth surface, D equals to 4. As D decreases towards unity, the structure changes from a compact smooth particle with rough surface to open ramified polymer-like character and finally to rod-like particles. Schematic models and their corresponding fractal dimensions are shown in ***Figure 1.7*** along with typical results from SAXS experiments [43]. If silica polymerization produces colloidal particles, a $K^{-4}$ power law is predicted [73]. The lower curves in Figure 1.7 show a $K^{-4}$ power dependence for two known colloidal systems: LUDOX HS40, a colloidal silica, and ferrofluid, a dispersion of colloidal magnetite. The scattering curves obtained for acid and base catalyzed silica solutions are shown in the upper part of this figure. During polymerization both systems show a Porod slope near -2, [43]. In the acid-catalyzed case, Porod slopes are consistently more positive than -2, while for the base-catalyzed system Porod slopes are consistently more negative than -2. Although deviations from -2 are not great in either case, deviations towards slopes more positive than -2 indicate a cross over between branched and

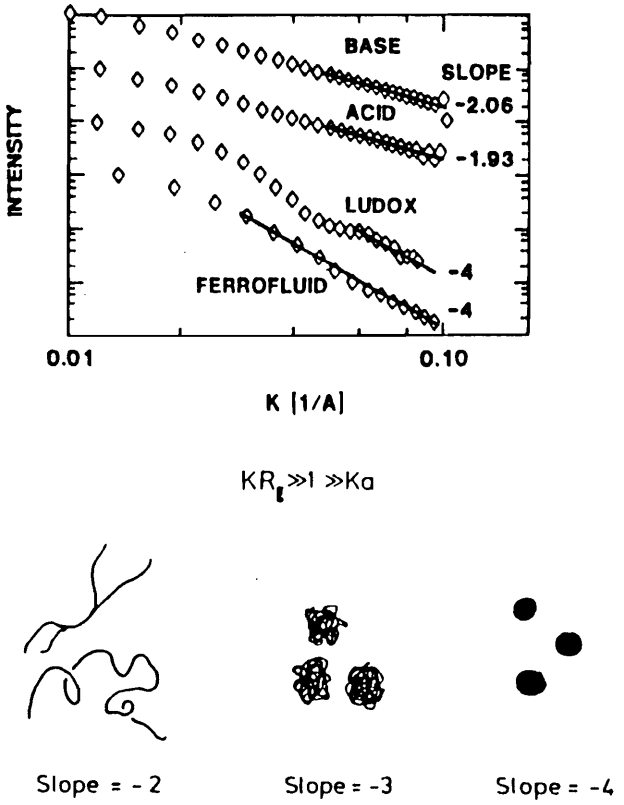


***Figure 1.7.*** SAXS profiles of base and acid-catalyzed sol-gel reactions, near their respective gel points, compared to colloidal sols. In the Porod regime the scattered intensity is proportional to $K^{-D}$. Slope analyses differentiate between linear or randomly branched chains, D=2, and colloidal particles, D=4 [43].

swollen linear chains. This suggests that the acid-catalyzed molecules are so slightly branched that the distance between branches is comparable to $K^{-1}$ (20Å). Deviations towards more negative slopes suggest that either the base-catalyzed molecules are more highly branched so that crossover toward dense structures (slope - 4) is observed or that base-catalyzed molecules are collapsed relative to ideal random linear polymers. SAXS results can be widely interpreted and can agree with more than one model of gelation. For example the observed slopes of -2 have been interpreted as self-avoiding branched polymers by Schaefer and Keefer [72], as loosely packed multiple clusters by Zarzycki [79] and Yoldas [80], and as possibly percolation clusters by Martin [81]. The evidence to date generally indicates that the acid-catalyzed polymerization occurs through growth of loosely crosslinked polymers, where-as the base-catalyzed gels behave similar to colloids, except that the particles are not dense like colloids, but are porous, highly ramified but not interpenetrating. This description of gelation for the various cases was put forward by Brinker and Scherer [82].

Although the Porod law analysis clearly demonstrate the existence of polymer molecules, the method is rather insensitive to the degree of branching. To gain further insight into branching, Guinier radius can be measured at different dilutions. If the macromolecules are compact, highly branched clusters, the Guinier radius will then be independent of the degree of dilution [72]. If the chains are nearly linear, however, they should become strongly overlapped soon after condensation begins. In this case, the measured Guinier radius is substantially less than the radius of gyration of the chains, i.e., the polymer solution is semidilute [72]. Upon dilution the chain disentangle and the Guinier radius approaches the radius of gyration. ***Figure 1.8*** and ***Figure 1.9*** show the effect of dilution on the Guinier radius as a function of time to gelation ($T_{gel}$-t) for an acid and base-catalyzed sol-gel reaction respectively [43]. The radius of gyration, $R_g$, is measured on diluted samples while the correlation range, $\zeta$, is measured on concentrated

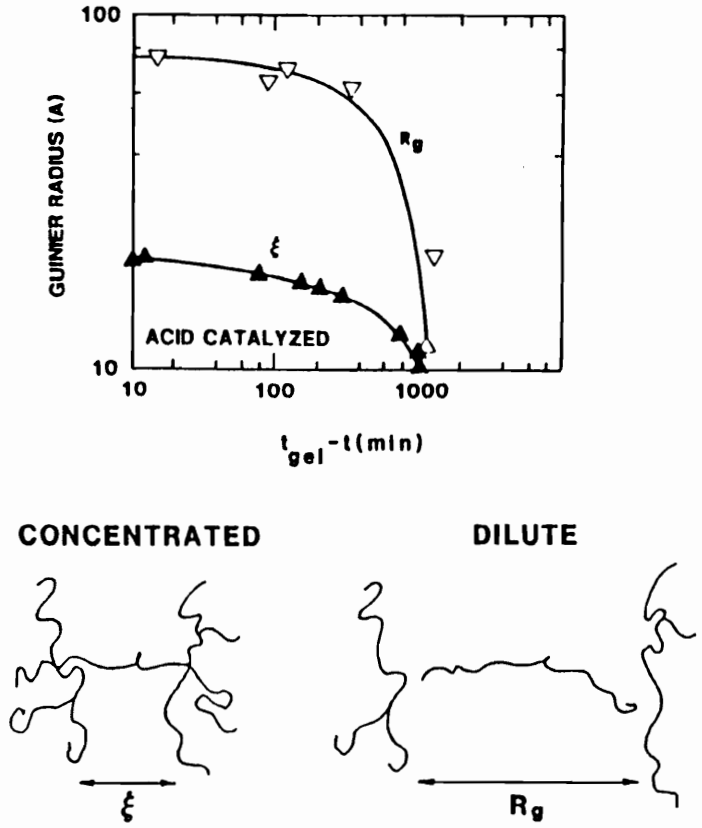


***Figure 1.8.*** Guinier radius as a function of time-to-gelation for an acid-catalyzed sol-gel reaction based on tetraethylorthosilicate (TEOS) [43].

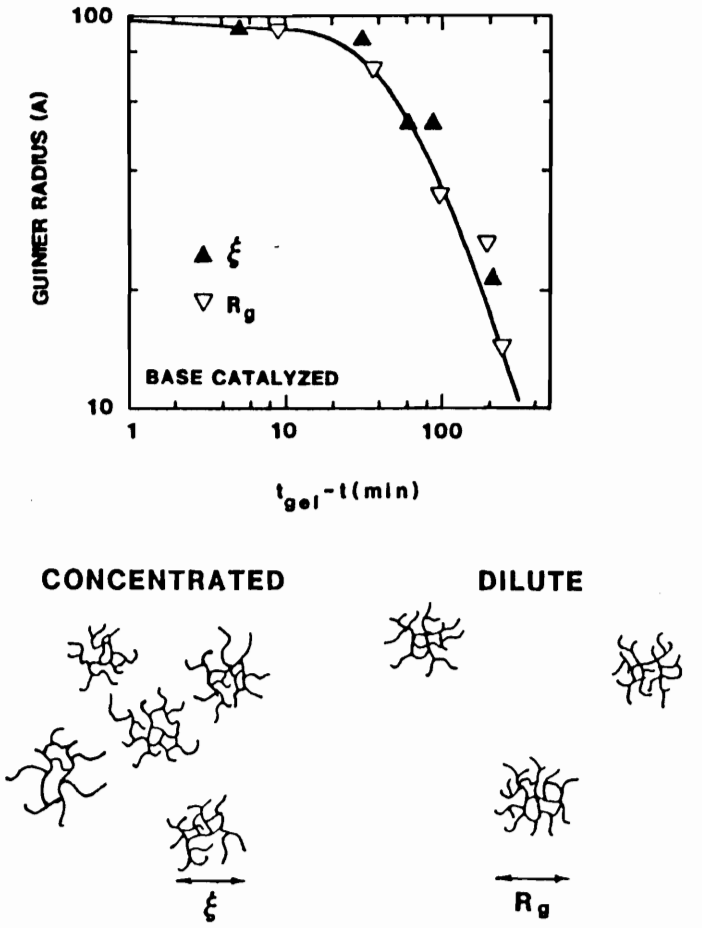


***Figure 1.9.*** Guinier radius as a function of time-to-gelation for a base-catalyzed sol-gel reaction based on tetraethylorthosilicate (TEOS) [43].

samples. For the acid catalyzed system in Figure 1.8, except near the start of the reaction, $R_g$ is considerably larger than the correlation range, $\zeta$. This discrepancy implies that for all later stages of reaction the silicate molecules are strongly overlapped in the undiluted solutions. Because for equivalent initial concentrations of monomer and equivalent amounts of polymerization chains are more likely to overlap than highly branched entities, these results suggest that the polymers formed in the acid-catalyzed solutions are extended, weakly branched chains. On the other hand, in the base-catalyzed system the Guinier radius of gyration, Rg, is concentration-independent, as shown in Figure 1.9. This implies that these molecules must be sufficiently dilute so that little overlap occurs prior to gelation. These results suggest that polymers formed in base-catalyzed solutions are discrete, more highly branched clusters.

The combined results of SAXS, GC, and NMR data [43] suggested a difference in the polymer growth prior to gelation for acid and base-catalyzed reactions. Consideration of both Porod and Guinier regimes by different authors [43,72,83,84] led to the conclusion that the degree of branching is controlled by the reaction conditions, most strongly by the catalytic conditions and the $H_2O$/alkoxide ratio. Linear chains are favored in acid catalyzed conditions and at low water content. Branching is favored in the opposite conditions. These conclusions are also supported by other lines of evidence. There is qualitative evidence for colloid formation in the base catalyzed hydrolysis of TEOS [85]. Colloidal particles represent the highly branched limit. By contrast, Sakka [86] found that fibers can be spun from silicates formed in acidic alcoholic solutions. Spinability is a characteristic of linear chains. The properties of the gels derived under different conditions are also consistent with the above conclusions [72]. The acid-catalyzed gels with low water addition are clear and rubbery as expected for a weakly crosslinked system. The base-catalyzed gels, on the other hand, are often brittle and cloudy, characteristic of highly crosslinked systems.

These observed differences in the growth mechanisms under different reaction conditions can be explained by the behavior at the molecular level during the hydrolysis and condensation reactions. For example, the tendency of silicon to form dense, colloidal particles may be explained by the nucleophilic mechanism during the base-catalyzed condensation reactions as discussed in previous sections. According to this mechanism, a deprotonated silanol reacts with a protonated silanol, displacing an $OH^-$ (Scheme 1.5). The favored condensation, therefore, is between the most acidic and most basic silanols in the system. The acidity of a silanol proton depends on the other substituents on the silicon atom. When very basic substituents $OH^-$ are replaced by less basic $SiO^-$, the reduced electron density on silicon increases the acidity of the protons on the remaining silanols. The most acidic silanols are, therefore, on the most highly condensed silicate units and the least acidic on orthosilicic acid. As a result, the condensation reactions preferentially remove the least polymerized species from solution and form very highly condensed species [27].

On the contrary, in the acid-catalyzed solutions, the first hydrolysis is easier than the second, so a growing polymer will have an even distribution of hydroxyls. It is generally accepted that if the charge on the attacking species is positive, the reactivity of a tetrahedron should increase as the electron density around the silicon increases. The more highly esterified silicate species should be the most prone to attack, rather than the least as in alkaline solutions. The forgoing arguments imply that tetraalkoxide monomers should be more rapidly hydrolyzed than the end groups on the chains, which in turn will be more rapidly hydrolyzed than the middle groups on the chains, etc. As a result, acid-catalyzed hydrolysis tend not to produce orthosilicic acid monomers and condensation could start between incompletely hydrolyzed species. The pattern of hydrolysis rates would therefore lead to less highly crosslinked polymers than those resulting in alkaline solutions [43].

### *2.5.2. Analysis of sol-to-gel transitions by TEM techniques*

A direct and independent method to study the growth mechanism during sol-gel reactions is transmition electron microscopy (TEM). The direct imaging of microstructure in fluid materials is made possible by cryogenic TEM of vitrified samples. In cryo-TEM , a thin liquid sample is rapidly frozen to prevent crystallization of the solvent and to freeze any structure which has developed in the liquid state. The vitrified solvent is transparent to the electron beam, so this technique allows for direct observation of liquid microstructures. TEM results can be further correlated with macroscopic flow behavior of the sol-gel reaction to better understand the growth mechanism during these processes [87].

The TEM reveals that under base-catalyzed conditions, the alkoxide firstly polymerizes into small silica clusters which are approximately 40Å in diameter, ***Figure 1.10*** [87]. These clusters agglomerate to form large networks. The networks are not continuous, but can be seen to be built up of ~ 40 Å individual clusters. These results support the conclusions of Brinker and Scherer [82] that under base conditions the reaction proceeds by the formation of highly branched structures which then bond together in a non-interpenetrating manner. The above results also correlate with macroscopic viscosity measurements, ***Figure 1.11*** [87]. The initial slow increase in viscosity corresponds to the formation of small clusters of branched silica polymers. As the reaction proceeds, more of these clusters are formed and the viscosity rises as they begin to aggregate. As they continue to aggregate, the viscosity rises rapidly until they have formed a sample spanning network. For acid-catalyzed sol-gels, the micrographs indicate that if particles are formed similar to base- catalyzed system, the particles would have to be on the order of 15 Å or less. If the structures that formed were nearly linear polymers which were of monomer thickness and uniformly distributed and entangled, the features would also be too small to observe. This is consistent to either the linear polymerization-gelation model of Brinker and

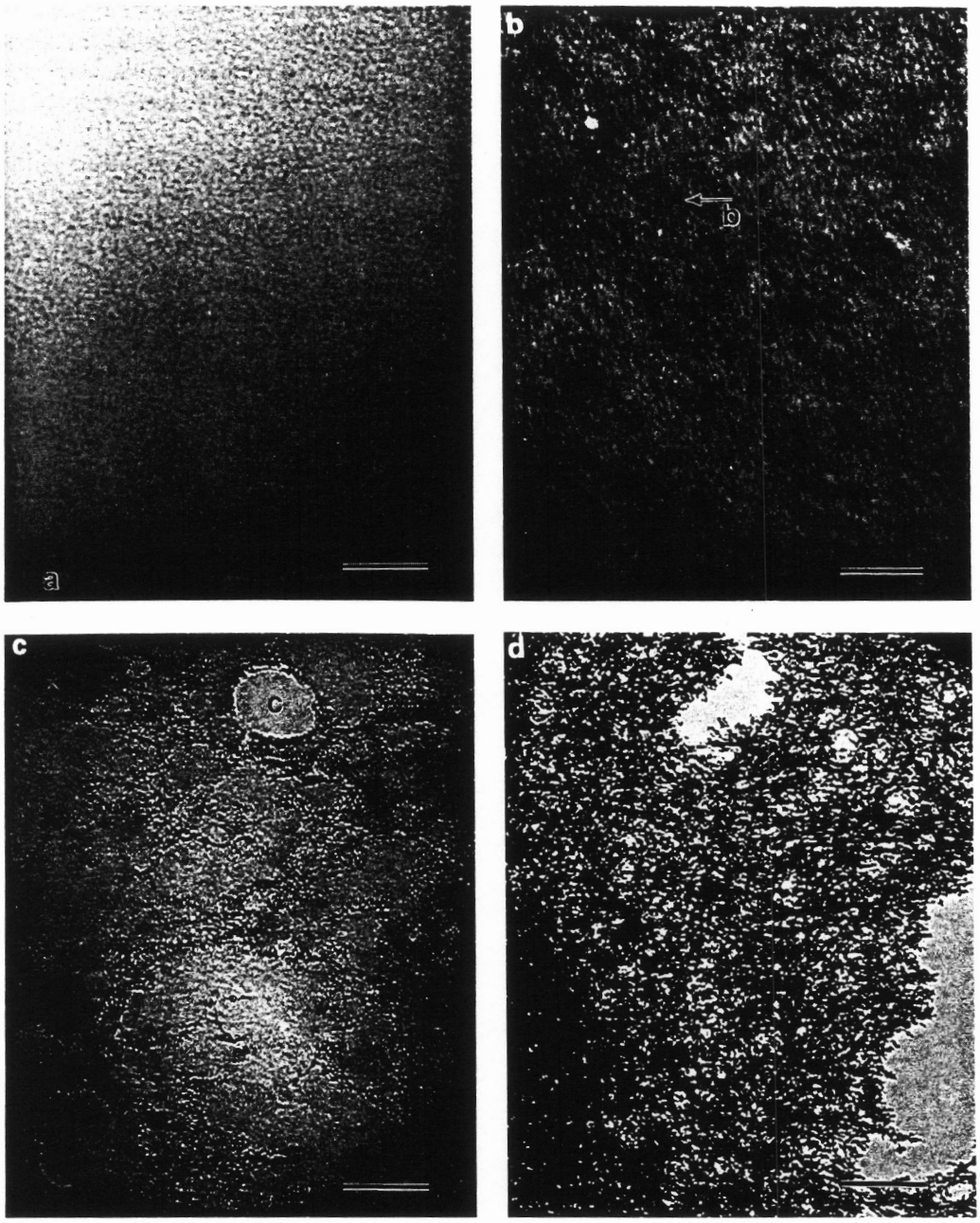


***Figure 1.10.*** Cryogenic TEM as a function of $t/t_{gel}$ in a base-catalyzed TEOS system [87]. ***(a)*** $t/t_{gel}$ =0.3; Corresponds to point A in Fig. 1.11; ***(b)*** $t/t_{gel}$ =0.48; Corresponds to point B in Fig. 1.11; ***(c)*** $t/t_{gel}$ =0.91; Corresponds to point C in Fig. 1.11; ***(d)*** $t/t_{gel}$ =1. 0 Corresponds to point D in Fig. 1.11; Bar = 100nm.

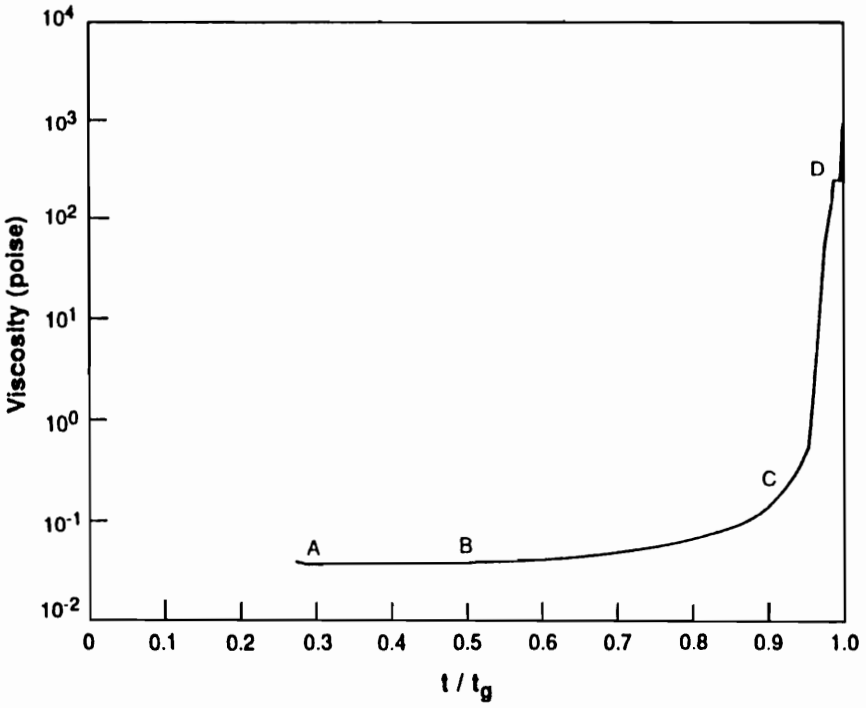


***Figure 1.11.*** Viscosity versus reduced time for a base-catalyzed TEOS sol-gel reaction [87].

Scherer [82] or Sakka and Kazuka [81]. The results could also be consistent with the evidence of small condensed silica clusters of about 10Å reported by Himmel et al. [88], provided that these particles agglomerated homogeneously. Although the exact fine structure of the acid-catalyzed gel is still somewhat ambiguous, one can clearly see by cryo-TEM a significant difference in the development of structure in the acid- and base-catalyzed gels. For the acid catalyzed sol-gel system, the viscosity curve-***Figure 1.12*** shows the same general trend as the base catalyzed system except that the viscosity increased more uniformly and the rapid rise in viscosity was less sharp [87]. The structures observed by cryo-TEM do not show the dramatic change in structure that the base catalyzed sols do, as shown in ***Figure 1.13*** [87].

### *2.6. GEL TO GLASS TRANSITIONS*

Among the questions still open in the sol-gel process is that of the mechanism of transformation of gel into glass. In particular, it is highly desirable to understand the transformations at the molecular level and the continuous or discontinuous character of the phenomenon. Most researchers who have attempted to describe the gel-to-glass transition for alkoxide derived gels [89] have utilized structural models based on Iler's representations of colloidal silica gels formed in aqueous solutions [27]. These gels are considered to be composed of fully polymerized (anhydrous) particles of 10-100Å in diameter which may be single or clustered. Based on these models, gel densification has been considered to be essentially a sintering process [89], and differences in densification behavior have been attributed to differences in texture, e.g. the characteristic particle size and/or differences in oxide composition. Investigations by different workers [40,90-92] revealed that it is seldom appropriate to strictly employ Iler's model of aqueous silicate gels to describe the structure of alkoxide-derived gels from alcoholic solutions. Bertoluzza [90] et al. have studied the chemical transformations taking place at the molecular level during heating from 40 to 800°C, using IR and Raman spectroscopy. The study revealed that the

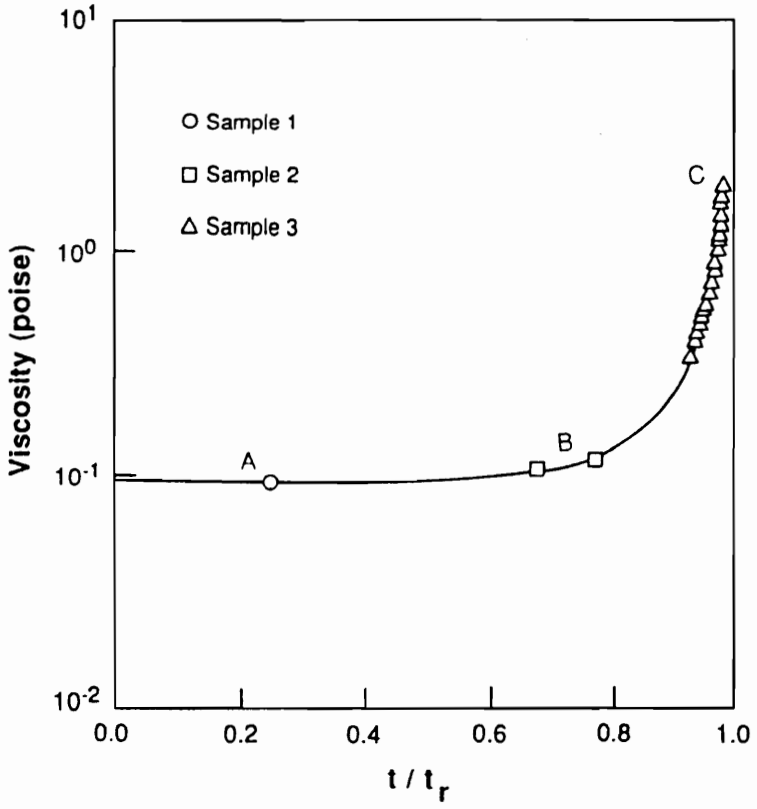


***Figure 1.12.*** Viscosity versus reduced time for an acid-catalyzed TEOS sol-gel reaction [87].

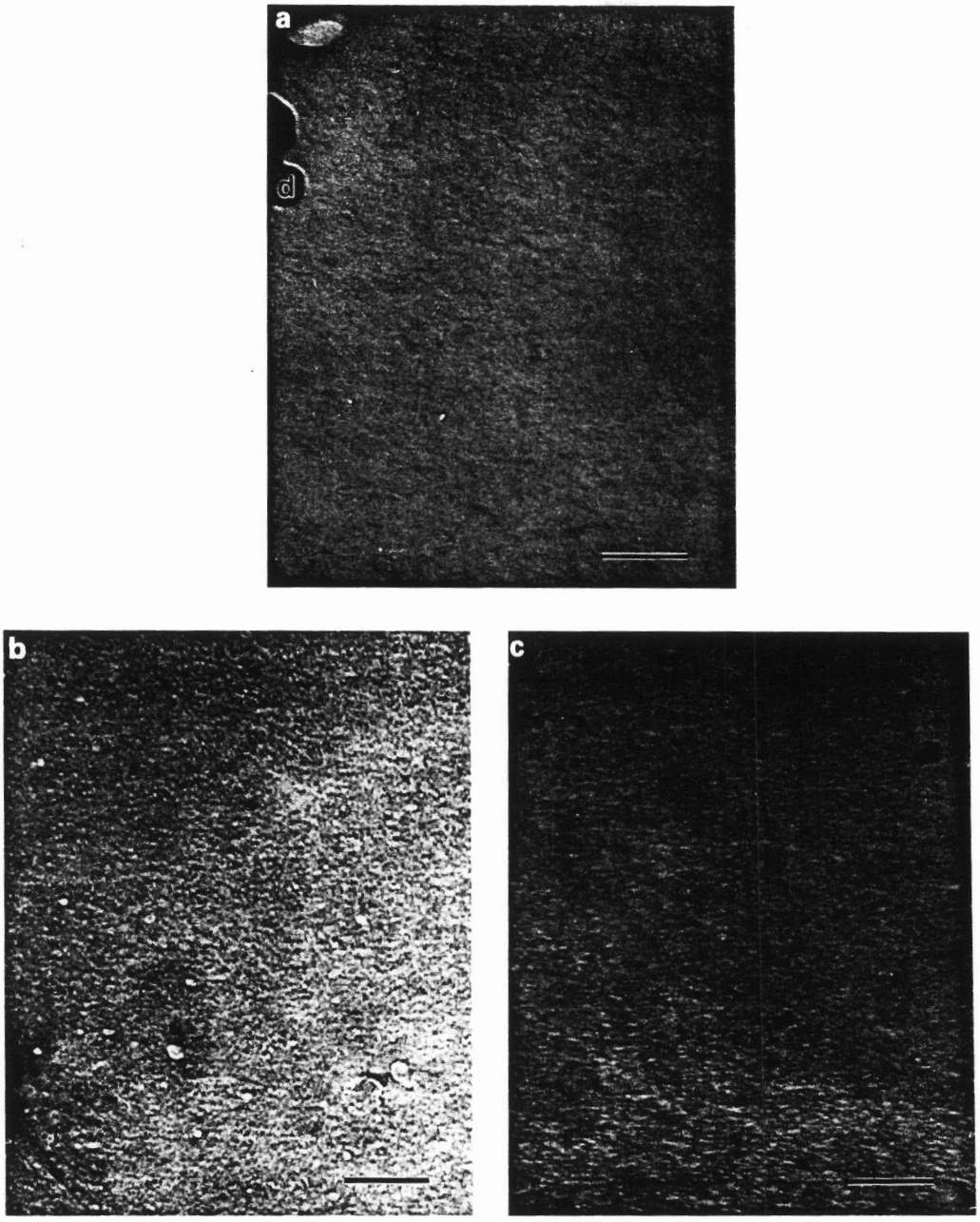


***Figure 1.13.*** Cryogenic TEM as a function of $t/t_{gel}$ in an acid-catalyzed TEOS system [87]. ***(a)*** $t/t_{gel}$ = 0 (immediately after mixing); Corresponds to point A in Fig. 1.12; ***(b)*** $t/t_{gel}$ = 0.78; Corresponds to point B in Fig.1.12; ***(c)*** $t/t_{gel}$ = 0.91; Corresponds to point C in Fig.12; Bar = 100nm

transformation of gel into glass, which is a hydrolytic polycondensation process, occurs progressively and continuously and becomes practically complete at 800°C [90].

Brinker et al. [40] summarized the chemical and physical transformations taking place during the gel-to-glass transition as follows [40]: (1) Physical desorption of water and solvents from the micropore walls,100-150°C; (2) Carbonization and combustion of residual organic groups (alkoxy), 200-300°C; (3) Exothermic combustion of carbon, 275-400°C; (4) Condensation polymerization (5) Volume relaxation, and (6) Viscous sintering. Of these transformations, 4,5, and 6 result in densification; therefore, it is expected that gels of different chemical compositions and morphologies should show markedly different densification behavior. Kawaguchi et al. [91] divided the bulk, macroscopic changes accompanying the drying into three stages corresponding approximately to the following trends: (I) weight loss without shrinkage (25-150°C), (II) shrinkage proportional to the weight loss (150-525°C), and (III) shrinkage without weight loss (>525°C). These macroscopic changes can be correlated with transformations at the molecular level.

***Figure 1.14*** shows the linear shrinkage and weight loss during the drying of the gel up to 700°C [92]. According to DTA analysis the weight loss measured in *Region I* is attributed to desorption of physically adsorbed water and alcohol. The small amount of shrinkage observed in this region results from the increase in surface energy due to desorption. Heat treatments above 150°C will result in dehydration according to equation (26), causing a further increase in surface energy [92].

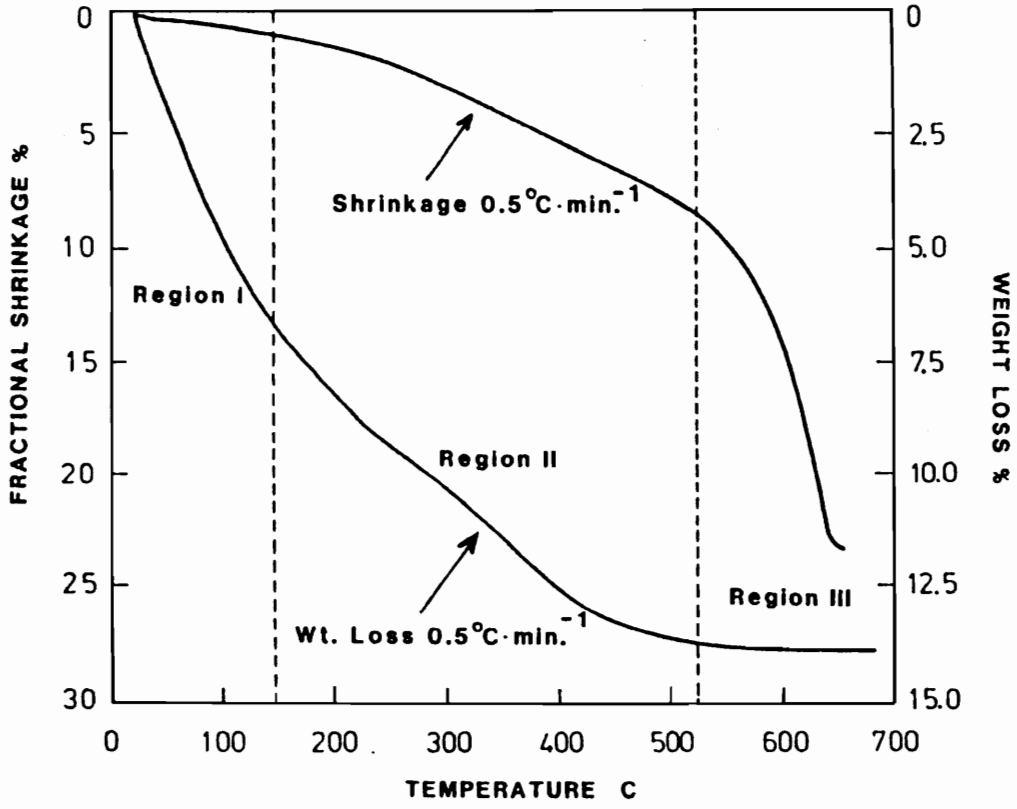


***Figure 1.14.*** Linear shrinkage and weight loss for a multicomponent silicate gel measured at 0.5 °C/min [92].

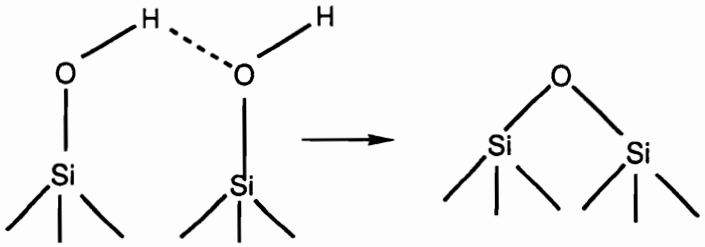


$$+ \quad H_2O \qquad (26)$$

The maximum additional contraction expected if the surface energy increased to a value corresponding to a completely dehydrated surface (280 erg/cm$^2$) is only 0.13% [92]. This additional linear shrinkage would occur between 150 and 650°C and represents a small contribution to the total measured linear shrinkage accompanying densification.

In Region II, weight loss and shrinkage occur concurently. Weight loss is attributed both to the removal of water as a by-product of polycondensation reactions :

$$\equiv Si\text{-}OH \quad + \quad HO\text{-}Si\equiv \quad \longrightarrow \quad \equiv Si\text{—}O\text{—}Si\equiv \quad + \quad H_2O \qquad (27)$$

and to the oxidation of carbonaceous residues. Conceivably, shrinkage in Region II can occur by both increased packing efficiency and skeletal densification (through polymerization and structural relaxation) [40]. The contribution of each of the proposed mechanisms to shrinkage in Region II is difficult to quantify. It is well established for melt prepared glasses that relaxation processes (which reduce "excess" free volume) occur at temperatures slightly below Tg. However, as the skeleton densifies in Region II, its Tg increases continuously so there is no narrow temperature range in which structural relaxation is predicted to take place.

Region III corresponds to a temperature interval where considerable shrinkage occurs with little associated weight loss. This behavior is associated with a viscous sintering mechanism.

In summary, previous literature data considering densification basically a sintering process are not correct. At least four mechanisms contribute to shrinkage [40, 91,92]: *(1)* Capillary contraction

due to the increase in surface energy, contributing ~3% to the total observed shrinkage and which is the predominant shrinkage mechanism below 150°C; *(2)* Condensation polymerization and *(3)* Structural relaxation; Polymerization and structural relaxation result in skeletal densification which closely account for the observed shrinkage and reduction in surface area in the temperature range 150-525°C. Skeletal densification which contributes ~33% to the total shrinkage, occurs without dramatically changing the local environment of the basic structural units. Thus, the dimensional scale of motion required for skeletal densification is very small, explaining how this process can occur at quite low temperatures. *(4)* Viscous sintering accounts for ~63% of the total shrinkage and appears to be the predominant mechanism above 525°C. High temperatures are generaly required to densify particulate gels by viscous sintering (>800°C) and even higher temperatures are required for gels with coarser microstructure. In contrast, a lower temperature (800°C) is sufficient to densify the non-particulate gels obtained through acid catalysis. These non-particulate gels start to densify significantly at 600°C. The low temperature densification was explained by a process consisting of polymer relaxation followed by condensation and pore collapse. This process is possible due to the larger amount of randomly distributed OH and OR groups existing in less highly condensed gels and their much finer pore size. It is obvious that the gel-to-glass conversion is highly dependent on the sol-to-gel transition. This implies that optimization of the solution conditions will serve to minimize the gel-to-glass conversion temperature and, therefore, result in lower temperature applications for sol-gel derived glasses.

A very important observation [91] is that the pathway along which the gel evolves toward a glass is very dependent on thermal hystory. Generally, as the heating rate is increased, the low temperature structure is retained to higher temperatures resulting in an enhancement of densification kinetics. Thus, shrinkage in Region II and III exhibits a complex heating rate

dependence, i.e. although the mechanisms which are responsible for shrinkage are all kinetically limited, the reduced time spent at each increment of temperatures as the heating rate is increased is partly or completely compensated for by increased rate of structural relaxation or viscous sintering. In fact, at sufficiently high rates, the reduced viscosity in Region III more than compensates for the reduced time and the gel densification temperature is reduced. This effect (reduction in densification temperature with heating rate) should be very important for gel-derived thin films which can be densified at very high heating rates.

## *2.7. MICROSTRUCTURE OF THE SOL-GEL DERIVED MATERIALS*

The overall sol-gel process is considered in two major steps, both important in determining the main features of the microstructure, such as pore diameter, D, and the pore distribution. First is the chemistry of the sol-gel formation and second is the drying and thermal treatment of the gel to form the porous glass. It is of utmost importance to correlate the reaction conditions (pH of the gelling solution and the water/silica ratio being the most important), to network microstructure (pore diameters, pore size distribution and packing mode).

It is generally accepted that hydrolysis of alkoxides at low pH and low $H_2O$/Si ratio result in weakly crosslinked polymeric silica chains which, when desiccated and heated below their densification temperature yield polymeric type glasses [82]. Since the structural unit in these materials can be considered chainlike, having crossections of only a few Angstroms, it is expected that the porosity (which occurs between dehydration and complete densification) will consist of a large number of small interconnected pores. This is in fact what is observed - the smallest pores are seen in glasses prepared under these conditions - ***Table 1.3*** [93]. On the other hand, high pH, high $H_2O$/Si ratio and high temperatures favor the formation of highly branched silica chains resulting in

more particle like structure having larger interconnecting channels, i. e. larger pore sizes. This chemistry has been discussed in previous sections.

The pore diameter D changes with temperature, dD/dT. A linear increase is observed until about 850°C, at which point there is a rather sharp decrease due to densification, ***Figure 1.15*** [93]. These changes with temperature are very dependent on other factors, the most important ones being the reaction parameters in the initial reaction stages. For example, a greater dD/dT is observed for the particle-like glasses, obtained at higher pH and larger $H_2O$/Si ratio which can probably be explained by a model which says that at favorable interparticle contact points "necks" grow during the initial stages of sintering and the overall structure changes from a strictly random particle type to one which has some characteristics of an array of intersecting cylinders [94]. This "necking" is observed in TEM micrographs of a particle like glass [93]. Since the polymeric glasses are non-particle like, a lower dD/dT is expected and this is what was observed experimentally for the acid catalyzed samples, ***Figure 1.16*** [93].

The type of microstructure leading to different pore size or pore size distribution can be characterized using high resolution TEM . At the supramolecular level, a spherical nature of the particle is seen. The substructure of the individual particles is definitely filamentary where the individual filaments are more or less randomly interconnected and in some cases even twisted [93]. The average single-filament diameters are in the $0.4 \pm 0.2$ nm and are possible individual chains of linked $SiO_4$ tetrahedra. Chain width estimates from bond distances can vary between 0.27 -0.53 nm and average about 0.4 nm [95]. An important observation from the high resolution TEM is that even the samples prepared under basic conditions, still do not show any evidence of

***Table 1.3.*** Summary of preparation conditions and pore sizes of sol-gel glasses [93]. A refers to alkoxide, E to ethoxide, M to methoxide, F to formamide. The numbers indicate the solution pH.

| Alkoxides sample | $H_2O$/Si | Temp. °C | *D* (nm) |
|---|---|---|---|
| AE-2.8 | 15 | 600 | <3.0 |
| AE-2.8 | 10 | 400 | <2.0 |
| AE-2.8 | 10 | 800 | <3.0 |
| AE-2.8 | 4 | 700 | <2.0 |
| AE-3.5 | 10 | 600 | 5.4 |
| AE-5.2 | 10 | 600 | 6.3 |
| AE-8.5 | 10 | 600 | 8.3 |
| AE-8.5 | 12.5 | 600 | 8.0 |
| AE-8.5 | 6 | 400 | 4.1 |
| AE-8.5 | 6 | 600 | 5.4 |
| AE-8.5 | 6 | 800 | 7.8 |
| AE-9.5 | 4 | 500 | 6.2 |
| AE-11.6 | 10 | 600 | 10.2 |
| AMF-9.1 | 12.5 | 500 | 8.3 |
| AMF-9.3 | 6 | 500 | 7.7 |
| AMF-10.6 | 12.5 | 500 | 9.4 |
| AMF-10.4 | 12.5 | 850 | 10.6 |

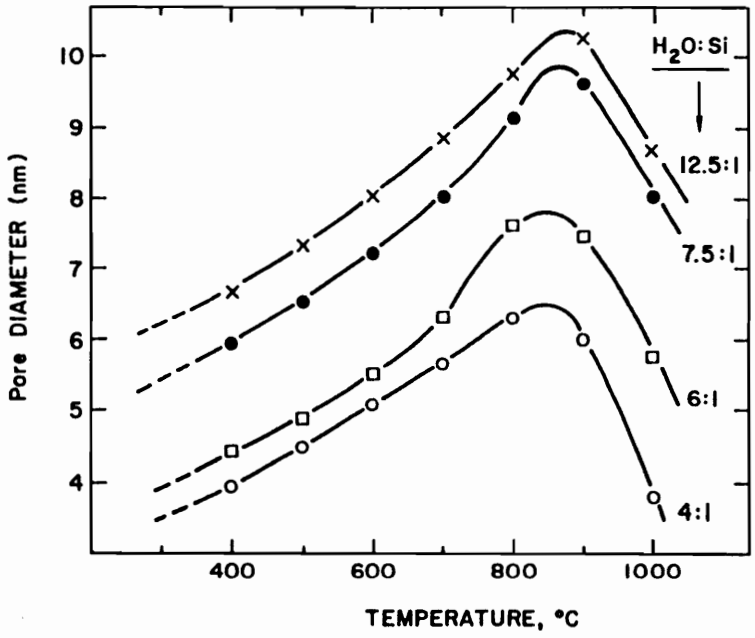


***Figure 1.15.*** Pore diameter vs firing temperature for alkoxide-type glasses (pH=8.5 ) [93].

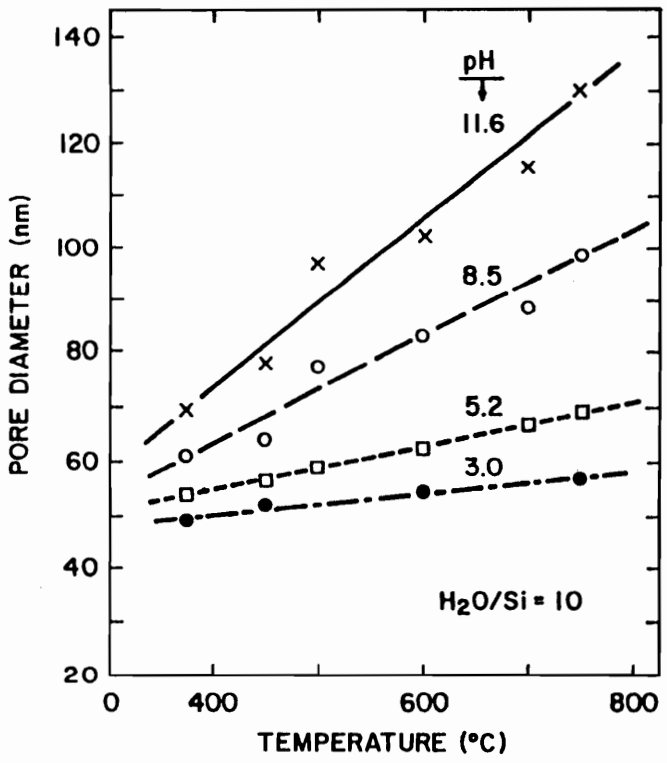


***Figure 1.16.*** Pore diameter vs firing temperature for alkoxide glasses prepared at four different pHs [93].

colloid-type behavior, even though it does appear to be more highly crosslinked than the acid catalyzed gels which are definitely polymeric [93].

Further insight into the organization at the supramolecular level can be obtained by combining the results of SAXS obtained for solutions and for solid films. From the analysis of Guinier region it was found that near the gelation point the sols are formed of particles of about 60 Å in diameter compared to scattering units of about 20Å in diameter for the films, [40,84]. These results suggest that the gel structure is developed at two different levels. Orcel [83,84] et al. proposed that primary particles of about 20Å in diameter agglomerate in secondary particles of about 60Å in diameter. Gelation occurs when the secondary particles are linked to each other forming a three-dimensional network all across the sample. Similarly, Elkins et al. [96] estimated from small angle x-ray scattering, that the average size of primary particles, assumed to be spherical, in freshly prepared silica gel was around 30-60 Å. This picture of the supramolecular building structure can be correlated as well with the results in the Porod regime. The fractal dimension of these systems, which can be computed by analysis of Porod region and which is dependent on the shape and geometry of the diffraction centers, also indicates a possible growth mechanism in which secondary particles made up of several primary particles agglomerate to form a gel.

Thermal aging studies of silica gels by Shapiro and Kolthoff [96] suggested that the structure of silica gel could best be visualized as being made up of discrete particles. The conversion of a sol of spherical particles to a uniform gel is not easily understood. When particles collide it is assumed that the attachement is through the formation of Si-O-Si bonds. The same factors that promote polymerization of monomer and low molecular weight silicic acids also promote the conversion of a sol of silica particles to a gel.

*2.8. ORGANIC MODIFICATION OF THE SOL-GEL MATERIALS*

In the past, glasses were mainly used as typical non-composite materials due to some excellent properties such as chemical durability, transparency and optical properties. But with increasing demand for special optical or mechanical properties, glasses became more and more modified by other components. This type of modification takes place on the macroscopic scale which means that a two or more step process has to be applied. The question arrises whether it makes sense to develop "composites at the molecular scale". The first question which has to be answered is what possibilities exist to combine typical inorganic with organic structures? The idea of combining organic and inorganic materials is not new. As Dr. Rochow was anticipating in the early 60s, "...there must be a way to combine inorganic and organic materials into a new type of products, using the basic principles of the silicone preparation and this task should be solved by the new generation of researchers" [98].

The conventional fusion method of making glasses excludes the possibility of organic modification because of the high temperature treatment. However, with the success of the sol-gel process, this approach has become feasible. Several studies have been already carried out to consider the possible incorporation of organic compounds into inorganic glass networks, and the results are very encouraging. However, in order to generate dense, pure inorganic glasses it is necessary to apply temperatures of about $T_g$ which are still too high for organic components. This means that the typical densification step of the inorganic sol-gel process by heat treatment cannot be applied without any modification. The organically modified sol-gel glass systems can generally be devided into two categories:

(1) When the organic modifiers are nonhydrolyzable substituents on the alkoxide monomers; the molecular weight of such organic groups is usually low to avoid dangling ends in the networks.

(2) When the organic modifiers are functionalized low molecular weight or polymeric organic molecules capable to either become a part of the inorganic glass network or form a network in itself, resulting into an interpenetrating network system (IPN).

### *2.8.1. Unhydrolyzable (Si-C) bonded ligands as the organic modifiers*

Organic components do not necessarily have to act as network formers: if they are not polymerizable, they may act as network modifiers, since they decrease the degree of crosslinking by reducing the monomer functionality. Gulledge [99] and Andrianov et al. [100,101] showed that silicon type networks with inorganic heteroatoms can be prepared by co-condensation of organosilicon with other network forming components like Ti, Al, P and others. The effect of decreased crosslink density in those cases led to dense products without high temperature treatment. These results encouraged the use of the method as a general possibility to develop new materials by introducing other organofunctional groups into the general sol-gel networks. The introduction of organic groups is expected to strongly affect the materials properties. For example substitution of one -Si-O- bridge in fused silica by one -Si-$CH_3$ group increases the thermal expansion coefficient from $0.5 \times 10^{-6}$ to about $100 \times 10^{-6}$ $K^{-1}$ [102]. In this type of modification the size of the organic group can strongly affect the structure. Differences should be expected for example from -Si-$CH_3$ or -Si-$C_6H_5$. It was already demonstrated that the substitution of -$CH_3$ by -$C_6H_5$ leads to very different properties of polymers [103]. Whereas -$C_6H_5$ containing polymers are thermoplastic and soluble in most organic solvents (probably due to the lower degree of crosslinking in this system, due to steric hindrance), the corresponding -$CH_3$ containing materials are insoluble and non-thermoplastic.

A wide variety of materials can be generated by the variation of R, composition or reaction conditions. The question arises whether materials based on these type of modifications might be

regarded as glasses or not. They surely are not glasses in the classical sense, but they can be considered as an interesting modification of sol-gel derived materials. In copolymerization type reactions between $Si(OR)_4$ and $R'_nSi(OR)_{4-n}$, the reaction conditions may be very strongly influencing the structure [98]. The control of the reaction rate is of special interest, if components with very different rates have to be used. Generally, the higher the amount of the organic unreactive substituents, the softer the product appear due to lower crosslinking density and as a consequence, dense materials are prepared at very mild conditions (100-200°C). Higher amount of inorganic components lead to more brittle products and, under certain circumstances, to porous gels [104]. Densification of porous gels by heat results in the destruction of organic functions.

### *2.8.2. Hydrolyzable organic modifiers*

Unlike the first type of modifications in which the organic containing species are dispersed within a continuous glass matrix, the second type of hybrid systems may show cocontinuous phases or even a dispersed inorganic phase, depending on the composition of the system. A very controlled modification of sol-gel structures is possible by the introduction of organic spacers *at regular intervals in the silicate framework* (V), [105]:

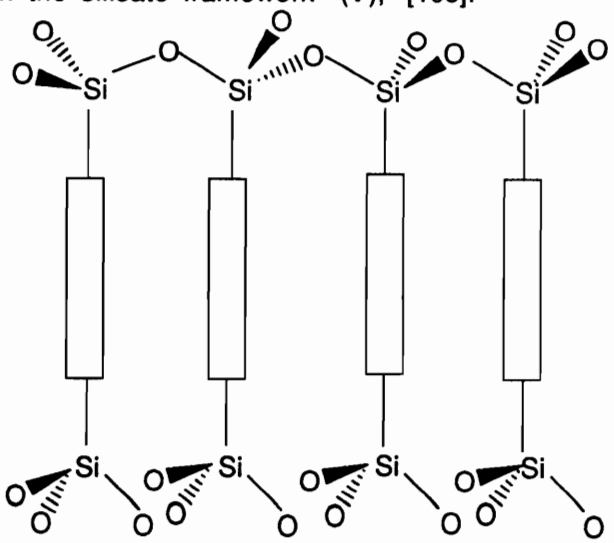

V

Such modifications have been reported [105], in which bis(triethoxysilyl) aryl monomers have been employed as the spacers:

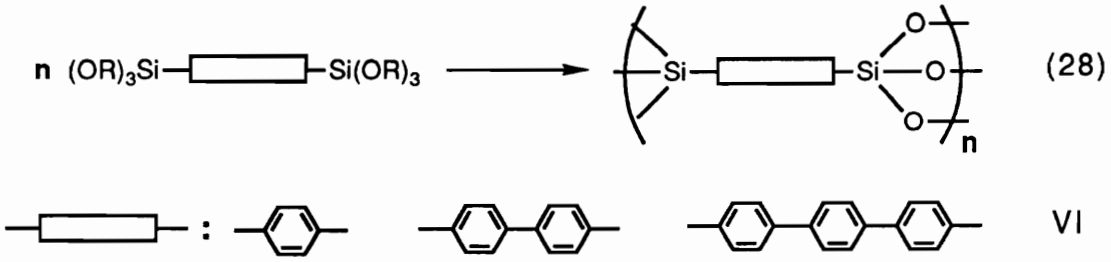


(28)



VI

The phenyl, biphenyl, and terphenyl groups separating the silicon atoms are rigid rod spacers with Si-aryl-Si distances of 0.67, 0.87 and 1.08 nm, respectively. The bis(triethoxysilyl) monomers can be represented by two silicon tetrahedra elongated by an aryl spacer. The monomers can condense at three vertices of each tetrahedra to produce an extended network without an opportunity for close packing. When highly condensed, such materials are expected to possess microporosity.

A new type of hybrid materials was introduced by Wilkes and co-workers [106-108]. The acronym CERAMER derived from CERamic polyMER was introduced by these authors to describe the new class of sol-gel derived materials in which functionalized polymeric components are incorporated into the silicate systems. Typically, the preparation of organically modified sol-gel glasses have primarily utilized elastomeric components as the organic modifiers. The first of these materials utilized silanol terminated poly(dimethylsiloxanes) (PDMS) as the organic component and TEOS as the inorganic component, reacted under acid catalysis [108]. The resulting gels were optically transparent and displayed a considerable amount of flexibility. The PDMS-$SiO_2$ systems often displayed bimodal and broadened $T_g$ transition in DMTA , instead of a sharp glass transition expected for pure PDMS system (~-120°C). The authors interpreted the observed broadening

and shifting of the Tg transition as an indication that the PDMS component was well dispersed throughout the matrix. SAXS studies on these systems showed no indication of a well defined phase separation, another proof that the systems are homogeneous or uniform in nature. (However, it was recognized that there may not be sufficient electron density difference between PDMS domains and $SiO_2$ networks to actually be able to measure any scattering from phase separation [108]). The main disadvantage of these systems, not always recognized, is that in the presence of catalysts usually employed for the sol-gel processes the polysiloxane chains can undergo redistribution reactions, especially when higher temperatures are used for drying of the gels. Materials incorporating functionalized polytetramethyleneoxide (PTMO) into the sol-gel system were also prepared by Wilkes and co-workers [109,110]. The use of DMTA and SAXS allowed the development of a simplified model for these systems. The bimodal tan $\delta$ behavior and the existence of a distinct correlation distance in these systems, the magnitude of which increased with the molecular weight of the PTMO component, was interpreted as the existence of $SiO_2$ -rich clusters dispersed within PTMO-rich areas [111].

There are fewer examples for the use of a glassy component (below $T_g$) as the organic modifier in sol-gel systems. A few years ago, Schmidt and Phillipp attempted to incorporate a glassy component (below $T_g$) in a sol-gel inorganic network (98, 112-114]. Their experimental method combines a sol-gel mechanism with an independent free radical reaction that requires a somewhat tedious and complex reaction procedure. Wilkes and co-workers and Mark and co-workers have used the basic approach described in the preparation of elastomer modified sol-gel systems [106,107,115-118], to incorporate glassy oligomeric components. In order to synthesize hybrid materials through this route, the organic oligomeric species to be incorporated into the inorganic networks must be functionally reactive with the silicon alkoxide precursor during the course of sol-gel reactions. Hence, an endcapping procedure in which silicon alkoxide functional groups are

placed at the end of the oligomer chains is usually employed. The endcapping scheme generally employed for the functionalization of such oligomers was the reaction of an amine or hydroxyl terminated oligomer with commercialy available isocyanate functionalized trialkoxy silanes. Polyetherketone amorphous oligomers (PEK) of controlled molecular weight were selected to prove, for the first time, this simple approach to the preparation of organic modified glasses in which the organic oligomer is glassy at the reaction temperature [119] (the $T_g$ of the PEK component is ca 150°C). In these systems, the conversion was found to be somewhat limited due to the vitrification, as the network buildup progresses, at least at lower reaction temperatures. However, the authors claim that further network development can be promoted by utilizing thermal post-gelation treatments. These materials maintain transparency in the optical frequency range but do illustrate that local microphase separation may occur. The main disadvantage of these systems is that the urea or urethane linkages connecting the chain ends of the oligomers with the reactive alkoxysilane end groups have relatively low thermal stability and a potential susceptibility for hydrolysis during the catalyzed sol-gel reactions.

## *2.9. POTENTIAL APPLICATIONS FOR SOL-GEL MATERIALS*

In terms of their usage, sol-gel materials can be classified into two categories : vitrified gels and non-vitrified gels.

### *2.9.1. Potential applications for vitrified gels*

These materials are usually vitrified at temperatures of ~ 900°C or higher and are generally dense and hard. The type of applications for these materials may include bulk glasses, thin sheets, coatings or particulate powders [120]. Formation of bulk glasses, even though a subject of high interest, is a difficult task, mainly due to the large volume shrinkage and the crack formation during the sol-to-gel and gel-to-glass transitions. The main applications for these materials would be in

making $SiO_2$ glass plates used as photomasks for integrated circuits and $SiO_2$-based glass rods for drawing optical fibers [85, 121,122]. Thin glass sheets ranging from several tens to several hundreds of microns can be obtained through sol-gel technology at temperatures below 1000°C [123]. The most serious difficulty associated with this technique arises from an enormous shrinkage in volume and area on solidification of the solution, which may cause deformation, crack formation and fracture of gel sheets. At present, these problems are not fully solved. Coating films, through dip-coating or spin-coating are techniques used for coating applications. In the years around 1970, dip-coating was applied by Schroeder and Schott Company in Germany [124] to modify the optical properties of glasses and plastics. In recent years the dip-coating technique has again attracted much attention as the demand for new electronic materials has increased. Sakka [120] gives a comprehensive table with examples of applications of the dip-coating using metal-alkoxide solutions. These applications range from mechanical and chemical protection of substrate, to films of particular optical characteristics (colored and absorbing film [7,125], reflecting film [126], antireflection film [127], photoconductive,etc) or electrically conducting films [128,129] and ferroelectric films [84,129], etc. Particulates from oxide powders made by precipitation from metal alkoxides [130] are excellent starting materials for sintered polycomponent ceramics because they are uniform in chemical composition and very fine in particle size.

### *2.9.2. Potential applications for non vitrified gels*

Sol-gel derived materials used as "gelled" or with minimum post gelation treatment are non-vitrified gels and they can be used in this form for a variety of applications. Such materials would retain much of the porous microstructure resulting in a very large surface area and so they are excellent candidates for catalyst carriers or as separation media [128-130]. The combination of "inorganic" and "organic" materials through a sol-gel process opened the door for a wide variety of new applications, as described below.

Bulk materials: The introduction of organic functions into inorganic networks lead to more flexible products which may have properties more related to organic polymers. In addition, it may help to overcome the difficulties of shrinking and cracking which are known to be a problem in the inorganic sol-gel systems. The use of the flexible sol-gel technology for example, allowed the combination of organic and inorganic monomers in designing materials for contact lenses. A typical reaction scheme used for the synthesis of contact lenses is described in ***Scheme 1.10*** [131]. In this reaction the network was synthesized by the hydrolysis and condensation of an epoxysilane and Ti-alkoxides; in this way it was possible to unify the main requirements of good wettability and $O_2$-permeability in one and the same product. Additionally, methacrylates were used as linear crosslinking elements to generate polymethacrylate linear chains for improvement of the overall mechanical properties. The incorporation of methacrylates was achieved by employing methacryloxysilane (a polymerizable and condensable component) able to act as a hook between the sol-gel networks and the methacrylate, respectively polymethacrylate.

Special coatings : Protective coatings to improve scratch resistance have been reported to be produced through sol-gel chemistry [92]. Such coatings are known to be used for protection of GE Lexan polycarbonate. Functional coatings can also be produced by introducing corresponding organic substituents in the system. For example amino groups can be used as coupling groups for biochemical materials such as enzymes or antibodies or as adsorption centers for acids [98].

These few examples, by no means exhaustive, show the potential offered by the combination of inorganic with organic materials on the molecular scale. If the influence of different properties determining parameters is known, the tailoring of the materials with very special properties becomes possible. Even though more knowledge was accumulated in this field, more fundamental work is necessary in order to understand and optimize these systems. Firstly, the

***Scheme 1.11.*** Reaction scheme for the synthesis of organic-inorganic hybrid networks[131].

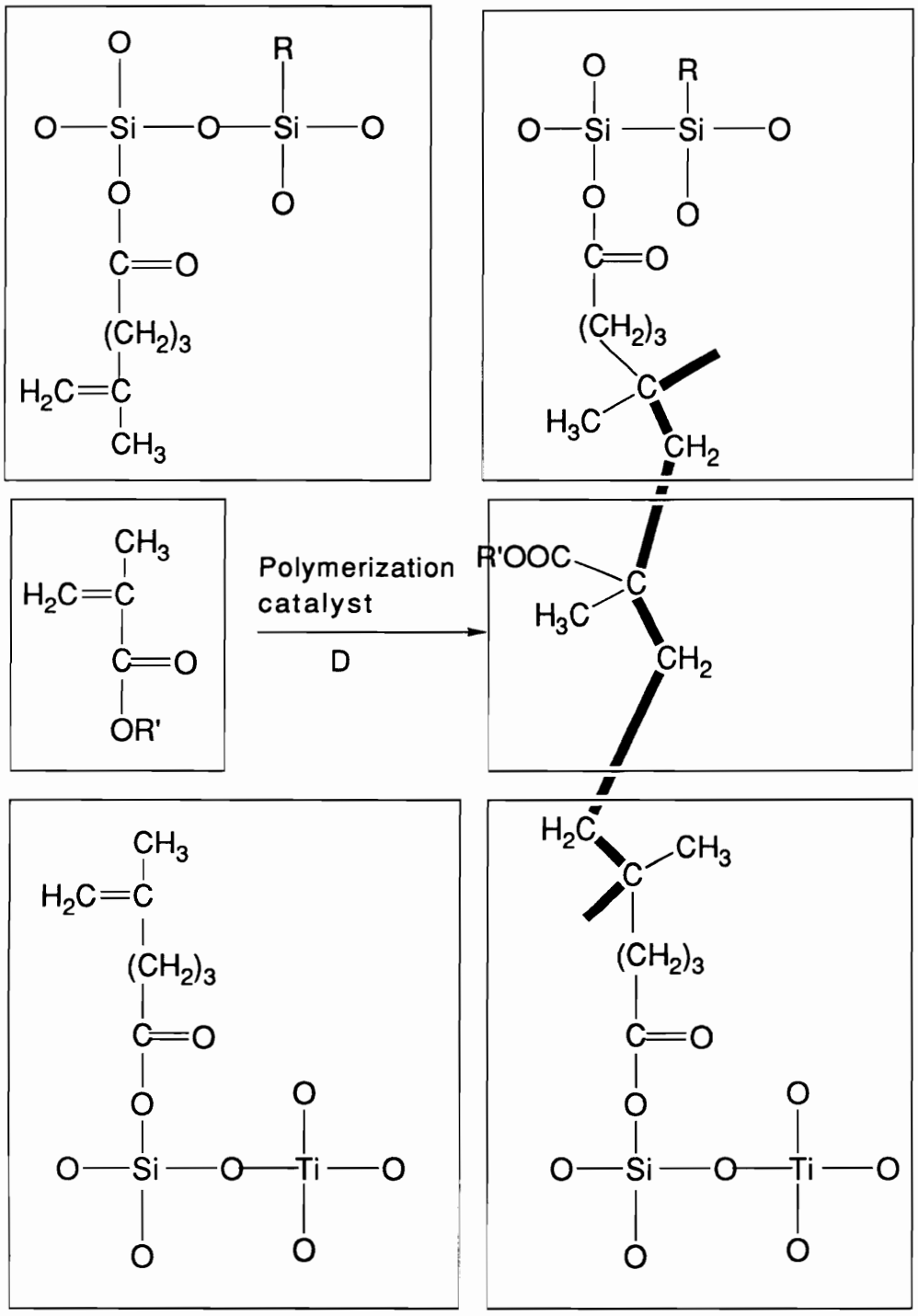

reactivity towards hydrolysis and condensation of starting compounds under standardized reaction conditions have to be known. This is important for the understanding of structures to be built up during copolymerization reactions. Secondly, these structures have to be determined. Thirdly, the correlation between structural parameters and materials properties have to be evaluated. This could be the basis for a successful material development of the described type of polymers.

*CHAPTER 3*

*EXPERIMENTAL TECHNIQUES*----------

# *CHAPTER 3*

# *EXPERIMENTAL TECHNIQUES*----------

## *3.1. PURIFICATION OF REAGENTS*

### *Nitrogen*

Prepurified nitrogen (99.99%) (Airco) was regulated through a 11/2 in steel drying column at ca 50psi. The drying column was packed with freshly activated 4Å molecular sieves and supported by glass wool at both ends. After passing through the drying column, the dried nitrogen was regulated to 5-10 psi and connected to a glass nitrogen/vacuum manifold fitted with Teflon rotoflow stopcocks. The vacuum manifold was connected to a mechanical vacuum pump with an in-line dry-ice cold trap and an in-line pressure transducer.

### *3.1.1. Solvent purification*

A variety of solvents were employed in the synthesis of inorganic networks, organic oligomers and model compounds, and for the copolymerization of organic oligomers with the inorganic alkoxides. Anhydrous solvents were utilized for kinetic investigations of sol-gel reactions. The solvents utilized for the synthesis of controlled molecular weight oligomers with different functionalities were previously purified by distillation. Solvent transfer during chemical reactions was generally conducted via syringe techniques. Synthesis of organic/inorganic networks was usually carried out using certified grade solvents without distillation. Structures of the most commonly used solvents are listed in **Table 4**.

*Tetrahydrofuran.* Tetrahydrofuran (THF) (Fisher, Certified grade) was refluxed under a nitrogen atmosphere in the presence of a sodium dispersion in paraffin wax. After complete dissolution of the paraffin wax with heating and stirring, a fine dispersion of sodium with a large

***Table 1.4.*** Common solvents for polyimide, polysiloxane and sol-gel reactions

| STRUCTURE | SOLVENT | ACRONYM | BP, °C |
|---|---|---|---|
| 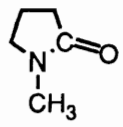 | N-Methyl-2-Pyrrolidinone | NMP | 82 @ 10mm |
| 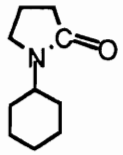 | N-Cyclohexyl-2-Pyrrolidinone | CHP | 154 @ 7mm |
| 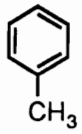 | Toluene | Tol | 111 |
| 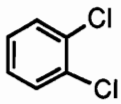 | o-Dichlorobenzene | DCB | 179-180 |
| 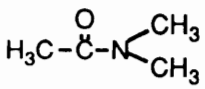 | N,N-Dimethyl-acetamide | DMAc | 166 |
| 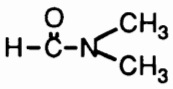 | N,N-Dimethyl-formamide | DMF | 153 |
|  | Tetrahydrofuran | THF | 67 |

surface area remains to efficiently dry the solvent. Benzophenone in relatively small amounts was used as an indicator of solvent purity due to the formation of a highly colored dianion when reacted with sodium in the absence of protic sources or oxygen. Immediately upon addition of benzophenone a blue color was observed due to the formation of a benzophenone radical anion. After several hours the color changed from blue to purple as the radical anion was converted to a dianion, indicating that the solvent was completely dry and oxygen free [132]. After the color change, THF was refluxed for several hours prior to distillation. A sodium excess must be used to prevent distillation of the benzophenone. The distilled THF was collected into a previously cleaned, flamed, and nitrogen purged flask fitted with a rubber septum. The rubber septum was secured in place with copper wire and a positive pressure of nitrogen was maintained at all times. The distilled THF was used as a solvent in hydrosilation reactions or for the synthesis of the poly(amic acid)s.

*Toluene.* Toluene (Fisher, Certified grade) was employed as an azeotropic agent. Toluene was allowed to stir overnight over calcium hydride ($CaH_2$), refluxed for at least two hours under nitrogen atmosphere and then fractionally distilled. The distillation was conducted under a low nitrogen flow through the apparatus. The constant boiling middle fraction was collected in a round bottom flask, sealed with a rubber septum, and stored under nitrogen pressure.

*Other solvents.* Other solvents used in the synthesis of polyimides or for potentiometric titrations (NMP, CHP, DCB, DMAc, chlorobenzene) were allowed to stir over phosphorous pentoxide ($P_2O_5$) for at least four hours (usually overnight), refluxed for approximately two hours, and then fractionally distilled under reduced pressure. The constant boiling middle fraction was collected in a round bottom flask, sealed with a rubber septum, and stored under low nitrogen pressure.

*Miscellaneous.* Chloroform-d (Aldrich, 99.8 atom % D), methyl-$d_3$ alcohol-d (Aldrich, 99.5 atom % D), N,N-dimethylformamide-$d_7$ (Aldrich, 99 atom % D) were used as received for routine NMR

analysis. Anhydrous methyl alcohol (Aldrich, 99+%, water<0.005%) was utilized for the study of reaction kinetics in sol-gel systems. Methanol (Fisher) used for precipitation of polyimide oligomers was employed as received, without purification.

### *3.1.2. Purification of monomers*

*3.1.2.1. Monomers for sol-gel reactions*

*Tetramethylorthosilicate (TMOS)*

| | |
|---|---|
| *Supplier(s):* | Petrarch Systems, Inc. |
| *Empirical Formula:* | $C_4H_{12}O_4Si$ |
| *Molecular weight, g/mol:* | 152.22 |
| *Boiling point/mm, °C:* | 121-122 |

*Structure:*

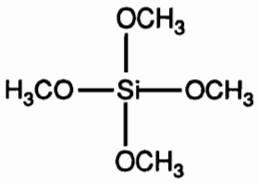


*Purification:* The TMOS utilized for kinetic investigations was fractionally distilled under nitrogen and the middle fraction of constant boiling point was collected in a previously cleaned, flamed, and nitrogen purged flask fitted with a rubber septum. The rubber septum was secured in place with copper wire in order that a positive pressure of nitrogen could be maintained at all times. For other sol-gel reactions the TMOS was used as received, without distillation. The reagent was storred under dried nitrogen at all times. Due to the very high level of toxicity (orl-rat LD50:700mg/kg) and potential cause of blindness rubber gloves were used and all the handling was done in well ventilated hoods.

*3.1.2.2. Monomers for polysiloxane synthesis*

*Octamethylcyclotetrasiloxane (D4)*

*Supplier(s):* Union Carbide

*Empirical Formula:* $C_8H_{24}O_4Si_4$
*Molecular weight, g/mol:* 296.61
*Boiling point/mm, °C:* 175-176
*Structure:*

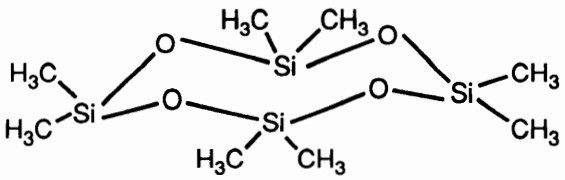

*Purification:* $D_4$ was dried over calcium hydride and distilled, under reduced pressure.

*1,3-Divinyltetramethyldisiloxane*

*Supplier(s):* Petrarch Systems, Inc.
*Empirical Formula:* $C_8H_{18}OSi_2$
*Molecular weight, g/mol:* 186.40
*Boiling point/mm, °C:* 139
*Structure:*

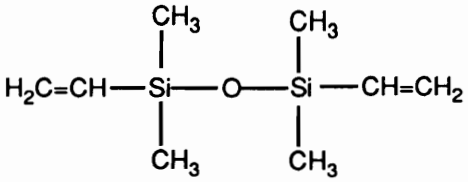

*Purification:* 1,3-divinyltetramethyldisiloxane was fractionally distilled. The middle fraction of constant boiling point was collected and stored under nitrogen.

*Trimethoxysilane*

*Supplier(s):* Petrarch Systems, Inc.
*Empirical Formula:* $C_3H_{10}O_3Si$
*Molecular weight, g/mol:* 122.20
*Boiling point/mm, °C:* 86-87
*Structure:*

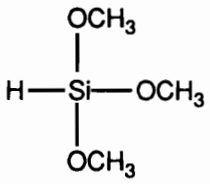

*Purification:* Trimethoxysilane was distilled under nitrogen atmosphere right before use. The middle fraction of constant boiling point was collected in a previously cleaned, flamed, and nitrogen purged flask fitted with a rubber septum. The rubber septum was secured in place with copper wire in order that a positive pressure of nitrogen could be maintained at all times. In order to avoid premature hydrolysis and condensation of the reactive methoxysilane any further handling was conducted via syringe technique. Due to the high toxicity (orl-rat LD50:8,024mg/kg) and the potential cause of blindness, the same precautions were taken as for TMOS reagents.

*Methyldimethoxysilane*

| | |
|---|---|
| *Supplier(s):* | Petrarch Systems, Inc. |
| *Empirical Formula:* | $C_3H_{10}O_2Si$ |
| *Molecular weight, g/mol:* | 106.20 |
| *Boiling point/mm, °C:* | 61 |
| *Structure:* | |

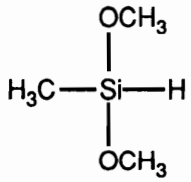


*Purification:* Methyldimethoxysilane was purified in a similar manner as tetramethoxysilane and trimethoxysilane previously described. Due to its high reactivity and sensitivity to moisture the reagent was handled via syringe techniques.

### *3.1.2.3. Monomers for the synthesis of polyimides*

*5,5'-[2,2,2-Trifluoro-1-(trifluoromethyl)ethylidene]bis-1,3-isobenzofuranedione (6F)*

| | |
|---|---|
| *Supplier(s):* | Hoechst Celanese Corporation |
| *Empirical Formula:* | $C_{19}H_6F_6O_6$ |
| *Molecular weight, g/mol:* | 444 |
| *Melting Point (pure), °C:* | 247 |
| *Structure:* | |

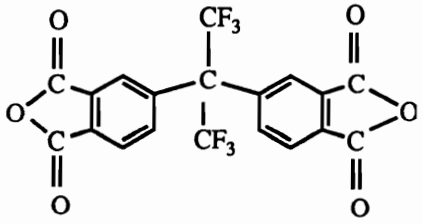

*Purification:* Electronic grade 6F of high purity was used as received.

*4,4'-isopropylidene dianiline (Bis A)*

| | |
|---|---|
| *Supplier(s):* | Air Products and Chemicals, Inc. |
| *Empirical Formula:* | $C_{15}H_{18}N_2$ |
| *Molecular weight, g/mol:* | 226 |
| *Melting Point (pure), °C:* | 132 |
| *Structure:* | |

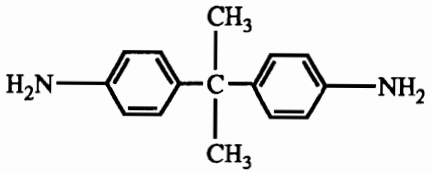

*Purification:* Bis A was received as a high purity white powder and it was used without further purification.

*cis-5-Norbornene-endo-2,3-dicarboxylic anhydride*

| | |
|---|---|
| *Supplier(s):* | Aldrich Chemical Company, Inc. |
| *Empirical Formula:* | $C_9H_8O_3$ |
| *Molecular weight, g/mol:* | 164.16 |
| *Melting Point (pure), °C:* | 165-167 |
| *Structure:* | |

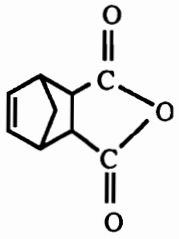

*Purification:* Norbornene dicarboxylic anhydride was purified by vacuum sublimation and was stored in the desicator until use.

*Aniline*

| | |
|---|---|
| *Supplier(s):* | Aldrich Chemical Company, Inc. |
| *Empirical Formula:* | $C_6H_5NH_2$ |
| *Molecular weight, g/mol:* | 93.13 |
| *Melting Point (pure), °C:* | -6 |
| *Boiling point, °C* | 184 |
| *Structure:* | |

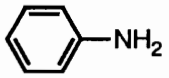

*Purification:* Aniline was dried over calcium hydride, distilled under reduced pressure, and stored under nitrogen and in the absence of light. Aniline was used in the synthesis of phenyl-nadimide, model compound for hydrosilation reactions employed for polyimide functionalization.

### *3.1.3. General Reagents and catalysts*

Tetramethylammonium hydroxide pentahydrate (TMAH·$5H_2O$) used in the preparation of the silanolate catalyst for siloxane equilibration reactions was obtained from Aldrich and used as received. Hydrogen hexachloroplatinate (IV) pentahydrate [$H_2PtCl6·5H_2O$], the hydrosilation catalyst, was purchased from Aldrich and stored under inert atmosphere until use.

## *3.2. SYNTHESIS OF INORGANIC $SIO_2$ NETWORKS*

Tetramethylorthosilicate (TMOS) was selected as the starting alkoxide monomer for the present study. The use of TMOS was imposed by the requirement of a highly reactive alkoxysilane, capable to undergo hydrolysis and condensation reactions at relatively high rates, in the absence of added catalyst. This was important for the synthesis of organic/inorganic networks, since many organic modifiers display limited stability in the presence of acid or base catalysts usually employed for sol-gel reactions. These aspects will be detailed in Chapter 4. The experimental procedure for the generation of three-dimensional $SiO_2$ networks from multifunctional alkoxides can be subdivided into two parts: a) the initial solution reaction up to the gel point and b) the post-gelation treatment.

### *3.2.1. Initial reaction up to the gel point*

The sol-gel reactions (up to the gelation) were carried out at room temperature, in a one-necked round bottom flask equipped with a Teflon coated magnetic stir bar. The glassware was rinsed with hydrofluoric acid (49%), followed by rinses with dilute base, water and acetone. The glassware was then dried in a forced air convection oven at 120°C. The reactants were charged into the reaction flask in the order TMOS, $CH_3OH$ and $H_2O$, at the desired molar ratios. The flask was then closed using a fitted rubber septum, and allowed to stir at room temperature. At desired time intervals, samples were removed as a function of reaction time and analyzed by $^{1}H$ and $^{29}Si$ NMR for the extent of hydrolysis and condensation reactions. Most of the compositions investigated generated homogeneous reaction mixtures. For a few compositions, however, the initial reaction mixtures were heterogeneous, but they became homogeneous as the water coreactant was consumed in hydrolysis reactions and more methanol was generated as a reaction by-product. A continuous increase in viscosity accompanies the increase in the molecular weight. The viscosity increase is somehow faster when the reaction approaches the gelation point (the formation of the insoluble three-dimensional networks). Prior to gelation, the reaction mixture was poured into 10 ml glass vials (approximately 2.0-2.5 grams reaction mixture in each) and allowed to gel at room temperature (~20°C). The gel point was considered the point at which the reaction mixture would no longer flow and it was assessed visually.

### *3.2.2. Post-gelation treatment*

The 10 ml glass vials containing 2.0-2.5 grams of the gelled reaction mixture and equipped with relatively tightly fitting caps were slowly heated to 65°C, where the gel was allowed to age for approximately 16 hours. Subsequently, the temperature was slowly increased to 100°C and the gel was further dried at this temperature for an additional 16 hours. Finally, the temperature was raised to 150°C and maintained for another 16 hours. During these heating stages, the vials were

kept closed, therefore the aging and drying were usually done under a modest pressure. Following the above treatment, the dried gels were removed from the sealed vials and further dried in a vacuum oven up to a maximum temperature of 150°C, prior to analyses. The rate of temperature increase during all of the above aging and drying cycles was maintained at values of approximately 0.5 deg per minute in order to avoid sample cracking at higher heating rates. In some cases, higher processing (drying) temperatures were investigated ($T_{max}$=500°C) as detailed in Chapter 4 Results and Discussions.

## *3.3. SYNTHESIS OF REACTIVE OLIGOMERS*

### *3.3.1. Poly(dimethylsiloxane) (PSH) oligomers*

*3.3.1.1. Vinyl functionalized polysiloxanes:* Vinyl terminated polydimethylsiloxane oligomers of controlled molecular weight were synthesized by the anionic ring opening equilibrium polymerization of the cyclic siloxane monomer octamethylcyclotetrasiloxane ($D_4$).

1,3-Divinyltetramethyldisiloxane was used as the end-capper or chain transfer agent (and provided the molecular weight control and the vinyl endgroup functionalities), and tetramethylammonium silanolate was used as the transient catalyst. The reaction was conducted in a three-necked round bottom flask equipped with a mechanical stirrer, reflux condenser, inert gas inlet, thermometer, and a rubber septum to allow for removal of samples at desired time intervals. The disiloxane and the cyclic siloxane tetramer were added to the reaction flask and heated to 80°C under inert atmosphere, with continuous stirring. The tetramethylammonium silanolate catalyst which was synthesized and titrated prior to equilibration according to procedures detailed elsewhere [133] was added to the reaction mixture at an approximate concentration of 0.1 mole percent based on the total moles of starting materials. The reaction temperature was maintained at 80°C using a programmable hot plate. The equilibration was allowed to proceed for 24 hours, during which time samples were continuously removed and

analyzed by GPC All reactions were completely equilibrated after 24 hours. At the end of equilibration (when GPC indicated no further change in molecular weight and/or molecular weight distribution) the reaction temperature was increased to 140°C for 30 minutes under efficient nitrogen flow, in order to decompose the silanolate catalyst into noncatalytic species [134-136]. After cooling at room temperature, the viscous product was transfered into a Kugelrohr vacuum distillation apparatus and the low molecular weight, unfunctionalized cyclics were stripped off under vacuum (aprox. 500mtorr) and heat (up to 150-180°C).

The molecular weight of the siloxane oligomer (PSX) was controlled by the initial ratio of the cyclic tetramer ($D_4$) to the disiloxane end-capper (DSX). A sample calculation for the synthesis of controlled molecular weight polydimethylsiloxane oligomers is given below. Calculations are for the preparation of **A** grams PSX oligomer with $M_n$ number average molecular weight.

$$\text{Grams DSX} = A[\text{grams}] \times \frac{\text{MW DSX [g/mole]}}{\bar{M}_n \text{ PSX [g/mole]}} = A \times \frac{186.4}{\bar{M}_n \text{ PSX}} \text{ [grams]} \qquad (29)$$

$$\text{Grams } D_4 = A[\text{grams}] \times \frac{\{\bar{M}_n - \text{MW DSX}\} \text{ [g/mole]}}{\bar{M}_n \text{ PSX [g/mole]}} = A \times \frac{\bar{M}_n - 186.4}{\bar{M}_n \text{ PSX}} \text{ [grams]} \qquad (30)$$

where MW is the molecular weight of the siloxane dimer and is equal to 186.4 grams/mole.

*3.3.1.2. Methoxy functionalized polysiloxanes:* The methoxysilane functionality was achieved by hydrosilation at the vinyl double bonds using methoxysilanes as hydrosilation agents and hydrogen hexachloroplatinate pentahydrate ($H_2PtCl_6x5H_2O$) as the reaction catalyst. The hydrosilation reaction was carried out in a three-necked round bottom flask equipped with a magnetic stirrer, a reflux condenser, nitrogen inlet, thermometer, addition funnel and a rubber septum to allow sampling via syringe. The glassware was previously dried in a forced air

convection oven at 120°C, flame dried after assembly and purged with prepurified nitrogen prior to charging the reaction. A low flow of dried nitrogen was maintained through the apparatus during the entire reaction. The olefin component (vinyl terminated polysiloxane oligomer or 1,3-divinyltetramethyldisiloxane) was charged into the reaction flask with a small amount of freshly distilled THF. Fresh catalyst solution was prepared before each reaction using distilled THF and a few drops of IPA. The catalyst solution was added to the reaction mixture at a molar ratio R = $[H_2PtCl_6]$/[Vinyl double bond] $=5x10^{-4}$. Upon addition of catalyst the solution becomes sometimes cloudy. In this case more freshly distilled THF was added to the reaction to ensure a homogeneous mixture. In general, the reaction was carried out at approximately 50% solids. The catalyst was allowed to complex to the vinyl double bond for aproximately 30 minutes prior to methoxysilane addition. The methoxysilane hydrosilating agent was transfered into an addition funnel via syringe in order to avoid hydrolysis and subsequent condensation of the reactive methoxy groups in the presence of moisture contaminants. The silane was then added in small portions (10% excess overall) to the reaction mixture. When the silane addition was carried out at room temperature no exotherm was observed. However, when the reaction temperature was increased to 30-35 °C an immediate exotherm was observed after each silane addition when the DSX was used as the olefin. The rate of silane addition in this case was controlled such as the temperature would not exceed 45-50°C. The entire addition required 15 to 30 minutes, depending upon the size of the reaction and the concentration of reactive groups. The hydrosilations were allowed to proceed for two more hours after the last silane addition. When PSX oligomers were employed as the olefin component, no exotherm was usually observed due to the relatively low concentration of reactive vinyl groups present at the ends of high molecular weight chains. In this case the reaction temperature was increased to 40-45°C and the addition of silane was carried out over a period of approximately 15 minutes. The reaction was then allowed to proceed for an additional two hours at the end of which $^1H$ NMR usually indicated a complete

unsaturation. Occasionally slightly longer reaction times were required (for higher molecular weight oligomers, with lower concentration of reactive groups); however, all reactions were allowed to proceed untill $^1$H NMR indicated complete disappearance of the unsaturation. The reaction mixture was then filtered through Celite, the reaction solvent and excess silane were removed by vacuum stripping, and the hydrosilated product was stored in the desicator until use.

### *3.3.2. Polyimide (PI) oligomers*

*3.3.2.1. Amine terminated polyimides* : Polyimide oligomers based upon 6F dianhydride and Bis A diamine, with controlled molecular weight and amine end groups, were synthesized by a two-step reaction. The poly(amic acid) intermediates were synthesized in a three necked, round bottom flask equipped with a mechanical stirrer, inert gas inlet, and a drying tube, at a solids concentration of 20 w/v percent. The glassware was previously dried in a forced air convection oven at ~ 120° C, flame dried after assembly, and purged with dried nitrogen prior to charging the reaction. A low flow of dried nitrogen was maintained through the apparatus during the entire reaction. A calculated excess of Bis A diamine, as determined by the Carothers equation (section 3.3.2.2.), was added first into the flask, as a powder, and enough NMP solvent was added to completely dissolve the diamine with stirring. NMP was also used for rinsing the weighing pan to ensure quantitative transfer of monomers into the reaction flask. The 6F dianhydride was slowly added to the previous reaction mixture as a solution in NMP, via cannula, under slight nitrogen pressure. The rate of addition of dianhydride solution was controlled in order to maintaim the reaction temperature at approximately ambient values. The reaction mixture stayed clear all the way through addition and reaction. The amic acid reaction was stirred for 4-6 hours at room temperature, and then immediately imidized. Conversion of the poly(amic acid) intermediates to the fully cyclized polyimide was accomplished by using previously documented solution imidization techniques [138,139]. Solution imidizations were conducted in a four necked flask

equipped with a mechanical stirrer, inert gas inlet, thermometer and Dean Stark trap with a condenser and a drying tube. The reaction flask was heated in an oil bath (~170°C) using a programmable hot plate. A thermocouple connected to the temperature controller was inserted into the reaction mixture through a rubber septum in order to allow continuous temperature control inside the reaction flask. The amic acid solution was added into the flask containing prewarmed (~150°C) cosolvent mixture of CHP and NMP, to result in a final solvent ratio of 20% CHP/80% NMP and a final solids concentration of ~18 percent. The reaction temperature was regulated at 160°C, and never allowed to fall below 120°C during the addition of the amic acid solution. The imidization reaction was allowed to proceed for approximately 24 hours at 160°C, maintaining a continuous inert gas flow throughout the reaction. After approximately 24 hours, the reaction mixture was allowed to cool at room temperature, under nitrogen, and the polyimide oligomer was recovered by precipitating the solution into a ~10 fold excess of a rapidly stirring methanol, filtering in a sintered glass funnel, rinsing with more methanol and air drying for several hours. The coagulated oligomer was then placed in a vacuum oven and the temperature was slowly increased to ~ 180-200°C. The oligomer was dried at this temperature for at least 24 hours.

*3.3.2.2. Molecular weight and end group control:* The Carothers equation can be employed to control the molecular weight and endgroup functionalities of oligomers synthesized through step growth polymerizations. For the above polyimide system of the type (AA + BB), the molecular weight and endgroup control was achieved by using a calculated stoichiometric imbalance of the diamine monomer. A complete derivation of the Carothers equation can be found in basic polymer books [140-142]. The Carothers equation relates the extent of reaction (p) and degree of polymerization ($X_n$) to the average functionality of the polymerizing system ($f_{av}$):

$$\overline{X}_n = \frac{2N_o}{2N_o - N_o p f_{av}} = \frac{2}{2 - p f_{av}} \qquad (31)$$

For 100% conversion of monomer to polymer (p=1) and perfectly difunctional monomers ($f_{av}$=2), the molecular weight of the step growth polymer is predicted to become infinite. Therefore, any stoichiometric deviation which decreases the average functionality to less than 2 will limit the molecular weight of the polymer. On the other hand, the number average degree of polymerization, $X_n$, in the (AA + BB) system, is related to the desired polymer molecular weight, $M_n$, through equation 32:

$$\overline{X}_n = 2\,DP = 2\,\frac{\overline{M}_n}{\text{molecular weight of the repeat unit } (M_{ru})} \qquad (32)$$

where $M_{ru}$ is the molecular weight of the repeat unit. In the context of polymerization of AA monomers with BB monomers, the repeat unit in the polymer is the aabb unit (each repeat unit contains the residue of two monomers). The number of aa plus bb units is twice the number of aabb units, hence the number average degree of polymerization, $X_n$, is twice the number of repeat units in the polymer molecule, DP. The value of $X_n$ for a desired molecular weight, $M_n$, can therefore be calculated from equation 32 above. The number average degree of polymerization may be further related to the stoichiometric imbalance ( r ) and the extent of conversion (p) by:

$$\overline{X}_n = \frac{1+r}{1+r-2pr} \qquad (33)$$

which for p =1 becomes

$$\overline{X}_n = \frac{1+r}{1-r} \qquad (34)$$

If $X_n$ is known, the value of the desired stoichiometric imbalance ( r ) can be calculated from equation 34. The stoichiometric imbalance, r, is defined by the ratio of the number of A and B functional groups, such that, by definition this ratio can not exceed unity. If amine endgroups are desired for the polyimide oligomers the stoichiometry must be upset by using an excess of diamine monomers (i.e. monomer B):

$$r = \frac{\text{Moles of difunctional A monomer}}{\text{Moles of difunctional B monomer}} \qquad (35)$$

The moles of difunctional A monomer may by arbitrarily established as 1; from equation 35 above, the moles of difunctional B monomer is then equal to r. These values may be scaled accordingly for any batch size.

A sample calculation for the synthesis of a 5,000g/mole amine terminated 6F-Bis A polyimide oligomer is given below :

$$X_n = 2\,\frac{5000}{(444 + 226) - 36} = 15.77$$

where

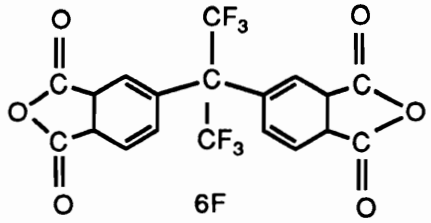

molecular weight = 444g/mole

6F

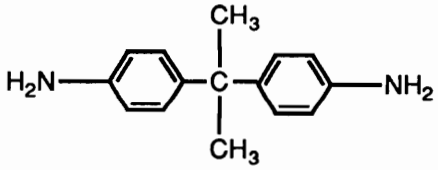

molecular weight = 226g/mole

Bis A

Also,

$$X_n = \frac{1 + r}{1 - r} \qquad \text{or} \qquad r = \frac{X_n - 1}{X_n + 1} = \frac{14.77}{16.77} = 0.8807$$

therefore the stoichiometric imbalance required is:

$$\frac{\#\text{ moles anhydride}}{\#\text{ moles diamine}} = 0.8807$$

In the above calculations it was assumed that the chain length of the oligomer is high enough to make unnecessary any correction for the chain ends. However, for relatively low molecular weight oligomers such corrections for the chain ends become necessary. In this case, equation 32 becomes:

$$\overline{X}_n = 2\,DP = 2\,\frac{\overline{M}_n - \overline{M}_{eg}}{\text{molecular weight of the repeat unit } (M_{ru})} \qquad (32')$$

where $M_{eg}$ is the molecular weight of the end-group units. For the particular sample calculation given on page 106, the expression for the degree of polymerization becomes:

$$X_n = 2\,\frac{5000 - 2\cdot 226}{(444 + 226) - 36} = 14.347$$

and

$$X_n = \frac{1 + r}{1 - r} \qquad \text{or} \qquad r = \frac{X_n - 1}{X_n + 1} = \frac{13.347}{15.347} = 0.8697$$

*3.3.2.3. Nadimide terminated polyimides:* The second reaction step in the synthesis of reactive polyimide oligomers involved the conversion of amine terminated polyimides to nadimide functionalized oligomers. The amine endgroups of the dried, recovered polyimide oligomers were titrated with 0.02 N HBr (detailed in section 3.5.1) to determine the actual number average molecular weight and hence, the amount of nadic anhydride (NA) needed for quantitative end-capping, i.e., 2 moles NA per mole of oligomer. The reaction was carried out in a four-necked round bottom flask equipped with a mechanical stirrer, inert gas inlet, thermometer and an inverse Dean Stark trap with a condenser and drying tube. Thus, the stoichiometric amount of NA plus 10 mole percent excess was added to the reaction flask containing the prewarmed (110°C) polyimide solution in cosolvent DMAc (80%) and chlorobenzene (20%) to yield a final solids concentration of 17 to 20 w/v percent. The reaction was allowed to proceed for three hours at 110°C followed by

a higher temperature (130°C) imidization of the amic acid end groups for approximately 12 hours. The resulting oligomer solution was cooled at room temperature, under nitrogen atmosphere. The polyimide was recovered by precipitating the solution into a ~10 fold excess of vigorously stirring methanol, filtering in a sintered glass funnel, rinsing with more methanol, and air drying for several hours. The coagulated oligomer was then placed in a vacuum oven and dried for a minimum of 24 hours at 150°C. Usually the above operations were repeated by redissolving the oligomer and reprecipitating and drying in the vacuum oven, to ensure the complete removal of excess unreacted nadic anhydride which would interfere in the next reaction step. A similar reaction procedure was employed for the synthesis of phenyl-nadimide used as the model compound for hydrosilation at the nadimide double bond. Hence, the stoichiometric amount of NA plus 10 mole percent excess was added to the reaction flask containing the prewarmed (110°C) aniline solution in cosolvent DMAc (80%) and chlorobenzene (20%) to yield a final solids concentration of 17 to 20 w/v percent. The reaction was allowed to proceed for three hours at 110°C followed by a higher temperature (130°C) imidization of the amic acid for approximately 12 hours. The clear, slightly yellow reaction mixture was then allowed to cool at room temperature under nitrogen, precipitated into a ten-fold excess diionized water, and filtered in a sintered glass funnel. The coagulated product was then redissolved in THF, recrystallized from a mixture of $CH_3OH$ (40%) and $H_2O$ (60%), and dried in the vacuum oven at 80°C. Spectral characterization of this compound ($^1H$ and $^{13}C$ NMR) is detailed in Chapter 4.

*3.3.2.4. Methoxy functionalized polyimides:* Silicon alkoxide functional groups were introduced at the end of the polyimide chains through a hydrosilation reaction at the nadimide double bond of the nadimide functionalized oligomers. Trimethoxysilane [$H\text{-}Si(OCH_3)_3$] was used as the hydrosilating agent and hydrogen hexachloroplatinate pentahydrate ($H_2PtCl_6x5H_2O$) as the reaction catalyst. Due to the low concentration of reactive groups on the

relatively high molecular weight polyimide oligomers (hence less accurate monitoring of the reaction), the reaction conditions for the hydrosilation at the nadic double bond were established on a model study in which N-phenyl nadimide was used as the model olefin substrate. The same procedure was then employed for the polyimide oligomers.

The hydrosilation reaction was carried out in a four-necked round bottom flask equipped with a mechanical stirrer, inert gas inlet, drying tube, thermometer, reflux condenser, addition funnel and a rubber septum to allow for sampling via syringe. In order to prevent any moisture contaminants (which can give premature hydrolysis and condensation of methoxy groups), the equipment was previously dried in a forced air convection oven at ~ 120°C, flamed after assembly, and continuously purged with dried nitrogen. The nadimide containing component (PI oligomer or phenyl-nadimide model compound) was charged into the reaction flask, dissolved in freshly distilled THF and heated at the reaction temperature of 65°C. The methoxysilane was transfered into the addition funnel via syringe.

Prior to silane addition freshly prepared catalyst solution (in THF with a few drops of IPA) was added to the unsaturated component in the reaction flask and allowed to complex for approximately 30 minutes. A relatively large amount of catalyst was required to perform the hydrosilation at the nadimide double bond (R = [catalyst]/[double bond] = $10^{-3}$ to $10^{-2}$). The total amount of catalyst solution utilized for each hydrosilation reaction was divided into four portions. Similarly, the required amount of freshly distilled methoxysilane was added to the reaction in approximately four fractions. A new portion of catalyst was utilized with each addition of methoxysilane hydrosilating agent. Shortly after the first addition of methoxysilane and catalyst the initially light brown reaction mixture became dark brown but it stayed visually clear. This change in color was previously observed for platinum hydrosilation catalysts, under different

conditions [137,143]. The $^{1}H$ NMR indicated that a fast decrease in the concentration of nadimide double bonds accompanied these changes. However, after the initial fast conversion the reaction arrived to a stop, even though the silane added in this first portion was not fully consummed. In order to produce further reaction, a new portion of catalyst solution and methoxysilane reagent were added and the reaction was continuously monitored by $^{1}H$ NMR. Again, a fast decrease in the concentration of nadimide double bonds was observed shortly after the addition, followed by a much slower conversions at longer reaction times, etc. An excess amount of hydrosilating agent (20-30%) was usually required in order to observe this initial fast conversion and in order to complete the hydrosilation. The reaction was generally completed within 24 hours at 65°C. The completion of the reaction was attested by the complete disappearance of unsaturation in both $^{1}H$ and $^{13}C$ NMR. The reaction was cooled at room temperature, a small amount of charcoal was added to it, and the solution was filtered through Celite to remove most of the platinum catalyst. All these opperations were conducted under anhydrous conditions, using closed systems with slight nitrogen pressure in order to prevent premature hydrolysis and condensation of the silicon-methoxide groups. Following the filtration, the solvent and the excess (unreacted) methoxysilane were vacuum distilled from the reaction mixture and the silicon-methoxide containing compound was stored in the desiccator, under nitrogen atmosphere, until use.

## *3.4. SYNTHESIS OF ORGANIC/INORGANIC HYBRIDS*

### *3.4.1. Polysiloxane modified silicates*

All reactions for the synthesis of polysiloxane modified silicates were carried out under relatively neutral conditions, in a catalyst free environment in order to avoid undesirable redistribution of the polysiloxane chains, especially at higher temperatures required for the drying of the gels. The preparation of organic/inorganic hybrid networks through sol-gel reactions involves two distinct

steps, as previously described for the synthesis of $SiO_2$ inorganic networks: the initial solution reaction, up to the gelation point, and the post-gelation treatment.

*3.4.1.1. Initial solution reaction:* The copolymerization of reactive functional PSX oligomers with TMOS was carried out in a one-necked round bottom flask equipped with a magnetic stirrer and a fitted rubber septum.Two main approaches were investigated for the above copolymerizations.

In the first approach, the organic (PSX) and inorganic (TMOS) reactants were both added at the beginning of the reaction. The reactants were charged into the reaction flask in the order TMOS, $CH_3OH$, $H_2O$ and PSX solution in THF. The reactive siloxane oligomer was added slowly as a solution in THF to the TMOS+$CH_3OH$+$H_2O$ solution (1.0:1.4:4.0 molar ratio), with continuous stirring, in order to prevent the precipitation of the PSX in the highly polar reaction environment. When necessary, more THF was added during the PSX addition in order to ensure a homogeneous reaction environment. All copolymerization reactions were carried out using a stoichiometric amount of water required for complete hydrolysis of all methoxy groups, in the absence of condensation reactions, and a minimum amount of solvent required to obtain an initially homogeneous reaction mixture. The initial cosolvent ratio of $CH_3OH$/THF was approximately1/10, w/w. High dilutions were generally required in order to maintain a homogeneous coreactant system (final concentration of approximately 20 weight percent solids). The main disadvantage of this experimental approach was that due to the high dilutions very slow reaction rates, hence long gelation times, were observed (from two weeks to few months, depending upon the reaction composition and the PSX molecular weight). The use of higher reaction temperatures in order to increase reaction rates often resulted in particle formation from the dilute reaction solutions.

In a second, more successful approach, the TMOS was prereacted to a controlled extent of conversion to generate soluble network precursors. This initial reaction was carried out at room temperature in a one-necked round bottom flask equipped with a magnetic stirrer and a fitted rubber septum. The reactants were charged into the reaction flask in the order TMOS, $CH_3OH$, $H_2O$ at a molar ratio of 1.0:1.4:4.0 respectively. The above reaction was allowed to proceed at room temperature, with continuous stirring for approximately 6 hours at which time 80-85 % of the initial methoxy groups were hydrolyzed (as indicated by $^1H$ NMR). At this point the PSX solution in THF was slowly added to the inorganic precursor. Enough THF was utilized in the second step to ensure a homogeneous coreactant solution. However, due to the fact that a large amount of water has already been used in hydrolysis reactions, higher reaction concentrations (25-30 w/w percent solids) could be employed. Consequently, faster reaction rates and shorter gelation times were obtained (usually the reactions gelled within approximately 12 hours at room temperature, after the addition of the PSX modifier). Prior to gelation, a considerable increase in viscosity was observed. At this point, the reaction mixture was poured into 10 ml glass vials equipped with relatively fitted caps (approximately 2.0-2.5 grams reaction mixture per vial) and allowed to gel at room temperature. The gelation was defined as the point at which the reaction mixture would no longer flow.

*3.4.1.2. Post-gelation treatment:* A similar post gelation treatment as the one described for the unmodified inorganic $SiO_2$ networks (section 3.2.2) was applied to the PSX/$SiO_2$ hybrids.

### *3.4.2. Polyimide modified silicates*

*3.4.2.1. Initial solution reaction:* The reaction conditions for the generation of polyimide/silicates were slightly modified from the previously discussed polysiloxane/silicate synthesis (section 3.4.1.). The THF/$CH_3OH$ cosolvent system (which generated opaque hybrids

upon initial drying, for all compositions) was replaced by DMF/$CH_3OH$ (which generated clear dried hybrids for lower PI compositions). Also, the initial solution reaction was carried out at 65°C. The reaction was carried out in a one necked round bottom flask equipped with a magnetic stirrer and a reflux condenser.

In the first approach the organic and inorganic reactants were both added at the beginning of the reaction. The reactants were charged into the reaction flask in the order TMOS, $CH_3OH$, $H_2O$ and PI solution in DMF. The reactive polyimide oligomer previously dissolved in DMF was slowly added to the TMOS+$CH_3OH$+$H_2O$ solution (1.0:1.4:4.0 molar ratio, respectively), with continuous stirring, to prevent the precipitation of the PI organic oligomer into the highly polar reaction environment. The initial ratio of $CH_3OH$/DMF was approximately 1/10. All reactions were carried out at approximately 20% solids. When the reactions were carried out at room temperature, very long gelation times were observed (sometimes the reactions never gelled). Increasing the reaction temperature to 65°C (refluxing temperature of $CH_3OH$) resulted in increased reaction rates but particle formation was often observed due to highly diluted solutions.

In the second approach the TMOS was prereacted at room temperature until approximately 80-85% of the methoxy groups were hydrolyzed (as described for the PSX/silicate hybrid systems). To this soluble network precursor the PI solution in DMF was slowly added, with continuous stirring, employing enough solvent to allow for a homogeneous reaction mixture at all times. The reaction temperature was then increased to 65°C. More concentrated solution could be used in this procedure (25-30% solids, depending upon the PI molecular weight and the reaction composition). When a viscosity increase was noticeable, indicating the approaching of the gelation, the reaction was poured into 10 ml glass vials equipped with relatively fitted caps (2.0-2.5 grams reaction mixture in each vial) and allowed to gel at 65°C in a heated oven.

*3.4.2.2. Post-gelation treatment:* A similar procedure developed for the inorganic $SiO_2$ networks was employed, with the difference that a higher final temperature was used in the last drying step (165°C, above the boiling point of the DMF solvent).

## *3.5. EXTRACTION EXPERIMENTS*

A soxhlet apparatus with a 2 liter THF reservoir was employed to perform extraction experiments. Samples selected for extraction were dried to constant weight in vacuum at ~ 22°C then loaded into cellulose thimbles which had also been dried in vacuum to constant weight. Cellulose thimbles containing ~1-3 grams of material were placed into the soxhlet apparatus to be extracted for 72 hours in refluxing THF. After extraction, the thimbles were removed, dried to constant weight in vacuum and weighed.

## *3.6. CHARACTERIZATION TECHNIQUES*

A variety of techniques were used for the characterization of the starting materials, reaction intermediates, functionalized oligomers and inorganic or organic/inorganic networks.

### *3.6.1. Potentiometric endgroup titrations*

In order to determine the number average molecular weight of functional oligomers or the concentration of the silanolate species in the silanolate catalyst, potentiometric titrations were performed on a MCI GT-05 (COSA Instruments Corporation) automatic potentiometric titrator. The samples were accurately weighed into a 150 ml beaker, and dissolved in 50-100ml solvent. The size of the sample was chosen such that the endpoint would require a total titrant volume between 2 and 4 ml. When the sample was completely dissolved, the electrode and the titrant delivery tip were inserted into the stirring solution and the titration was conducted in the automatic endpoint seeking mode. The potential of the solution at the endpoint was noted, and the total

volume of titrant consumed was stored in the computer memory. The molecular weight was then calculated automatically. The results were the average of three samples. The amine terminated polyimide oligomers based upon 6F and Bis A were dissolved in a chlorobenzene/glacial acetic acid cosolvent mixture (2/1 v/v) and titrated potentiometrically with 0.02-0.03N anhydrous HBr in glacial acetic acid. The HBr solution was standardized against potassium hydrogen phthalate dissolved in chlorobenzene/glacial acetic acid (2/1 v/v). The silanolate catalyst was dissolved in isopropanol/THF and titrated with 0.1 N alcoholic HCl.

### *3.6.2. Multinuclear Magnetic Resonance Spectroscopy (solution techniques)*

Multinuclear magnetic resonance spectroscopy has been used extensively throughout the different aspects of the present work. The technique was employed to check the purity of the reactants, to follow the extent of conversion in different systems, to determine the number average molecular weight or the paths of different chemical reactions. The use of the technique for the above mentioned studies will be detailed in Chapter 4 Results and Discussions.

***$^1H$ NMR.*** $^1$H NMR data were acquired at room temperature on a Bruker WP 270 spectrometer operating at 270.132 MHz with a sweep width of 3000 Hz. A variable number of transients were accumulated (depending on the sensitivity required) and were Fourier transformed with a line broadening equivalent to the Hz per point resolution. $CDCl_3$, $CD_3OD$, or d-DMF used as the NMR solvents also provided the deuterium lock signal. All chemical shifts were referred to tetramethylsilane (TMS) at 0.00ppm.

***$^{13}C$ NMR.*** The carbon-13 NMR spectra were obtained at room temperature on a Bruker WP 270 spectrometer operating at 67.932 MHz. Scans were accumulated using complete proton decoupling. Additional conditions: acquisition time, 0.188ss; delay time, 3s; sweep width, ~20,000 Hz. The samples were 10-20% by weight in $CDCl_3$ solvent wich also served as an

internal standard (77.0ppm from TMS) and provided the internal deuterium lock. Typically, 3,000-4,000 scans were accumulated and a line broadening of 2Hz was used.

*$^{29}Si$ NMR.* Quantitative $^{29}Si$ NMR spectra were acquired at room temperature on a Bruker WP 200 spectrometer operating at 39.765 MHz. The NMR experiments were carried out in a 10 mm multinuclear broad band probe with a 16,000 Hz sweep width. An inversegated pulse sequence was used in order to decouple the protons; the decoupler was on during the acquisition and off during the delay, to supress any negative nuclear Overhauser effect (NOE). Chromium (III) acetylacetonate [$Cr(acac)_3$] was added at ~ 0.04M concentration to reduce the $^{29}Si$ spin lattice relaxation times (T1). Generally, a pulse repetition rate of 6s was used. A variable number of transients were accumulated and were Fourier transformed with a line broadening of 2.0 Hz.

### *3.6.3. $^{29}Si$ Solid State NMR*

Solid state NMR spectra were measured at room temperature on a Bruker CXP-300 spectrometer equipped with an ASPECT 3000 computer and a Bruker double-bearing CP/MAS probe. The silicon-29 frequency was 59.601 MHz. A bullet-type zirconium oxide rotor with a total sample volume of ~0.5$cm^3$ was used. By using CP/MAS techniques, one can obtain $^{29}Si$ NMR spectra on silica gel in reasonable times (minutes to hours) and with a highly useful level of resolution [143,144]. However, **$^{29}Si$-$^{1}H$ cross-polarization restricts detection to silicon nuclei that are near protons, i.e., at or near the surface** . The highly cross-linked sol-gel samples contain a considerable amount of $Q^4$ units, corresponding to silicon atoms reacted through all four of their functionalities into the three-dimensional $SiO_2$ networks. The Si atom in this environment is removed by at least four bonds from the nearest hydroxyl proton, resulting in the largest value for the $^{29}Si$-$^{1}H$ cross polarization relaxation parameter, $T_{SiH}$. As a result, the use of CP/MAS techniques discriminates against these species. In order to obtain quantitative

information on the sol-gel systems, cross-polarization was not utilized in any of the $^{29}Si$ NMR data presented in this study. Instead, Magic Angle Spinning techniques, with the MAS frequency of 3.0 -3.5 KHz, and 30s between the r.f. pulse sequences were used, requiring longer acquisition times. Approximately 1,000-2,000 transient scans were acquired and Fourier transformed using a band broadening of 25Hz. For quantitative evaluation each spectrum was fitted in an iterative fitting program by the superposition of three Gaussians curves.

### *3.6.4. Gel Permeation Chromatography (GPC)*

The molecular weight and molecular weight distributions of polyimide oligomers were analyzed by GPC using a variable temperature Waters 150-C17 GPC, operating at 30°C and equipped with Ultra Styragel columns of 500, $10^3$, $10^4$, $10^5$, $10^6$ Å porosity. A Waters 490 programmable, multiwavelength UV-visible detector set at 218 nm was utilized with uninhibited HPLC grade THF as the elution solvent at a flow rate of 1.0 ml/minute. Polystyrene standards purchased from Polymer Laboratories, Inc. were used to prepare a GPC calibration curve. A different column set was used for the PSX oligomers:100, 500 and 1000Å porosities, in toluene as the elution solvent and with a differential refractive index (DRI) detector. Polysiloxane standards prepared in our laboratories [133] were employed to prepare a calibration curve for the characterization of the polysiloxane oligomers.

### *3.6.5. Fourier transform infrared spectroscopy (FTIR)*

The amic acid to imide transformation was monitored by FTIR using a Nicolet MX-1 spectrophotometer. Samples were removed during the course of imidization to monitor the progress of the cyclization, or at its completion to ensure quantitative conversion. The disappearance of the amic acid peak at 1546 $cm^{-1}$ and the appearance of the imide peak at 1778 and 725 $cm^{-1}$ were taken as evidence that imidization was quantitative. This technique was used

during the polyimide synthesis, nadimide end-capping reaction or the synthesis of phenyl-nadimide compound. The analysis was done either using a thin film of the reaction mixture on a KBr plate or using KBr pellets.

### *3.6.6. Thermal gravimetric analysis (TGA)*

TGA was performed on a DuPont 951 instrument on samples in powder form. Scans were run at a heating rate of 10 deg per minute in air or nitrogen with a flow rate of 10 ml per minute. Thermogravimetric analysis-Mass spectroscopy (TGA-MS) was also used. TGA s of the dried gels were obtained on a Perkin-Elmer TGS-2 analyzer. The volatile products were subsequently conveyed to a mass selective detector (Hewlett-Packard 5970 series MSD) via a two-meter long, 10μm ID, deactivated capillary column. This capillary also served to restrict the flow between the TGA experiment carried out at ambient pressure (in a self generated atmosphere, with no sample purge) and the MS experiment performed in vacuum (~$2x10^{-5}$ torr). The samples were heated from 30°C to 800°C at a constant heating rate of 20 deg per minute. Total ion chromatograms as a function of analysis time were constructed for selected ions at the mass to charge ratio for the base peak of each component (ex: m/e=18, water; m/e=31, methanol).

### *3.6.7. Dielectric thermal analysis (DETA)*

In Dielectric Thermal Analysis (DETA) an electrical stress is applied to the sample which is placed between two electrodes. The electrical displacement is then analysed using bridge techniques to give the so called dielectric constant (e'), dielectric loss (e") and loss factor (tan $d_e$). The samples used for DETA measurements in this study were thin discs of approximately 12-14 mm in diameter and 0.5 mm thick. The sample was held horizontally between a spring loaded top electrode and a fixed lower electrode. The electrodes used were 10mm in diameter. A demountable oven covered the entire assembly and allowed temperature control over the range of -150°C to +300°C.

Frequency multiplexing was used during scanning. Frequency multiplexing over a large frequency range is easy in DETA because the higher frequencies (up to 100KHz) can be accessed and measured rapidly. Indeed, each single measurement is normally averaged over at least eight measurements. The frequencies employed for the present measurements were:1, 5, 10, 50, and 100KHz. Computer control allows all the required frequencies to be clocked through continually during a slow thermal scan. The curves at each frequency are both displayed and stored. The sample specimens were dried in a vacuum oven at 120°C for at least three days prior to analyses. The sample preparation involved gold coating on both sides on a 10 mm diameter disc. To avoid short-circuiting during DETA measurements, the edges of the sample were protected during gold coating by covering the sample with removable tape in which a hole of 10 mm diameter has been cut, as shown in the sketch below. A temperature range from 30° C to 300°C and a heating rate of 1 deg per minute were used. The DETA scans were run in a nitrogen atmosphere. The sketch below shows a typical DETA sample preparation:

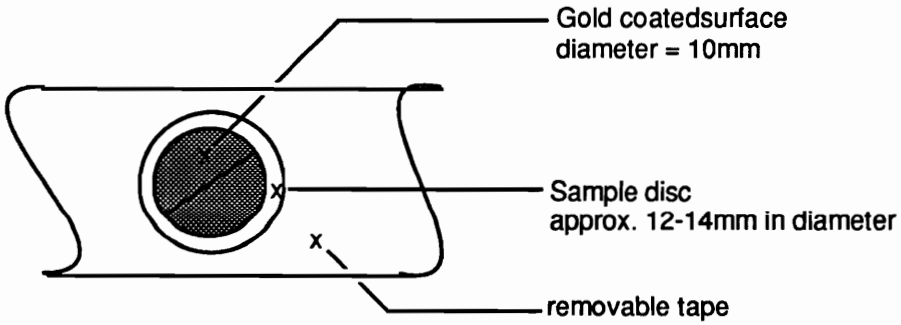


### *3.6.8. Scanning electron microscopy (SEM)*

SEM analysis was performed to study the topography of various fracture surfaces for the sol-gel derived materials. A Phillips IL 420 STEM was used in the SEM mode. Samples were coated with gold in order to minimize charging effects. High resolution micrographs (up to 100,000

magnification) were obtained for fracture surfaces of both unmodified $SiO_2$ inorganic networks and the organic/inorganic hybrid networks. The method was used for a qualitative estimation of the toughness of different sol-gel derived materials.

### *3.6.9. Water Contact Angle Analysis*

Monolithic samples with approximately 10 mm in diameter were used for contact angle measurements. Prior to analysis the samples have been dried in the vacuum oven for 1 week at 120°C and stored in sealed vials until the measurement was performed. The sample was placed in the instrument at room temperature and at atmospheric conditions. Water was added dropwise in 0.002 ml increments until an equilibrium contact angle was measured. This angle was referred to as the advancing contact angle. The reported contact angle values are averages of approximately four readings.

*CHAPTER 4*

*RESULTS AND DISCUSSION*----------

# *CHAPTER 4*

# *RESULTS AND DISCUSSION*----------

## *4.0. INTRODUCTION*

Silica glass is a very representative material in the inorganic field and it is well known for its good optical properties, high hardness and modulus and its outstanding thermal and dimensional stability. However, it also has certain drawbacks which limits its applicability:

(1) Although in the early days silica glass was viewed as an aggregation of colloidal silica, it is now generally accepted that silica glass is a *highly crosslinked*, defect containing $SiO_2$ network. Such materials are known to be quite brittle. (2) Additionally, the silica glasses obtained via sol-gel low temperature techniques are known to be characterized by an incomplete extent of conversion when produced below their glass transition temperature ($T_g(SiO_2)$ ~650°C). Consequently, such materials possess residual alkoxy and hydroxy groups which will impart *high polarity* to their surfaces. The highly polar and inherently microporous $SiO_2$ networks generated this way are readily wet and penetrated by water and other solvents, which will further limit their applicability.

Modification of the inorganic $SiO_2$ glasses with organic components, through chemical reactions, is one important way to improve upon these undesired features. Hence, the objective of this study was to investigate the possibility of generating organic modified $SiO_2$ networks using the sol-gel chemistry. Specifically, the incorporation of high molecular weight functionalized organic oligomers into the inorganic glasses was of particular interest due to the belief that such modifiers can exist as a second microphase and can more effectivelly tailor the properties of the hybrid. The synthesis of organic/inorganic networks through this technique would involve copolymerization of inorganic silicon alkoxides with functionalized organic oligomers capable to react under sol-gel conditions. Tetraethylorthosilicate (TEOS) is the most commonly used alkoxide starting material

for the generation of $SiO_2$ networks via sol-gel processes. Relatively strong acid or base catalysts are required in such systems, in order to promote hydrolysis and subsequent condensation of TEOS at fast reaction rates. However, many of the organic materials which would otherwise be of interest as network modifiers, display a relatively low stability in the presence of strong acids or bases employed in sol-gel reactions, especially at higher temperatures required for the drying of the gels. For a successful modification of the inorganic networks with organic components, the inorganic alkoxide starting material must be able to generate $SiO_2$ networks, at reasonable reaction rates, in the absence of added catalyst. Tetramethylorthosilicate (TMOS) is the most reactive silicon tetraalkoxide in the series, as discussed in Chapter 2 Literature Review; therefore, TMOS was selected as the starting alkoxide material for the present study.

During the initial investigations it was essential to establish that TMOS can react at acceptable rates, in the absence of added catalyst; therefore it can provide a catalyst free route for the synthesis of $SiO_2$ networks. In addition, it was important to investigate the effect of the most important reaction parameters on the hydrolysis and condensation rates, in order to determine the reaction conditions resulting in higher rates and conversions. Also, since the type of catalyst (reaction pH) is known to play a key role in determining the reaction mechanism, it was important to evaluate the relative contribution of hydrolysis and condensation reactions to the overall conversion, in order to understand the growth mechanism under the uncatalyzed reaction conditions employed in this study. The first section of this chapter (section 4.1.) will discuss such aspects associated with the synthesis of reference (unmodified) $SiO_2$ inorganic networks. The following sections (4.2. and 4.3.) will describe two organic modified systems investigated in this study: PSX/$SiO_2$ and PI/$SiO_2$ hybrid networks.

## *4.1. REFERENCE (UNMODIFIED) $SiO_2$ NETWORKS*

The generalized reaction conditions for the conversion of TMOS starting material into three-dimensional insoluble $SiO_2$ networks are described in ***Scheme 1.12***. The process involves two major steps: the initial solution reaction (up to the formation of the insoluble gel) and the post-gelation treatment. The chemistry of the process involves two reaction steps: hydrolysis and condensation-polymerization. The major difference of the present TMOS-based sol-gel reaction from other sol-gel systems investigated in the field is that hydrolysis and condensation reactions were carried out in the absence of catalysts, under relatively neutral reaction environments. The chemistry of the process is most important in the initial solution reactions where the chemical transformations predominate. It is at this initial stage that the topology of the network precursors (therefore the microstructure of the resulting network) is defined by the relative rates of hydrolysis and condensation reactions. Hence, the effect of the most important reaction parameters on the rate and conversion with respect to both hydrolysis and condensation reactions in this particular system were investigated at this initial stage. Following gelation the chemical transformations are slower and the flexibility in adjusting the structure through reaction parameters is highly reduced.

### *4.1.1. Effect of the reaction parameters on the hydrolysis rate*

The effect of different reaction parameters on the hydrolysis rate was investigated using $^1H$ NMR solution techniques. Sol-gel reactions based on TMOS starting alkoxide were carried out using anhydrous $CH_3OH$ as the reaction solvent (as detailed in Chapter 3). NMR samples were removed from the reaction flask at desired time intervals, diluted with $CD_3OD$ and immediatelly analyzed. Usually, 16 transient scans were accumulated and the entire sampling and analysis time was no longer than ca 5 minutes. Therefore, it was assumed that no reactions occured between sampling and the acquisition of the $^1H$ NMR spectra. The reported reaction

***Scheme 1.12***. General scheme for the synthesis of three-dimensional, insoluble $SiO_2$ networks from TMOS starting alkoxide via uncatalyzed sol-gel reactions.

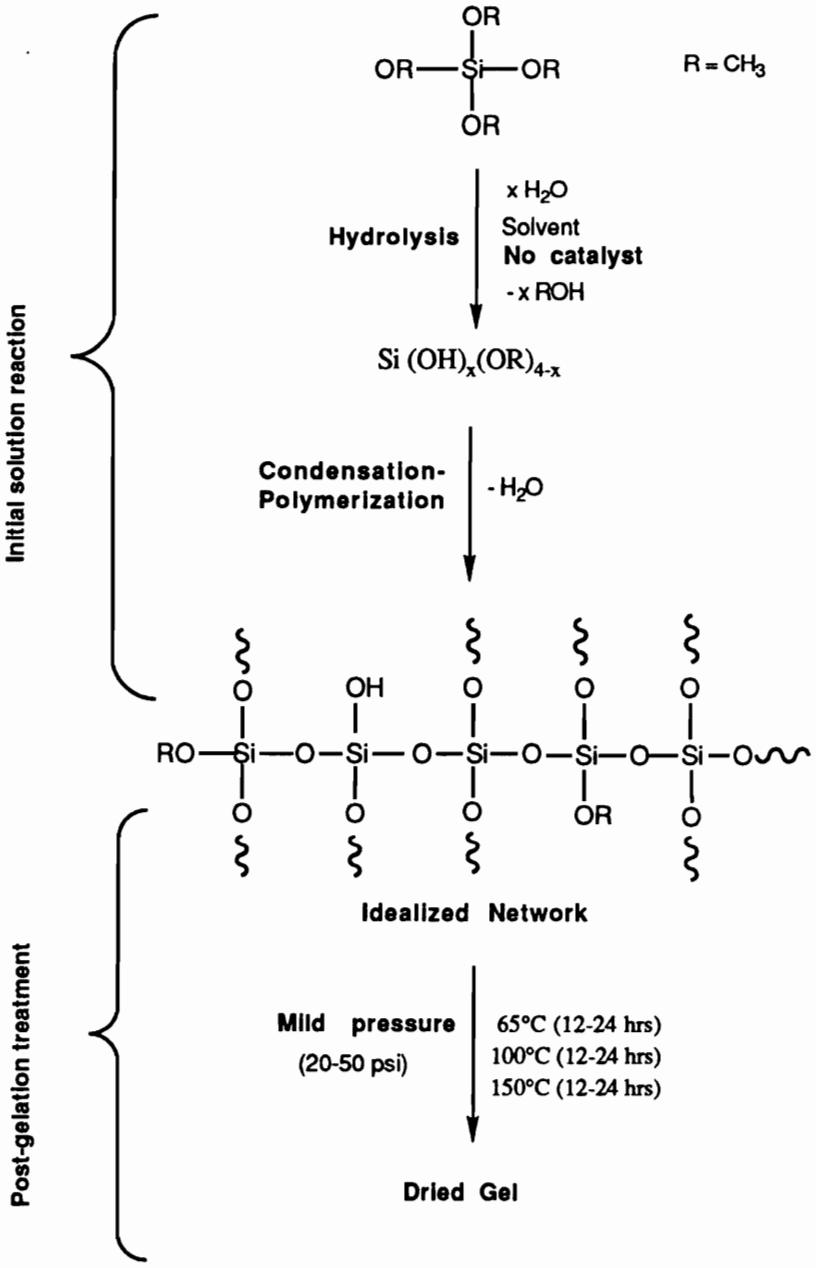

times correspond to sample removal. Typical $^1$H NMR spectra for a TMOS based sol-gel reaction are shown in ***Figure 1.17*** for two different reaction times. The resonances of interest are the ones at ca 3.5 and 3.3 ppm corresponding to the methoxy (Si-OC$\underline{H}_3$) and methanol protons (C$\underline{H}_3$OH), respectively. The methanol resonances in the $^1$H NMR spectra derive from two sources: from the reaction solvent and hydrolysis by-product. A decrease in the intensity of the methoxy protons and a corresponding increase in the intensity of the methanol protons accompanies the progression of the hydrolysis reaction. Therefore, for a mixture of known initial concentration, the extent of hydrolysis at any reaction time can be calculated from the ratio of the two peaks in the $^1$H NMR spectrum. It is important to point out that there are a number of reactions involving the species of interest in the system investigated, as summarized below:

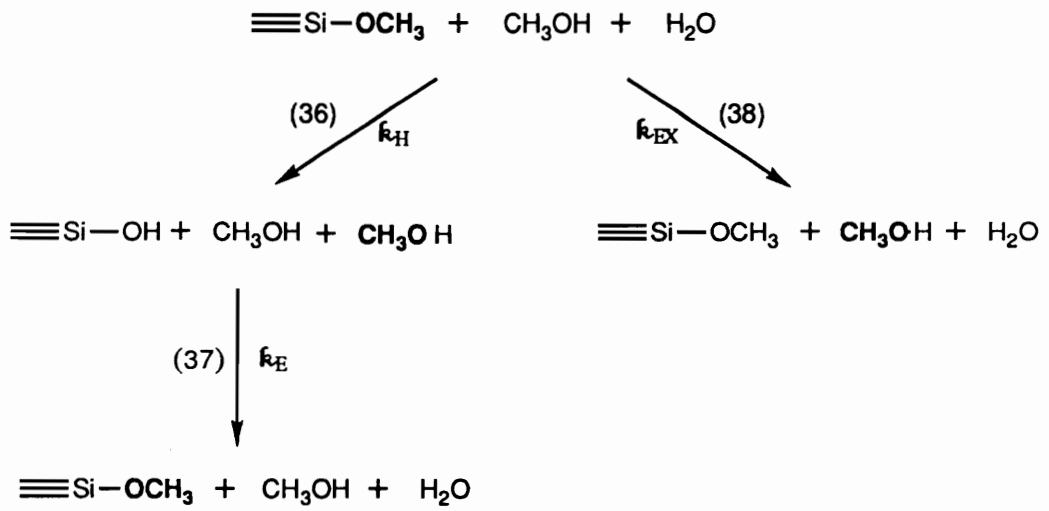


The hydrolysis reaction ($k_H$) described by equation (36) involves the conversion of silicon methoxide to silanol groups, with generation of methanol. Hence, as the hydrolysis proceeds, a decrease in the concentration of methoxy and a corresponding increase in the concentration of methanol protons will be observed in $^1$H NMR. This is considered to be by far the major reaction under the conditions investigated. Reesterification of silanol groups

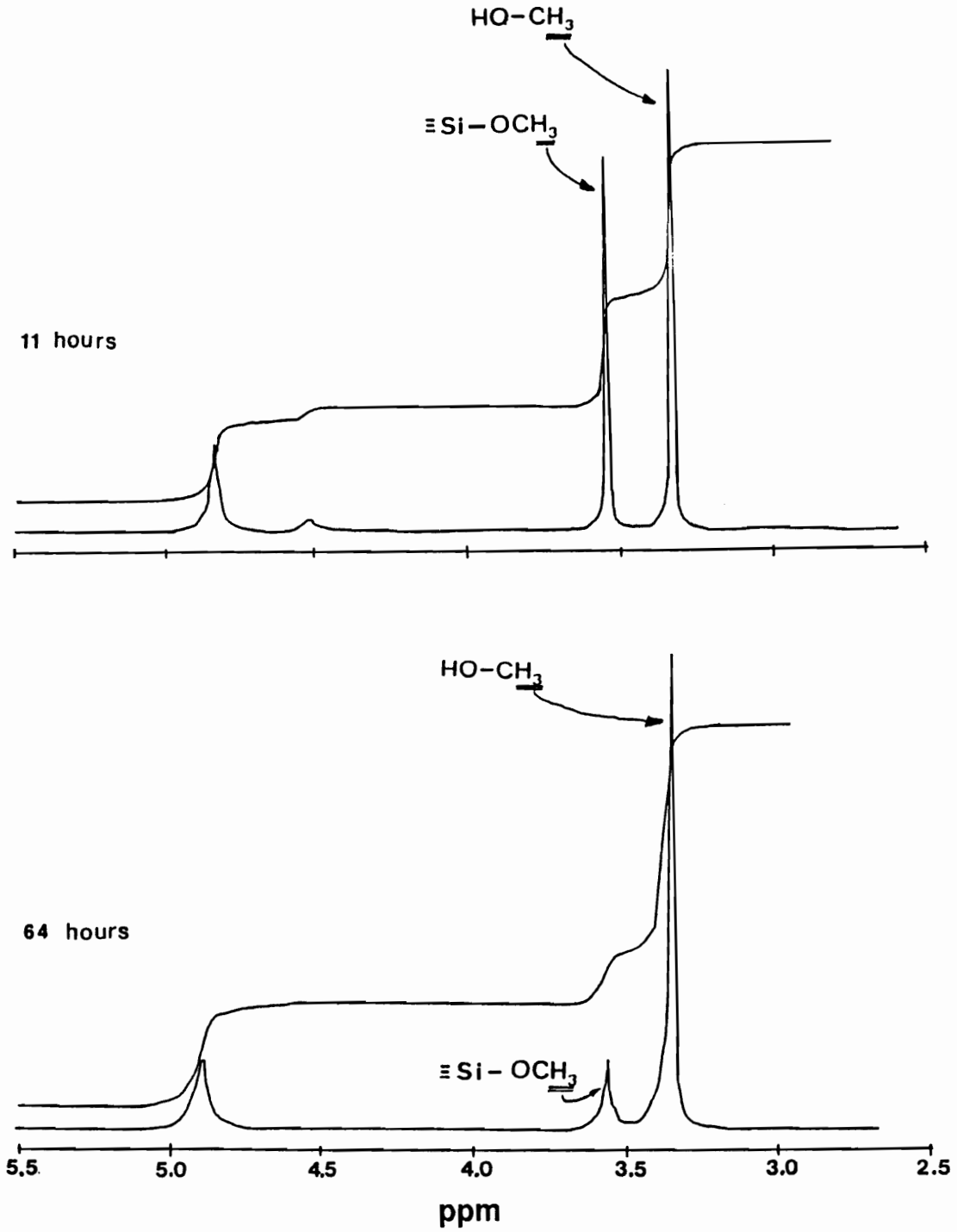


***Figure 1.17.*** $^{1}H$ NMR spectra at two different reaction times for a sol-gel reaction with initial composition TMOS:$CH_3OH$=1.0:5.0

($k_E$), which is the reverse of hydrolysis reaction can, in principle, take place according to equation 37. During these reactions, methanol is consumed and methoxy groups are generated, therefore an inverse effect would be seen during the $^1$H NMR measurements. The two processes (hydrolysis and reesterification) can not be separated from each other under the experimental conditions employed, and the net result is that an apparently lower hydrolysis rate would be measured if reesterification reactions have any considerable contribution under these conditions. Although the reesterification reactions are more important under acid-catalyzed conditions (see Literature review section 2.3.3), their contribution under the uncatalyzed conditions employed in this study is not known. For this reason, under the experimental conditions employed, relative rather than absolute hydrolysis rates are observed, since no corrections were made to account for the reverse hydrolysis in this system. Finally, a third reaction which can, in principle, take place in the system investigated is the methoxy-methanol exchange ($k_{EX}$) described by equation 38. This reaction has no effect on the observed $C\underline{H_3}OH/OC\underline{H_3}$ ratio in the $^1$H NMR, therefore it does not affect the observed rate. It is also assumed that no rapid exchange occurs between Si-$OCH_3$ and $CD_3OD$ during the acquisition time.

#### *4.1.1.1. Effect of TMOS:$H_2O$ ratio*

The amount of water utilized for the hydrolysis is one of the most important parameters affecting both the reaction rates and the network microstructure. As detailed in the Literature review, higher hydrolysis rates are obtained at higher water levels, while lower rates and incomplete conversions are achieved at low water concentrations, under both acid and base-catalyzed conditions. Furthermore, at very low or very high water concentrations low density gels are usually produced. Intermediate water concentrations that would result in relatively high reaction rates and high density gels were considered of interest for this study. Since incorporation of organic modifiers (functionalized oligomers) was intended to be carried out during the next stage of this

study, a minimum water concentration which would result in relatively high reaction rates, was desired. These reaction conditions would allow the hybrid synthesis at relatively high concentrations, without the risk of precipitating the organic oligomers.

Investigating the effect of the TMOS/$H_2O$ ratio in the particular sol-gel system selected for the present study was important for several reasons: Firstly, it was essential to determine the rate of TMOS hydrolysis, and its dependence on the concentration of water utilized in the initial hydrolysis stage. Secondly, it was important to determine the effect of water concentration on the condensation rates, and on the molecular growth mechanism in the sol-gel system investigated. Finally, it was desirable to determine if the amount of water utilized (in the intermediate water level) would be important for the generation of monolithic dried gel specimens. The effect of water on the hydrolysis rate will be discussed in this section, while aspects related to condensation reactions will be discussed in section 4.1.2.

Two water levels, corresponding to the $H_2O$:TMOS molar ratio of 2.5 and 4.0 respectively, were investigated in the intermediate water range. The ratio of 4.0 corresponds to the stoichiometric amount of water required for complete hydrolysis in the absence of condensation reactions. However, both water levels investigated were higher than the theoretical amount (2.0) required to complete the reaction under the conditions in which an infinite polymerization takes place (equation 22). Four series of experiments were carried out, corresponding to four different reaction concentrations. In each series, a constant molar ratio of $CH_3OH$:TMOS was maintained while the $H_2O$:TMOS ratio was varied from 2.5 to 4.0. The change in the concentration of methoxy reacting groups, [$OCH_3$], as a function of reaction time, is shown in ***Figure 1.18 (a, b, c,*** and ***d )***, for the above series of experiments. The data points in these plots were calculated

*Figure 1.18a.*

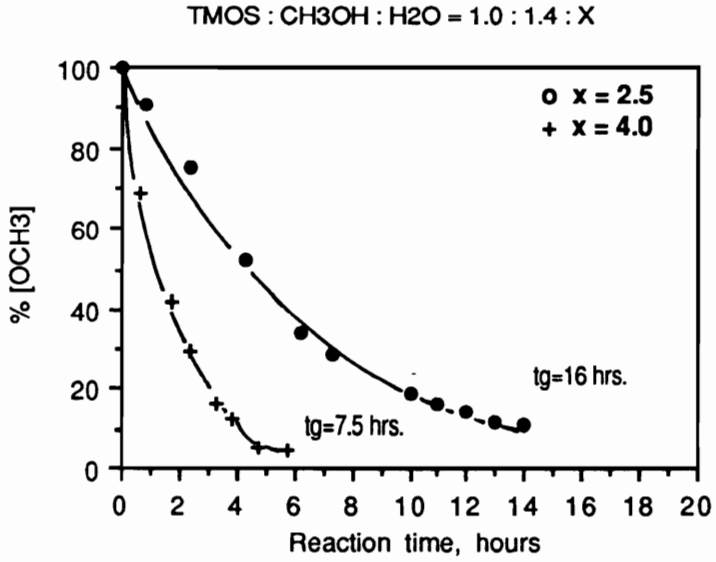


*Figure 1.18b.*

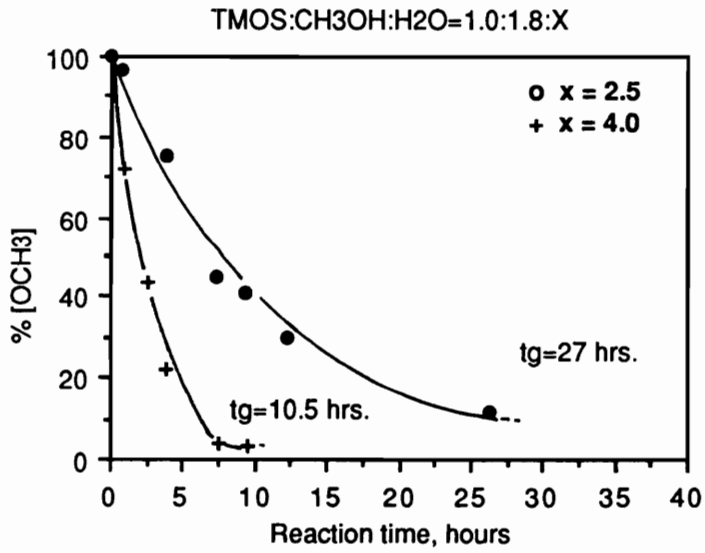

*Figure 1.18c.*

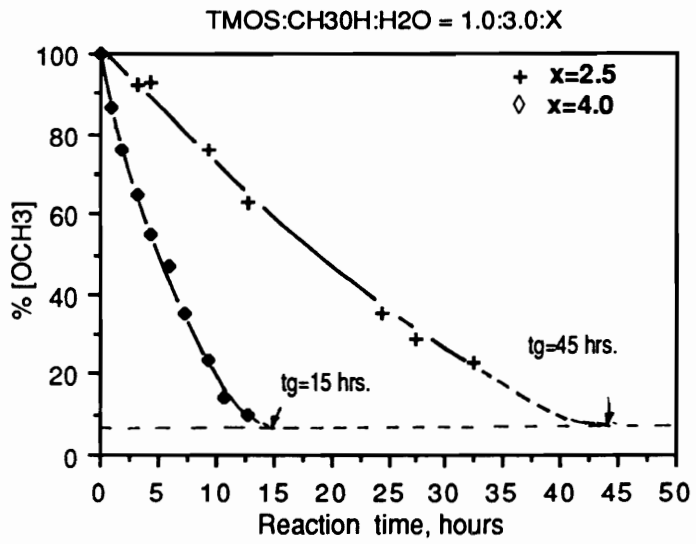


*Figure 1.18d.*

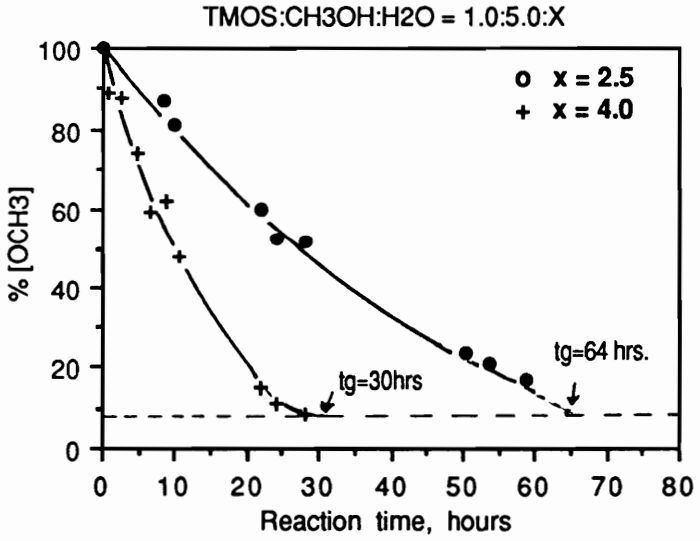


***Figure 1.18.*** The effect of water level on the hydrolysis rate at four different reaction concentrations.

from the $^{1}H$ NMR spectra at the corresponding reaction times. The last data point of each curve corresponds to the reaction composition right before gelation. The gelation times were also marked on each plot.

Increased hydrolysis rates and shorter gelation times were observed at higher water concentration, in all four series of experiments. In addition, a higher extent of hydrolysis at the time of gelation was accomplished for the reaction conditions in which higher water content was employed in the initial reaction stage. The gelation times and the extents of conversion at the gelation points are summarized in ***Table 1.5*** and ***Table1.6,*** respectively. It is worth pointing out that even though no direct information on condensation reactions is available from $^{1}H$ NMR, the above analysis indicates that condensation reactions must start before hydrolysis is completed. In the absence of condensation reactions, a maximum extent of hydrolysis of 62.5% would be achieved in the reaction in which an initial $H_2O$:TMOS ratio of 2.5 was employed. However, conversions as high as 89% were observed, as shown in Table 1.6, indicating that additional water was provided to the reaction mixture. The source of additional water was, most probably, the occurance of condensation reactions in which the water was generated as a reaction by-product. These observations are in agreement with the $^{29}Si$ NMR measurements which will be discussed later in this chapter.

#### *4.1.1.2. Effect of concentration*

The concentration of the reacting species was also known to be important for the hydrolysis rate. Four different concentrations were investigated, corresponding to the $CH_3OH$:TMOS molar ratios of 1.4, 1.8, 3.0 and 5.0 respectively. For each solvent concentration, two series of experiments were carried out, corresponding to a $H_2O$:TMOS molar ratio of 4.0 and 2.5 respectively. The

***Table 1.5.*** Effect of the initial water concentration on the gelation time in a TMOS sol-gel reaction

| $TMOS:H_2O$ / $TMOS:CH_3OH$ | Gelation time ($t_g$), [hours] | |
|---|---|---|
| | $TMOS:H_2O$ = 1.0:2.5 | $TMOS:H_2O$ = 1.0:4.0 |
| $TMOS:CH_3OH$ = 1.0:1.4 | 16 | 7.5 |
| $TMOS:CH_3OH$ = 1.0:1.8 | 27 | 10.5 |
| $TMOS:CH_3OH$ = 1.0:3.0 | 45 | 15 |
| $TMOS:CH_3OH$ = 1.0:5.0 | 64 | 30 |

***Table 1.6.*** Effect of the initial water concentration on the extent of hydrolysis at the gelation point in a TMOS sol-gel reaction

| $TMOS:H_2O$ / $TMOS:CH_3OH$ | Conversion,% | |
|---|---|---|
| | $TMOS:H_2O$ = 1.0:2.5 | $TMOS:H_2O$ = 1.0:4.0 |
| $TMOS:CH_3OH$ = 1.0:1.4 | 89 | 95 |
| $TMOS:CH_3OH$ = 1.0:1.8 | 87.5 | 95 |
| $TMOS:CH_3OH$ = 1.0:3.0 | 84 | 92 |
| $TMOS:CH_3OH$ = 1.0:5.0 | 84 | 91.5 |

conversion versus time results are summarized in ***Figure 1.19a*** and 1.***19b*** for the two series of experiments. These graphs were constructed from the same data used to generate Figures 1.18a through 1.18d, however, rearranged such as to indicate the effect of concentration.
The reaction concentration highly affected the hydrolysis rate and the gelation time: increased hydrolysis rates, and correspondingly decreased gelation times were observed at higher reaction concentrations. However, the reaction concentration did not have a significant effect on the extent of conversion at the gelation point. These concentration effects are summarized in ***Table 1.7*** and ***Table 1.8*** respectively, generated by rearranging the data in Table 1.5 and Table 1.6.

Based on the above data, it follows that in order to achieve faster hydrolysis rates and higher conversions, under the experimental conditions investigated, it is important to use higher water levels and higher reaction concentrations. Gelation times as short as 7.5 hours were obtained for higher water concentration (TMOS:$H_2O$ =1.0:4.0) and for more concentrated solutions (TMOS:$CH_3OH$ =1.0:1.4), which is quite a remarkable reaction rate for an uncatalyzed, room temperature reaction.

#### *4.1.1.3. Effect of pressure*

During our investigations of sol-gel reactions we found that the use of mild pressures (30-50psi) for the drying of the gels was essential for the generation of monolithic type samples. In order to understand how the moderate pressure affects the drying process, it was of interest to investigate its effect on the reaction rates. It has already been discussed (section 2.4.1.7) that high pressures have a dramatic accelerating effect on the reaction rates. In this study, the range of moderate pressures was of interest. The reactions for this investigation were carried out in a pressure reactor, shown in ***Figure 1.20*** which was designed and built in our labs. The pressure reactor was based on the commercially available Fisher-Porter bottles (Lab Crest Scientific Glass

*Figure 1.19a.*

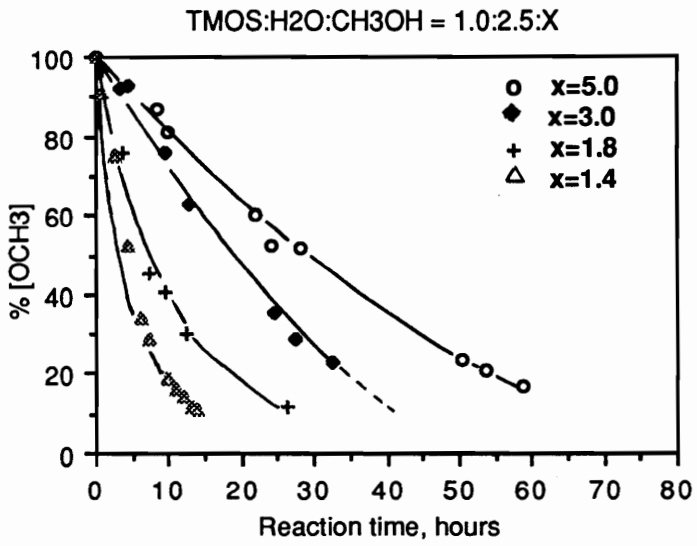


*Figure 1.19b.*

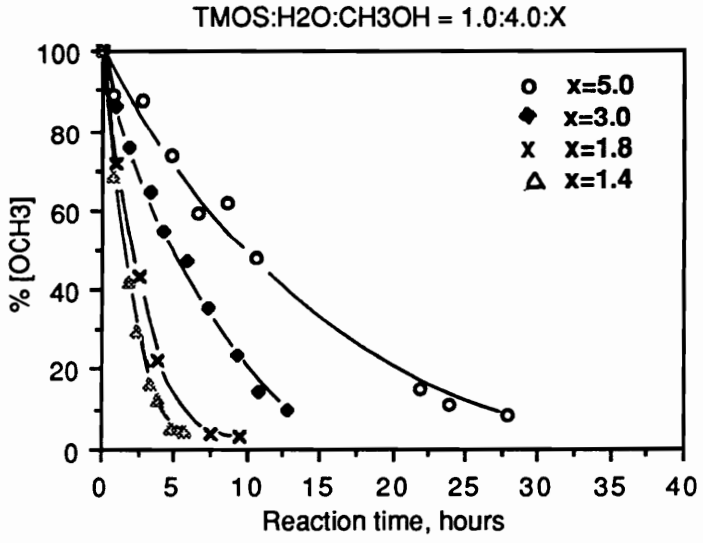


***Figure 1.19.*** Effect of reaction concentration on the hydrolysis rate in a TMOS sol-gel reaction

***Table 1.7.*** Effect of reaction concentration on the gelation time in a TMOS sol-gel reaction

| | **Gelation time ($t_g$), [hours]** | | | |
|---|---|---|---|---|
| | **TMOS:$CH_3OH$** | | | |
| | 1.0:1.4 | 1.0:1.8 | 1.0:3.0 | 1.0:5.0 |
| **TMOS:$H_2O$** = 1.0:2.5 | 16 | 27 | 45 | 64 |
| **TMOS:$H_2O$** = 1.0:4.0 | 7.5 | 10.5 | 15 | 30 |

***Table 1.8.*** Effect ofreaction concentration on the extent of hydrolysis at the gelation point in a TMOS sol-gel reaction

| | **% Conversion** | | | |
|---|---|---|---|---|
| | **TMOS:$CH_3OH$** | | | |
| | 1.0:1.4 | 1.0:1.8 | 1.0:3.0 | 1.0:5.0 |
| **TMOS:$H_2O$** = 1.0:2.5 | 16 | 27 | 45 | 64 |
| **TMOS:$H_2O$** = 1.0:4.0 | 7.5 | 10.5 | 15 | 30 |

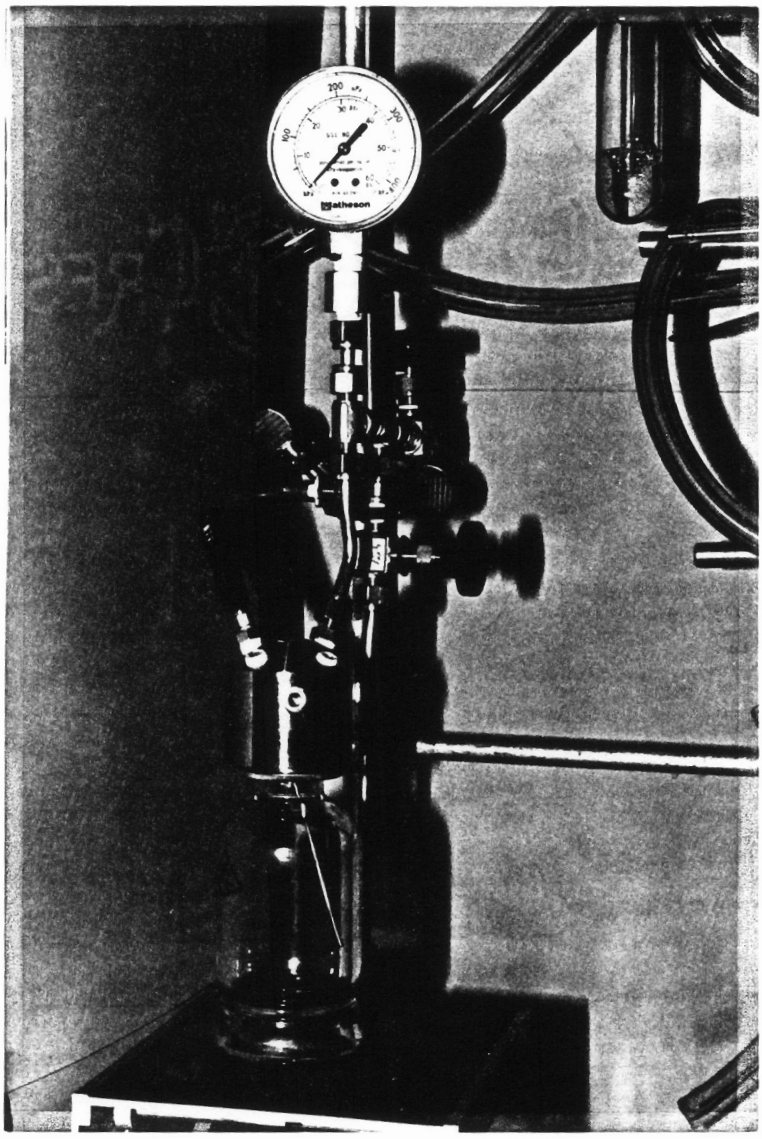


***Figure 1.20***. Laboratory reactor for controlled pressure and temperature.

Company, Warminster, PA, (215) 674-6614). For more details on the design of the pressure reactor the reader is refered to [146]. Two pressures were investigated in the range of interest: 20psi (1.4 atm), and 50 psi (3.4 atm). $^1$H NMR samples were removed from the reactor as a function of reaction time, and the extent of hydrolysis was calculated, as previously described. The change in the concentration of the methoxy groups as a function of the reaction time, for the conditions investigated is plotted in ***Figure 1.21***. It is evident that in the range of pressure employed for drying of the gels, there is no apparent effect on the hydrolysis rate. The role of pressure on the drying of the gels will be discussed later in this chapter.

#### *4.1.1.4. Effect of temperature*

As described in Chapter 2 Literature Review, increasing temperature generally results in an increased reaction rate and shorter gelation times. The use of temperature as an alternative approach for rate increase would be highly desirable for the uncatalyzed TMOS system. To investigate this effect, two reactions of similar compositions (TMOS:$CH_3OH$:$H_2O$=1.0:1.4:2.5) were carried out side by side at room temperature and 60°C respectively. $^1$H NMR samples were removed as a function of time and the extents of hydrolysis were determined at the corresponding reaction times. While the reaction carried out at room temperature required approximately 5 hours to reduce the concentration of methoxy groups to half of their initial value, the same reaction occured in less than 2 hours at 60°C. Correspondingly, the gelation time was reduced from 16 hours (at room temperature) to 4 hours (at 60°C). However, the gels generated at elevated temperature were cloudy and showed a particulate nature. It is possible that the temperature increase resulted in a change of the growth mechanism during the condensation-polymerization reactions. While no detailed investigations were carried out to prove this assumption, the use of higher temperatures as a mean to increase the reaction rate in the initial

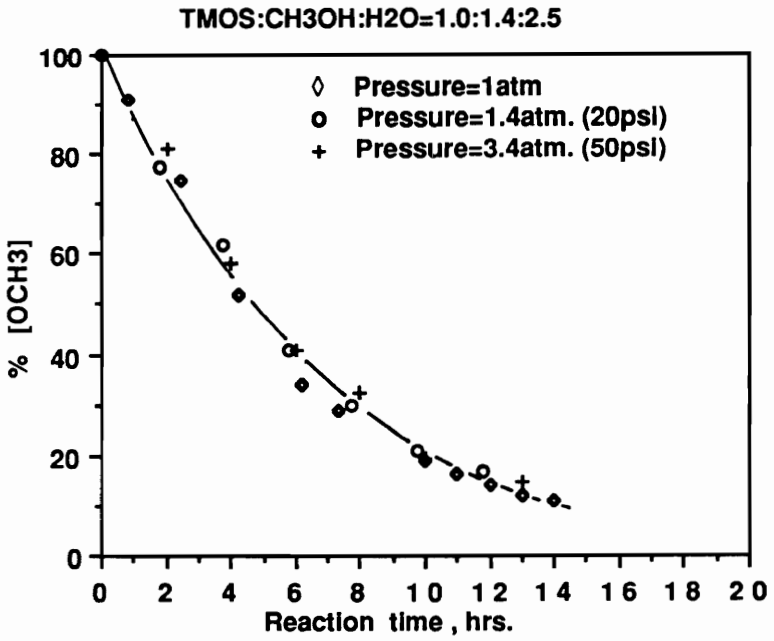


***Figure 1.21.*** Effect of pressure on the initial reaction rate in a catalyst-free, TMOS based, room temperature sol-gel reaction

reaction stages was not considered in this study, due to the observed undesired changes in the macroscopic properties of the networks generated under these conditions.

### *4.1.2. Effect of reaction parameters on the condensation rate*

$^{1}H$ NMR techniques discussed in the previous section are very useful for the study of hydrolysis rates in sol-gel reactions. However, they provide little or no information about the competing condensation reactions which may be occuring simultaneously into the system. $^{29}Si$ NMR, a technique very sensitive to the silicon local environment, is a complementary technique for the study of sol-gel reactions. A typical $^{29}Si$ NMR spectrum for a sol-gel reaction based on TMOS is shown in ***Figure 1.22(A).*** A commonly encountered problem in $^{29}Si$ NMR studies is the presence of a broad resonance signal centered at approximately -110 ppm and which arises from the glass sample tube or the probe insert, and obscures a large portion of the high resolution spectrum. This broad signal interferes with resonances arising from sol-gel reactions. Because of the above mentioned spectral interference, the use of $^{29}Si$ NMR techniques for the study of sol-gel reactions has been previously limited to qualitative studies [147] or made use of a special probe [148]. In the present study, subtraction techniques were developed in order to eliminate the spectral interference. ***Figure 1.22(B)*** shows the same spectrum after subtraction. The spectral assignments which are detailed in ***Figure 1.23,*** are reproduced from published literature [148]. These assignments are based upon numerous reference spectra (specifically work done by Harris, Engelhardt, Hoebbel, and their collaborators [149-154]). The symbol $Q^{i}$ is used to represent specific silicate structural units, where i refers to the number of siloxane bridges generated through condensation reactions. Hence, $Q^{0}$ designates the silicate units which did not undergo any condensation reactions, i.e., monomers and partially or completely hydrolyzed monomers (in which R is either methoxy or/and hydroxy). Depending upon the extent of hydrolysis, a total of five monomeric units of the type $[Si(OCH_3)_x(OH)_{4-x}]$ may exist, where x can

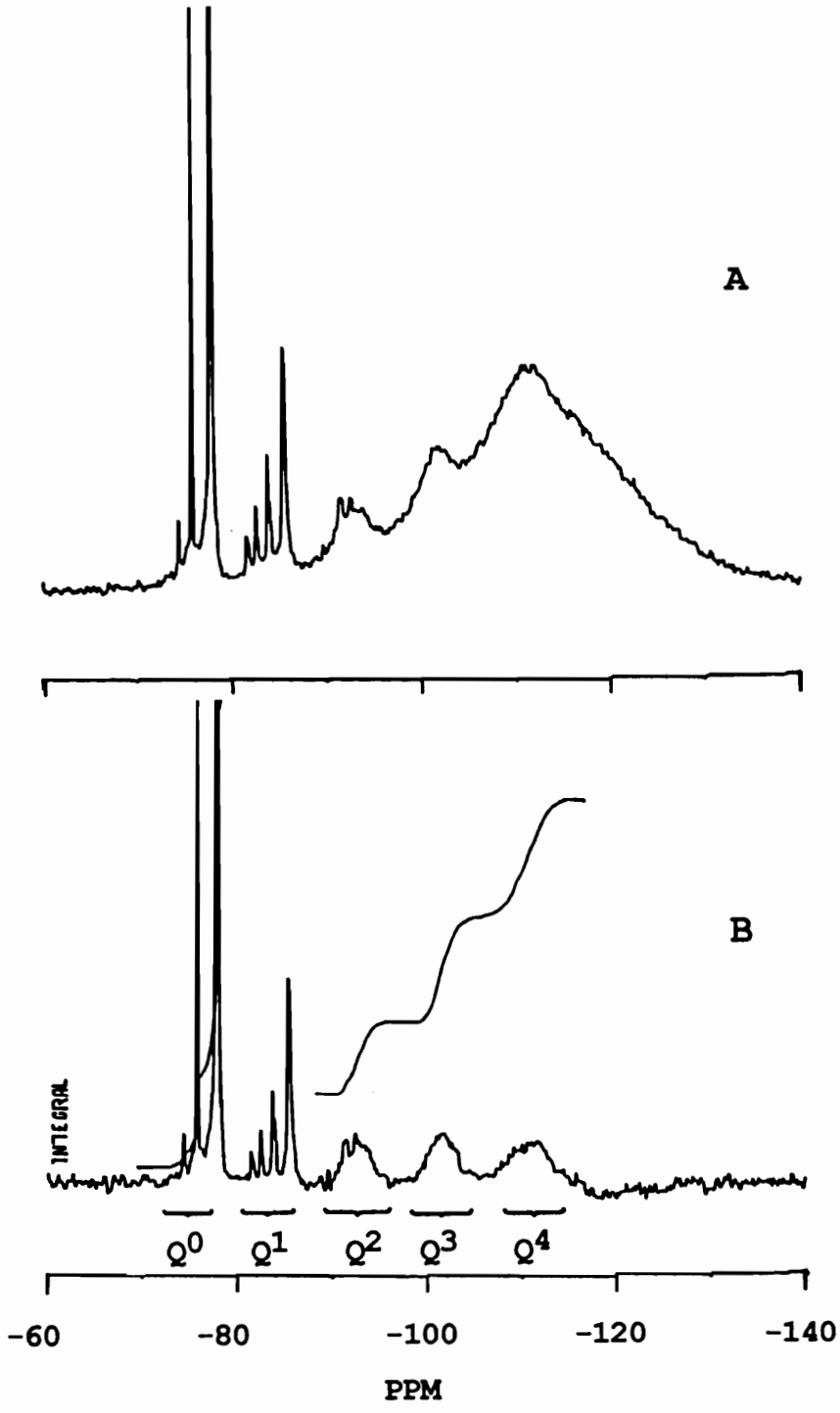


***Figure 1.22.*** $^{29}Si$ NMR spectra for a sol-gel reaction with initial molar composition TMOS:$H_2O$:$CH_3OH$=1.0:4.0:1.4 ; (A) before and (B) after subtraction.

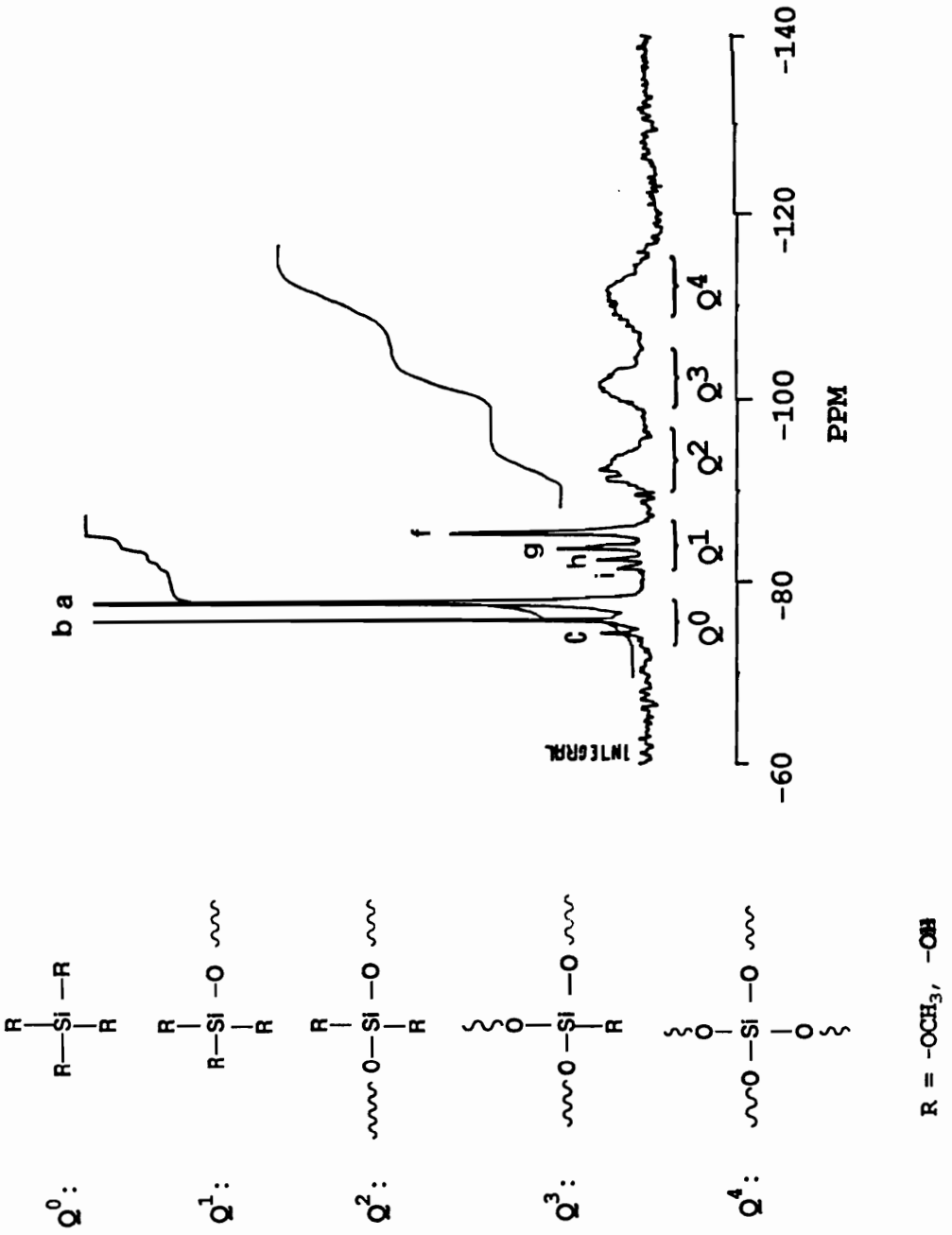


***Figure 1.23.*** Spectral assignments for $Q^i$ silicate units generated during sol-gel reaction [148]. Initial reaction composition TMOS:$H_2O$:$CH_3OH$=1.0:4.0:1.4

vary from 0 to 4. The exact assignment of the individual resonances in the monomeric group was based on the relative position of tetrasilicic acid, $Si(OH)_4$ [154] with respect to unreacted TMOS [$Si(OCH_3)_4$]. All chemical shifts are summarized in ***Table 1.9.*** The resonances of the group labeled $Q^1$ are assigned to the silicate units which underwent one condensation reaction (i.e., end group silicones).

Again, depending upon the character of the substituents directly attached to the silicon nucleus giving rise to the signal, four resonances may exist, as listed in Table 1.9. Each of these resonances exhibits fine structure due to the additional chemical shift caused by the nature of the substituents attached to the silicon adjacent to the silicon nucleus giving rise to the signal. These fine structures are difficult to resolve with the 39.765 MHz instrument employed for this investigation. $Q^2$ bands refer to the silicate units which underwent two condensation reactions (i.e., middle groups on a linear chain); $Q^3$ designates the silicate units which developed three siloxane bridges , and $Q^4$ refers to the silicate units which reacted through all four of their functionalities into the three dimensional network (i.e., branching and crosslinking points). Therefore the general trend is that as the number of siloxane bridges generated through condensation reactions increases from zero to four, the silicon nuclei become more polarizable, and the respective silicate units will resonate at higher and higher field. As it can be observed from Figure 1.23, the $Q^2$, $Q^3$, and $Q^4$ bands are quite broad. The breadth of these bands is due to the overlap of a large number of single resonance lines produced as a result of the highly varied chemical environment surrounding the silicon nuclei of condensed oligomeric species.

Due to the complexity of these structures, the use of $^{29}Si$ NMR spectroscopy as a structure identification tool is limited to the study of the initial stage of the sol-gel process, before the formation of the highly condensed oligomeric species. The use of high field NMR instruments

***Table 1.9.*** $^{29}Si$ chemical shifts for the $Q^0$ through $Q^4$ structural units (given in ppm with respect to TMS) [66]

| Silicate unit/type | | Structure | $d_{Si}$, ppm |
|---|---|---|---|
| $Q^0$ | a | $Si(OCH_3)_4$ | -79.0 |
| | b | $Si(OCH_3)_3(OH)$ | -77.0 |
| | c | $Si(OCH_3)_2(OH)_2$ | -75.6 |
| | d | $Si(OCH_3)(OH)_3$ | -74.5 |
| | e | $Si(OH)_4$ | -73.7 |
| $Q^1$ | f | $\underline{Si}(OCH_3)_3$-O-Si- | -86.5 |
| | g | $\underline{Si}(OCH_3)_2(OH)$-O-Si- | -85.1 |
| | h | $\underline{Si}(OCH_3)(OH)_2$-O-Si- | -83.9 |
| | i | $\underline{Si}(OH)_3$-O-Si- | -83.0 |
| $Q^2$ | | -O-Si$(OR)_x(OH)_{2-x}$ - O- | -91.0 to -95.0 |
| $Q^3$ | | -O-Si$(OR)_x(OH)_{1-x}$ - O-<br>O | -99.0 to -106 |
| $Q^4$ | | O<br>—O—Si—O—<br>O | -108 to -116 |

with increased sensitivity and spectral dispersion can provide further details on the structure of oligomers and polymers of reacting sol-gel systems [154]. When investigating the hydrolysis-condensation reaction as a function of time by means of $^{29}Si$ NMR spectroscopy, one usually has to make a choice between a prolonged measurement, resulting in a spectrum with a good signal-to-noise ratio but mean (average) reaction time [156-160], and a measurement during a short period, giving a less accurate spectrum but a better defined reaction time [156, 161]. Another possibility to avoid this problem is to follow the reaction at such a low temperature that during the measurement the changes are negligibly small [162]. In this way, a good signal-to-noise ratio can be obtained at each moment of reaction time. However, this procedure is more difficult and time consumming. During our study the first approach was taken, using a prolonged measurement in order to obtain a good signal-to-noise ratio. For each $^{29}Si$ NMR sample, 600 scans were accumulated over approximately a one hour period (a pulse repetition rate of 6 seconds being used). The reported times of the spectra are the midpoints of data acquisition.

In order to apply the subtraction technique, a blank measurement was carried out for each sample. The blank consisted of 600 scans of the same NMR tube employed for that particular sample and containing only the deuderated solvent. These scans were acquired under identical conditions to those employed for the sample itself.

The alkoxide-to-water ratio is one of the most important parameters affecting the hydrolysis and condensation reactions in sol-gel processes. Unlike other parameters such as concentration, pressure, etc., the water participates directly in the reaction and its concentration is believed to affect not only the reaction rate, but also the growth mechanism. The effect of water on the condensation reactions was investigated by $^{29}Si$ NMR techniques detailed in this section. This investigation was important for two reasons. Firstly, it was of interest to evaluate the relationship

between hydrolysis and condensation reactions, in order to develop an understanding of the growth mechanism during condensation-poymerization reactions, under the particular conditions investigated (no added catalyst, hence relatively neutral reaction environment). Secondly, it was important to determine if small changes in the concentration of water, in the range of intermediate water levels used in this study, may affect the growth mechanism in the system.

The sol-gel reactions for the $^{29}Si$ NMR investigations were performed in deuderated methanol ($CD_3OD$) which was also the NMR solvent. Samples were removed as a function of reaction time, mixed with small amounts of $Cr(AcAc)_3$ such as to result in an approximately 0.4 M concentration of the relaxation agent, and immediately analyzed. All resonances are reported with respect to TMS which was used as an external standard. Two water concentrations were investigated corresponding to an $H_2O$:TMOS ratio of 4.0 and 2.5, respectively. As previously described, the ratio of 4.0 corresponds to the stoichiometric amount of water necessary for complete hydrolysis in the absence of any condensation reactions, while the ratio of 2.5 corresponds to less than stoichiometric amount of water. As already known from the $^1H$ NMR analysis, the two reactions occured on a different time scale. In order to allow for a direct comparison of the two reactions, a reduced time was employed. The reduced reaction time, $\tau$, is defined as the ratio between the reaction time (t) and the gelation time ($t_g$).

Subtracted $^{29}Si$ NMR spectra as a function of reduced reaction time, for the two reaction conditions investigated are shown in ***Figure 1.24***. The most important qualitative observations are summarized below: Firstly, the two series of spectra indicate that the same type of silicate units were formed under the two reaction conditions, as the reactions progressed. This implies that a similar growth mechanism operates under the two reaction conditions investigated, and that the mechanism was not affected by the change in the water level from the ratio of 2.5 to 4.0.

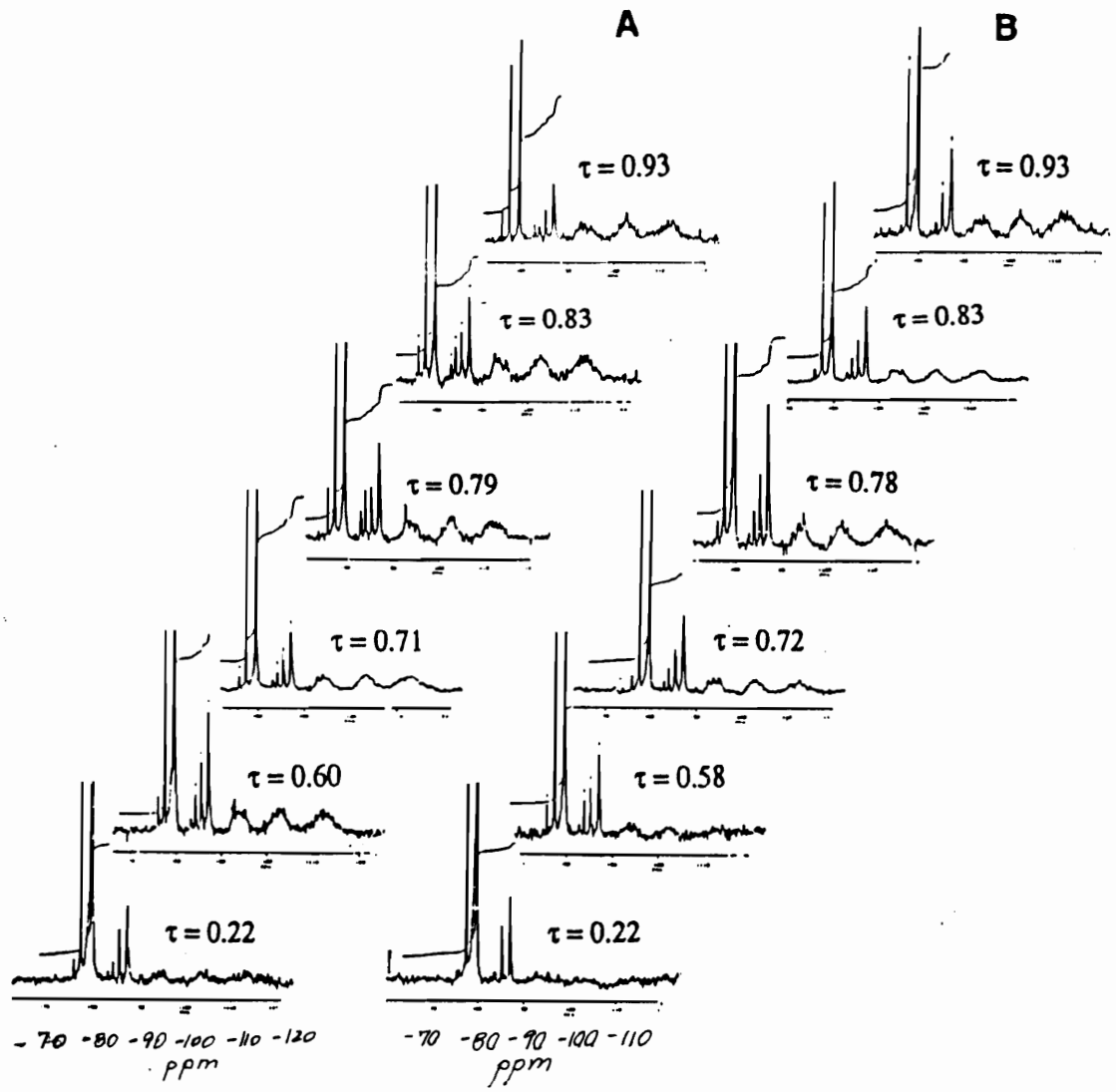


***Figure 24.*** Subtracted $^{29}Si$ NMR spectra as a function of reduced reaction time τ ($\tau=t/t_g$)

(A) TMOS:$H_2O$:$CH_3OH$=1.0:**4.0**:1.4

(B) TMOS:$H_2O$:$CH_3OH$=1.0:**2.5**:1.4

Secondly, the relationship between hydrolysis and condensation reactions becomes evident. The $^{29}Si$ NMR spectra indicate the presence of condensed species (up field from -80 ppm), at short reaction times (low $\tau$), for both reaction conditions. This suggests that condensations began early in the reaction, long before hydrolysis was completed. Additionally, monomer and partially hydrolyzed monomer species (down field from -80 ppm) were still present in both reaction mixtures, at long reaction times (high $\tau$), indicating that hydrolysis reactions were not completed at times close to gelation. The overall observation is that under the conditions investigated hydrolysis and condensation reactions were highly competitive, taking place simultaneously. This is an intermediate behavior between an acid and a base-catalyzed sol-gel reaction and it is what would be expected for a non-catalyzed system. It becomes therefore obvious that the TMOS sol-gel reaction described by Scheme 1.12 is just a schematic representation. The hydrolysis and condensation reactions are not sequential processess as implied by this oversimplified representation, but rather a complex process in which the two reactions take place simultaneously, generating siloxane type species with a complex chain topology. Finally, it is important to notice that highly hydrolyzed monomeric species are not formed, at any reaction time, for any of the two conditions investigated. This is more clearly ilustrated in ***Figure 1.25*** in which the spectral region corresponding to the $Q^0$ and $Q^1$ silicate units was expanded. The assignments **(a)** through **(l)** for different species corresponding to $Q^0$ and $Q^1$ silicate units have been explained in Table 1.9 of this section, page 141.

The $^{29}Si$ NMR spectra in Figure 1.24 were integrated and typical results for the change in the concentration of monomeric and polymeric species as a function of reduced reaction times are described in ***Figure 1.26*** for both reactions investigated. In these plots, all the silicate units which did not undergo any condensation reactions ($Q^0$ type silicate units) are included under the

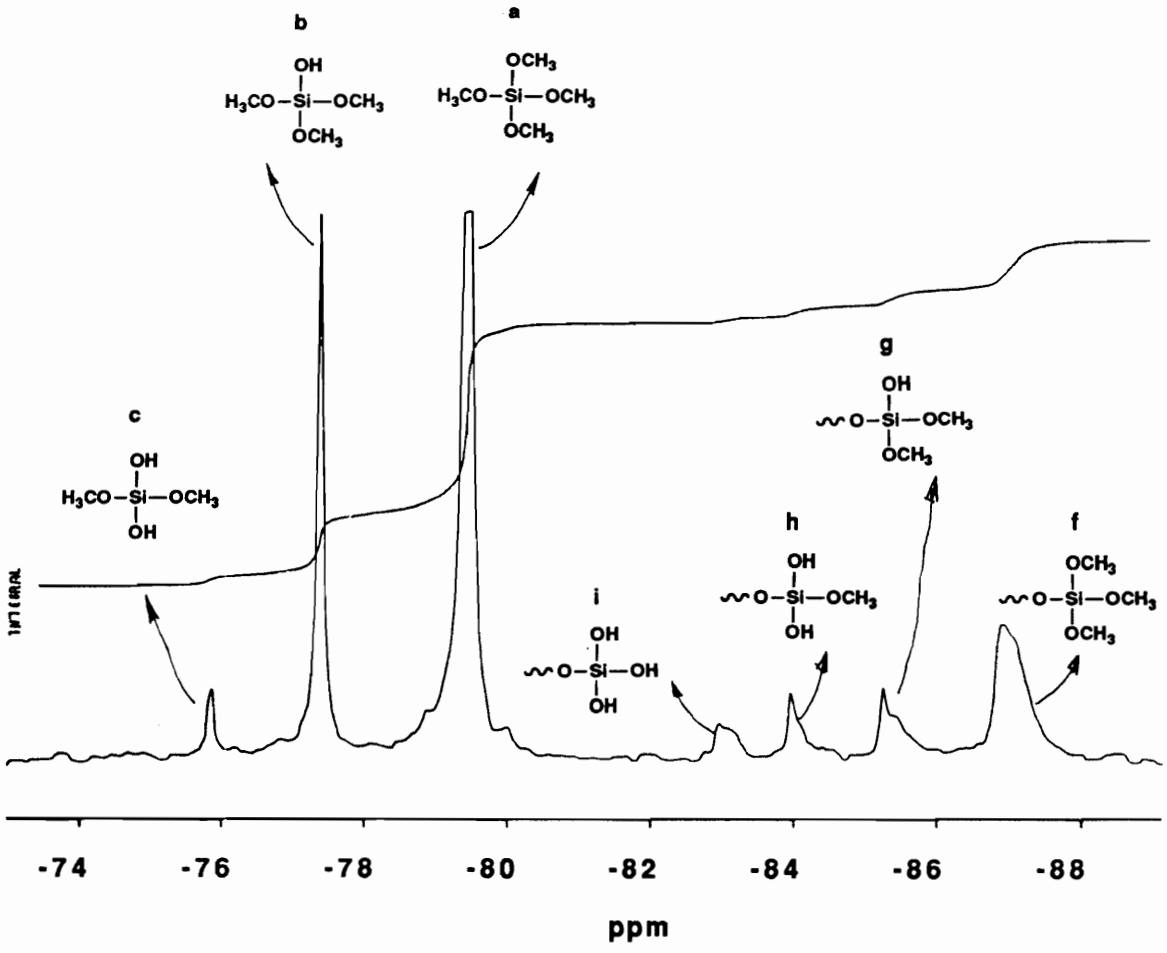


***Figure 1.25.*** $^{29}Si$ NMR spectrum for a sol-gel reaction with initial composition TMOS:$H_2O$:$CH_3OH$=1.0:**4.0**:1.4 (reaction A), at $\tau$=0.79 (where $\tau$ is the reduced reaction time; $\tau=t/t_g$) . Expanded $Q^0$ and $Q^1$ regions.

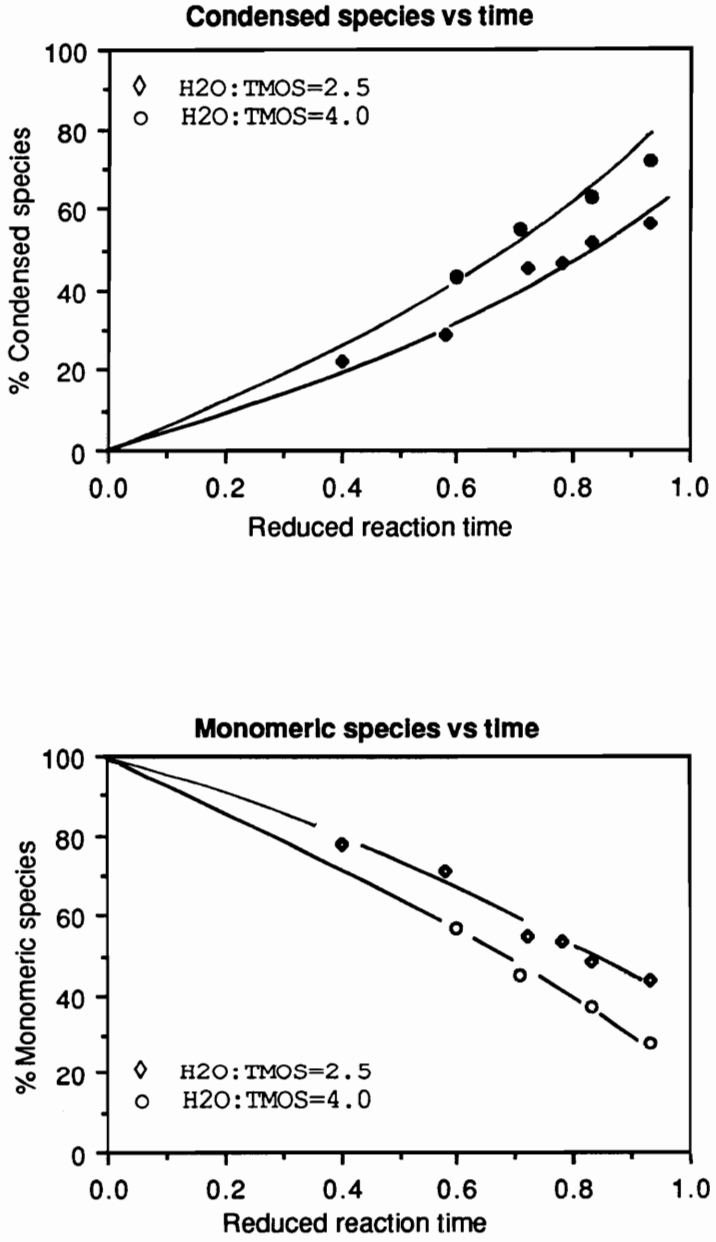


***Figure 1.26.*** Concentration of polymeric and monomeric species as a function of reduced reaction time (calculated from $^{29}Si$ NMR spectra in Figure 1.24)

monomeric species; the condensed or "polymeric" species comprise all the other silicate units ($Q^1$ through $Q^4$). At any reaction time, the concentration of polymeric species is higher and the concentration of monomeric species is correspondingly lower for the reaction conditions in which a stoichiometric amount of water was utilized in the initial hydrolysis step; in other words, faster condensation rates and higher conversion were achieved under these reaction conditions.

The distribution of species with different degree of hydrolysis within $Q^0$ and $Q^1$ silicate units was determined by integration, and the results are plotted in ***Figure 1.27a*** and 1.***27b*** respectively. At any reaction time, the concentration of **a** species (tetraalkoxide monomer) is higher than the concentration of **b** species (monomer units which underwent one hydrolysis reaction), which in turn, is higher than the concentration of **c** species (monomer units which underwent two hydrolysis reactions). Higher hydrolyzed monomeric units (d,e) were not observed, within the limits of detection of the NMR instrument. This trend indicates that, under the reaction conditions investigated, the first hydrolysis of the tetraalkoxide monomer was more favored than the second, and a third hydrolysis was not likely to occur. A similar trend was observed for the species **f** through **I** belonging to the $Q^1$ type silicate units (end groups): the first hydrolysis of the end groups was more favored than the second, which in turn was more favored than the third. The described trends imply that under the reaction conditions investigated hydrolysis did not produce orthosilicic acid monomers and condensation started between incompletely hydrolyzed species. The result is that under the relatively neutral reaction conditions employed, less highly crosslinked polymers than those produced in alkaline solutions [43], are usually formed. Of course, this is true in the range of intermediate water level investigated in this study, and it may change at high water concentrations. This growth mechanism more closely resembles the acid-catalyzed sol-gel reactions.

**(a)** a, b, and c species ($Q^0$ type silicate units), where a= $Si(OCH_3)_4$; b=$(HO)Si(OCH_3)_3$; c=$(HO)_2Si(OCH_3)_2$

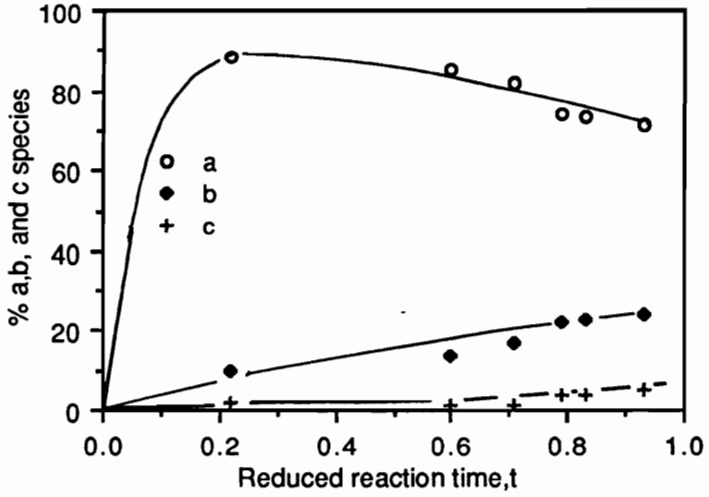


**(b)** f, g, h, and i species ($Q^1$ type silicate units), where f = -O-$Si(OCH_3)_3$; g = -O-Si(OH)$(OCH_3)_2$; h = -O-$Si(OH)_2(OCH_3)$; i = --O-$Si(OH)_3$

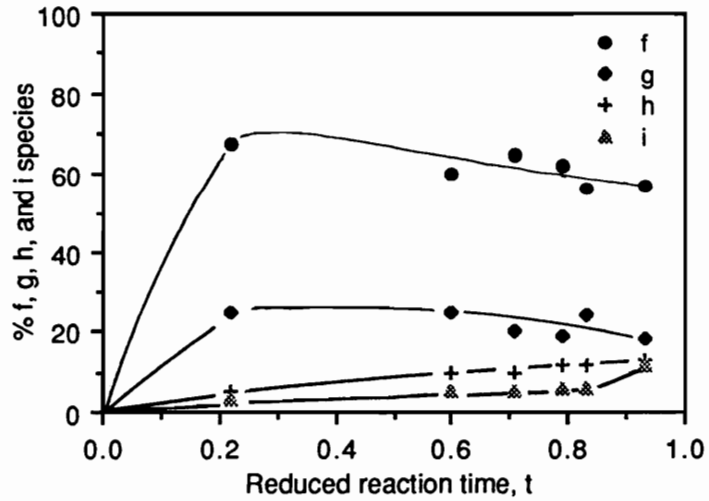


***Figure 1.27.*** Percent silicate species with different extent of hydrolysis as a function of reduced reaction time.

### *4.1.3. Effect of reaction parameters on the extent of conversion*

#### *4.1.3.1. Solid state MAS $^{29}Si$ NMR*

The previously discussed solution NMR techniques can be employed to study the progression of hydrolysis and condensation reactions up to the development of the insoluble three-dimensional networks (gel point). Beyond gelation, however, such solution techniques can no longer be used. The extent of conversion in the gelled samples can be determined by solid state NMR. The solid state $^{29}Si$ NMR.analyses were carried out under the conditions detailed in section 3.6.3. Two typical MAS $^{29}Si$ solid state NMR spectra are shown in ***Figure 1.28*** for two of the $SiO_2$ gels which were previously dried up to a maximum temperature of 500°C and room temperature respectively. Both samples contain three resonances corresponding to the silicate units which reacted through two ($Q^2$), three ($Q^3$), or all four ($Q^4$) of their functionalities into the three dimensional $SiO_2$ network. The spectral assignments are similar to those just discussed for the solution $^{29}Si$ NMR and detailed in Table 1.9 (Section 4.1.2.).

It is notable that resonances corresponding to $Q^1$ silicate units are not present and only very small $Q^2$ resonances are observed. This indicates that the dried gels do not contain any dangling ends ($Q^1$) and that only a few linear segments ($Q^2$) are still present. Furthermore, since $Q^0$ resonances were not observed in any of the gels (even the one reacted at room temperature), one can conclude that unreacted precursors are not likely present as trapped species in the gel network. Since these gels were not extracted prior to NMR analysis, any unreacted precursors trapped in the gel network would have been observed in the NMR spectra.

In the MAS $^{29}Si$ NMR the observed peaks are inherently quantitative with respect to the amount of a given silicate species present in the sample, provided the delay time between pulses is at least three times longer than the $T_1$ of the slowest relaxing species. In the system under

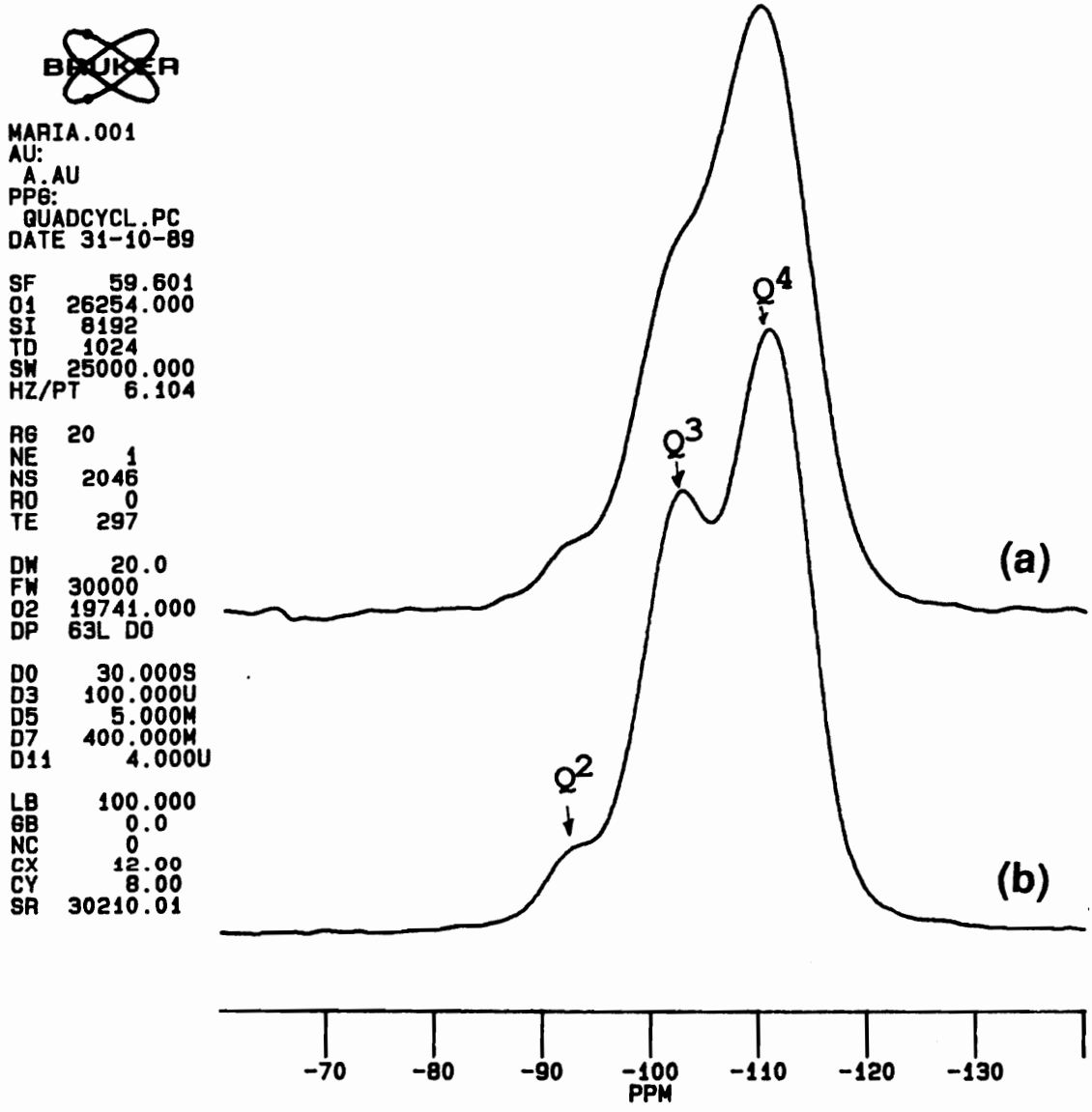


*Figure 1.28.* Typical Magic Angle Spinning $^{29}Si$ Solid State NMR for $SiO_2$ gels;

(a) $T_{max}$ = 500°C, and (b) $T_{max}$ = RT.

investigation the slowest relaxing species are the $Q^4$ silicates. In order to be able to meaningfully quantitate the MAS spectra obtained for the various gels, determination of the $T_1$ for the $Q^4$ type silicons would be necessary. For the present investigation a 30 s relaxation delay between scans was used. Relaxation delays between 5s and 300s have been reported in the literature for these systems [162]. Hartman et al., [162] reported that an increase of the relaxation delay from 5s to as much as 300s between scans did not significantly change the peak width (in ppm) or relative peak area.

Each spectrum obtained for gels generated under different reaction and processing conditions can be fitted quite well in an iterative curve fitting program by the superposition of three Gaussians centered at -93 ppm ($Q^2$), -102.5 ppm ($Q^3$) and -112ppm ($Q^4$). ***Figure 1.29*** gives an example of the deconvolution method employed in analyzing the $^{29}Si$ NMR spectra, and ***Table 1.10*** summarizes the relative percentage of the various silicate structures in the gelled materials. The amount of each type of $Q^i$ silicate units (listed in column 2), contained in the dried gels generated under the reaction and prodessing conditions listed in column 1, was calculated using the peak height % H, (column 3), as well as the peak area % A (column 4) from the deconvoluted spectra. The compiled NMR data in Table 1.10 allow for the calculation of the degree of reaction which is also tabulated in column 7. The extent of conversion (p) for a given gel system was calculated by comparing the number of reacted functional groups ($N_r$) given in column 6, to the number of theoretical functional groups ($N_{th}$) listed in column 5:

$$p = \frac{N_r}{N_{th}} \times 100 \qquad (39)$$

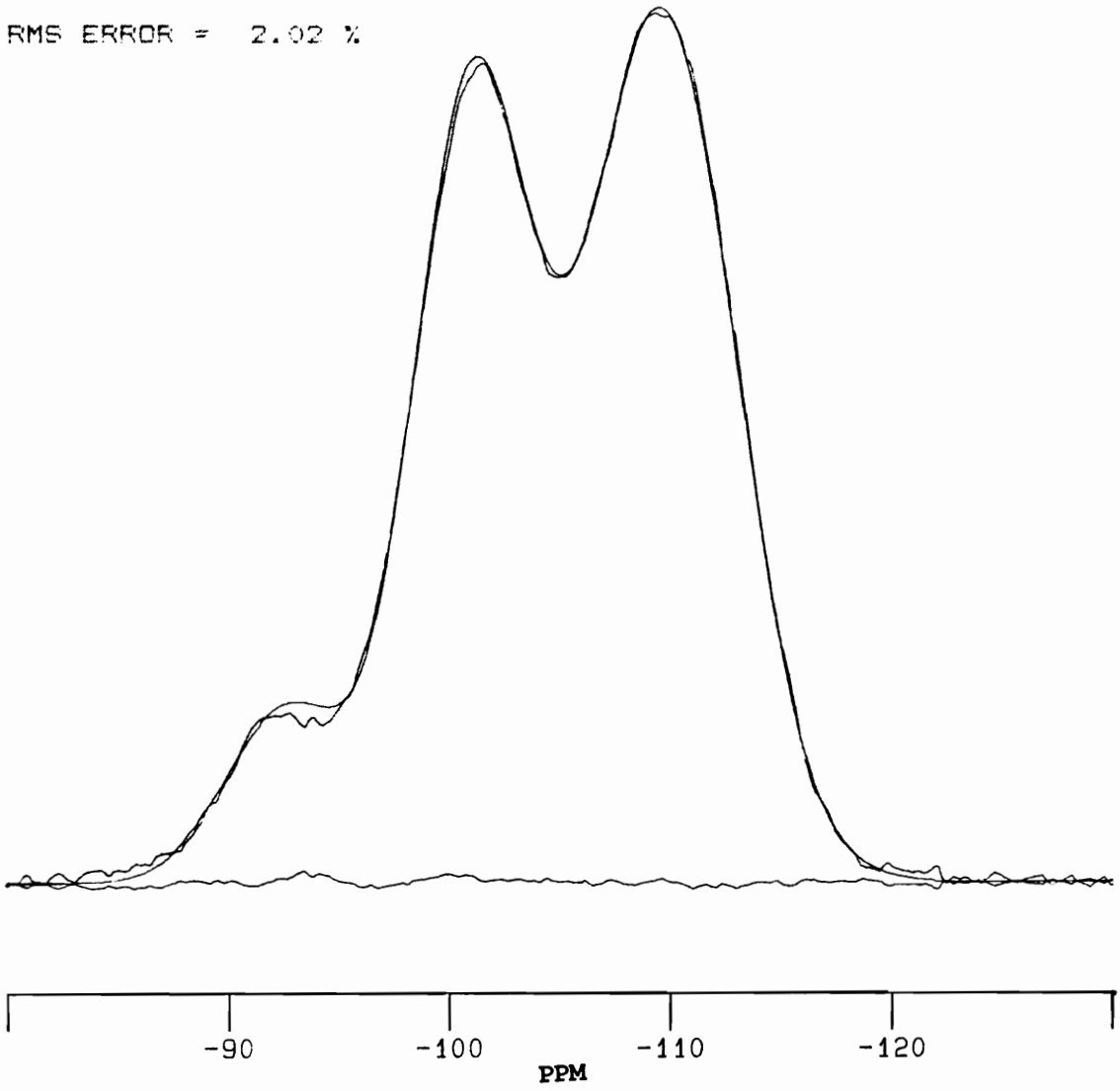


***Figure 1.29***. Deconvolution of solid state $^{29}Si$ NMR spectrum by superposition of three Gaussian curves

***Table 1.10.*** Calculated percentage of various silicate structures in dried $SiO_2$ sol-gel samples and the overall reaction conversion measured from solid state MAS $^{29}Si$ NMR

| | Reaction conditions or Processing conditions | Silicate unit | $\%Q^i$ (% H) | $\%Q^i$ (% A) | Total functional groups | Reacted funct. groups | Conversion, % (p) |
|---|---|---|---|---|---|---|---|
| 0 | 1 | 2 | 3 | 4 | 5 | 6 | 7 |
| Const. process. cond. $T_{max}$ = 150°C | TMOS:$H_2O$= 1.0:2.5 | $Q^2$ | 9.1 | 8.9 | 400 | 351 (344) | 88 (86) |
| | | $Q^3$ | 37.9 | 31.1 | | | |
| | | $Q^4$ | 53.0 | 60.0 | | | |
| | TMOS:$H_2O$= 1.0:4.0 | $Q^2$ | 8.5 | 8.3 | 400 | 350 (346) | 88 (86.5) |
| | | $Q^3$ | 36.7 | 33.0 | | | |
| | | $Q^4$ | 54.8 | 58.7 | | | |
| Constant reaction conditions TMOS:$H_2O$ = 1.0:4.0 | $T_{max}$=RT | $Q^2$ | 8.1 | 7.2 | 400 | 352 (347) | 88 (86.7) |
| | | $Q^3$ | 37.0 | 32.9 | | | |
| | | $Q^4$ | 54.9 | 59.8 | | | |
| | $T_{max}$=150°C | $Q^2$ | 9.1 | 8.9 | 400 | 350 (346) | 88 (86.5) |
| | | $Q^3$ | 37.9 | 31.1 | | | |
| | | $Q^4$ | 53.0 | 60.0 | | | |
| | $T_{max}$=500°C | $Q^2$ | 6.2 | 5.0 | 400 | 371 (361) | 93 (90) |
| | | $Q^3$ | 27.0 | 19.3 | | | |
| | | $Q^4$ | 66.8 | 75.7 | | | |

**RMS ERROR** =2-4% (for estimated peak area); This translates in less than 2% error in calculated conversion values. See Appendix 1.1.

The theoretical number of functional groups is always 400 since the calculations were done per 100 silicate units, each silicate unit possessing a maximum (theoretical) functionality of 4. The number of reacted functional groups listed in column 6 was calculated from:

$$N_r = \sum_{i=2}^{i=4} n_i x_i \qquad (40)$$

where $x_i$ is the molar fraction of the $Q^i$ silicate unit (from column 3 or 4) and $n_i$ is the number of reacted groups from each $Q^i$ unit. Hence, $n_2=2$ (for $Q^2$ units), $n_3=3$ ($Q^3$units), and $n_4=4$ ($Q^4$ units). The first series of values for the reacted functional groups listed in column 6 correspond to calculations based on the peak area and the second series of numbers, in parentheses, correspond to the values obtained using the peak hight. Similarly, column 7 contains two series of conversion values. The first set of values was calculated from the peak area, while the second one, in parentheses, was evaluated from the peak height. The conversions calculated from the peak hight are consistently lower than those estimated from the peak area, but the difference is not higher than 3%. The RMS of the fitting Gaussian curves were < 4% which translates into a maximum 3% error in the calculated conversion values (± 1.5%).

It is notable that a limiting extent of conversion of approximately 88% was obtained for gels generated under a number of reaction and processing conditions. Higher conversions were observed only when higher processing temperatures (500°C) were employed. However, the gel processed at 500°C is also incompletely reacted (approximately 93%). The limiting extent of conversion achieved in these systems is undoubtedly related to their physical state (the occurance of vitrification). This phenomenon can be explained in terms of the familiar time-temperature-transformation (TTT) effect observed for thermosetting resins [163]. The Tg of the sol-gel reacting system steadily increases as the crosslinking reaction proceeds. When the

reaction temperature becomes equal to the glass transition temperature of the developed gel, vitrification occurs. Beyond vitrification the reaction becomes diffusion controlled and it would take place only at infinitely slow rates. In order to fully react such systems, one would have to carry out the reaction above the glass transition temperature of the $SiO_2$ gels (>650°C). However, for organic modified systems the use of high processing temperatures (>650°C) is not desirable since none of the organic modifiers would withstand such temperatures for any considerable length of time.

### *4.1.3.2. TGA-MS and CP/MAS $^{13}C$ solid state NMR*

Solid state $^{29}Si$ NMR analyses discussed in the previous section indicated that $SiO_2$ gels generated through low temperature sol-gel processes were incompletely reacted. These gels contain residual $-OCH_3$ and -OH groups which can further react at elevated temperatures. In order to determine the temperature range within which further condensation-polymerization reactions are most likely to occur, TGA-MS techniques were employed. From TGA one can determine the extent of weight loss and the temperature range within which the weight loss occurs. Thermograms obtained for dried gels produced under a variety of conditions indicated that the weight loss was dependent on both reaction and processing parameters, as shown in ***Figure 1.30*** and ***Figure 1.31*** respectively. The weight loss can be divided into two main temperature intervals: (1) the low temperature weight loss, below 200°C, and (2) the high temperature weight loss, above 200°C. The low temperature weight loss was generally associated with desorption of physically adsorbed water and alcohol , while the high temperature weight loss was attributed to the removal of water (by-product of polycondensation reactions), and to the oxidation of carbonaceous residues [92]. Therefore, the weight loss above 200°C can be qualitatively related to the extent of conversions of the gels. It is observed that samples reacted at lower temperatures (e.g. RT), or at higher dilutions (e.g. TMOS:$H_2O$=1.0:**2.5** vs TMOS:$H_2O$=1.0:**4.0**) show a higher

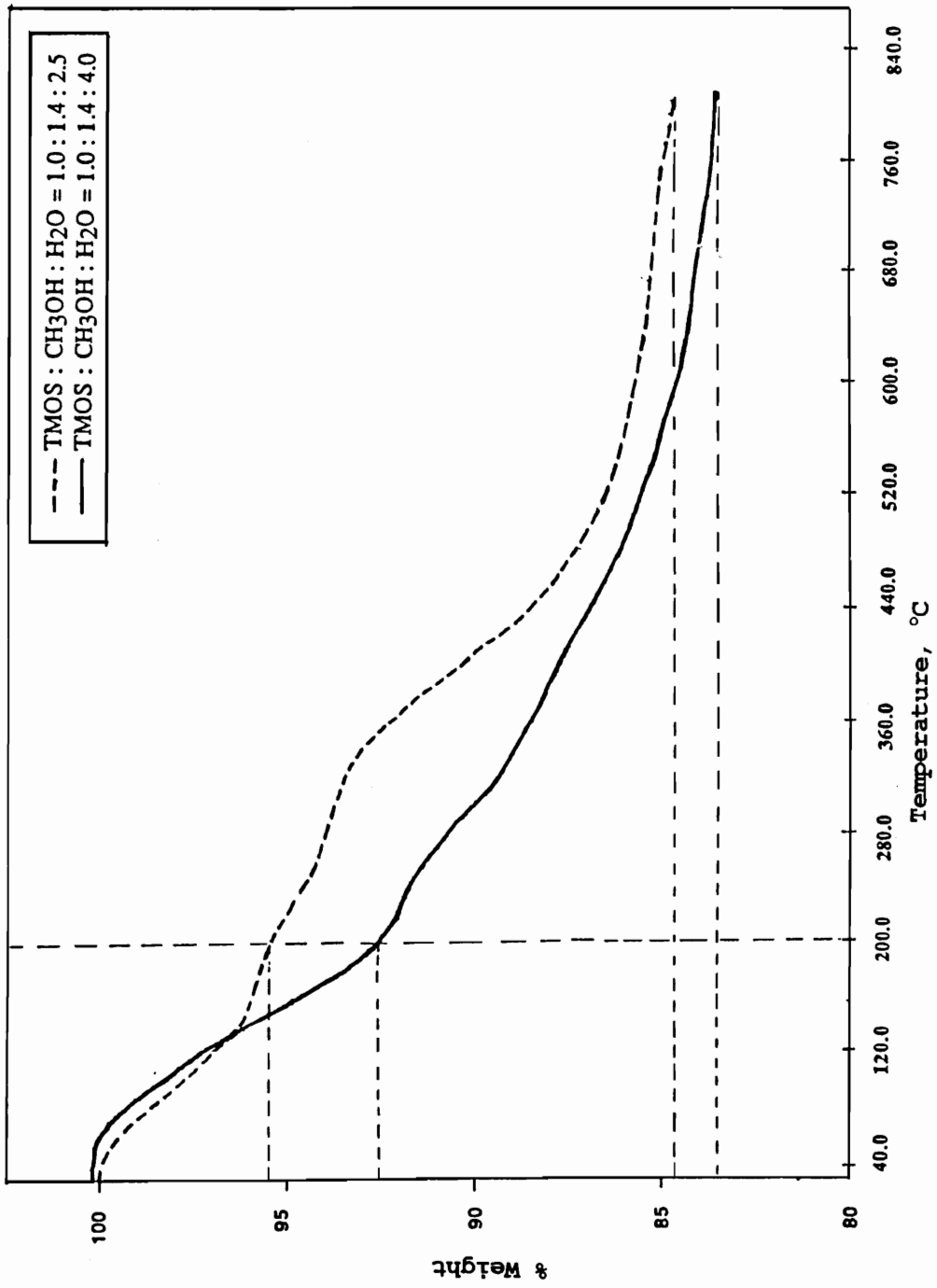


***Figure 1.30***. Dynamic TGA scans of dried $SiO_2$ gels produced under different reaction conditions (Heating rate = 20deg/min; in air).

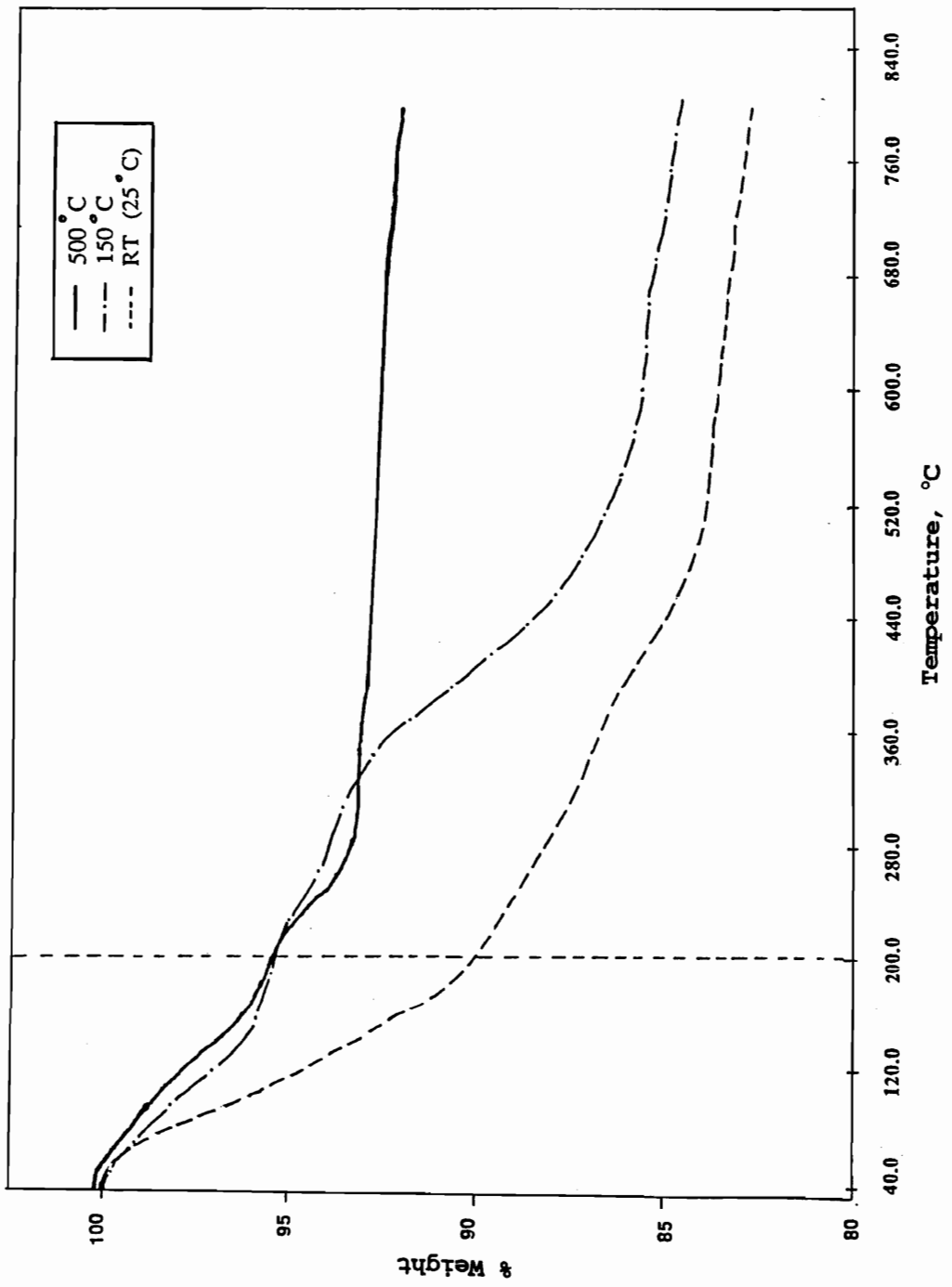


***Figure 1.31.*** Dynamic TGA scans of dried $SiO_2$ gels generated under different processing conditions (Heating rate = 20deg/min; in air); Reaction comp.: TMOS:$CH_3OH$:$H_2O$=1.0:1.4:4.0.

percentage of initial weight loss due to desorption of reaction solvent and by-products. The high temperature weight loss shown by a variety of samples is relatively similar. The most significant difference was observed for the sample reacted at higher temperature ($T_{max}$=500°C), Figure 1.31, which shows a much lower weight loss above 200°C. This observation is in agreement with the calculations from solid state $^{29}Si$ NMR which indicated similar conversions (~88%) for all samples reacted under a variety of conditions but at relatively low upper temperatures, while a higher conversion was obtained for the sample reacted at high temperature ($T_{max}$=500°C).

If the volatiles evolved in the thermogravimetric analyzer are conveyed to a mass selective detector, the species generated during the weight loss processes can be identified and the type of transformations taking place at higher temperatures can be ascertained. For the system investigated, it was of interest to determine if further condensation-polymerization reactions of the incompletely reacted networks would take place in the gelled samples at higher temperature. The type of condensation-polymerization reactions which could take place in these systems can be described by equations 41 and 42 below:

$$\equiv Si-OH + \equiv Si-OCH_3 \longrightarrow \equiv Si-O-Si\equiv + CH_3OH \uparrow \qquad (41)$$

$$\equiv Si-OH + \equiv Si-OH \longrightarrow \equiv Si-O-Si\equiv + H_2O \uparrow \qquad (42)$$

Since methanol and water are generated as by-products of polycondensation reactions, ion chromatograms were constructed at the charge to mass ratio for the base peak of the two species. Typical ion chromatograms for methanol and water are shown in ***Figure 1.32*** and ***Figure 1.33***, respectively. Both ion chromatograms contain two peaks, corresponding to two different weight loss events during which methanol and water are generated. The low temperature weight loss in the thermogravimetric analyzer, taking place over a relatively narrow temperature range, gives rise to a sharp peak in the ion chromatograms. This is consistent with a low activation energy process

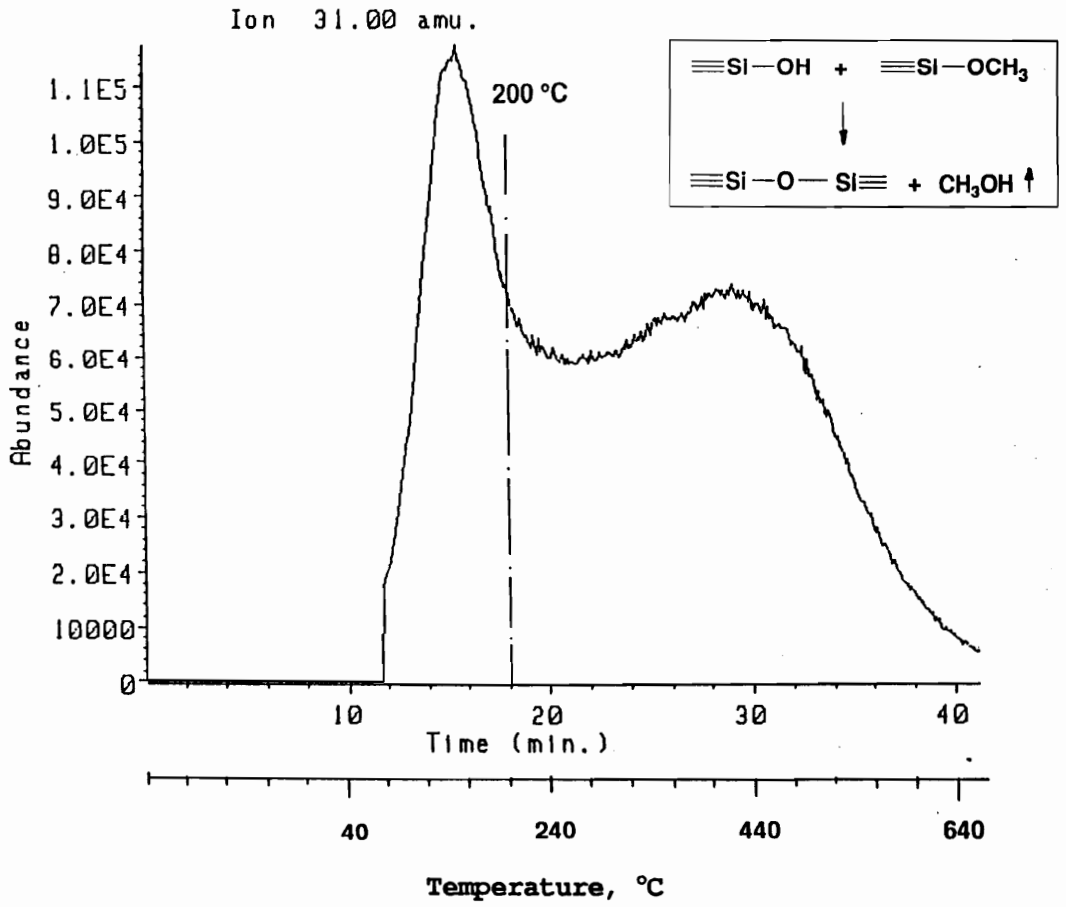


TMOS:$H_2O$:$CH_3OH$ = 1.0:4.0:1.4
Maximum Drying Temperature = 150°C

***Figure 1.32.*** Ion chromatogram for $CH_3OH$ evolution during heating of a $SiO_2$ dried gel.

(Heating rate =20.0 deg/min)

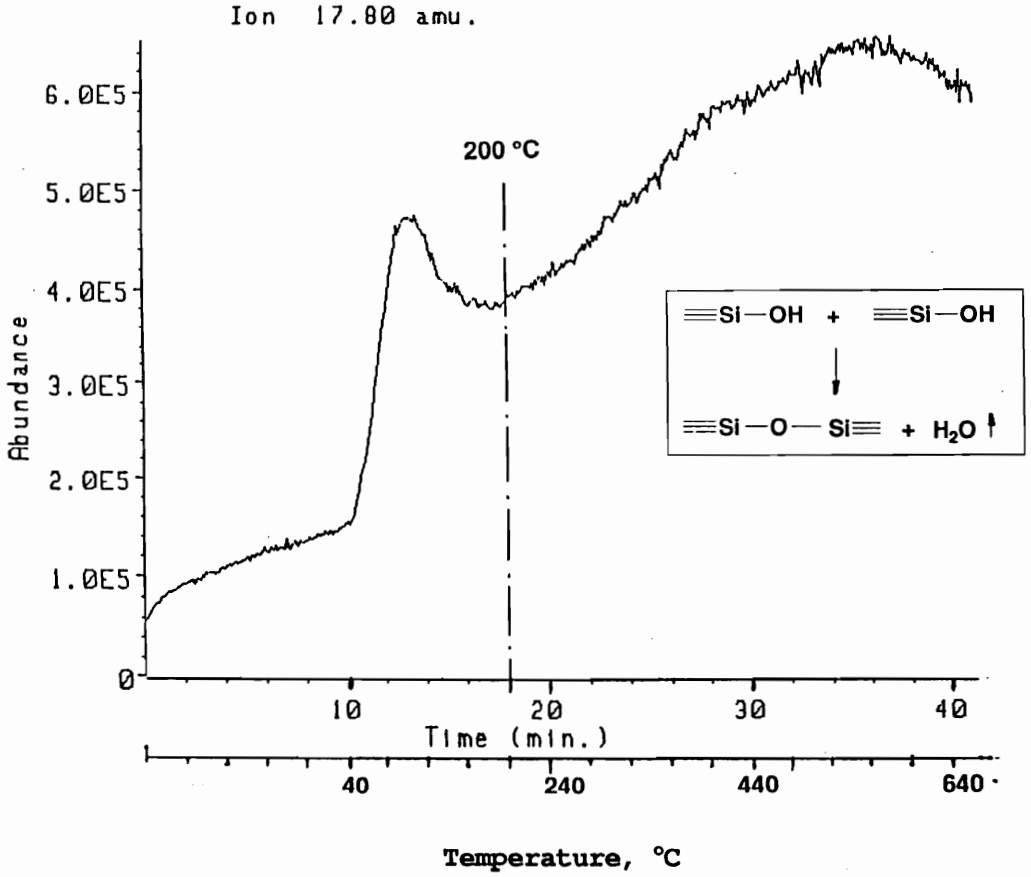


TMOS:$H_2O$:$CH_3OH$ = 1.0:4.0:1.4
Maximum Drying Temperature = 150°C

***Figure 1.33.*** Ion chromatogram for $H_2O$ evolution during heating of a $SiO_2$ dried gel.

(Heating rate =20.0 deg/min)

which can be attributed to the desorption of physically adsorbed methanol and water, and it is in agreement with previous literature assumptions. The weight loss above 200°C gives rise to a second peak in both ion chromatograms, corresponding to a higher temperature event during which both methanol and water are generated. This event is not as well defined in the ion chromatograms: the peaks are much broader, the evolution is slower, and it takes place over the whole temperature range from 250 to 600-650°C. The evolution of methanol and water in this temperature range can be attributed to further condensation reactions of the type described by equations 41 and 42. The occurance of these reactions over the broad temperature range can be explained by the continuous competition between the reaction temperature and the glass transition temperature of the reacting network. At any given temperature there is a limited amount of reaction taking place, until the glass transition temperature ($T_g$) becomes equal to the reaction temperature (T). At this point the reaction stops. A new temperature increase is followed by further reaction until the $T_g$ increases again to the T value, etc. The polycondensation processes seem to be completed around 600-650°C. The above description of the transformations brought about by the temperature increase in this type of highly crosslinked, microporous, inorganic networks is a somehow simplistic representation of the complex process, and it depicts only the chemical changes taking place. As discussed in Chapter 2 Literature Review, chemical changes are usually accompanied by complex physical transformations when the temperature is increased.

$^{13}C$ solid state NMR was used to confirm the presence of unreacted methoxy groups at the end of a typical drying cycle of $SiO_2$ gels (Tmax=150°C). Such groups must be present if the type of condensation reactions described by equation 41 were to occur at higher temperatures, as suggested by TGA-MS experiments. Although the solid state $^{29}Si$ NMR analysis indicated an incomplete conversion of the $SiO_2$ dried gels, the technique did not allow identification of the nature of the unreacted groups (whether methoxy or/and hydroxy). A typical solid state

CP/MAS $^{13}C$ NMR spectrum of a dried gel is shown in ***Figure 1.34.*** Spiking techniques were used to identify the resonance corresponding to the methoxy ($O\underline{C}H_3$) and methanol ($\underline{C}H_3OH$) carbons. The $^{13}C$ NMR spectra in Figure 1.34 indicate that unhydrolyzed methoxy groups, capable of high temperature condensation reactions of the type described by equation 41, are indeed present in the incompletely reacted $SiO_2$ gels, at the end of a typical drying cycle. This observation is in agreement with solution NMR data which indicated that the hydrolysis was not completed at the gelation point and that the condensation reactions started to occur at early stages between partially hydrolyzed species. The free $CH_3OH$ observed in the $^{13}C$ NMR spectrum of the dried gel is the residual solvent retained within the micropores and eliminated at higher temperatures (up to 200°C), as determined by the TGA-MS experiment.

### *4.1.4. Drying of the gels*

The most promising route to obtain glasses from gels through the sol-gel method is to first prepare monolithic dried gels. However, due to the very high compression forces developed inside the pores during the drying of the gels, when a liquid-gas curved interface is formed within the pores, the material, most often, loses its integrity [164]. According to the theory of drying gels introduced by Scherer [165], the stress developed in a plate during drying is dependent upon the solvent evaporation rate and the mechanical properties of the gels. When drying is very slow, and the relaxation time is smaller than the drying time, the stress is independent of the mechanical properties of the gel [165]. This is probably the reason of some succes in generating monolithic gels by very slow drying at room temperature [166]. However, when the relaxation time of the gels becomes much greater than the drying time, the stress developed will also depend on the mechanical properties of the gel, therefore, the stronger the network becomes, one expects it will better withstand the stresses developed during drying.

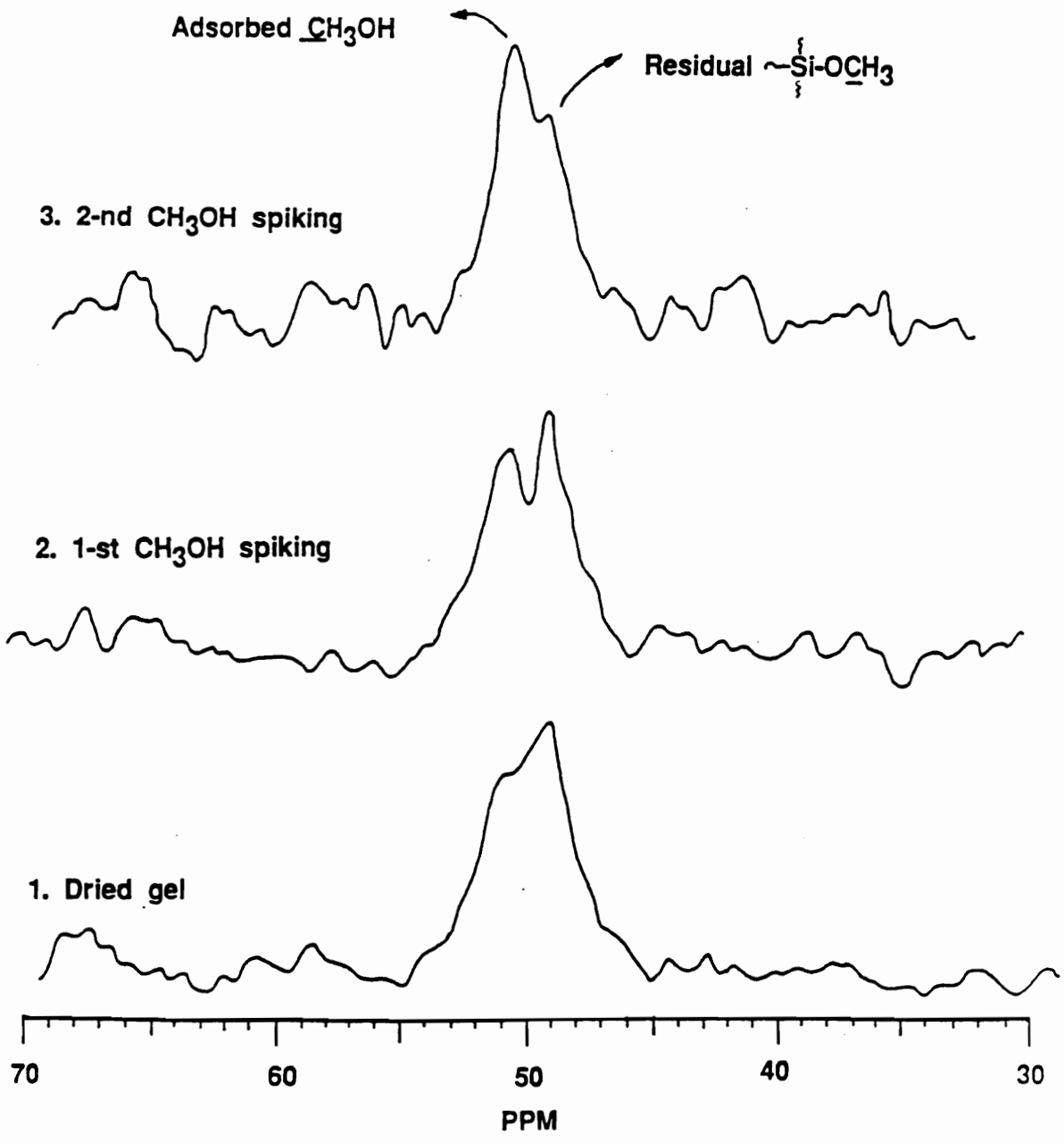


***Figure 1.34.*** Solid state CP/MAS $^{13}C$ NMR spectra for a dried $SiO_2$ gel ($T_{max}$=150°C)

With this understanding of the factors involved during drying of the gels, we believed that the use of relatively high temperatures and mild pressures during the drying process would allow us to approach the following conditions: (a) low evaporation rates due to low vapor pressure of the solvent at high external pressure; (b) decreased compressive forces in the capillaries of the gels, as a result of decreased solvent surface tension at higher temperatures; (c) increased overall conversion of the gel in earlier stages of the drying with increasing temperature, resulting in a stronger, higher consolidated network, capable of withstanding the stresses during drying.

The drying step for all the experiments was conducted in glass vials equipped with relatively tight fitting caps as detailed in Chapter 3. The amount of water employed in the initial hydrolysis step was found to be the most important reaction parameter for producing monolithic dried gels, while the concentration of the reaction had no significant effect. For example, increasing the amount of water from 2.5 to 4.0 moles per mol of TMOS increased the occurance of monolithic samples from 38% to 93%. The addition of water at latter reaction stages did not have the same consequence, indicating that the influence of water is rather complex and it goes beyond the simple stoichiometric effect. These conclusions were obtained by carrying out side by side14 samples for each of the above conditions and determining the number of monolithic specimens obtained in each series.

The above observations are in agreement with previous literature data which indicate that the chain growth in later stages of the reaction is much more efficient when larger amounts of water are employed in the initial reaction. This behavior was attributed to the fact that the water content largely determines the nature of the terminal bonds, and thus their activity in modifying the molecular size. A significant size expansion occurs in later stages of the reaction in solutions containing active polymers, e.g. having OH terminal bonds [52].

## *4.2. ORGANIC MODIFIED $SIO_2$ NETWORKS*

***Introduction:*** $SiO_2$ networks generated by the low temperature sol-gel process possess residual hydroxy and methoxy groups (due to incomplete conversion) which contribute to a high polarity of these materials, as discussed in the previous section. In addition, the highly crosslinked inorganic networks are rather brittle, a behavior which is similar to highly crosslinked organic resins. These drawbacks highly limit the applicability of the sol-gel technology and modifications of the system are often required.

The use of organic modifiers for the inorganic systems, made possible by the development of the low temperature sol-gel techniques, is already known. For the vast majority of such modifications, the organic compounds employed are low molecular weight substituents bonded to the metallic atom of the inorganic alkoxide monomers, which do not form a linkage in the final network. The methyl or phenyl groups on the alkoxysilanes are typical examples of this type of system. The molecular weight of these organic groups is usually low, such as to avoid the formation of dangling ends in the resulting networks. Such systems are expected to show a continuous glass phase with uniformly dispersed organic species. The use of organic modifiers which can form a linkage, and either become a part of the inorganic glass network, or result in an interpenetrating network (IPN) is a more versatile approach. In this approach, higher molecular weight organic modifiers can be employed. Such systems may show cocontinuous phases or a dispersed first phase within a continuous second phase. Therefore, materials ranging from modified glasses (in which the inorganic glass is the continuous phase) to reinforced polymers (in which the organic component is the continuous phase) can in principle be generated this way. In the present study, modified $SiO_2$ networks in which the organic modifiers were functionalized organic oligomers, capable to coreact with inorganic alkoxides and to become part of the inorganic glass networks, will be

discussed. The emphasis will be placed on chemical compositions resulting in modified glasses (low concentrations of the organic modifiers).

An organic modifier for such systems should possess a number of features:

(1) The organic modifier should contain reactive groups capable to undergo copolymerization reactions with the inorganic alkoxides, under the sol-gel conditions. (2) The organic modifier should be stable under the reaction conditions employed. The major concern here is the general use of strong acids and bases for the sol-gel reactions. A large number of organic oligomers of potential interest as inorganic network modifiers, display a limited stability under the general sol-gel conditions. As previously discussed, this problem was avoided in the present study by employing a catalyst free sol-gel system based on TMOS, the most reactive silicon tetraalkoxide in the series. (3) The organic modifier should contribute to the improvement of the undesired properties, while preserving the most desired features of the inorganic networks.

### *4.2.1. Poly(dimethylsiloxane) modified $SiO_2$ networks*

Polysiloxane oligomers possess all of the above desired features: (1) Their synthesis is very versatile and they can be functionalized with reactive groups capable to undergo copolymerization reactions with inorganic alkoxides, under the sol-gel conditions. In this study, methoxy functional groups were used as reacting sites for polysiloxane copolymerization.

(2) The polysiloxane oligomers are stable under the reaction conditions employed in this study. Specifically, polydimethylsiloxane homopolymers are typically stable up to 350-400°C, in the absence of air, or 300°C in air. The (Si-O) bond is one of the most thermally stable bonds formed by silicon, and has a bond dissociation energy of 110 kcal/mole (460 kJ/mole) [12] compared with 85.5 (357) for (C-O), 82.6 (345) for (C-C) and 76 (318) for (Si-C) bonds [166]. The substantial thermal stability of siloxanes is thus partly a consequence of the high bond strength. The siloxane

backbone is sometimes considered to have an "organic-inorganic" nature as compared to typical organic elastomers. The value of the (Si-O) bond length is equal to 1.64 ± 0.03Å [12], substantially smaller than that of (Si-O) bond length calculated from the additivity of atomic radii (1.83Å). A shortening of the (Si-O) bond can be explained by its substantial ionic character (40-50%) and also, most probably, by its partial double bond character [12]. Though resistant to homolytic cleavage, the ionic nature of the siloxane bond renders it quite susceptible to attack by polar reagents such as acids and bases. Indeed, this heterolytic cleavage is used to an advantage in the preparation of oligomeric polysiloxanes, as will be discussed later in this chapter. However, it can also lead to redistribution reactions of polysiloxane chains, especially at elevated temperatures.

It becomes apparent that the use of a catalyst-free sol-gel system is critical, if polysiloxanes are to be used as organic modifiers for the $SiO_2$ networks. (3) Incorporation of oligomeric polysiloxanes into the inorganic $SiO_2$ networks can, in principle, contribute to a substantial improvement of the undesired properties of the inorganic networks: (a) The polysiloxane chains are known to be highly hydrophobic and to possess a low surface energy [167]. Consequently, polysiloxane (PSX) modified inorganic networks should result in materials with decreased surface polarity and increased resistance to water, when compared to the inorganic $SiO_2$ networks. (b) Additionally, the highly flexible, low glass transition temperature ($T_g$=~-120°C) polysiloxane oligomers are rubbers at room temperature; therefore, their incorporation may improve the toughness of the $SiO_2$ glasses. This is one of the advantages which are anticipated when relatively high molecular weight low glass transition temperature organic modifiers are used: such modifiers can microphase separate and generate a second rubbery phase into the glassy matrix, hence provide a mechanism for rubber toughening of the otherwise brittle $SiO_2$ networks.

#### *4.2.1.1. Synthesis of reactive PSX oligomers*

***Vinyl terminated PSX.*** Ring opening polymerization of octamethylcyclotetrasiloxane ($D_4$) with a suitable catalyst, also known as equilibration reaction, is an important commercial process for the synthesis of functionalized polysiloxane oligomers. The molecular weight and functionality of these oligomers can be controlled by the addition of specified amounts of a disiloxane (DSX) or endblocker [168-173]. A general reaction scheme for the equilibration-polymerization of $D_4$ in the presence of a disiloxane endblocker (DSX) is shown in ***Scheme 1.13***. During these reactions the (Si-O) linkages in a mixture of siloxanes (e.g. cyclic and linear) are continuously broken and reformed, in the presence of a catalyst, until the system reaches its thermodynamically most stable equilibrium state [167]. At equilibrium, the reaction mixture consists primarily of linear polymers (or oligomers) and to a lesser extent (~10-15% by weight) of cyclic species. Under the acid or base catalyzed equilibration conditions, although the (Si-O) bonds are cleaved fairly easily, (Si-C) and many other less polar organic bonds such as (C-C), (C-O), (C-N), etc. are stable. This feature provides the main strategy for the synthesis of a variety of functionally terminated siloxane oligomers with controlled structures. These processes will be discussed in more detail in Part 2 of this disertation.

The disiloxanes are used as chain transfer agents or "end-blockers" and they play two major roles. Firstly, they determine the type of the reactive functional end groups and secondly they regulate the number average molecular weight of the linear oligomers formed. Molecular weight control is achieved by varying the initial ratio of the cyclic monomers to the end-blocker. The type of catalyst used (acid or base) is primarily determined by the nature of the functional groups on the disiloxane so as to avoid undesired side reactions which may lead to the loss of functionality or poisoning of the catalyst. At the end of equilibration, the resulting linear oligomers are functionally terminated

***Scheme 1.13.*** General route for the preparation of functionalized poly(dimethylsiloxane) oligomers via equilibration (redistribution) reactions.

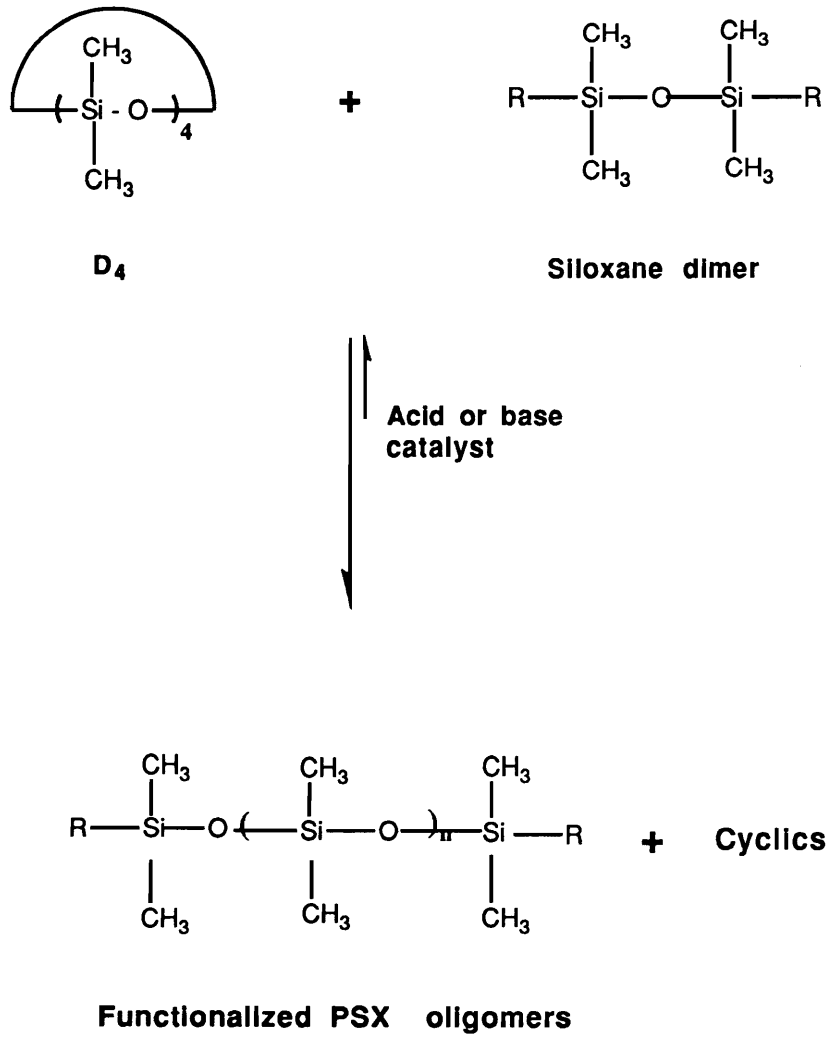

and the cyclic products are non-functional, provided that there are no side reactions involving the functional end groups. After the elimination of the catalyst, either by neutralization or decomposition [12,133,174,175], the cyclic species can usually be removed from the system by vacuum distillation at elevated temperatures. More details on equilibrium-polymerization reactions of cyclic siloxane monomers will be given in Part 2 of this thesis.

Synthesis of controlled molecular weight, vinyl terminated PSX oligomers was achieved by anionic ring opening polymerization of the cyclic siloxane monomer, $D_4$, in the presence of tetramethylammonium silanolate as a transient catalyst, and 1,3-divinyltetramethyldisiloxane as the chain transfer agent or end-capper, as described in ***Scheme 1.14.*** The synthesis and characterization of the silanolate catalyst was detailed elsewhere [133, 176]. Polysiloxanes with theoretical number average molecular weights ($<M_n>$) ranging from 1,000 (1k) to 12,000 g/mole (10k) were synthesized. The number average molecular weight of each oligomer was determined using GPC as a primary method. The siloxane oligomers as well as the cyclic structures and the siloxane dimer were detected by refractive index using toluene as the transport solvent. The molecular weights were determined with respect to poly(dimethylsiloxane) standards.

***Table 1.11*** summarizes the amount of siloxane cyclic and DSX end-capper in the initial reaction mixture, employed for each molecular weight desired, along with the theoretical and experimental values for the number average molecular weight, as measured by GPC. The GPC data indicate a relatively good molecular weight control in the range investigated. However, the experimental molecular weights were consistently higher than the theoretical values, partly due to the incomplete incorporation of the disiloxane end-capper, as confirmed by GPC analyses. The reaction progress is visualized in ***Figure 1.35*** by stacked GPC traces at increasing equilibration times. It was observed that the formation of high molecular weight oligomers started at very low reaction times (10 minutes) but the equilibrium composition of the reaction mixture was not

***Scheme 1.14.*** Synthesis of vinyl terminated poly(dimethylsiloxane) oligomers via anionic ring opening equilibrium polymerization of $D_4$

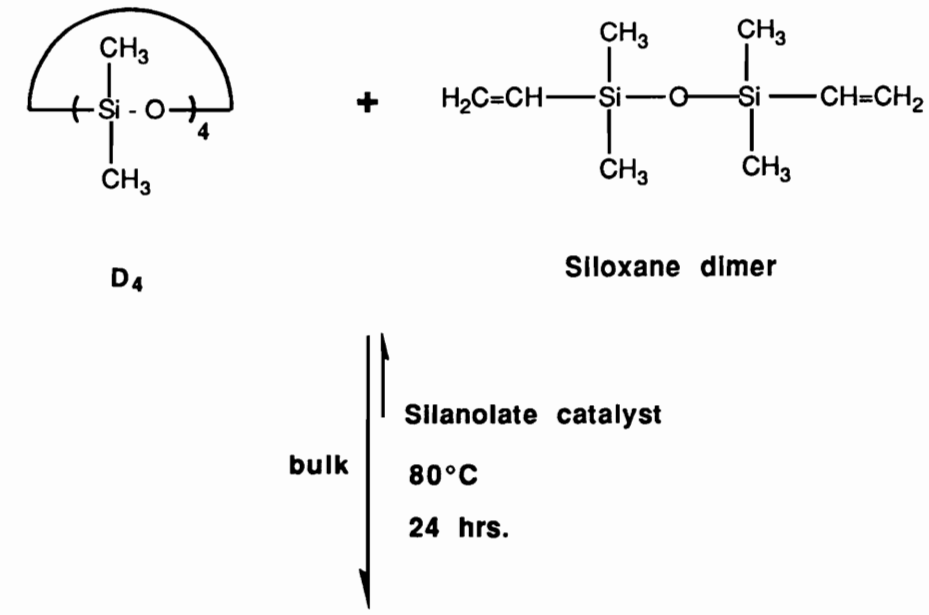

***Table 1.11.*** Theoretical vs experimental number average molecular weight for vinyl terminated poly(dimethylsiloxane) oligomers

| Sample No | D4 (g) | DSX (g) | Number average molec. weight, <Mn>, (g/mole) Theoretical | Experimental* |
|---|---|---|---|---|
| 1. | 81.3 | 18.7 | 1,000 | 1,400 |
| 2. | 90.7 | 9.3 | 2,000 | 3,700 |
| 3. | 93.8 | 6.2 | 3,000 | 5,600 |
| 4. | 96.3 | 3.7 | 5,000 | 8,000 |
| 5. | 98.1 | 1.9 | 10,000 | 12,600 |

* From GPC, according to poly(dimethylsiloxane) standards

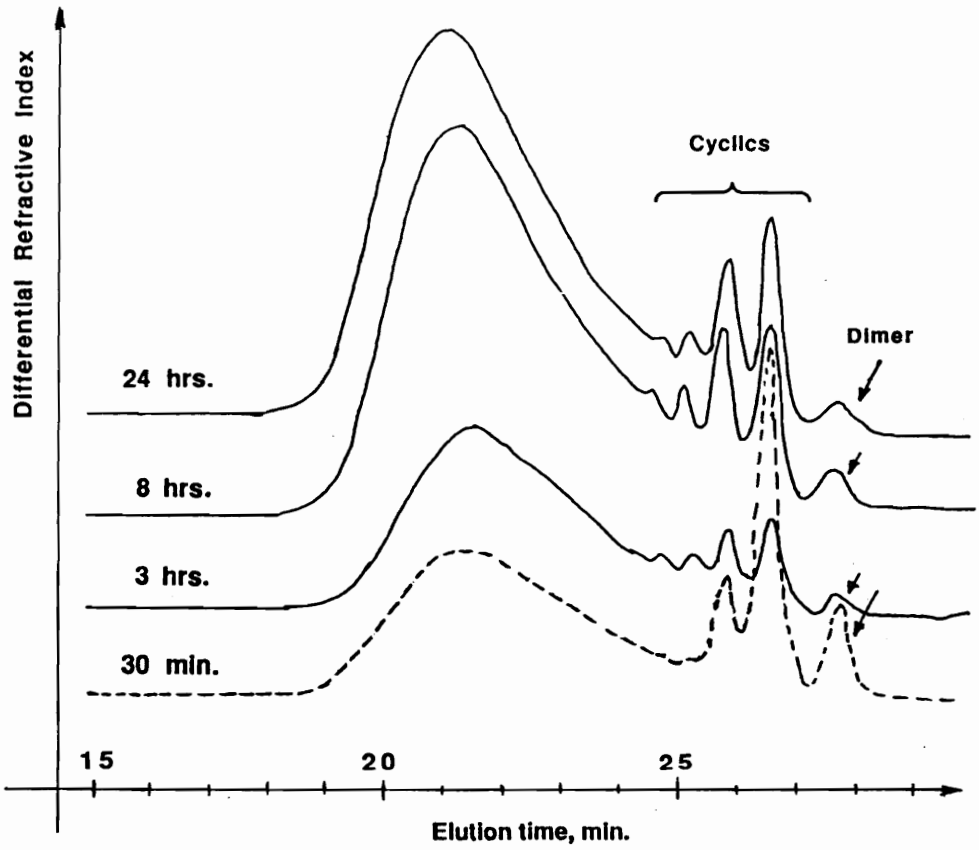


***Figure 1.35.*** Stacked GPC traces at different equilibration times; Vinyl terminated PSX oligomer; Theoretical molecular weight <Mn>=1 K.

achieved until later. After approximately 8 hours of equilibration at 80°C, GPC indicated a relatively constant composition, molecular weight and molecular weight distribution. No significant changes were observed between 8 hours and 24 hours of reaction at this temperature. However, all reactions were allowed to proceed for 24 hours in order to ensure that the system achieved its equilibrium distribution. The change in the concentration of siloxane dimer, as well as oligomeric and cyclic species, was calculated from GPC traces, and typical data are shown in ***Figure 1.36a*** and ***Figure 1.36b*** respectively. These data were obtained for an equilibration reaction with the initial chemical composition $D_4$:DSX=81.4:18.6 w/w, corresponding to a molar ratio $D_4$:DSX=73.3:26.7, for a theoretical $<M_n>$=1,000 g/mole.

The siloxane dimer was readily consumed, as shown in Figure 1.35a. Its weight percent in the reaction mixture dropped from the initial value of 18.6 to approximately 2%, in less than two hours of equilibration. However, the equilibrium composition still contains 1.0-1.5 weight percent DSX, which represents approximately 7.0-8.0 mole percent of the initial amount of DSX dimer added to the reaction. This incomplete incorporation of the dimer may be partly responsible for the consistently higher molecular weights observed. Meantime, the concentration of cyclics decreased readily from the initial value of 81.4 to the equilibrium value of approximately 10.5 weight percent, generating high molecular weight species, as shown in Figure 1.35b. At the end of equilibration, the catalyst was decomposed by heating the reaction mixture at 140°C under nitrogen flow, for 15-30 minutes. The viscous oil was then stripped off under vacuum (approx. 300mtorr, 150°C) to eliminate the nonfunctionalized cyclics. Typical GPC traces for vacuum stripped oligomers, ***Figure 1.37,*** indicate efficient removal of the non-functional cyclic species and a typical $^1$H NMR spectrum,***Figure 1.38,*** contains the resonances corresponding to the vinyl end-groups (5.7 to 6.2 ppm) along with Si-methyls on the siloxane backbone (0.1 ppm).

***Figure 1.36a.*** Siloxane dimer vs. equilibration time (weight percent in the reaction mixture)

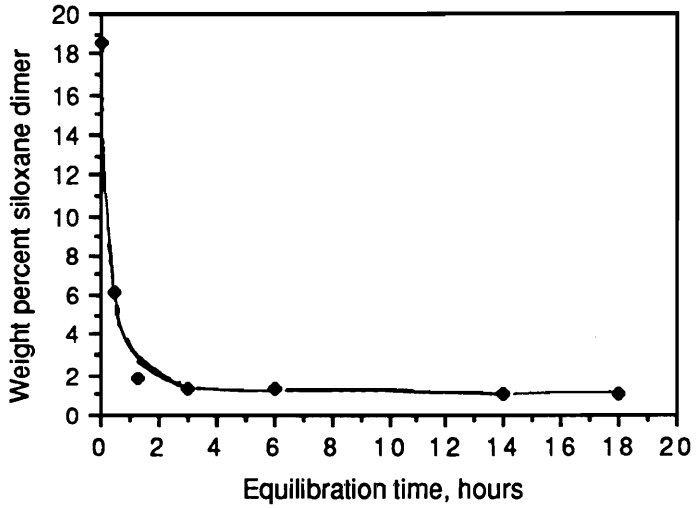


***Figure 1.36b.*** Polysiloxane oligomers and cyclics vs equilibration time (weight percent in the reaction mixture).

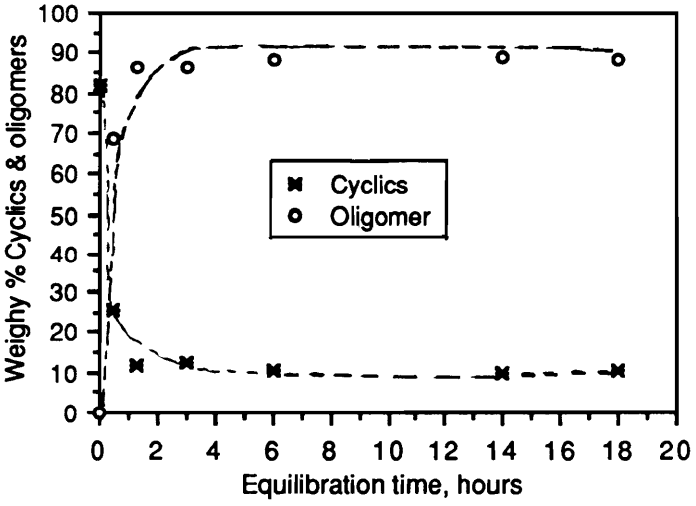


***Figure 1.36.*** Change in the concentration of dimer, cyclics, and oligomers during an equilibration reaction for the synthesis of vinyl terminated PSX oligomer

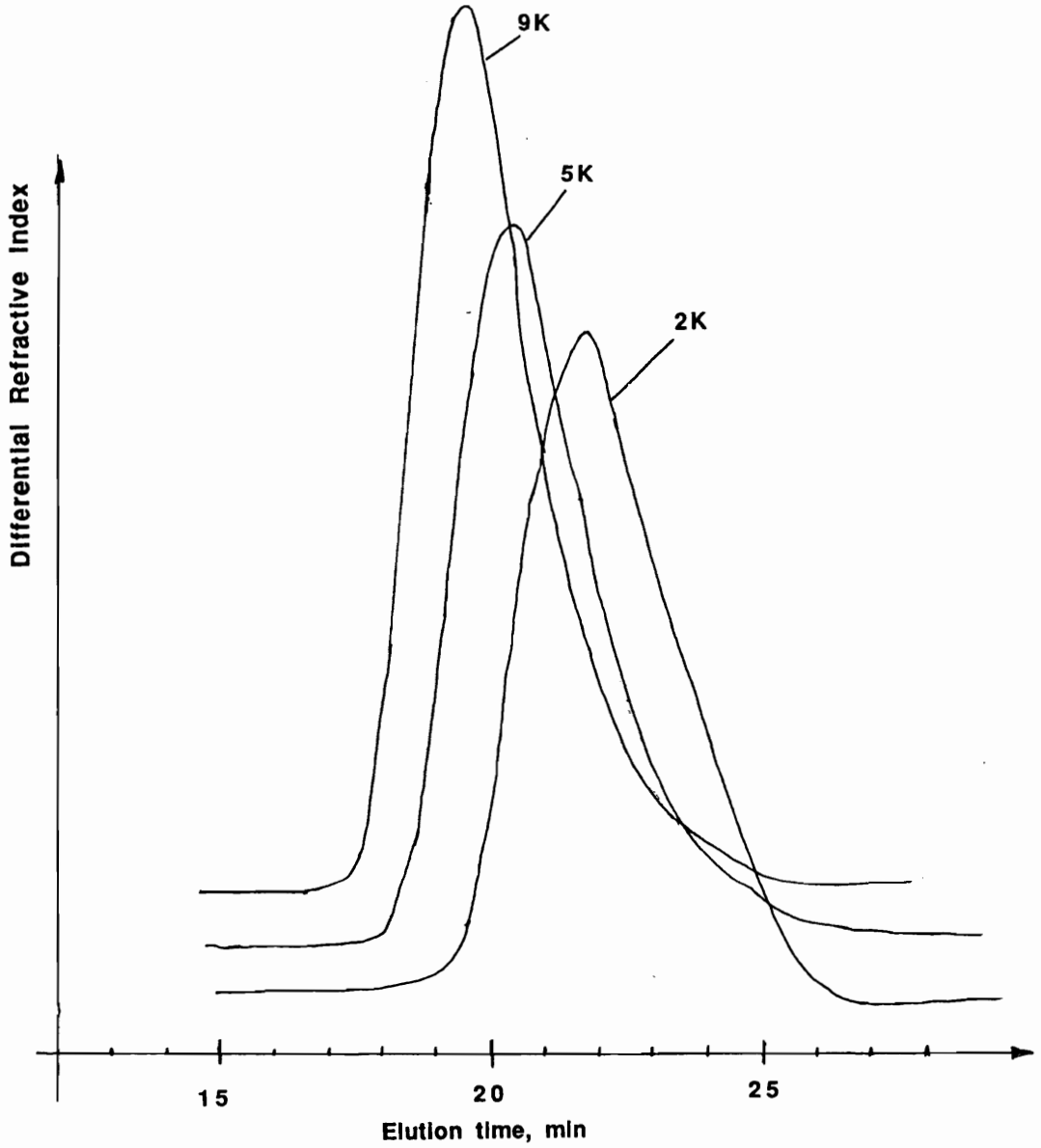


***Figure 1.37.*** Typical GPC traces for vinyl terminated PSX oligomers after vacuum stripping (free of cyclics)

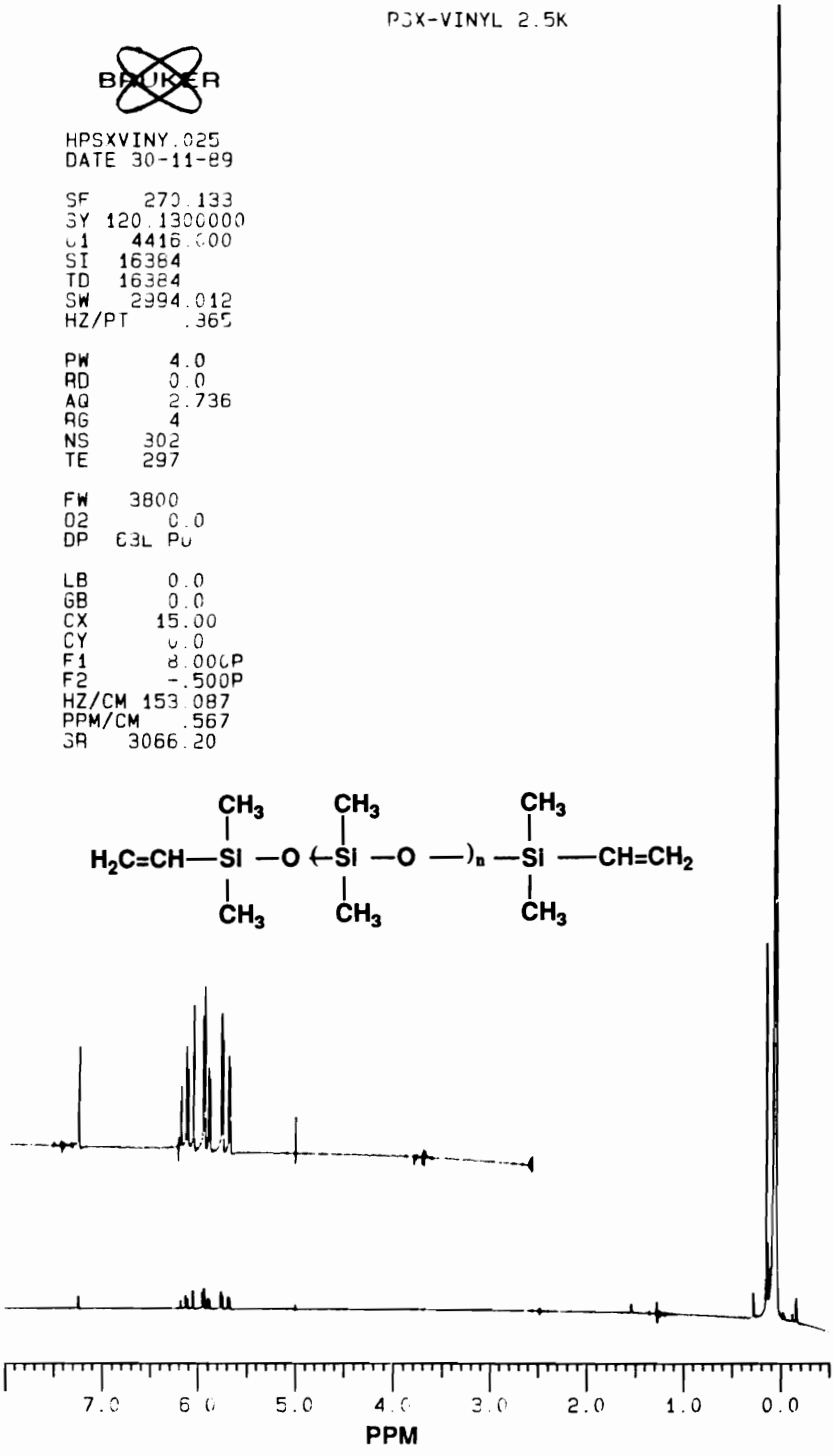


***Figure 1.38*** Typical $^{1}H$ NMR spectrum for vinyl terminated PSX oligomers.

***Methoxy functionalized PSX.*** The terminal vinyl groups in the polysiloxane oligomers were converted to methoxy groups using a hydrosilation reaction. Hydrosilation is the term used for the addition of silicon hydrides (Si-H) to multiple bonds such as olefins (C=C) or acetylenes (C=C) under the action of various catalysts. The hydrosilation reactions emerged from about six separate laboratories in the United States [177-181] between 1945 and 1947. In 1947, Sommer et al. [182], reported the successful addition of trichlorosilane to 1-octene in the presence of diacetyl peroxide. Other peroxides, UV and γ-radiation [182-189] have also been investigated as hydrosilation catalysts. In 1953, Wagner and Strother [190-192] proposed a completely new type of catalyst for the addition of silicon hydrides to unsaturated compounds, namely, platinum on carriers. The use of platinum on carriers made it possible to extend considerably the range of silicon hydrides and unsaturated compounds capable of undergoing addition. Silicon hydrides of the type $RSiHCl_2$, $R_2SiHCl$, etc., and also readily polymerizable unsaturated compounds which gave a poor yield of addition products in the presence of peroxides and other initiators, reacted readily under the influence of platinum catalysts [193,194]. It was soon found that not only platinum, but also other metals of the platinum group will catalyze the addition of silicon hydrides to unsaturated compounds [195-200]. Finally, Speier, Webster, and Barnes discovered that chloroplatinic acid has an exceptionally high catalytic activity in this reaction [199]. Chloroplatinic acid, $H_2PtCl_6$, is a more active addition catalyst than platinum on carriers [201,202].

Methoxy functionalized PSX oligomers were synthesized by the addition of methoxysilane hydrosilating agents to the vinyl end-groups of previously synthesized PSX oligomers. Both methyldimethoxysilane and trimethoxysilane were used as hydrosilating agents, to produce tetrafunctional and hexafunctional PSX oligomers, respectively. The general reaction for this post-functionalization is exemplified in ***Scheme 1.15*** for the synthesis of hexamethoxy functionalized PSX oligomers. In order to determine the reaction conditions for this hydrosilation,

***Scheme 1.15.*** Synthesis of methoxy functionalized poly(dimethylsiloxane) oligomers

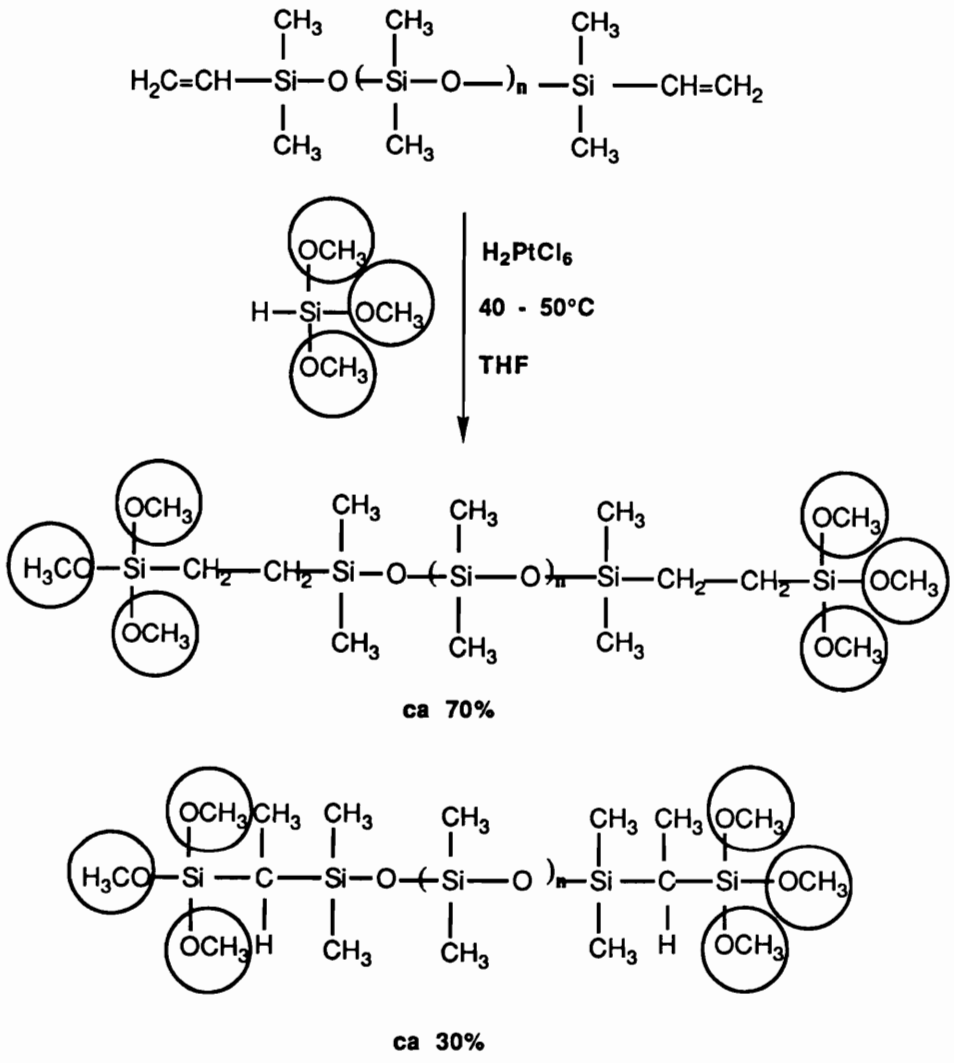

a model study was carried out. In the model reaction, the alkoxysilane was added to the vinyl double bonds of 1,3-divinyltetramethyldisiloxane, as described in ***Scheme 1.16*** The concentration of reactive vinyl groups of the disiloxane compound is much higher than for the vinyl terminated PSX oligomers, and the reaction could be more closely monitored. The hydrosilation was followed by $^1$H NMR, by monitoring the disappearance of the unsaturated vinyl protons. Typical $^1$H NMR spectra of the reaction mixture at two different reaction times are shown in ***Figure 1.39.*** The hydrosilation reaction was readily completed after 30 minutes at 40-50°C, as shown by the complete disappearance of the vinyl protons in the NMR spectrum at the top. Under the above reaction conditions, both $\beta$ and $\alpha$ additions to the asymmetrical double bond occured, at a ratio of 70% to 30%, respectively. The ratio of the two adducts was determined from $^1$H NMR, as shown in ***Figure 1.40.***

The usefulness of the hydrosilation reactions is sometimes limited by a number of side reactions that can not always be controlled. Polymerization and isomerization of the olefin are the major side reactions usually associated with hydrosilation [203]. However, in the system investigated, and under the reaction conditions employed, no side reactions were observed within the limits of detection of $^1$HNMR. Some side reactions have been reported for hydrosilations involving (Si-H) and (Si-CH=CH$_2$) groups [205], but only at higher reaction temperatures (90-110°C) and in the presence of excess silane component. Under the above mentioned conditions the authors observed the formation of highly branched species, and proposed that both dimethylsilyl functions and the chloroplatinic acid catalyst were involved in these side reactions, which may imply an attack of the functional Si-H groups at the polydimethylsiloxane backbone. Two mechanisms leading to the formation of branched species have been proposed, as shown in ***Scheme 1.17***, a and b. Both mechanisms would result in the formation of branched species which was confirmed by size exclusion chromatography techniques using both refractive index

***Scheme 1.16.*** Model reaction for the hydrosilation at the vinyl double bond

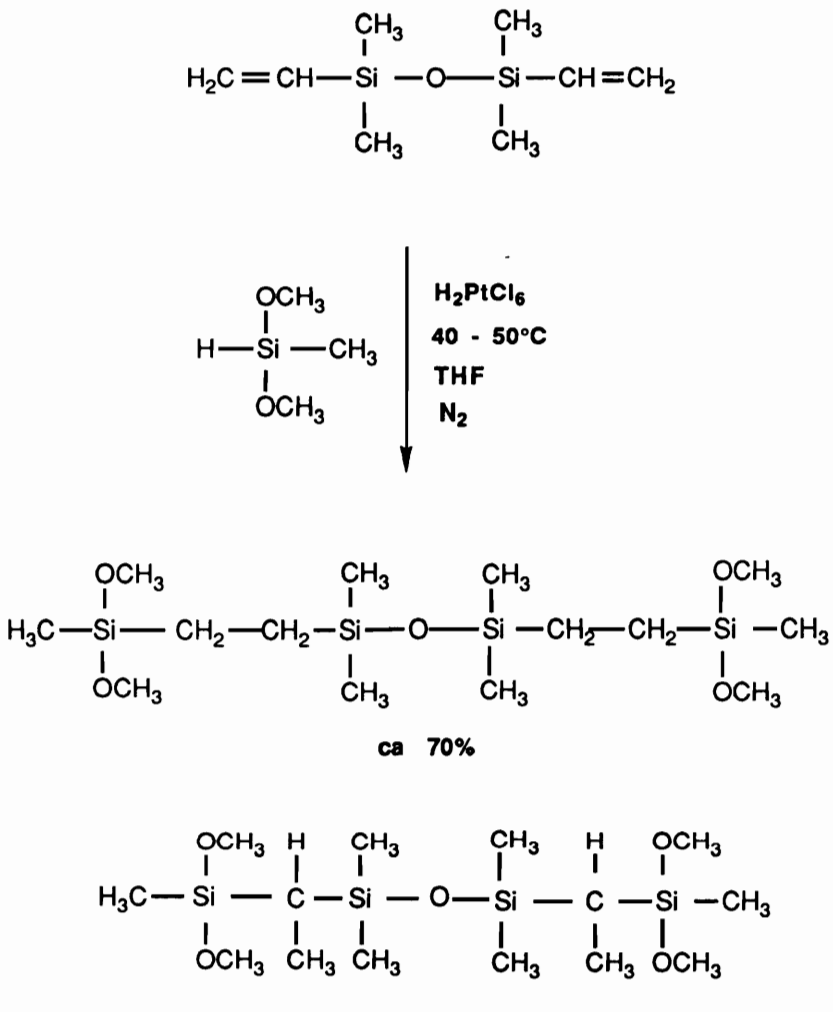

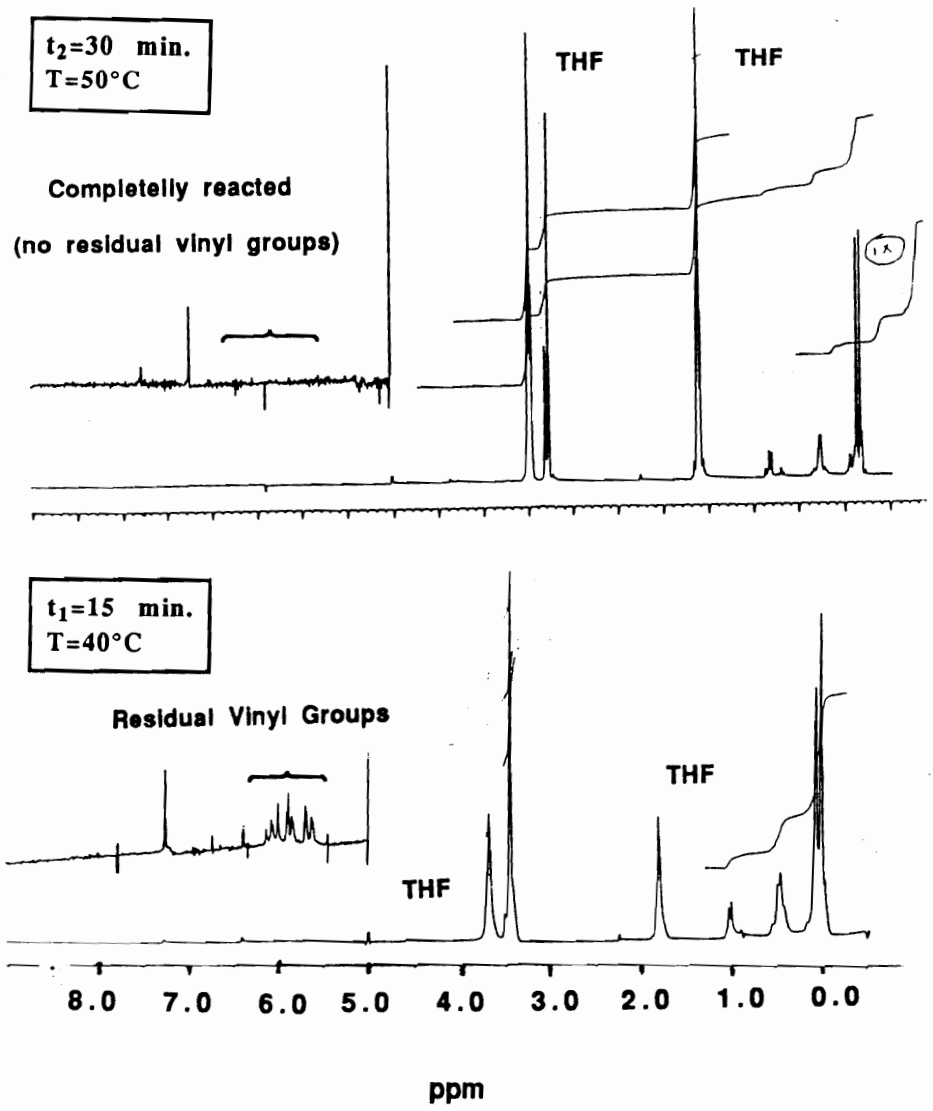


***Figure 1.39.*** $^{1}$H NMR spectra for the initial vinyl dimer, and the hydrosilation reaction mixture at two different reaction times

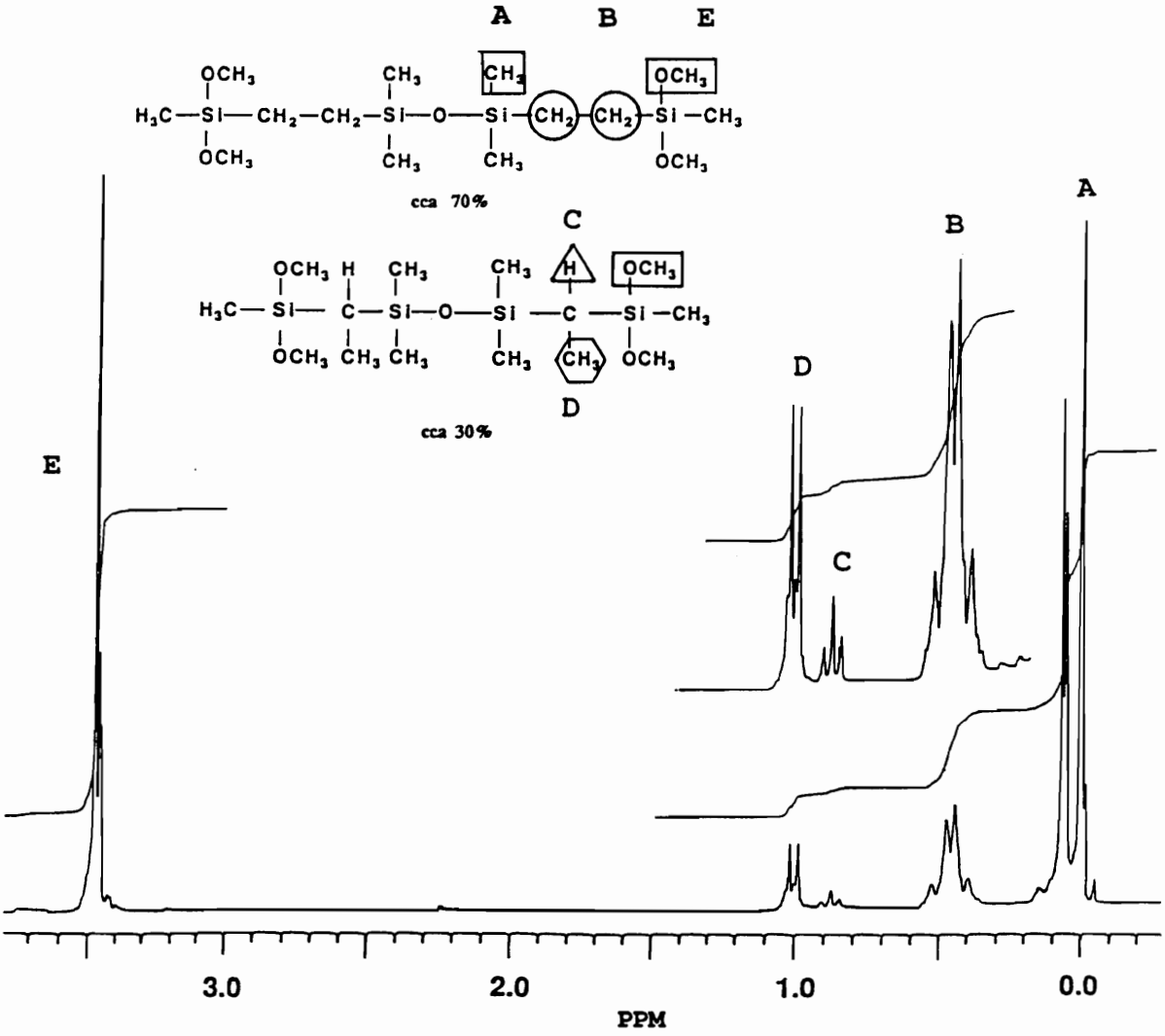


***Figure1.40.*** $^{1}H$ NMR spectrum for the hydrosilation adducts of 1,3-divinyltetramethoxydisiloxane hydrosilation adducts.

***Scheme 1.17.*** Proposed mechanisms for side reactions involving the silyl functionality and the polysiloxane backbone [218].

a)

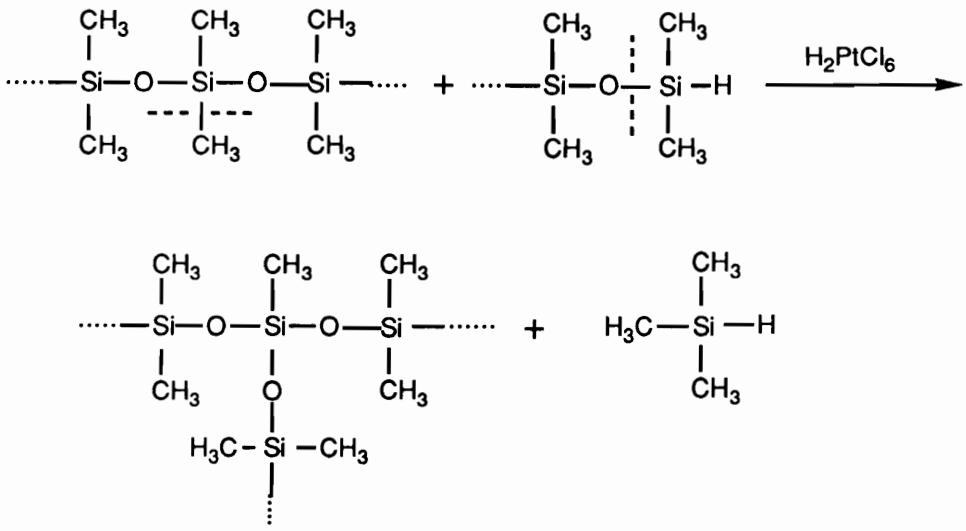


b)

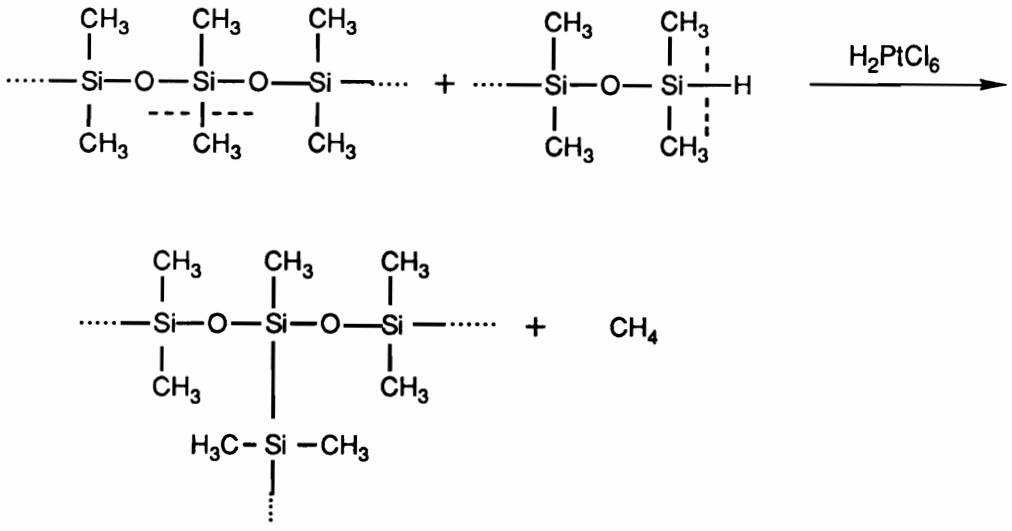

and light scattering detectors. However, the proposed mechanisms have not been proved.

Typical GPC traces for a polysiloxane oligomer before and after hydrosilation are shown in ***Figure 1.41***. No change in the molecular weight was observed during hydrosilation reactions, indicating: (1) no polymerization of vinyl groups, (2) no side reactions associated with hydrosilation, as mentioned above, and (3) no side reactions involving methoxy functionalities occured under the mild reaction conditions employed. It is important to emphasize that in the presence of moisture, the methoxy groups can hydrolyze and subsequently condense, resulting in a molecular weight increase.

Another problem often encountered in hydrosilation of asymmetrical olefins is the existence of two modes of addition, Markovnikov and anti-Markovnikov [203]:

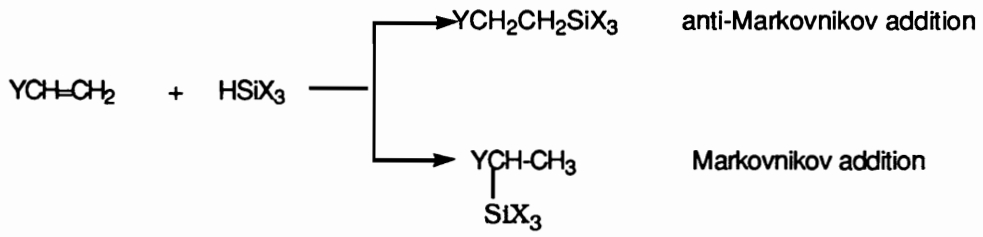


Ability to control the mode of reaction can be a major problem. For some systems, such as acrylonitrile and other functional olefins, the mode of addition is very critical because the Si-C bond in the $\alpha$-isomer cleaves under acid conditions, and products made from it are unstable [203]. The selectivity for $\beta$- addition can generally be improved by carrying out the reaction at lower temperatures, however, the most effective way to control the selectivity is by changing the catalyst system [204]. For the system under investigation, both adducts are satisfactory, and no efforts to improve the selectivity were made.

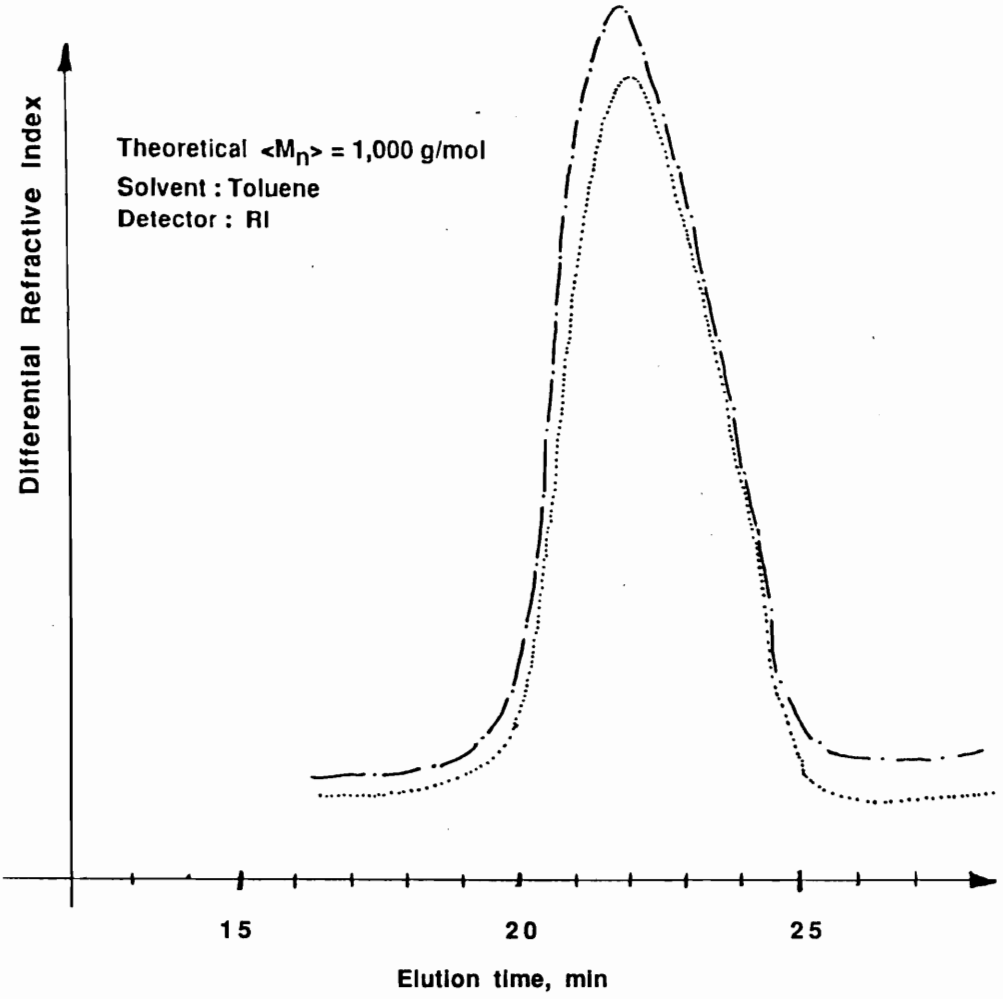


***Figure 1.41.*** Typical GPC traces for vinyl (-----) and methoxy (.....) terminated PSX oligomer

### *4.2.1.2. Synthesis of PSX-$SiO_2$ networks*

***Model hydrolysis and condensation reactions.*** The methoxy functionalized PSX oligomers should be able to hydrolyze and subsequently co-condense with TMOS, under the sol-gel conditions, providing a straightforward route for the synthesis of organic-inorganic networks. Before such copolymerizations were carried out, the efficiency of hydrolysis and co-condensation of hexamethoxy and/or tetramethoxy functional organic modifiers under the sol-gel conditions was investigated, using the previously synthesized methoxy functionalized siloxane dimer as the model compound. All model reactions were carried out using a stoichiometric amount of water required for complete hydrolysis in the initial reaction, e.g., a molar ratio of $[OCH_3]:[H_2O]=1.0:1.0$, and no catalyst was added.

The model hydrolysis reaction of methoxy functionalized disiloxane was followed by $^1H$ NMR, and the extent of hydrolysis was calculated from the ratio of methoxy and methanol protons, as previously described for TMOS reactions. Typical $^1H$ NMR spectra as a function of reaction time are shown in ***Figure 1.42*** for a reaction with the initial composition $DSX:H_2O:CH_3OH$ = 1.0:6.0:6.0, equivalent to a ratio of $TMOS:H_2O:CH_3OH=1.0:4.0:4.0$. At this composition the reaction mixture was initially heterogeneous, but it became clear and homogeneous within seconds, as the hydrolysis occured, the water was consumed, and more methanol was generated. The hydrolysis reaction started immediately upon addition of water, as indicated by the readily noticed reaction exotherm and by the $^1H$ NMR spectrum obtained immediately upon water addition (1 minute). 50% of the methoxy groups were already hydrolyzed by the time the first sample was analyzed. However, at this point an equilibrium seemed to be achieved between hydrolysis and the reverse reaction, esterification. After approximately 1 hour, the reaction "gelled", but it could be redissolved with a very large excess of $CDCl_3$ solvent. This suggested that, following the initial hydrolysis, the condensation reactions started to take place, generating

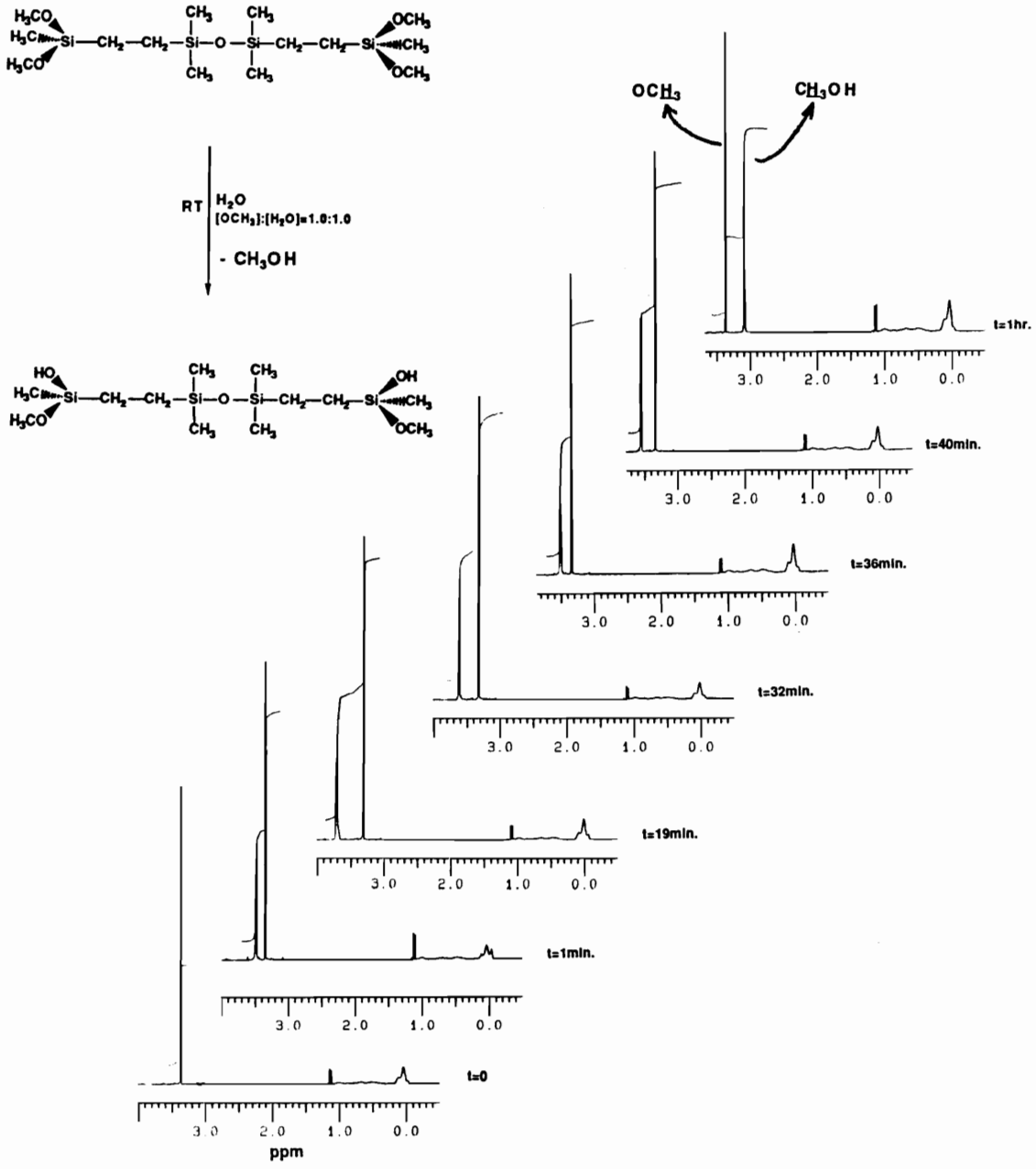


***Figure 1.42.*** $^{1}H$ NMR spectra as a function of time for a model hydrolysis reaction

$[OCH_3]:[H_2O]:[CH_3OH] = 1.0:1.0:1.0$

mostly linear or only slightly branched high molecular weight species, which could be redisolved in a large excess of solvent. Such observations are in agreement with the observed $^{1}H$ NMR data which indicated a limited number of available OH groups for condensations (approximatelly 3 OH groups per molecule).

The next step was to demonstrate that the methoxy functionalized organic compounds could undergo co-condensation reactions with the inorganic alkoxides, at competing rates, under the conditions employed for the polymerization of TMOS by the sol-gel techniques. A few experiments were carried out using the methoxy functionalized disiloxane as the model organic component and the TMOS as the inorganic component, at a molar ratio of TMOS:DSX=3.0:1.0. A stoichiometric amount of water required for complete hydrolysis in the absence of any condensations, e. g. $[OCH_3]:[H_2O]=1.0:1.0$, was used in all the experiments. The reactions were followed by $^{29}Si$ NMR. 600 scans were accumulated for each sample and the reported times are the midpoints of sample acquisition. Typical $^{29}Si$ NMR spectra are shown in ***Figure 1.43*** at different reaction times. Due to a lower concentration of these samples (lower solubility of the dimer), a relatively high signal to noise ratio was obtained after one hour of acquisition, and the subtraction techniques could not be succesfully applied. Therefore, all the spectra in Figure 1.43 contain the broad glass peak (NMR tube and probe) and only qualitative information was obtained. As previously discussed, upon condensation of silicon alkoxides and siloxane bridge formation, the silicon nuclei become more polarizable and resonate at higher field. The above series of spectra provide a number of valuable information: Firstly, the decrease in the intensity of the resonance at approximately -42ppm (corresponding to **Si**$(OCH_3)_3$ in the disiloxane) , and the appearance of a new resonance upfield from it, at approximatelly -53ppm, is undoubtedly an indication that these groups participate in condensation reactions. At longer reaction times the

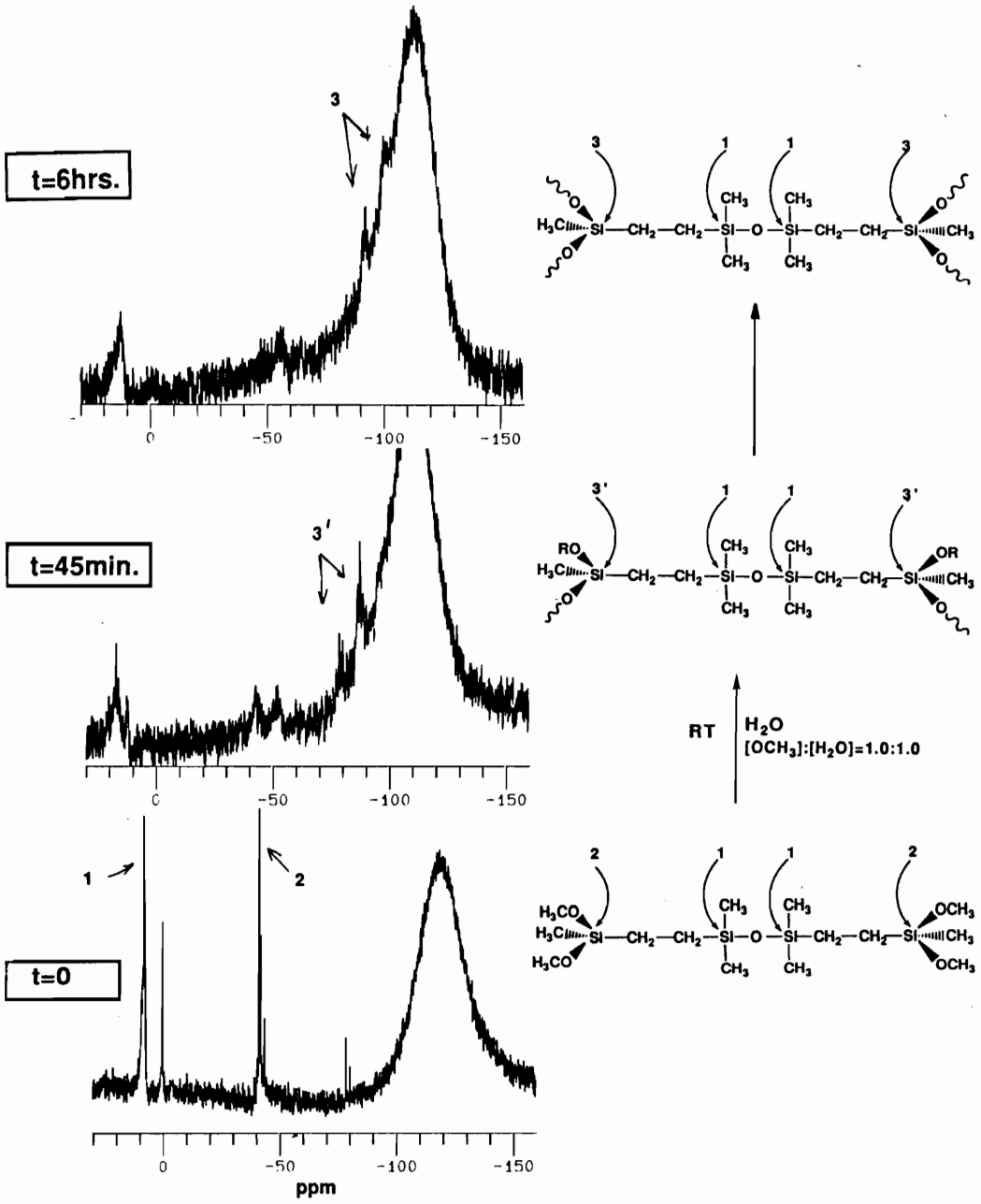


***Figure 1.43.*** $^{29}Si$ NMR spectra as a function of time for a model hydrolysis-condensation reaction; [DSX]:[TMOS] = 1.0:3.0, and $[OCH_3]:[H_2O]:[CH_3OH]$ = 1.0:1.0:1.0.

resonances at -42ppm completely disappear. Secondly, it is very important to notice that the TMOS resonance (at -78.5ppm) is not observed in the spectra, even at short reaction times (e.g. t=6hours), while higher field resonances corresponding to condensed species are effectively formed. This is very important if one recalls that in the homopolymerization of TMOS, previously discussed, unreacted TMOS species were present in considerable amount at times approaching gelation (see Figure 1.24). This observation suggests that copolymerization of TMOS with the hexamethoxy functionalized organic dimer may be faster than homopolymerization, and that TMOS may be preferentially involved in copolymerization reactions.

To summarize, both $^{1}H$ and $^{29}Si$ NMR indicate that the hexamethoxy functionalized organic disiloxanes can undergo rapid hydrolysis and subsequent co-condensation with TMOS, in the absence of catalyst, under the same conditions employed to carry out the inorganic sol-gel reactions. Furthermore, the $^{29}Si$ NMR results indicate that a much faster disappearance of the TMOS monomer was observed during copolymerization reactions, when compared to the homopolymerization, suggesting that under the conditions employed copolymerization reactions were favored. These represent excellent conditions for efficient incorporation of methoxy functionalized polysiloxane oligomers into $SiO_2$ inorganic networks by their copolymerization with inorganic TMOS.

***Copolymerization of functional PSX oligomers with TMOS.*** The copolymerization reactions were carried out under conditions similar to those employed for the homopolymerization of TMOS. However, due to lower solubility of the PSX oligomers in the highly polar reaction environment, a slight modification of the procedure was necessary, as described in the previous chapter, Experimental Techniques. In principle, a soluble network precursor was generated by prereacting the TMOS under the conditions known to lead to faster rates (e.g.,

TMOS:$H_2O$:$CH_3OH$=1.0:4.0:1.4), until approximately 85% of the methoxy groups were hydrolyzed, as indicated by $^1H$ NMR analysis. At this reaction stage, the still soluble network precursors consisted of various polysiloxane chains with a complex chain topology, as shown by $^{29}Si$ NMR (Figure 1.24). The methoxy functionalized polysiloxane oligomers were added to the soluble precursors as a solution in THF, making sure that enough THF solvent was utilized such as to result in homogeneous reaction solutions. Following the addition of polysiloxane solutions, the reactions gelled within 12 hours (depending upon the chemical composition and the PSX molecular weights). Prior to gelation the reaction mixture was poured into glass vials and the reaction was allowed to gel at room temperature. All PSX/$SiO_2$ gels were dried up to a maximum temperature of 150°C using the step-wise temperature profile described in ***Scheme 1.18***.

#### *4.2.1.3. Characterization of PSX-$SiO_2$ hybrid networks*

***Nomenclature.*** The different gel compositions in this study have been identified by the final weight percent of the components in the completely reacted networks which, in author's view, more suggestively describes these systems, than the conventional nomenclature in which the initial reaction composition is usually given [106,110,111]. For example a hybrid refered to as 40%PSX-60% $SiO_2$ (weight percent calculated based on complete conversion) was generated from 20%PSX-80%TMOS initial reaction composition. Molar concentrations involving the polysiloxane modifying component have been calculated in terms of the repeat segment, -$(CH_3)_2SiO$-, and ignore the effect of the methoxy endgroups on the molecular weight. A sample calculation of weight percent and mole percent initial and final composition for PSX-$SiO_2$ hybrids is given in Appendix 1.2.

***Reaction parameters.*** The following parameters were considered important for the generation of homogeneous PSX-SiO2 hybrid networks, and were briefly investigated:

- reaction solvent (or cosolvent system)

***Scheme 1.18.*** . General procedure for the synthesis of PSX-$SiO_2$ hybrid networks.

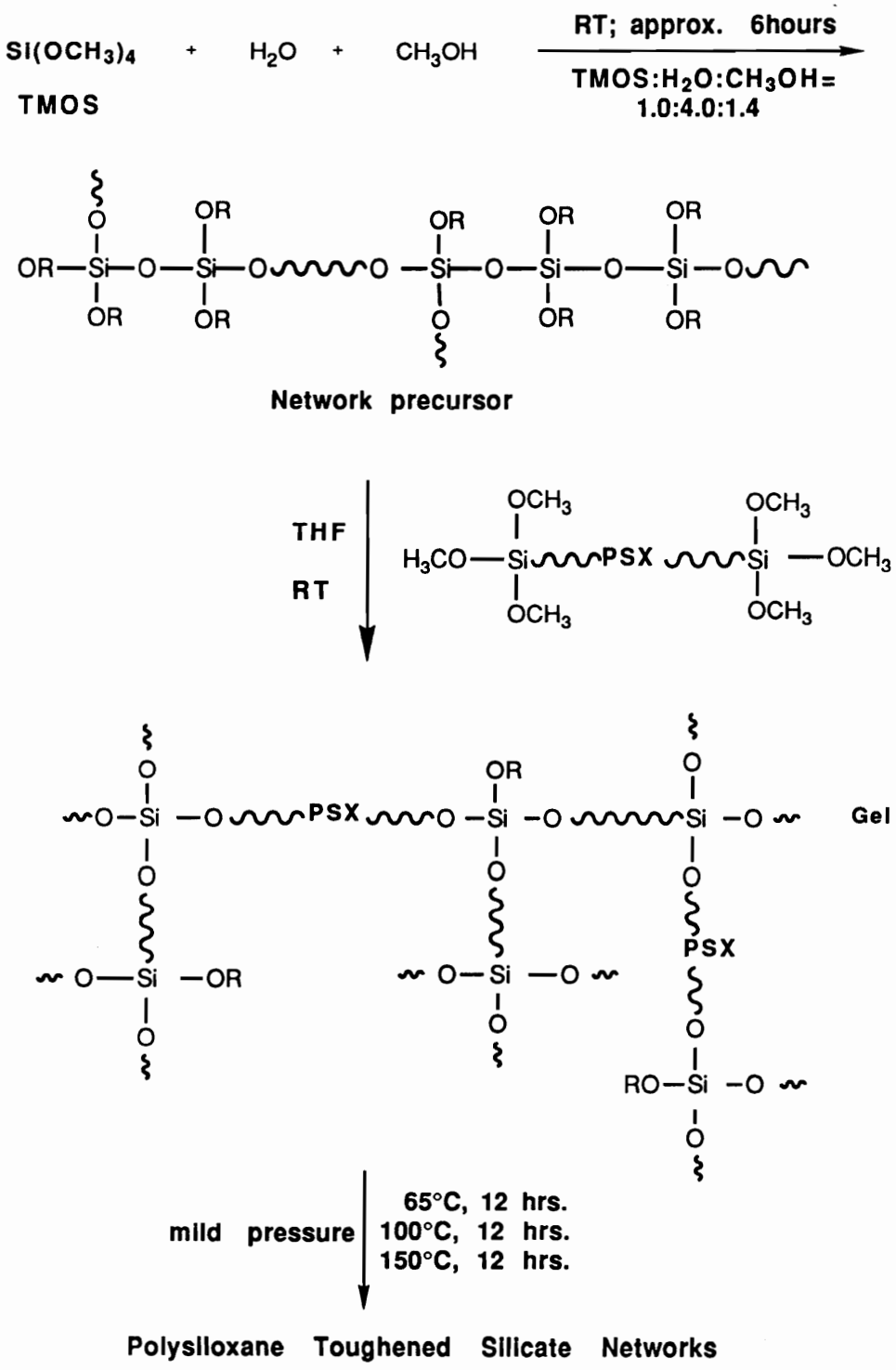

- molecular weight of the PSX oligomer (organic modifier)
- the average functionality of the polysiloxane network modifier
- hybrid chemical composition

A limited number of solvents were investigated for this reaction: methanol/isopropanol, methanol/THF and THF alone. Methanol/THF cosolvent system was selected for the described copolymerization procedure, for several reasons: methanol was preferred for the first stage of precursor synthesis, since kinetic data were available for the homopolymerization of TMOS in methanol solvent (from the initial study of the TMOS reactions); tetrahydrofuran (THF) was preferred for the second stage of copolymerization reactions, since it was a good solvent for the PSX oligomers; additionally, by using THF for the second reaction stage, instead of isopropanol (also a solvent for PSX), one does not have to worry about possible ester interchange reactions which could take place between methoxy and isopropoxy groups and could affect the reaction rates; finally, and most importantly, the selected cosolvent system generated homogeneous PSX-$SiO_2$ hybrids, after drying, for a broad composition range.

***Table 1.12*** summarizes the results for the other three parameters investigated in these systems: (1) PSX molecular weight, (2) average functionality of the PSX modifier, and (3) hybrid chemical composition. In general it was observed that: (1) As the molecular weight of the PSX organic modifier increased, the range of compositions resulting in transparent, homogeneous hybrids, narrowed (the transparency was evaluated by visual inspection). At PSX molecular weights above10-12K, as little as 10% PSX incorporation resulted in opaque hybrids. (2) The functionality of the PSX organic modifier seemed to be an important parameter: the hexamethoxy functionalized oligomers resulted in transparent hybrids over a broader composition range than the tetramethoxy functionalized oligomers. To make this point it is sufficient to notice that the tetrafunctional PSX-3K generated transparent hybrids only when

***Table 1.12.*** PSX-$SiO_2$ hybrid networks; Effect of PSX molecular weight, PSX functionality, and hybrid composition on macroscopic miscibility-Summary

| PSX $<M_n>$* [g/mole] | Hybrid Composition % PSX | Hybrid Composition % $SiO_2$ | Comments |
|---|---|---|---|
| **Tetramethoxy Functionalized PSX** | | | |
| 1,400 | <40 | >60 | T |
| | >40 | <60 | O |
| 3,000 | <30 | >70 | T |
| | >30 | <70 | O |
| 8,000 | <30 | >70 | T |
| | >30 | <70 | O |
| **Hexamethoxy Functionalized PSX** | | | |
| 5,600 | 20 | 80 | T |
| | 80 | 20 | T |
| >12,000 | 10 | 90 | T |
| | >10 | <90 | O |

*** From GPC (PSX standards)**

**T = Transparent Hybrid**
**O = Opaque Hybrid**

incorporated into hybrids at concentrations of less than 30%, while the hexafunctional PSX-5.6K produced transparent materials over the entire composition range. While the transparancy can be affected by a number of factors, the generation of transparent hybrids in these parallel experiments was taken as an indication of efficient incorporation of the PSX modifier into the glass component. (3) Finally, the composition of the hybrid plays a role: as expected, at lower PSX concentrations homogeneous hybrids were produced over a broader range of molecular weights and average functionality of the PSX component.

***Characterization of chemical composition.*** All the gels used for composition determination were dried at a maximum temperature of 150°C, according to the general procedure detailed in Chapter 3 and in Scheme 1.12. In order to determine the percentage of PSX that was actually incorporated into the hybrids, under the reaction conditions employed, the samples were extracted for a minimum of 72 hours in refluxing THF, and the composition before and after extraction was measured by MAS $^{29}$Si solid state NMR. A typical MAS $^{29}$Si NMR spectrum is shown in ***Figure 1.44*** for one of the chemical compositions investigated. The $^{29}$Si NMR spectrum contains two main silicon resonances corresponding to the polysiloxane component (approximately -22ppm) and glass component (between -90 and -120 ppm), respectively. The percentage of each component in the sample was calculated from simple integration. The results are summarized in ***Table 1.13.*** For each sample investigated, the composition before and after extraction, as well as the theoretical composition assuming 100% conversion, is tabulated. All compositions are expressed in mole percent, the molar concentrations involving the polysiloxane modifying component being calculated in terms of the repeat segment, $-(CH_3)_2SiO-$, as previously explained. These mole percent calculations based on polydimethylsiloxane repeat unit are very close to the weight percent of the components in the fully reacted gel, as shown for comparison by the theoretical values for which both mole and weight percent compositions are

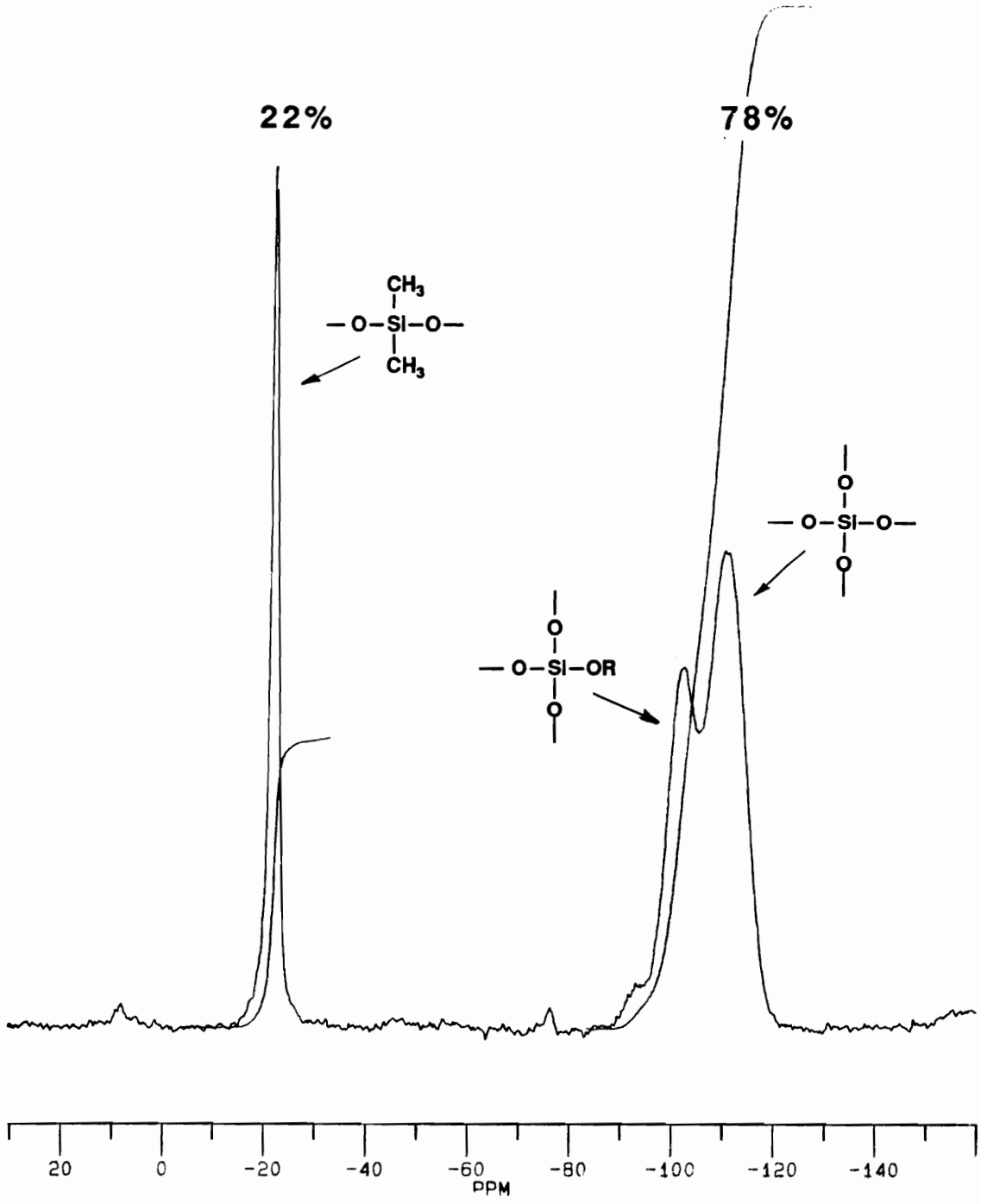


***Figure 1.44***. Typical MAS solid state $^{29}Si$ NMR spectrum for a PSX-$SiO_2$ hybrid. (theoretical molar composition 20%PSX-80%$SiO_2$)

***Table 1.13.*** Theoretical vs experimental compositions for PSX-$SiO_2$ hybrids, before and after THF extraction (experimental values calculated from solid state MAS $^{29}Si$ NMR).

| Sample No. | Chemical composition, % | | | | | | | |
|---|---|---|---|---|---|---|---|---|
| | Theoretical | | | | Experimental | | | |
| | Weight % | | Mole % | | Before extraction | | After extraction | |
| | PSX | $SiO_2$ | PSX | $SiO_2$ | PSX | $SiO_2$ | PSX | SiO2 |
| 1. | 20 | 80 | 17 | 83 | 21.2 | 78.8 | 22.0 | 78.0 |
| 2. | 40 | 60 | 35 | 65 | 42.8 | 57.2 | 43.0 | 57.0 |
| 3. | 50 | 50 | 45 | 55 | 46.0 | 54.0 | 46.0 | 54.0 |
| 4. | 60 | 40 | 55 | 45 | 59.2 | 40.8 | 59.0 | 41.0 |
| 5. | 70 | 30 | 65 | 35 | 66.0 | 34.0 | 62.0 | 38.0 |

a). **Typical error associated with quantitative $^{29}Si$ NMR analysis is approximatelly 5% in integrated values. This translates into less than 2% in calculated chemical compositions (± 0.8%) - see Appendix 1.3.**

b). The hybrids 1 through 5 were synthesized using a hexamethoxy functionalized polysiloxane oligomer with number average molecular weigh 5.6K, as determined by GPC, using PSX standards;

c). All samples were transparent;

d). All samples were reacted up to a maximum temperature of 150°C

e). All samples were extracted in boiling THF for 72 hours

indicated. The $^{29}Si$ NMR data indicate that the experimental compositions matched very well the theoretical compositions, and that the compositions before and after extractions were practically identical, within the experimental error (see Appendix 2). This demonstrated that a very efficient incorporation of PSX component was achieved under the reaction conditions employed.

It was previously discussed that due to the occurance of vitrification, the highly crosslinked sol-gel networks prepared below the glass transition temperature of the $SiO_2$ networks were not fully reacted. The incorporation of relatively high molecular weight PSX oligomers can increase the vitrification temperature, hence the ability of the system to react, by decreasing the network crosslink density. Furthermore, the low glass transition temperature PSX chains can depress the glass transition of the reacting networks, further increasing the temperature range within which the system can react. It was therefore of interest to determine if the incorporation of polysiloxane oligomers may result in an increased extent of conversion of the glass component in the PSX-$SiO_2$ hybrids.

The conversion of the glass component in the PSX-$SiO_2$ hybrids was calculated from MAS $^{29}Si$ NMR, by the superposition of three Gaussians corresponding to $Q^2$, $Q^3$, and $Q^4$ silicate units respectively, as previously described for the $SiO_2$ inorganic systems. ***Table 1.14*** summarizes the percentage of ($Q^2$+$Q^3$) and $Q^4$ species, and the calculated extent of conversion for the glass component of the PSX-$SiO_2$ hybrids of different compositions. These data are compared with the corresponding values for the reference $SiO_2$ network synthesized under similar reaction and processing conditions (Reference 150°C; Tmax =150°C). A consistently lower concentration of less reacted silicate species ($Q^2$+$Q^3$) and a correspondingly higher concentration of fully reacted units ($Q^4$) was observed for all the polysiloxane containing hybrids, when compared to the reference network (Ref. 150°C, Table 1.14). This resulted in increased conversion of the glass

***Table 1.14.*** The effect of polysiloxane incorporation on the extent of conversion of the glass component in PSX-$SiO_2$ hybrid networks.

| Sample No. | Hybrid comp. | $Q^l$ silicate unit | | RMS Error | Conversion |
|---|---|---|---|---|---|
| | % PSX/$SiO_2$ Mole % | $Q^2+Q^3$ % | $Q^4$ % | % | % |
| **Ref. 150°C** | **0/100** | **41.3** | **58.7** | **4.0** | **88** |
| 1. | 17/83 | 24.8 | 75.2 | 5.2 | 93 |
| 2. | 35/65 | 17.6 | 82.4 | 4.7 | 94 |
| 3. | 45/55 | 22.5 | 77.5 | 7.6 | 94 |
| 4. | 55/45 | 23.0 | 77.0 | 4.6 | 94 |
| 5. | 65/35 | 22.6 | 77.4 | 8.1 | 94.5 |
| **Ref. 500°C** | **0/100** | **24.3** | **75.7** | **2.5** | **93.0** |

a). **The RMS ERROR < 4% (for integrated surface areas). This translates into less than 2 % (±1.0%) in calculated conversion values; See Appendix 1.1 for sample calculation.**

b). The hybrids 1 through 5 were synthesized using a hexamethoxy functionalized polysiloxane oligomer with number average molecular weigh 5.6K, as determined by GPC, using PSX standards;

c). All samples were transparent;

d). Samples 1-5 & Ref 150°C were reacted up to a maximum temperature of 150°C; Ref. 500 was reacted up to a maximum temperature of 500°C

component in the hybrids, by 5-6.5%. Incorporation of even low concentrations of PSX (20 weight %) has a significant effect on the extent of conversion: its effect is equivalent to reacting the network at temperatures as high as 500°C (see Ref 500°C, Table 1.14).

***Physical characterization of PSX/$SiO_2$ hybrids***

The effect of PSX incorporation on the toughness of the $SiO_2$ inorganic networks was qualitatively estimated using high resolution Scanning Electron Microscopy (SEM). ***Figure 1.45*** shows a typical fracture surface for the inorganic $SiO_2$ network and for one of the PSX modified networks. The fracture surface of the inorganic material is relatively featureless, indicative of a relatively brittle fracture. On the other hand, the fracture surface of the PSX modified system shows the development of specific features associated with a ductile fracture, as defined by the strand pattern which can be connected with the local direction of failure [206]. The development of these features seems to be favored by increasing the molecular weight of the PSX modifier, ***Figure 1.46*** and/or increasing the percent of PSX in the hybrid ***Figure 1.47.***. The above SEM data suggest that the incorporation of the polysiloxane elastomeric component into the $SiO_2$ networks may provide an efficient mechanism for the rubber toughening of the otherwise brittle inorganic glasses. Unfortunately, quantitative measurements of the fracture toughness to confirm these effects was not possible, due to extreme difficulties encountered in sample preparation.

The effect of the polysiloxane incorporation on the surface polarity of the sol-gel materials was estimated from contact angle measurements. A qualitative experiment (depicted in ***Figure 1.48)*** was carried out in order to suggestively demonstrate this effect. Two samples consisting of an inorganic $SiO_2$ network and a polysiloxane modified hybrid (40%PSX, 5.6K) were placed side by side. Following, a drop of water (colored with $KMnO_4$ for visual purposes) was placed on the

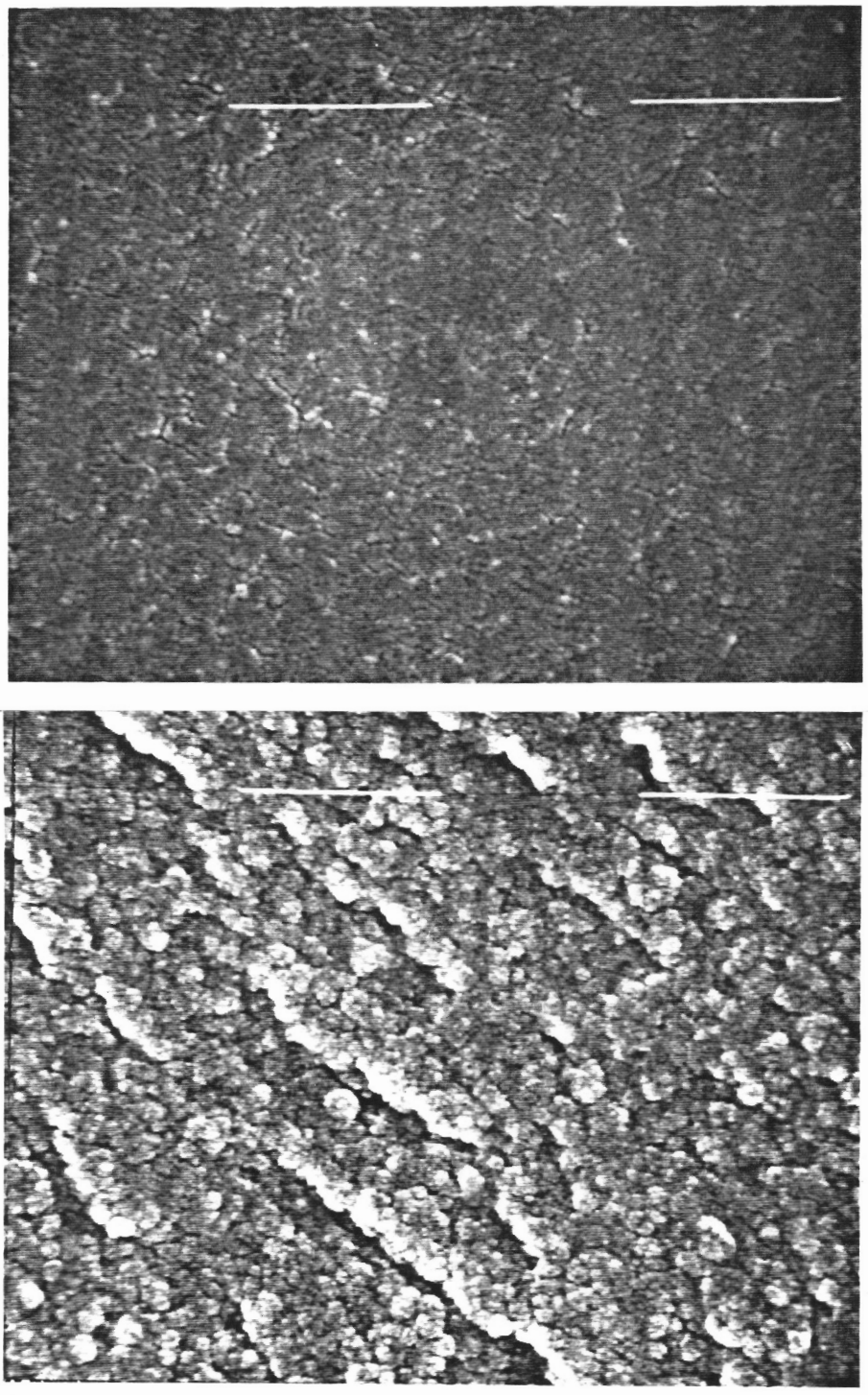

(a)

(b)

***Figure 1.45.*** Scanning electron micrographs of fracture surfaces: the effect of polysiloxane incorporation into the $SiO_2$ networks (50 Kx; 0.5μ bar); **(a)** Reference $SiO_2$; **(b)** 30/70 PSX 8K/$SiO_2$.

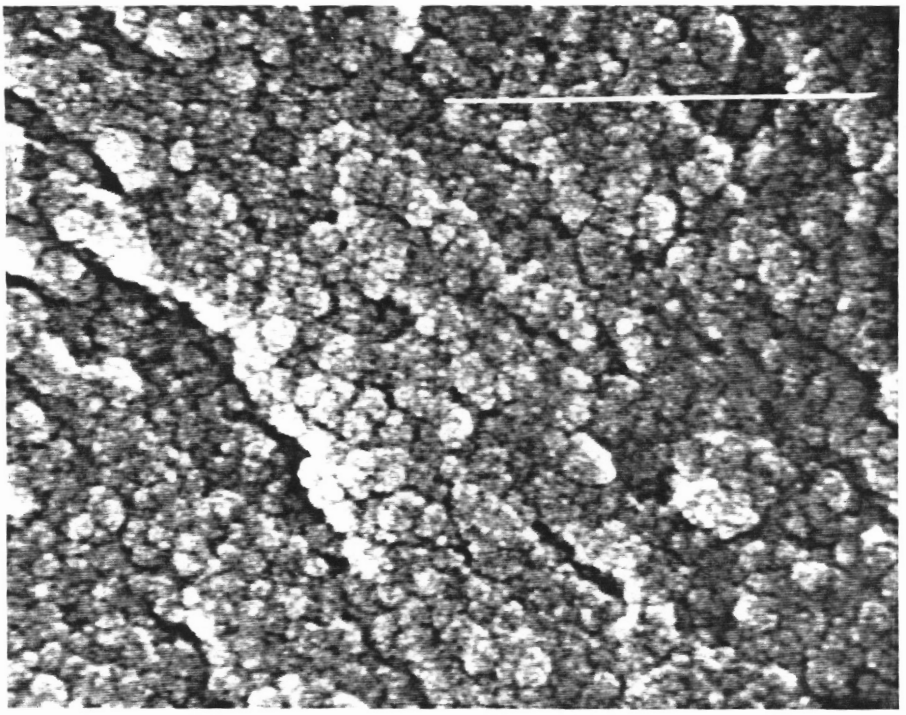

(a)

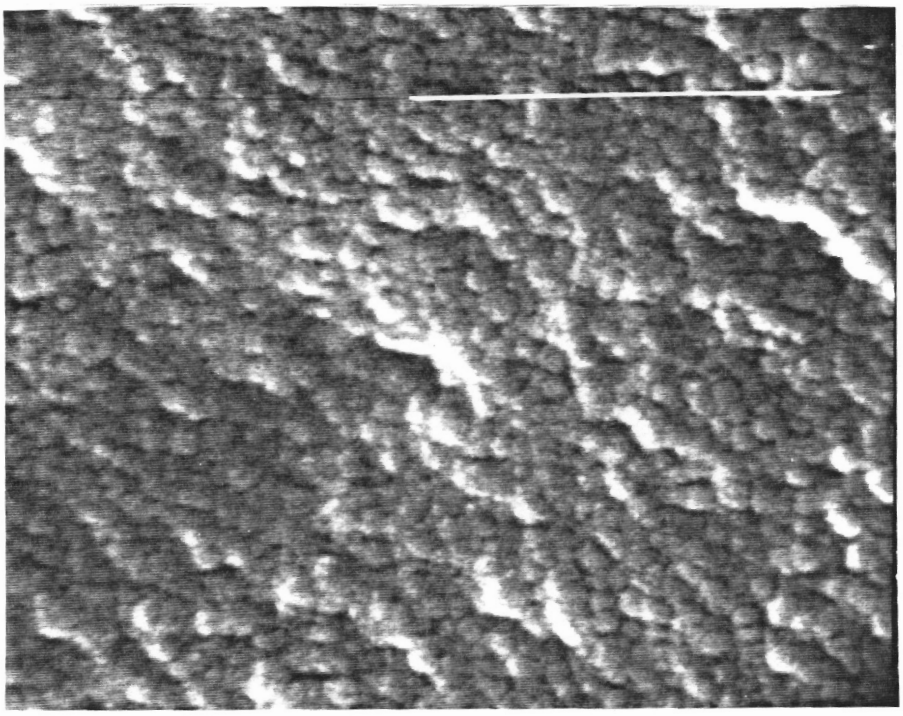

(b)

***Figure 1.46.*** Scanning electron micrographs of fracture surfaces: the effect of molecular weight of the PSX modifier (100 Kx; 0.5μ bar); **(a)** $SiO_2$ + 30% PSX 8K; **(b)** $SiO_2$ + PSX 1.4K

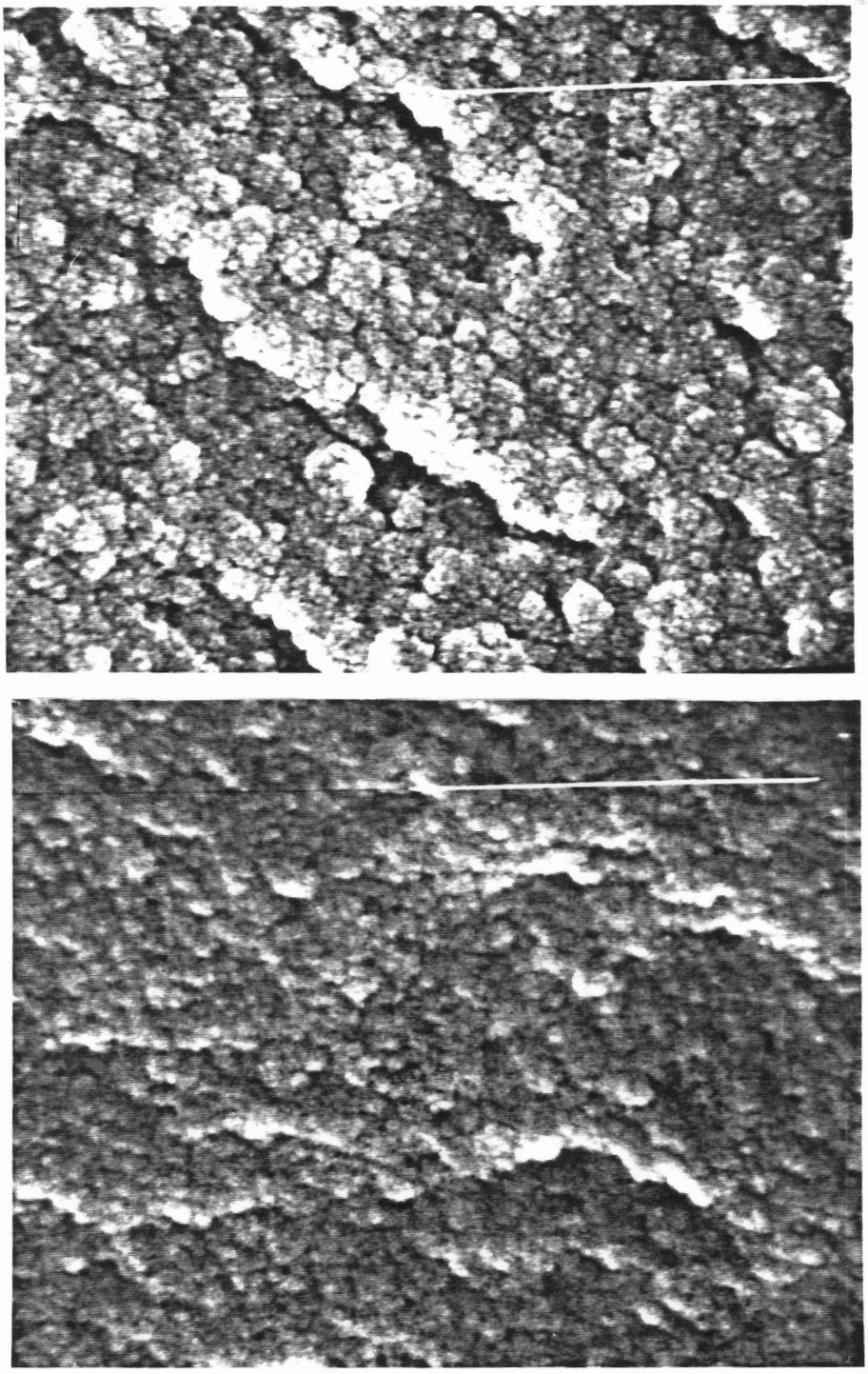

(a)

(b)

***Figure 1.47.*** Scanning electron micrographs of fracture surfaces: the effect of the concentration of the PSX modifier (100 Kx; 0.5μ bar); **(a)** 30% PSX 8K; **(b)** 15% PSX 8K

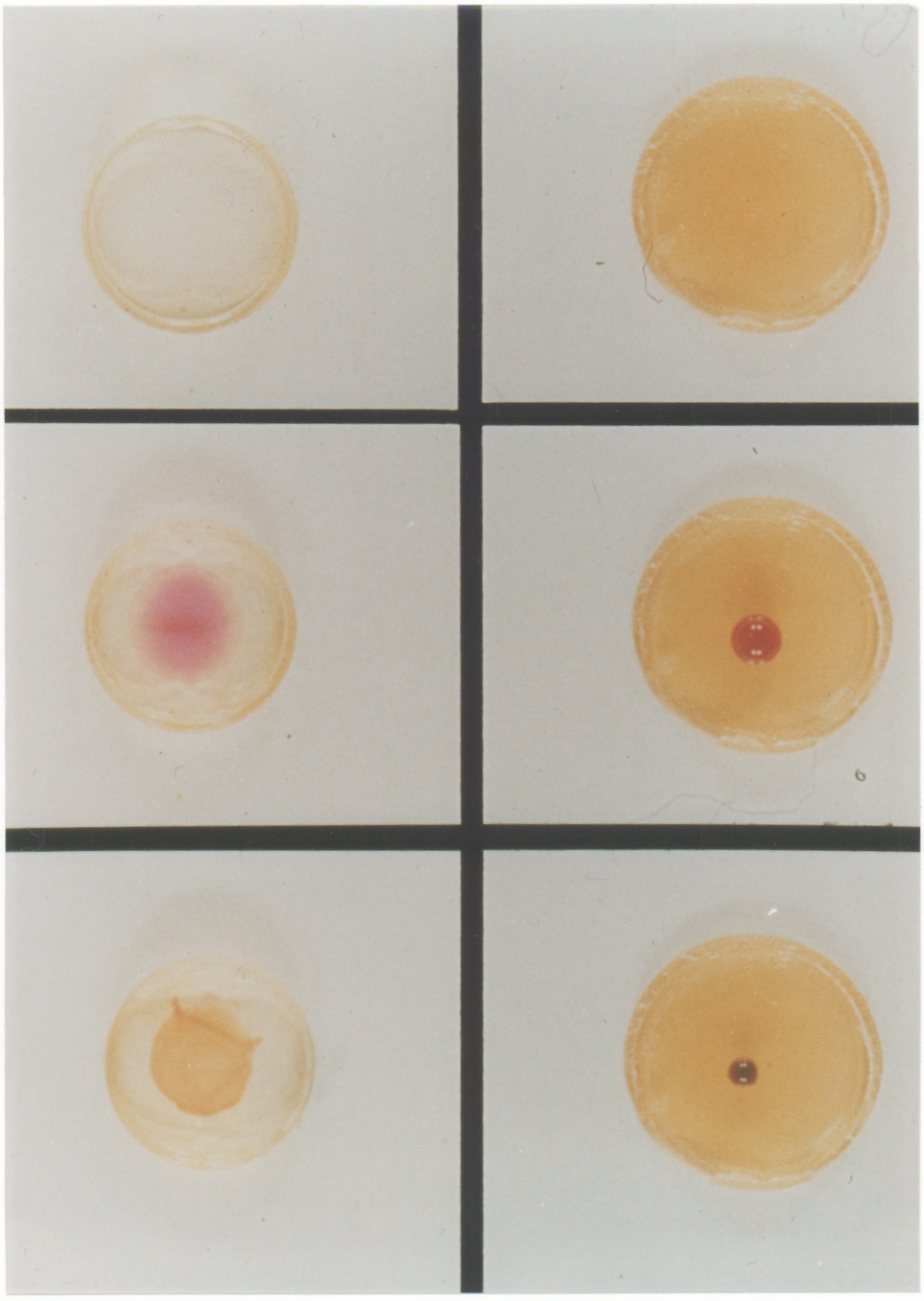

***Figure 1.48.*** Water "contact angle" experiments - qualitative evaluation of the surface polarity

**Left**: Reference inorganic SiO2; **Right**: PSX/SiO2, 40/60 weight %

**Top**: Initial samples; **Middle**: after1minute; **Bottom**: after 1 hour

surface of each sample. The water was observed to spread instantaneously on the surface of the inorganic network, but it did not wet the PSX modified material, as shown by the pictures taken one minute after the water was added. At longer contact times, the water completely penetrated the microporous inorganic $SiO_2$ network, while it did not interact with the PSX modified sample, as shown by the two pictures at the bottom, taken one hour after the water was added .

Because polydimethylsiloxanes have a low surface energy relative to the surrounding $SiO_2$ network, and are believed to exist, at least partially, in "oligomer rich areas" [207], it was anticipated that the PSX component would tend to dominate the air/solid interface of the hybrid networks. Advancing water contact angle were measured to verify these expectations and the results are listed in ***Table 1.15*** Water contact angle measurements indicated a change in the surface composition of the samples as a function of the hybrid composition: the hybrids with higher levels of PSX exhibit higher advancing water contact angles. However, all the measured values for this type of materials, including the reference PSX networks, are much lower than the reported contact angles for polydimethylsiloxane networks generated by a different crosslinking mechanism, in a less polar environment [146]. The samples for this study (including the reference PSX networks) were generated in sealed vials, as detailed in Chapter 3, under a permanent polar environment ($CH_3OH$ and $H_2O$), conditions which do not favor at all the migration of the PSX segments at the surface, but rather the orientation of the chains with their more polar segments (e.g. endgroups containing residual OH or/and $OCH_3$ groups) towards the surface. Even though all the samples utilized for the contact angle measurements were extensively dried in the vacuum oven for at least 48 hours prior to analyses, the chain orientation at the reaction stage appeared to be retained to a large extent, as suggested by the much lower values obtained for the water contact angles. A second factor for the relatively low water contact angles may have been the

***Table 1.15.*** Contact angle measurements for PSX/$SiO_2$ gels.

| Sample No. | Composition PSX/$SiO_2$, (wt%) | Advancing contact angle |
|---|---|---|
| 1. | 0/100 | – * |
| 2.*** | 20/80 | – * |
| 3.*** | 40/60 | 83 |
| 4.*** | 70/30 | 86 |
| 5. | 100/0** | 89 |
| **6.** | **PDMS X-linked** | **112** |

a). Water spread readily on samples 1 and 2 and cracked the samples before any reading could be made;

b). The reference PSX sample (100/0) was generated by crosslinking a hexamethoxy functionalized PSX-5.6 K.

c). The hybrids 2,3, and 4 were synthesized using the same hexamethoxy functionalized PSX-5.6K, as for the preparation of the reference sample;

‡ All samples were transparent;

retention of residual methanol and water which were very difficult to completely remove due to their hydrogen bonding to the residual OH groups.

***Thermal stability of PSX-$SiO_2$ hybrids.***. Thermo-gravimetric analysis (TGA) was carried out on selected PSX-$SiO_2$ hybrids in order to determine the thermal stability of the hybrid systems as a function of PSX content. The TGAs were carried out in air, at a constant heating rate of 10°C per minute according to the procedure outlined in Chapter 3. ***Figure 1.49*** gives representative thermograms for PSX-$SiO_2$ hybrids, along with the reference PSX and $SiO_2$ networks. The reference PSX network was generated by crosslinking the same hexamethoxy functionalized oligomer (5.6K) utilized for the preparation of the hybrids, using similar reaction and processing conditions. Prior to the recorded thermogram the reference $SiO_2$ material was rapidly heated at 500°C in the thermo-gravimetric analyzer, followed by fast cooling, in order to eliminate the residual solvent and reaction by-products retained in the microporous network.

These curves indicate a significant difference in the thermal stability of the hybrids when compared to the inorganic $SiO_2$ networks, which is to be expected. However, the thermal stability of the hybrids is quite good: the 5% loss does not occur until 375°C and the major weight loss does not take place until approximately 450°C. This indicates that (1) no redistribution reactions of the PSX chains occured at eleveted temperature, in the catalyst-free systems employed for these reactions, and that (2) such hybrids were stable at relatively high temperatures.

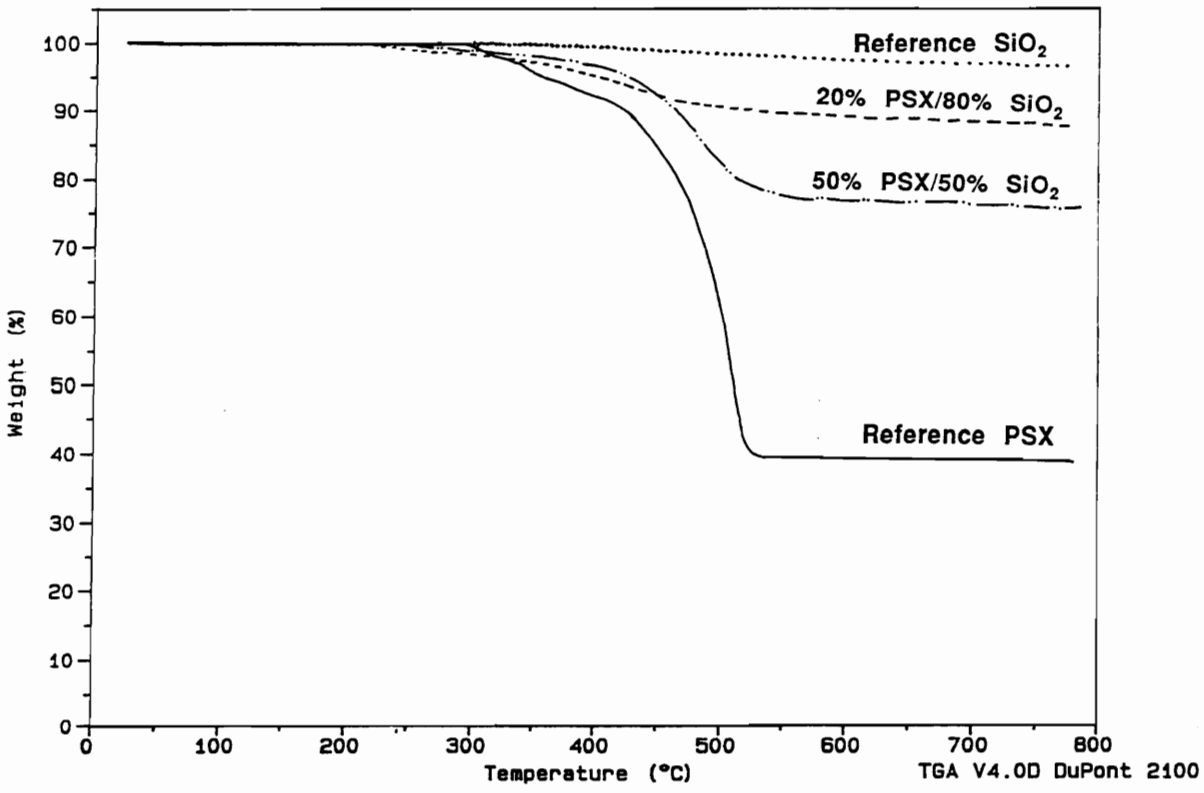


***Figure 1.49.*** Dynamic TGA scans for PSX/$SiO_2$ hybrids and the reference networks (Heating rate = 10 deg/min; Air flow 10 ml/min).

### *4.2.2. POLYIMIDE MODIFIED $SiO_2$ NETWORKS*

Typically, organically modified sol-gel glasses have been primarily synthesized with elastomeric components such as poly(dimethylsiloxane) or polytetramethylene oxide, and employing catalyzed sol-gel reactions [105-107]. A new route for the synthesis of polysiloxane modified $SiO_2$ glassses through a catalyst-free reaction was described in the previous section of this chapter. However, there are fewer attempts at this time for the incorporation of a glassy component (below the $T_g$) in a sol-gel inorganic network. Schmidt and Philipp combined a sol-gel mechanism with an independent free radical reaction [111-113] for the synthesis of organic modified glasses in which the organic modifier is a glassy component.

Wilkes et al. simplified this approach by using the same principle as the one developed for incorporation of elastomeric modifiers [118]. Polyetherketone (PEK) oligomers of controlled molecular weight were selected by Wilkes et al. to prove, for the first time, this simple approach to the preparation of organic modified glasses in which the organic oligomer is glassy at the reaction temperature. The $T_g$ of the PEK component is of ca 150°C. The PEK oligomers were functionalized by reacting hydroxyl or amine terminated oligomers with isocyanato propyl trialkoxysilane, therefore generating an urethane or urea linkage between the oligomer chain end and the reactive end groups. The alkoxysilane end groups provide the reactive site of the PEK oligomers in sol-gel type reactions. The conversion in such systems was found to be somewhat limited due to the vitrification, as the network buildup progresses, at least at lower reaction temperatures. However, the authors indicated that further network development could be promoted by utilizing thermal post-gelation treatments [118]. The main disadvantage of these systems is that the urea or uretane linkages generated during functionalization reactions have a relatively low thermal stability and a potential susceptibility for hydrolysis during the catalyzed sol-gel reactions.

The present study investigated a new functionalization route for such oligomers in order to produce more thermally and hydrolytically stable linkages to the reactive end-groups. Polyimide oligomers of controlled molecular weight were selected as the glassy organic component. Hence, the remaining of this chapter will discuss the synthesis and post-functionalization of polyimide oligomers of selected structure, and their subsequent incorporation into the inorganic glasses through sol-gel reactions.

### *4.2.2.1. Synthesis of reactive polyimide oligomers*

***Amine terminated polyimide oligomers.*** Amine terminated, fully imidized polyimide oligomers of controlled molecular weight were synthesized by the classic two-step procedure which initially involved the synthesis of a soluble poly(amic acid) intermediate from aromatic dianhydrides and aromatic diamines. A calculated excess of diamine component was utilized in order to control the molecular weight and to generate amine end groups (Section 3.3.2.2). From the wide variety of polyimide structures available the particular structure based on the less polar monomers 6F dianhydride and Bis A diamine was selected for these investigations. These structures generate polyimides with low dielectric constant values [138, 209] which was one important feature we were seeking to bring into the inorganic glass by polyimide incorporation. Conversion of the poly(amic acid) intermediates to fully cyclized polyimides was accomplished by solution imidization techniques. The two-step reaction is described in ***Scheme 1.19.*** The target moleculr weights for the polyimide oligomers used in this study ranged from 1K g/mole to 9K g/mole. The number average molecular weights were determined by potentiometric titration of amine end groups with 0.02 anhydrous HBr in glacial acetic acid (Section 3.5.1). ***Table 1.16*** summarizes these results and indicates that a good correlation exists between the theoretical and experimental molecular weights.

***Scheme 1.19.*** Synthesis of amine functionalized, fully imidized polyimide oligomers by the two-step solution imidization techniques.

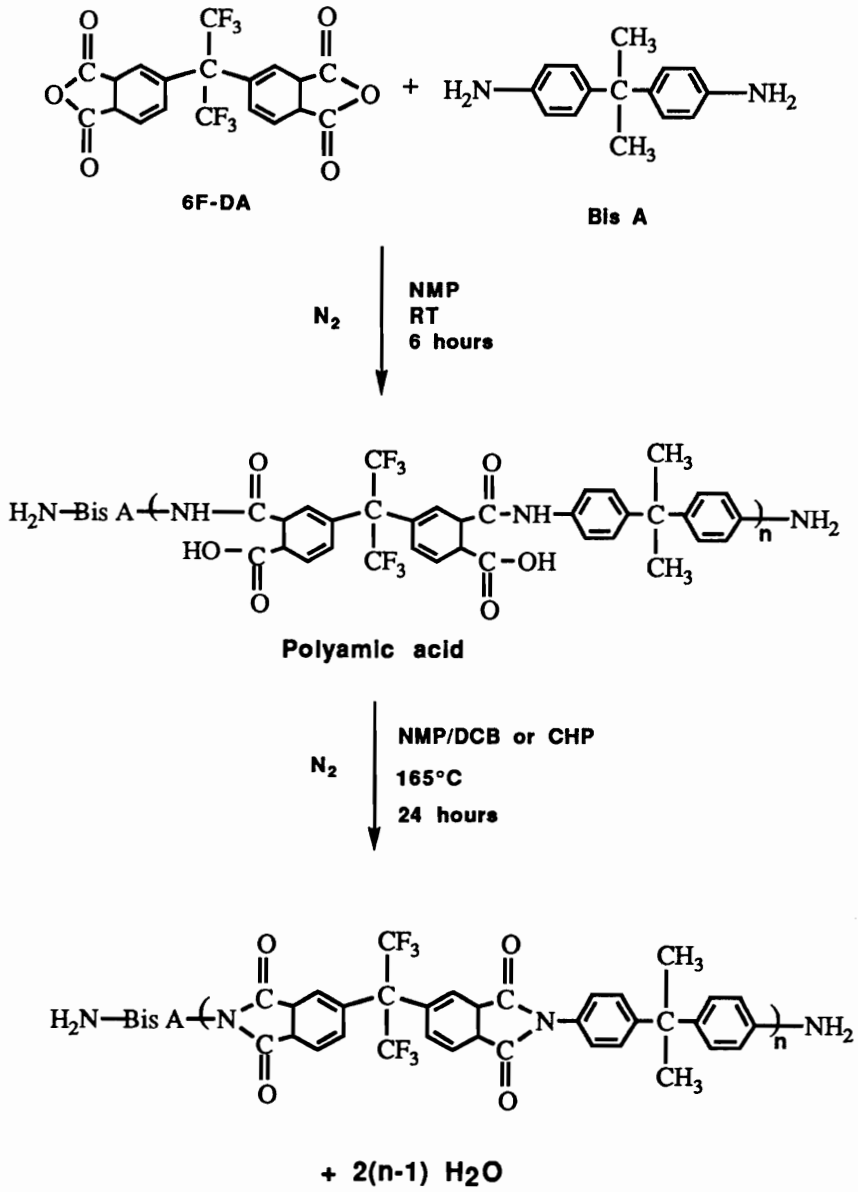

***Table 1.16.*** Theoretical vs experimental number average molecular weights for amine terminated polyimide (PI) oligomers

| Sample | Number average molecular weight, $<M_n>$, g/mole | |
|---|---|---|
| No. | Theoretical | Amine endgroup titrated |
| 1. | 950 | 1,300 |
| 2. | 284.0 | 3,070; 3,200; 3,400* |
| 3. | 4730 | 5,800; 6,300** |
| 4. | 8520 | 9,600 |

*three different reactions

**two different reactions

***Nadimide terminated polyimide oligomers.*** The amine terminated polyimide oligomers were reacted with cis-5-Norbornene-endo-2,3-dicarboxylic anhydride to convert the amine to nadimide end groups, ***Scheme 1.20.*** Quantitative conversion was achieved under the conditions described in Scheme 1.20, as indicated by $^1$H NMR analysis. ***Figure 1.50*** shows the $^1$H NMR spectra for the nadimide and amine functionalized 6F-Bis A polyimide. A down field shift of two of the aromatic protons at 6.6ppm and the appearance of the nadimide unsaturated protons at 6.2 ppm accompanies this conversion, as shown by $^1$H NMR spectra in Figure 1.50.

***Methoxy functionalized polyimides.*** During the last functionalization step, the nadimide functions were converted to silicon-methoxide end-groups which are reactive under the sol-gel conditions. This conversion was achieved through a hydrosilation reaction at the double bond of the nadimide end groups using methoxy silanes as hydrosilating agents and chloroplatinic acid as the reaction catalyst.

Hydrosilation reaction is a very useful tool for the synthesis of organosilanes however, it is very complex and it is not a simple matter to make really effective use of it. The reaction rate is highly dependent on the structure of olefin, silane and catalyst [203]. The structure of the silane is not very important except that the reactivity is decreased with increase in the electron density on the hydrogen atom. The catalyst is very important because it will determine whether or not the metal can coordinate to the olefin. Strongly coordinating ligands can displace the olefin from the metal complex thus prolonging the induction period or even stopping the reaction totally. The nature of the olefin has considerably more influence than that of the silane on the reaction rate. Both electronic and steric factors contribute to this effect. The reactivity is directly proportional to the electron density on the double bond, hence a conjugation or an electron withdrawing group

***Scheme 1.20.*** Synthesis of nadimide functionalized polyimide oligomers

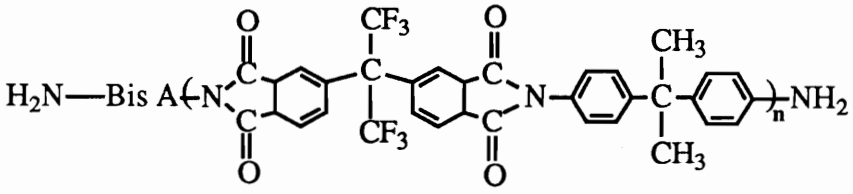

**Amine terminated polyimide**

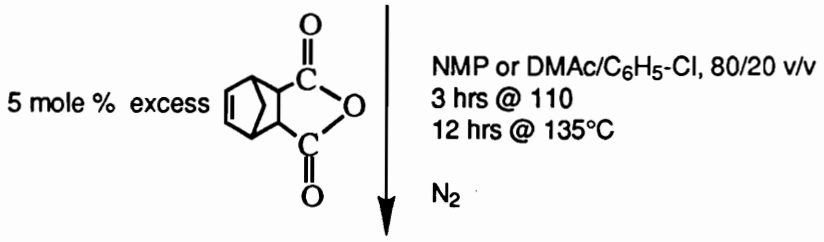


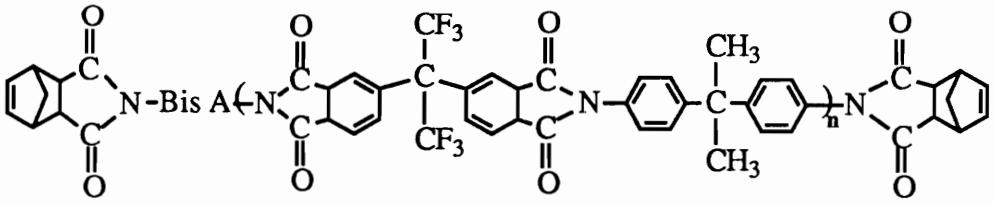

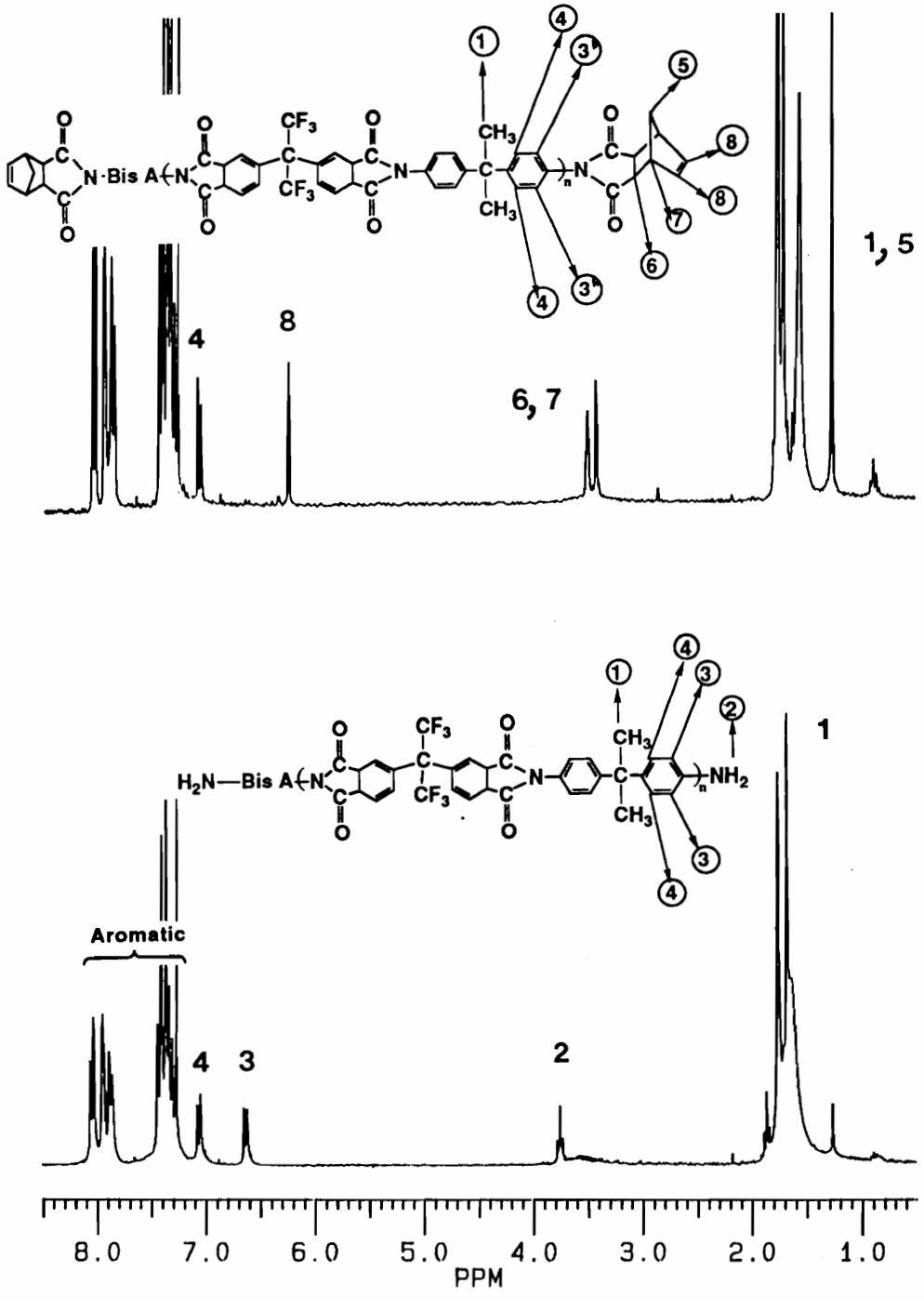


***Figure 1.50.*** $^{1}H$ NMR spectra of 6F-Bis A (2.5K) polyimide oligomer, amine (a) and nadimide (b) end group functionalized.

reduces the rate. Saam and Spier [210] found that a change of only 0.07 units in the sigma values of the substituents on the olefin was associated with a tenfold change in the reaction rate. The importance of substituents on the olefin was reinforced by experiments carried out by Plueddemann et al. [211]. They showed that addition to allyl acrylate occured entirely on the allyl group, not on the acrylate. Steric hyndrance also reduces the rate of hydrosilation. Addition to internal olefins is slower, but still fast if a terminal position is conveniently available [212]. Addition to cyclohexene structures is very slow and accompanied by every conceivable exchange and isomerization. Every example with a cyclohexene has proved hydrosilation to be very slow and difficult, but this difficulty was not experienced with cyclopentene structures [213]. This different reactivity can be attributed to the different ring strain which is present in the smaller rings as molecular geometry requires greater distortion from optimal bond angles, while the six-membered rings are nearly strain free [214]. The strain is further increased in cyclics containing double bonds when factors of molecular geometry do not permit all the bonds to the two $sp^2$-hybridized carbons to be coplanar [214].

In light of the above information available we believed that the hydrosilation at the nadimide double bond might be somewhat slower but it would not present special difficulties. While the electronic and steric effects in the nadimide structure are not too favorable, the ring strain should counteract to some extent these unfavoreble contributions. Hydrosilation of the related structure, nadic anhydride, has already been employed in the synthesis of organic compounds and the reaction was shown to proceed to high conversions [215,216]. Our goal was to carry out the hydrosilation reaction under the most favorable conditions such as to increase the reaction rate and hence the hydrosilation yield. Faster reaction rate means less time for competing side reactions (telomerization, polymerization, isomerization), while slower reaction rate normally leads to poor yields.

Due to the low concentration of chain ends in the high molecular weight nadimide terminated polyimide oligomers it was difficult to directly evaluate the efficiency of the hydrosilation reaction when polyimide oligomers were used as the olefin component. A model reaction in which a low molecular weight olefin component closely resembling the reactive end groups of the polyimide oligomers was employed, in order to carry out this evaluation. The model olefin compound, N-phenyl-nadimide, was synthesized from aniline and cis-5-Norbornene-endo-2,3-dicarboxylic anhydride according to ***Scheme 1.21.*** The hydrosilation to the N-phenyl nadimide, described in ***Scheme 1.22*** was closely monitored by both $^{1}H$ and $^{13}C$ NMR. In the $^{1}H$ NMR the hydrosilation reaction was characterized by the disappearance of the unsaturated nadimide protons at 6.2 ppm as well as by a down field shift of two of the aromatic protons from 7.15 to 7.25 ppm, as shown in ***Figure 1.51.*** The rate of disappearance of the nadimide double bond, under different reaction conditions, was calculated from $^{1}H$ NMR as a function of hydrosilation time. Typical results are summarized in ***Figure 1.52*** for two such reactions in which same amount of catalyst and similar reaction conditions were used as detailed in Chapter 3, but the reagents were added at different rates. In the reaction designated 6.31 the silane and catalyst portions were added at shorter time intervals, while in the second reaction designated 6.49, they were added over a larger period of time. The stepwise addition of both catalyst and silane reagent was detailed in Chapter 3, Section 3.3.2.4.

For both reactions it was observed that each fresh catalyst and silane addition was accompanied by a fast decrease in the concentration of unsaturated protons. However, following the initial fast dissapearance of unsaturation the reaction arrived at a plateau, even though the $^{1}H$ NMR indicated that the silane was not fully consumed. A new catalyst and silane portion was necessary for further reaction to occur and an excess silane was required for complete disappearance of unsaturation. This behavior, ilustrated by the stepwise shape of the conversion curve, is more

***Scheme 1.21.*** Synthesis of N-phenyl nadimide utilized as the model olefin compound for hydrosilation to the nadimide double bond.

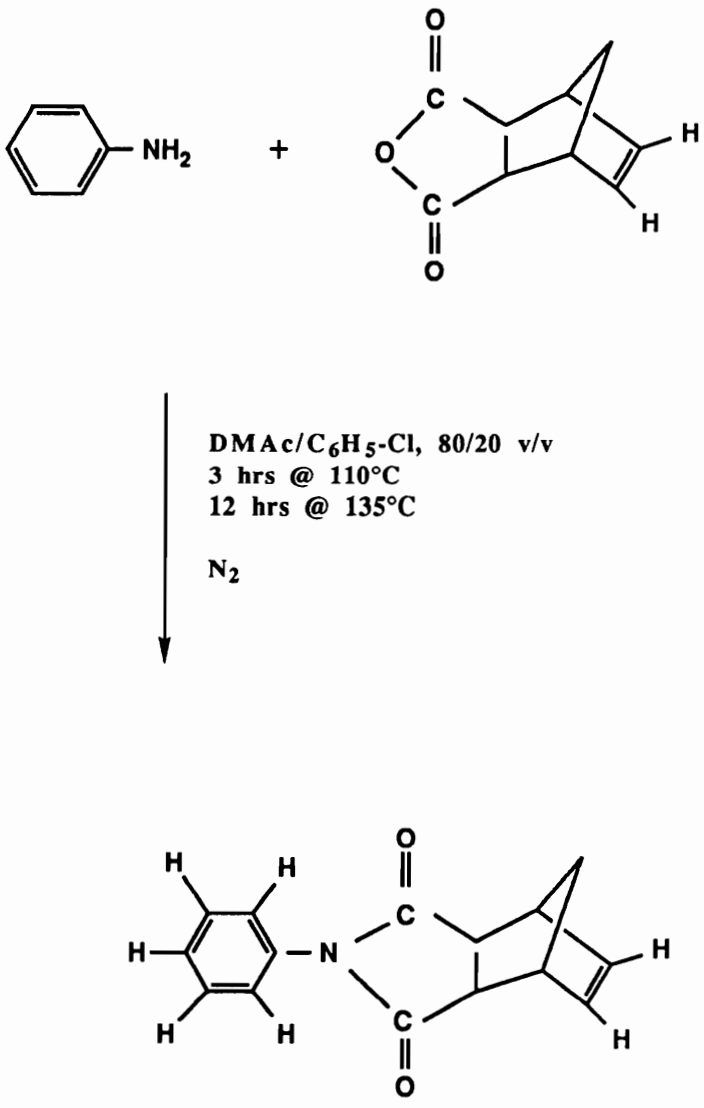


1

***Scheme 1.22.*** Hydrosilation reaction at the N-phenyl nadimide; Model reaction for the synthesis of methoxy functionalized polyimide oligomers

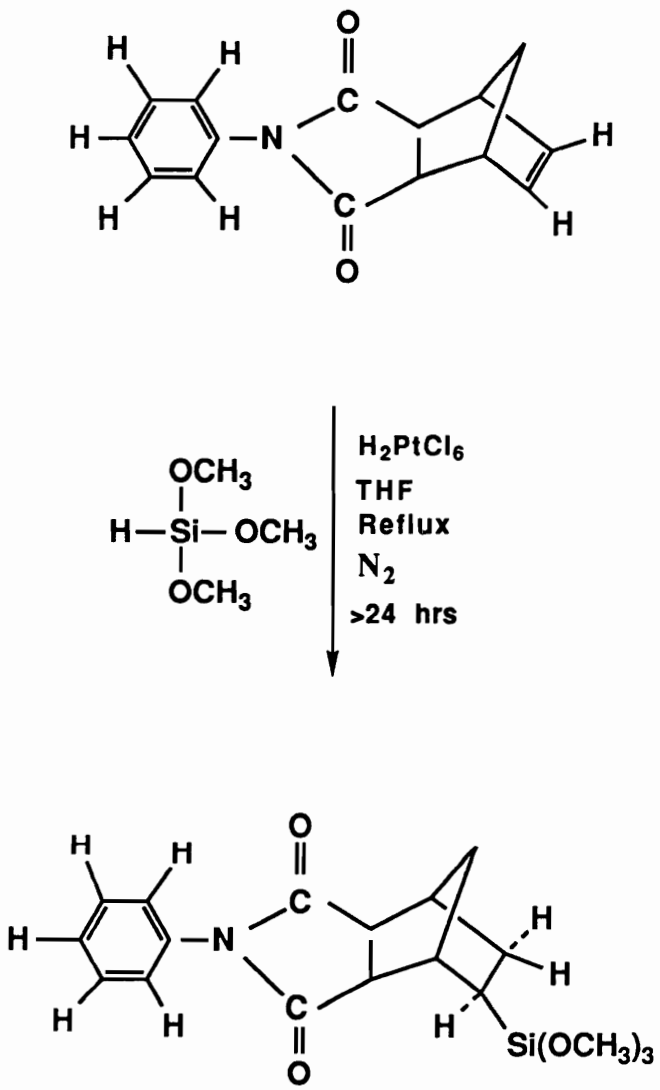

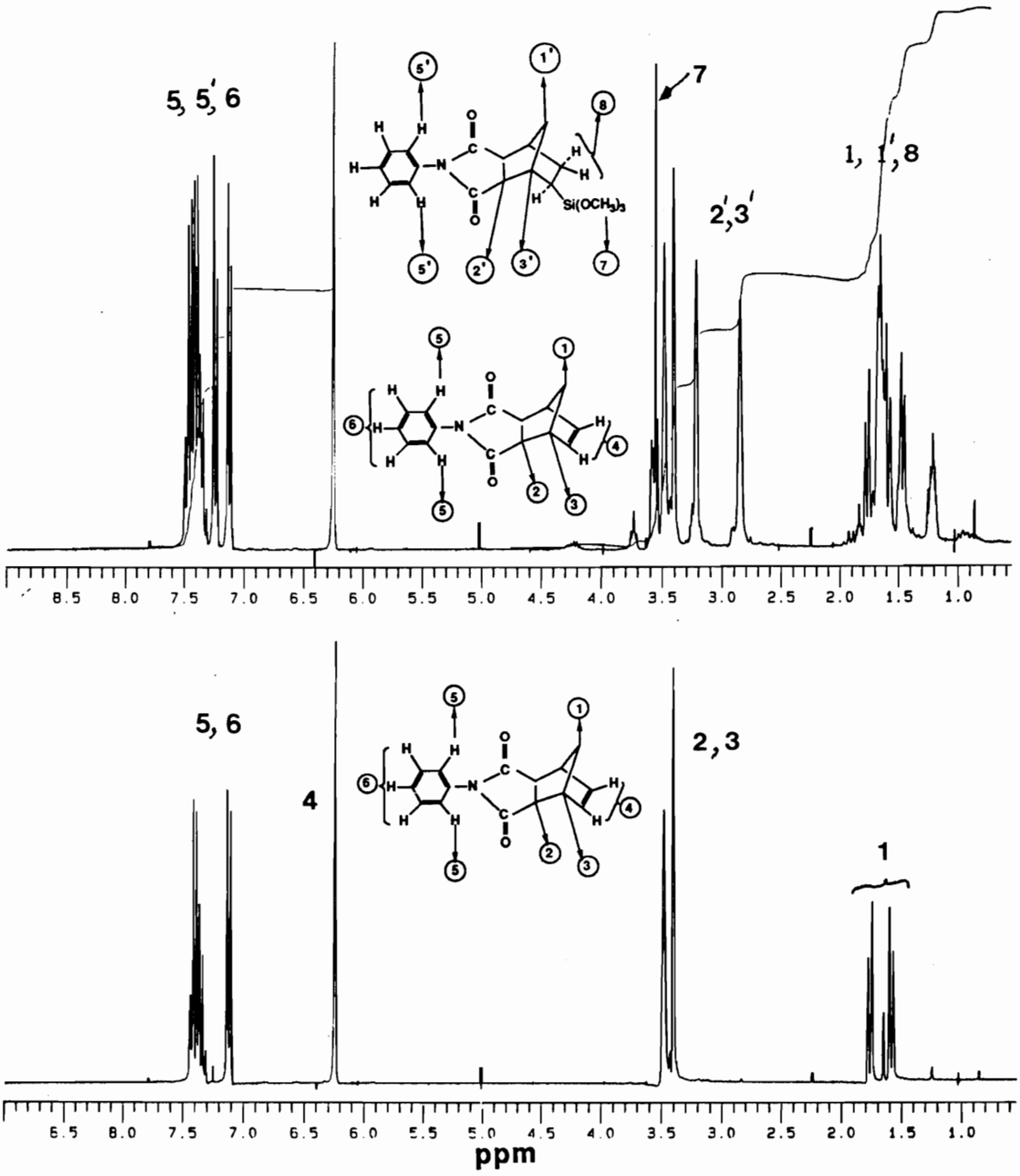


***Figure 1.51.*** $^{1}H$ NMR spectra showing the evolution of hydrosilation to the N-phenyl nadimide model compound.

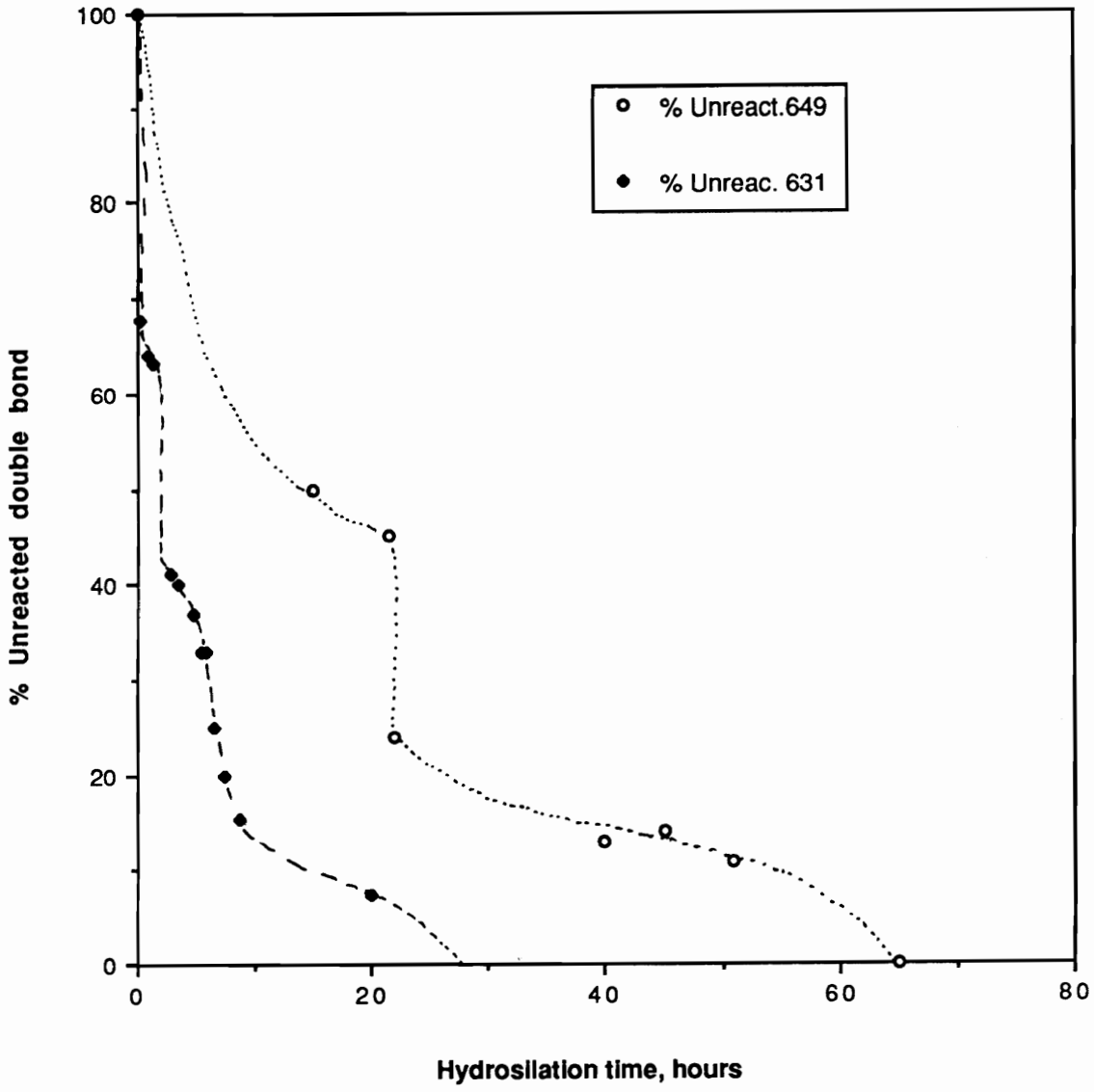


***Figure 1.52.*** Model hydrosilation at the nadimide double bond; Rate of disappearance of the unsaturated nadimide protons as a function of hydrosilation time. (Reactions 6.31 and 6.49 differ by the time interval between fresh reagent addition).

evident for the reaction labeled 6.49 in which the new catalyst and silane portions were added at larger time intervals. The fast conversion increase following the fresh catalyst and silane addition was preceded by a color change from yellow to very dark brown, but the solution remained visually clear. Such behavior was previously reported in the literature [143] for $Pt^{II}$ type hydrosilation catalyst, and it was associated with the formation of colloidal platinum ($Pt^0$) as the active catalyst. These colloidal species are believed to be more active than the compounds from which they are derived, and the induction period is greatly reduced upon their formation [143]. The formation of colloidal platinum ($Pt^0$) from $Pt^{II}$ complexes was proposed to be promoted by the reaction with the silane, according to equation 43 below:

$$CODPt^{II}Cl_2 + xs(EtO)_3SiH \longrightarrow \quad (43)$$

$$[Pt^0]_x + H_2\uparrow + ClSi(OEt)_3 + c\text{-}C_8H_{14} + c\text{-}C_8H_{16}$$

colloid

where COD = 1,5-cyclooctadiene.

Transmission electron micrographs (TEM) of the active colloidal platinum $Pt^0$ generated by equation 43 revealed a honeycomb structure, with a high surface area, in contrast to the lower surface area, hard spheres which were observed for the colloidal species formed from $H_2PtCl_6$ in isopropanol [212] as described by equation 44. Under the conditions described by equation 44, the catalytic activity was reduced or completely lost by such solutions after they turned brown.

$$H_2PtCl_6 \cdot 6H_2O \times 10\ i\text{-}PrOH + 28\ MeCl_2SiH \longrightarrow \quad (44)$$

$$Pt^0\downarrow + 6\ MeSiCl_3 + 6\ [MeCl_2Si]_2O + 10\ MeCl_2SiOi\text{-}Pr + 24\ H_2\uparrow$$

colloid

While elucidation of the structure of the active catalytic species was beyond the scope of this work, it was apparent that the change in color during our experiments was accompanied by a considerable increase in the catalytic activity, at least in the initial stages, as judged by the fast

decrease of the unsaturation following the color change. It is also important to emphasize that an excess silane was required for complete reaction, suggesting that the silanes were also involved in the formation of the reactive catalytic species.

Under these conditions the hydrosilation to the model olefin was usually completed in less than 24 hours, as indicated by both $^{1}H$ and $^{13}C$ NMR. Stacked $^{1}H$ NMR spectra of the aromatic and unsaturated region, indicating near complete disappearance of unsaturated protons, are shown in ***Figure 1.53***. The completion of hydrosilation was also confirmed by $^{13}C$ NMR. ***Figure 1.54*** shows the $^{13}C$ NMR spectra for the model olefin compound before and after hydrosilation, with the spectral assignments. The region of interest in the above spectra is expanded in ***Figure 1.55*** and indicates the complete disappearance of the unsaturated carbons at 134.6ppm.

Similar reaction conditions were employed for the hydrosilation of nadimide functionalized polyimide oligomers, as described in ***Scheme 1.23.*** All reactions were carried out in inert atmosphere in refluxing THF, using a catalyst concentration of $5x10^{-3}$-$1x10^{-2}$ mole catalyst/mole double bond and a 25-30% excess silane. Each reaction was closely monitored by $^{1}H$ NMR, and allowed to proceed until complete disappearance of unsaturated nadimide protons at 6.2 ppm was observed. Typical $^{1}H$ NMR spectra for nadimide and methoxy functionalized polyimide oligomers are shown in ***Figure 1.56.***

#### *4.2.2.2. Synthesis of polyimide-$SiO_2$ hybrid networks*

***Model hydrolysis and condensation reactions.*** Due to the low concentration of methoxy reacting end groups on the functionalized polyimide oligomers, it was difficult to directly attest their ability to react under sol-gel conditions. Consequently, model studies which allowed for a closer monitoring of such reactions by spectroscopic techniques were used.

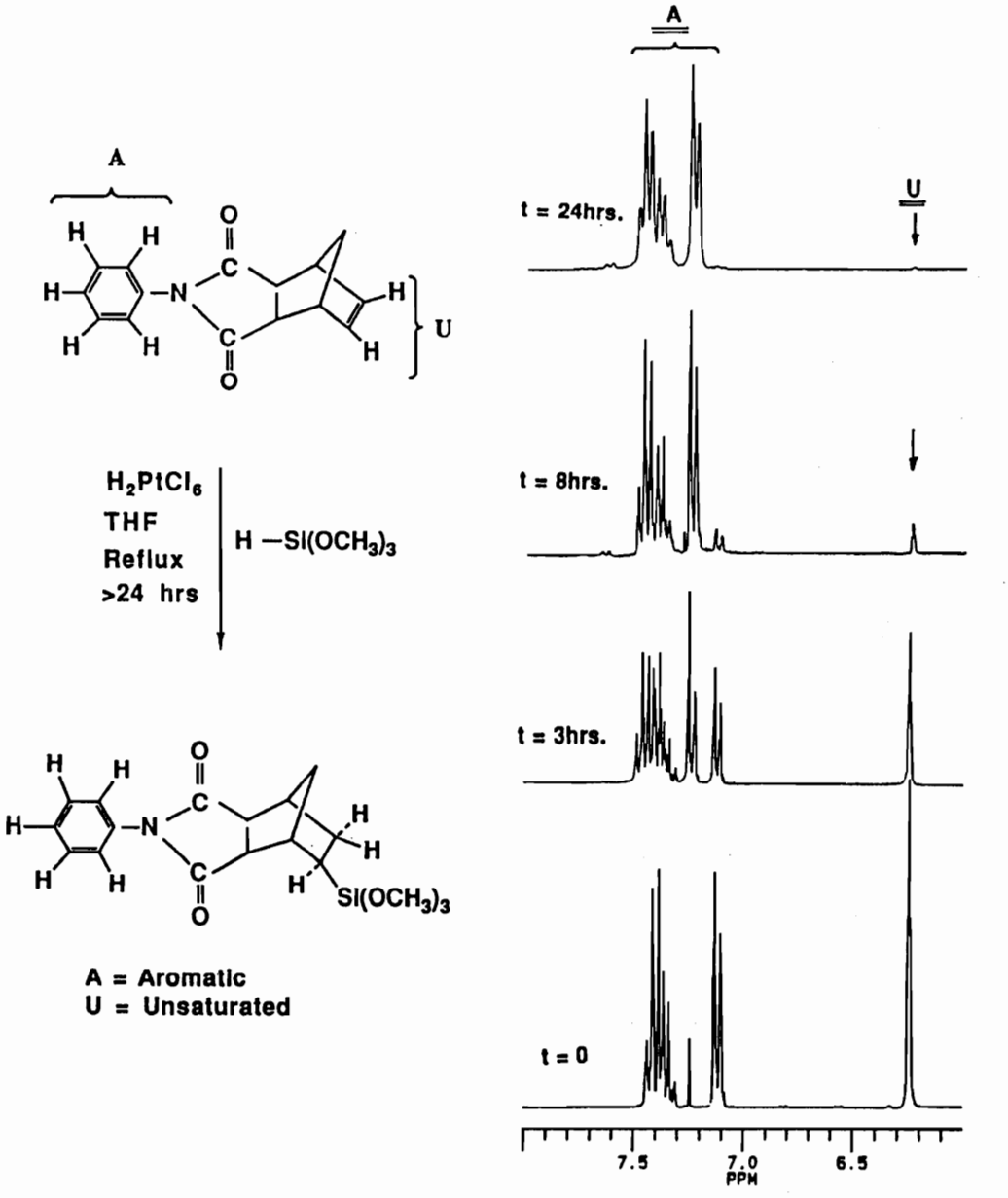


***Figure 1.53.*** $^1$H NMR spectra at different reaction times for the hydrosilation to the olefin model compound showing the complete disappearance of unsaturated protons (6.2 ppm).

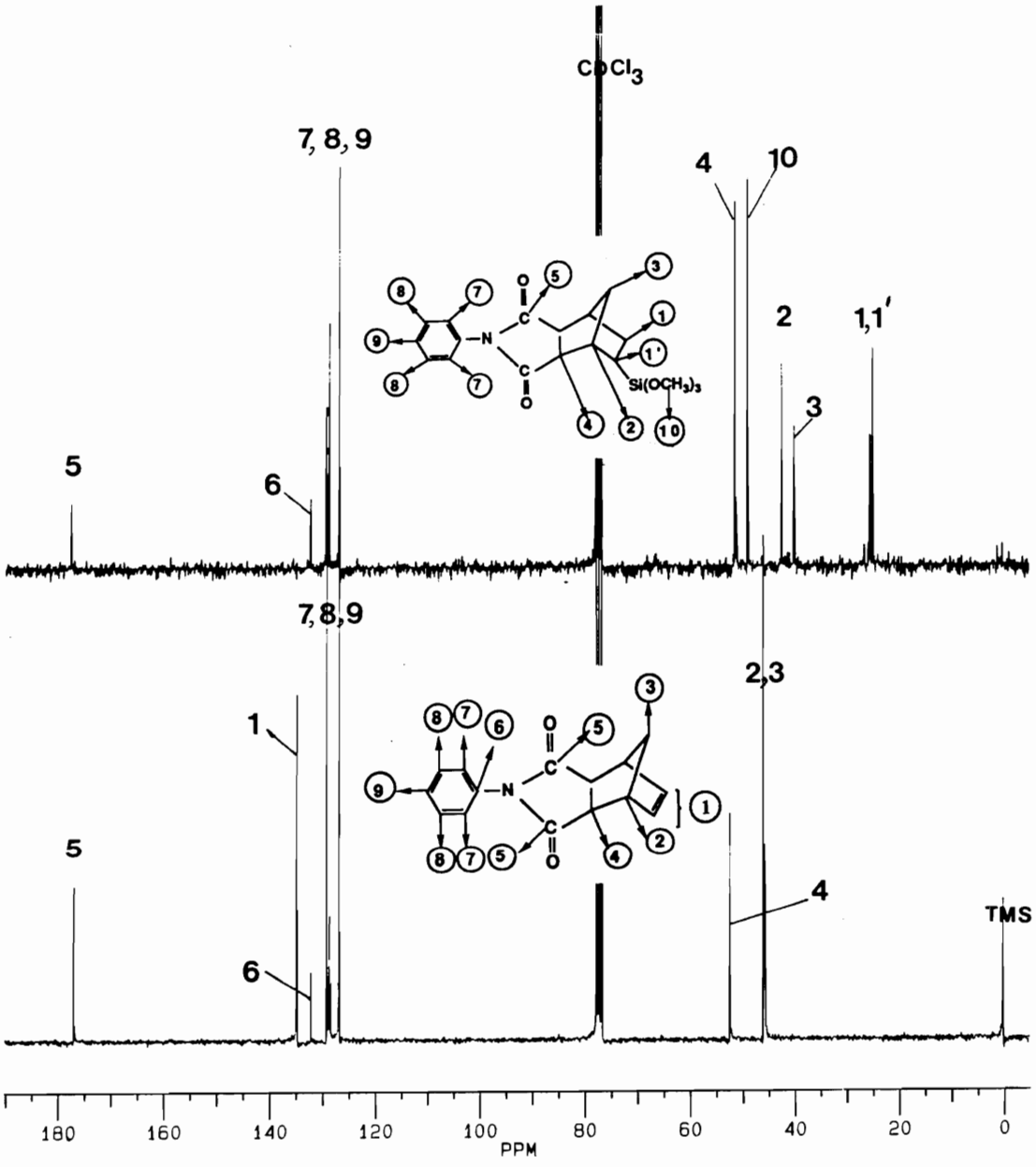


***Figure 1.54.*** $^{13}C$ NMR spectra of the olefin model compound before and after hydrosilation.

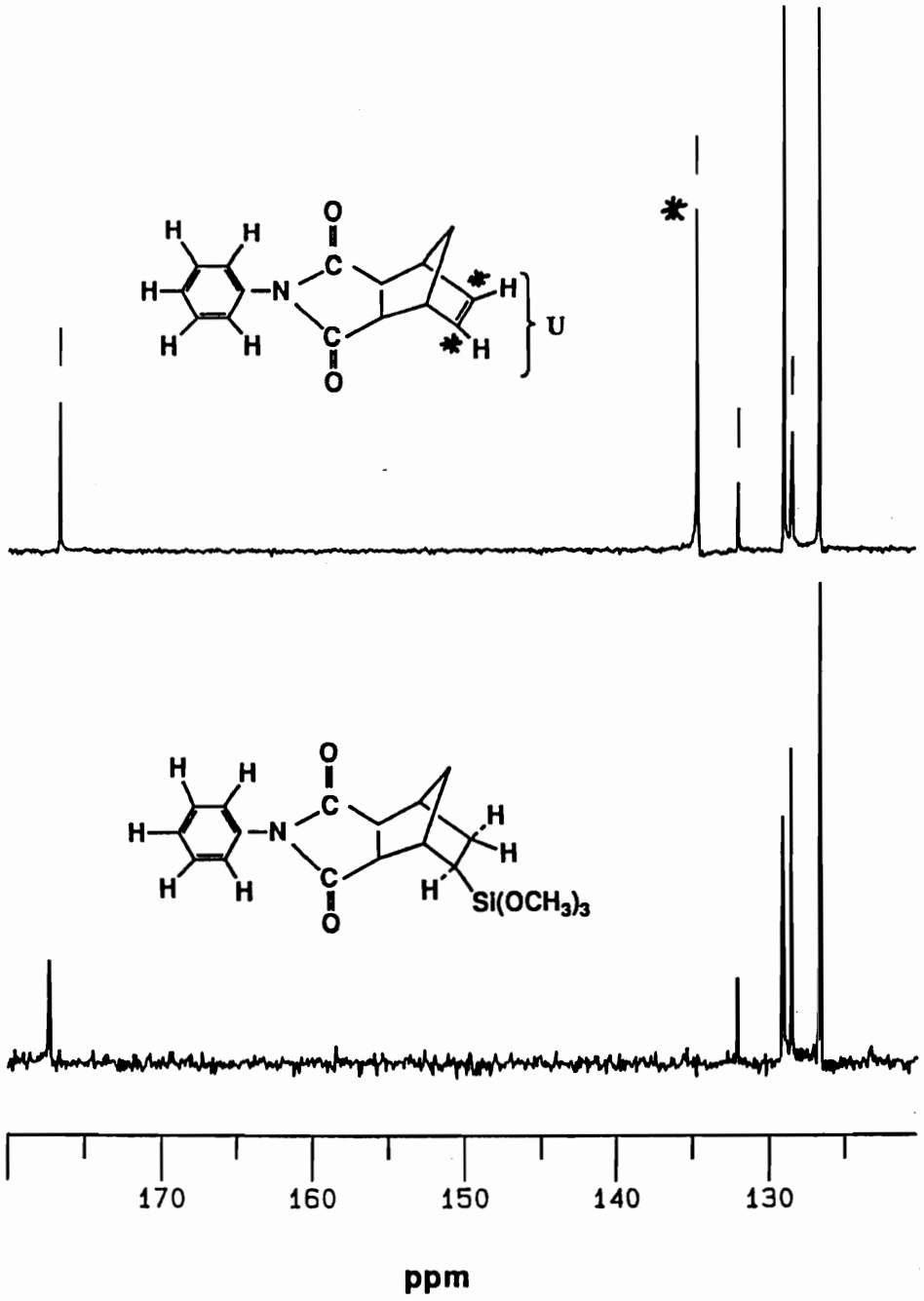


***Figure 1.55.*** $^{13}C$ NMR spectra of the olefin model compound before and after hydrosilation. Expanded aromatic and unsaturated region to show complete dissapearance of the unsaturation.

***Scheme 1.23.*** Synthesis of methoxy functionalized polyimide oligomers

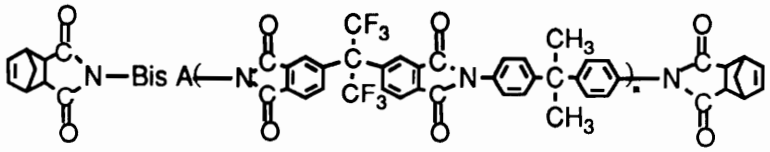


**Nadimide terminated polyimides**

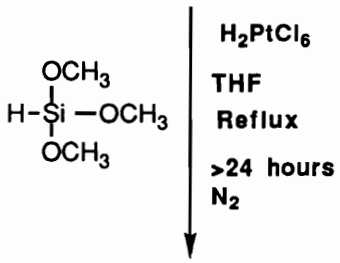


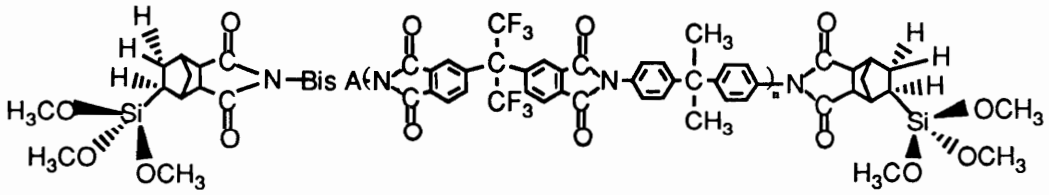

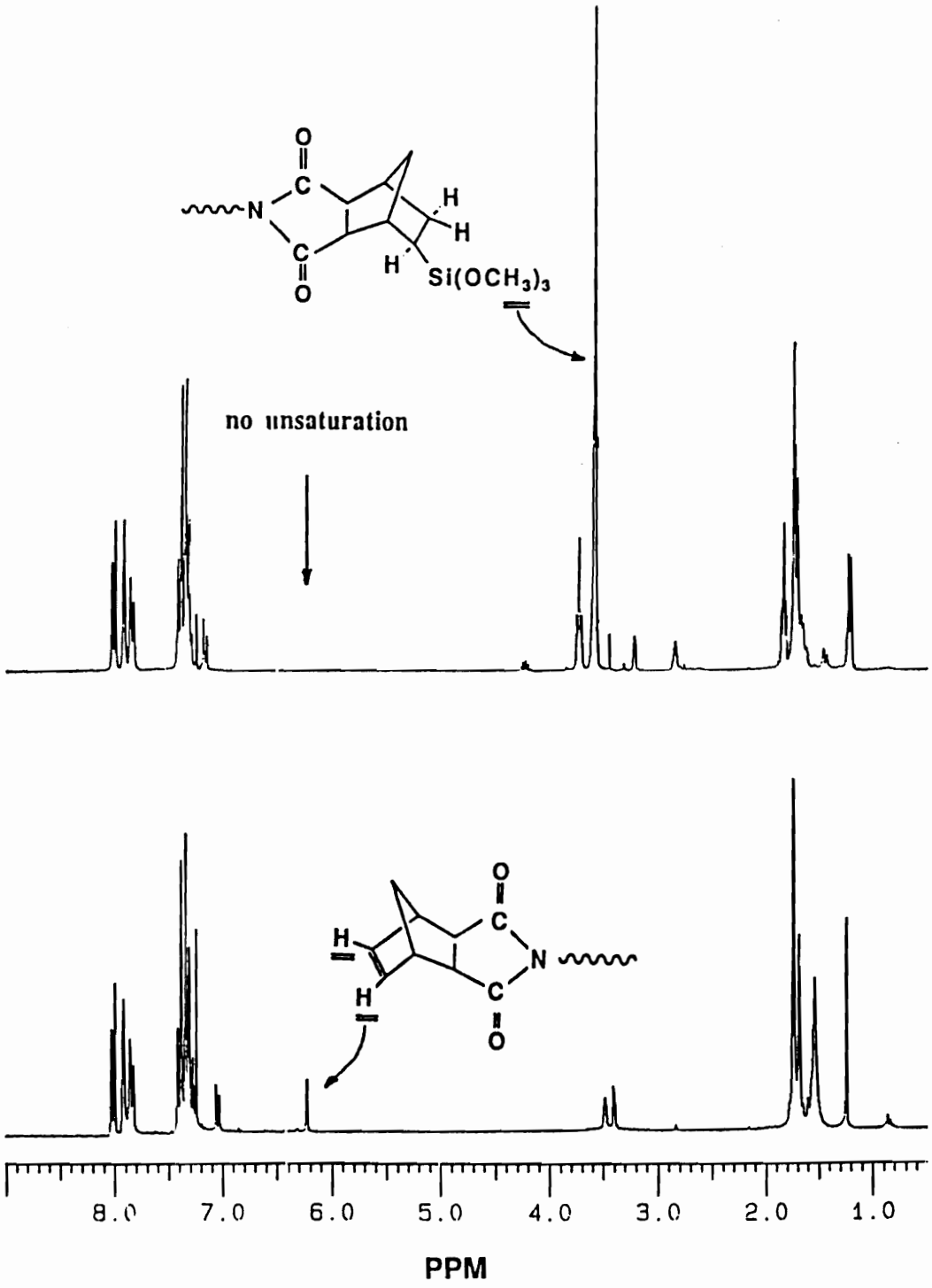


***Figure 1.56.*** $^{1}H$ NMR spectra for a 6F-BisA polyimide oligomer (3K) nadimide and methoxy functionalized.

Firstly, it was necessary to determine if the methoxy functionalized model compound (2) was capable of undergoing hydrolysis reactions under the sol-gel conditions to be employed for the synthesis of the polyimide modified glasses. Hence, model hydrolysis reactions were carried out at room temperature, in the absence of catalyst, and at a molar ratio of $[OCH_3]:[H_2O]=1.0:1.0$, corresponding to a stoichiometric amount of water required for complete hydrolysis in the absence of condensation reactions, ***Scheme 1.24***. $^1H$ NMR spectra before hydrolysis and 30 minutes after the water addition ***Figure 1.57,*** indicate that under the conditions employed the methoxy groups were readily hydrolyzed and methanol was generated.

Next, it was necessary to evaluate if the hydrolyzed species above (3) can further undergo condensation reactions. This was determined by using $^{29}Si$ NMR. However, due to the low concentration of silicon nuclei in the reaction mixture (high molar mass of the model compound, and high sample dilution) a relatively low signal to noise ratio was obtained and subtraction of the glass peak could not be succesfully applied for this study. Consequently, the $^{29}Si$ NMR data for these reactions are strictly qualitative. ***Figure 1.58*** shows typical $^{29}Si$ NMR spectra at different reaction stages for the model condensation described in Scheme 1.24. In order to understand these spectra it is important to recall that upon condensation and formation of siloxane bridges, the silicon nuclei in silicon alkoxide species become more polarizable and they resonate at higher field. Therefore, the upfield shift of the silicon resonances observed at longer reaction times and especially at higher reaction temperatures in Figure 1.58 was attributed to the formation of higher condensed species. The tentative spectral assignments in Figure 1.58 were based on analogies with the TMOS system (higher condensed species resonate at higher field) rather than a positive identification of the assigned species.

***Scheme 1.24.*** Model hydrolysis and condensation reactions of the methoxy functional N-phenyl-nadimide compound (**2**).

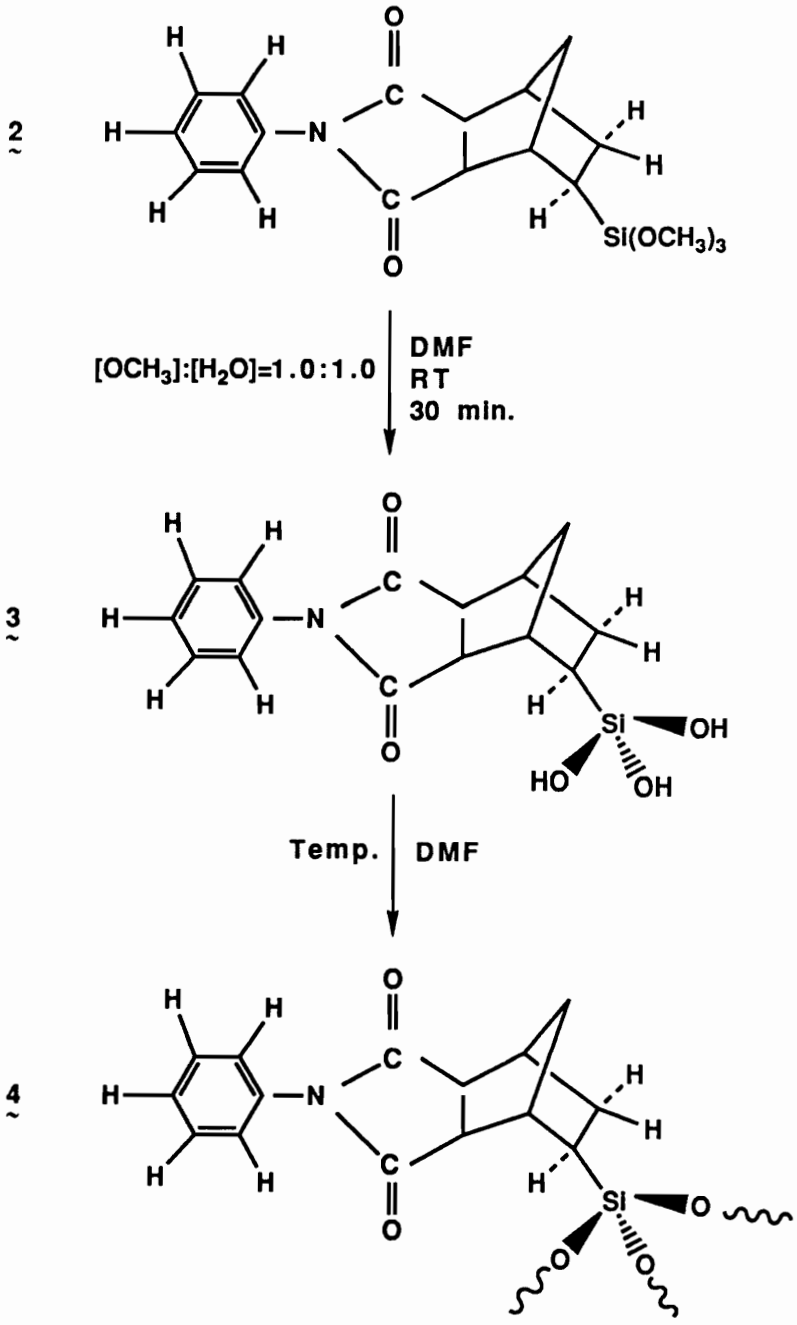

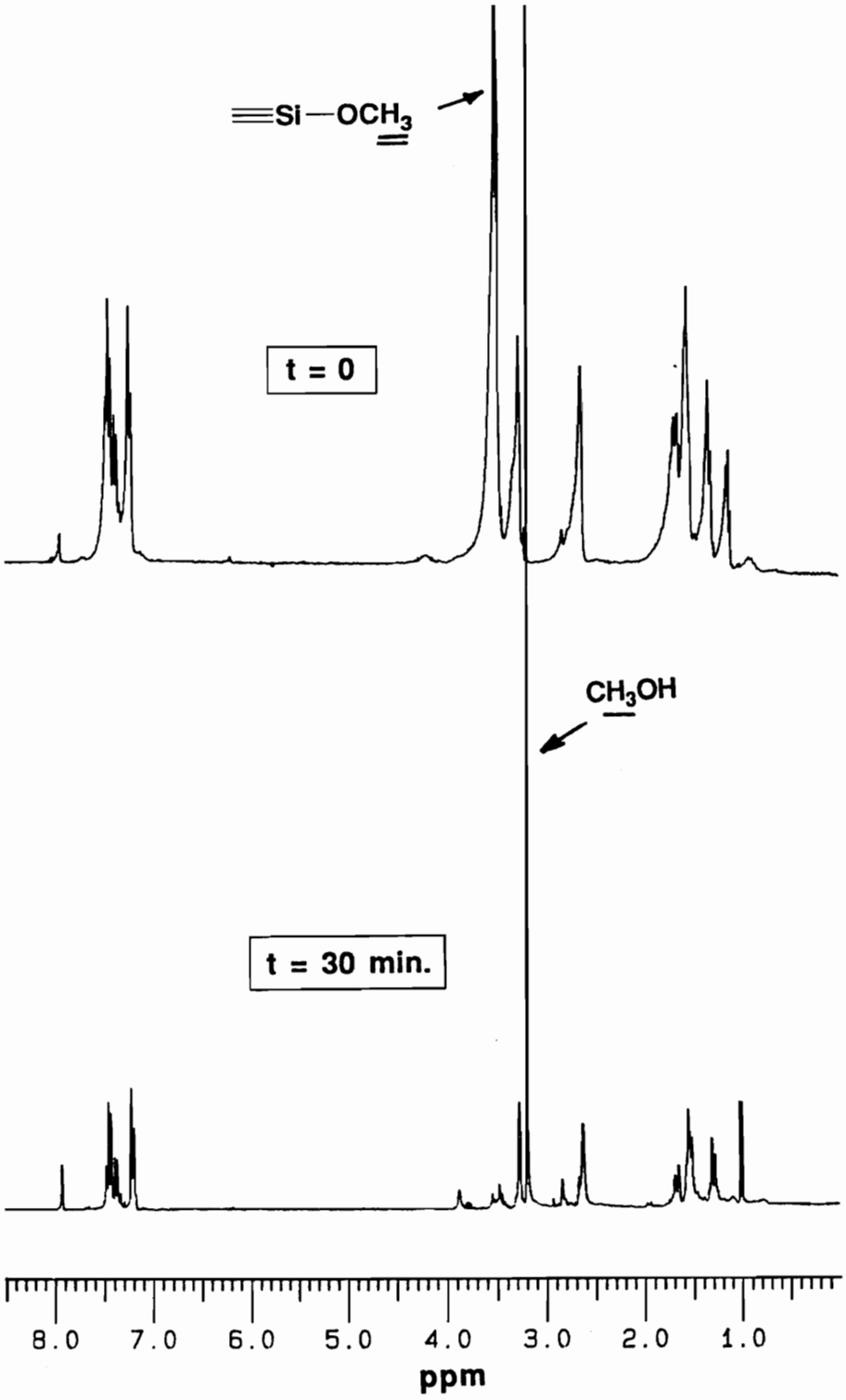


***Figure 1.57.*** $^{1}$H NMR spectra for the model hydrolysis reaction described in Scheme 1.24.

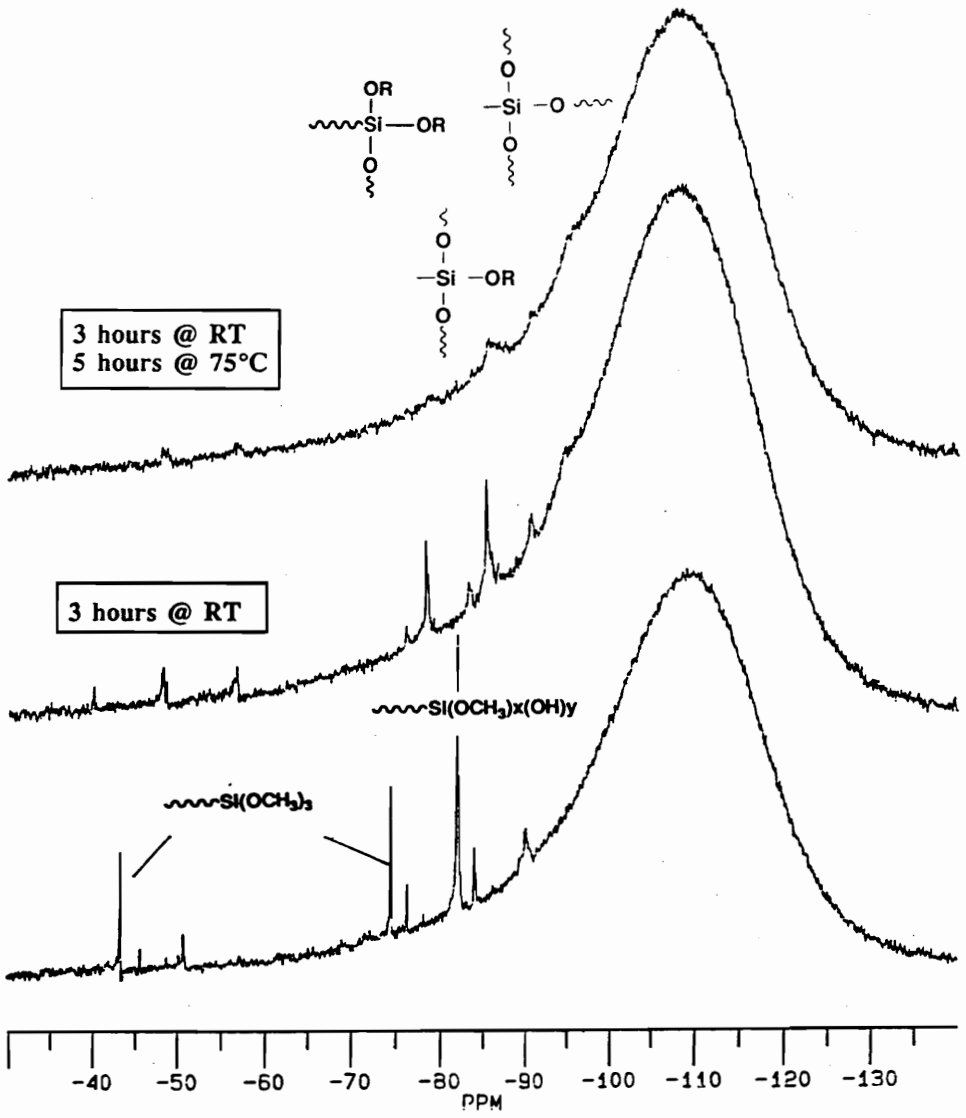


***Figure 1.58.*** $^{29}$Si NMR spectra at different reaction stages for the model condensation reaction described in Scheme 1.24.

The model study suggested that the low molecular weight methoxy functional compound with a similar structure to the reactive end groups of the polyimide oligomers can efficiently undergo hydrolysis and condensation reactions under the sol-gel conditions employed in this study. Consequently, the hexamethoxy functionalized polyimide oligomers should also react under the above conditions. In order to verify these expectations hydrolysis-condensation crosslinking reactions of methoxy functionalized polyimides were carried out under similar conditions to be employed for the synthesis of the PI/$SiO_2$ hybrids. At the end of a typical crosslinking process (maximum temperature 165°C), a very small insoluble polyimide fraction was obtained indicating that no considerable crosslinking took place. Additionally, TGA-MS analysis of the above "crosslinked" polyimide samples indicated further evolution of $CH_3OH$ and $H_2O$ (by-products of condensation reactions) at elevated temperatures, with a maximum evolution rate just above the glass transition temperature of the polyimide ($T_g$ = 260°C, for $M_n$ =~ 6K). The ion chromatograms for methanol and water, ***Figure 1.59*** and ***Figure 1.60*** respectively, contain two major peaks. The low temperature peaks in both ion chromatograms (200-360°C) can be associated with high temperature condensation reactions, while the high temperature peaks (above 480-500°C) can be attributed to the thermal decomposition process of the polyimide backbone, which is in agreement with the observed TGA behavior of the 6F-Bis A polyimides. Therefore the ion chromatograms indicated that by-products of condensation reactions ($CH_3OH$ and $H_2O$) are being formed in the thermogravimetric analyzer at elevated temperatures, suggesting that the condensation-crosslinking process was not completed at the lower reaction temperature. These preliminary experiments suggested that the methoxy functionalized polyimides may not efficiently crosslink at temperatures below their glass transition temperature, a potential problem for the synthesis of PI-$SiO_2$ hybrids, in which the vitrification of the network may occur before the glass transition temperature of the polyimide component is reached.

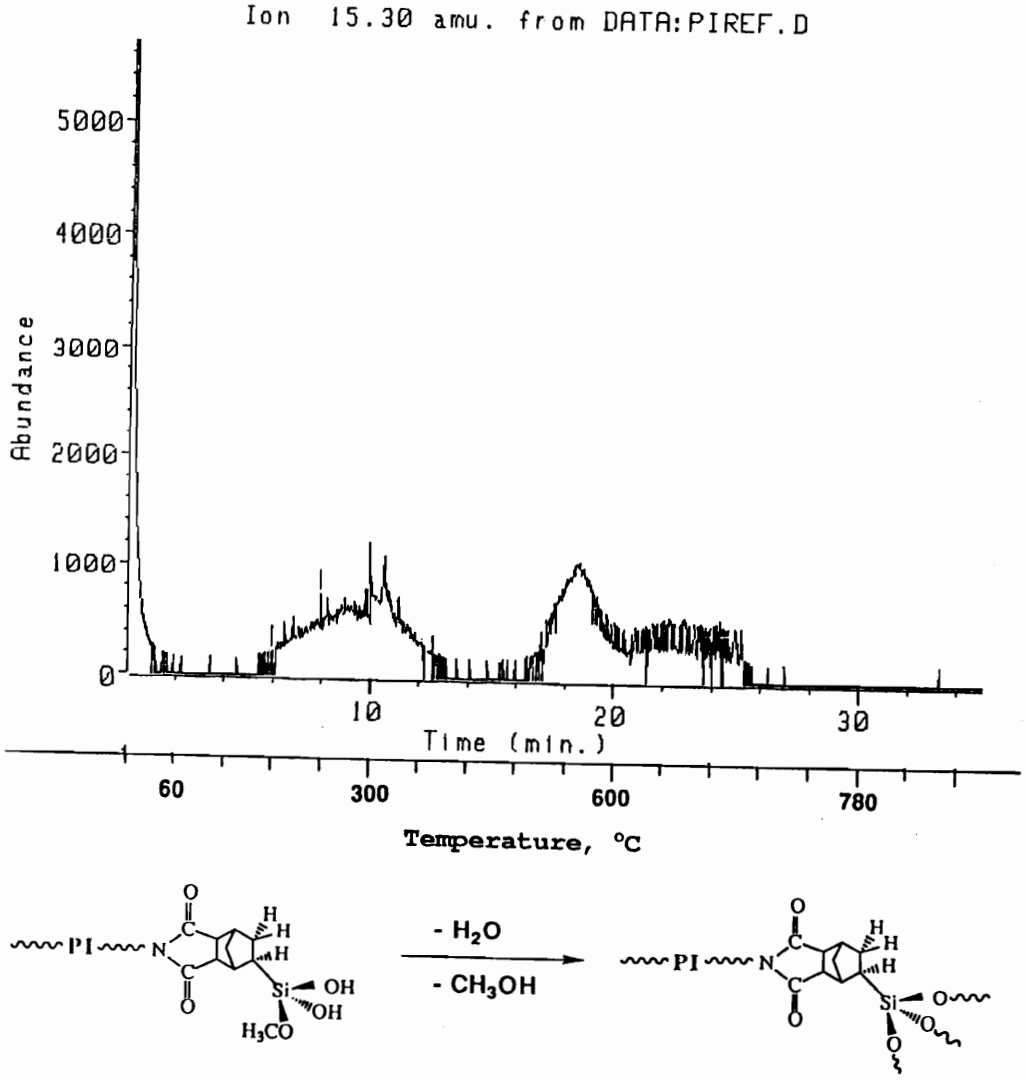


***Figure 1.59.*** Ion chromatogram for the $CH_3OH$ evolution during heating of "crosslinked" polyimide in the thermogravimetric analyzer (TGA); (Heating rate 30 deg/min)

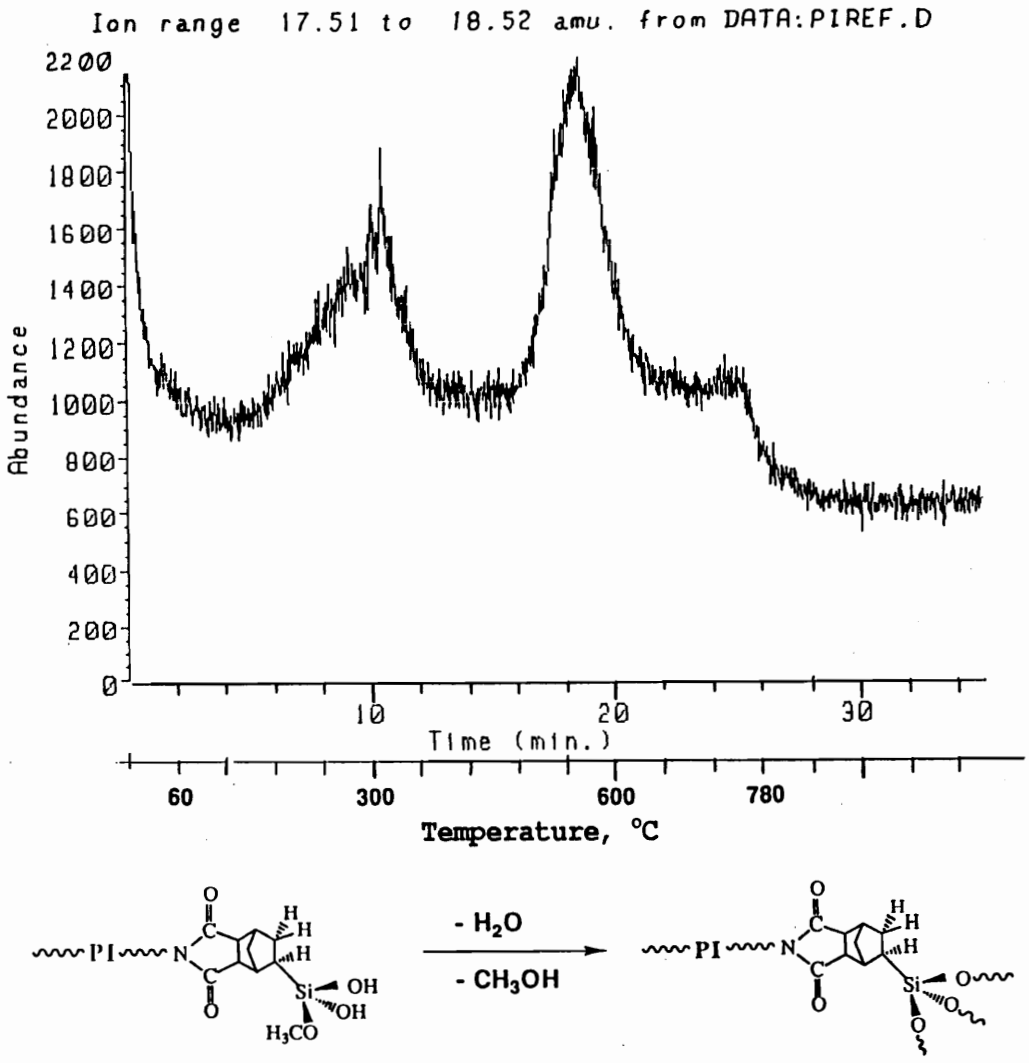


***Figure 1.60.*** Ion chromatogram for the $H_2O$ evolution during heating of "crosslinked" polyimide in the thermogravimetric analyzer (TGA); (Heating rate 30 deg/min).

***Synthesis of PI-$SiO_2$ hybrids.*** The reaction procedure for this synthesis was described in Chapter 3 (Section 3.4.2) and it was slightly modified from the PSX-$SiO_2$ system. As for polysiloxane modified glasses, TMOS was used as the inorganic component, and the reaction was usually carried out in the absence of catalyst, even though for the fully imidized polyimides this was not as critical as for PSX systems. TMOS was prereacted to a controlled conversion, as described for the PSX/$SiO_2$ systems. Methoxy functionalized polyimide oligomers dissolved in DMF were added to the still soluble network precursors and reacted at 75°C, as described in ***Scheme 1.25.*** A reaction temperature of 75°C was employed for the initial stages of copolymerization since the model study indicated a more efficient condensation under these conditions (see Figure 1.58). The reaction was allowed to proceed at 75°C until an increase in solution viscosity, indicating the approaching of gelation, was observed. At this point the reaction mixture was poured into glass vials equipped with relativelly fitted caps and the reaction temperature was slowly increased (approximately 1-2 deg/min) to a maximum value of 165°C. Generally the reactions gelled before or shortly after arriving at 165°C.

Following gelation, the samples were "aged" in the sealed vials at 165 °C for at least 12 hours, and the reaction solvents and volatile by-products were removed from the aged gels by very slowly releasing the pressure of the vials (through a small hole made in the cap). The relatively slow rate of drying was found to be essential for generating transparent hybrids. Premature solvent evaporation was observed to result in opaque hybrids, but at slow rates of solvent removal transparent hybrids were usually obtained, at least for up to 40-50% polyimide incorporated in the final networks. The reaction parameters investigated included: (1) hybrid composition, (2) polyimide molecular weight, (3) reaction solvent, and (4) maximum post-gelation temperatures. (1) Compositions ranging from 0 to 80% polyimide in the fully reacted networks were investigated.

***Scheme 1.25.*** General reaction scheme for the synthesis of PI-$SiO_2$ networks.

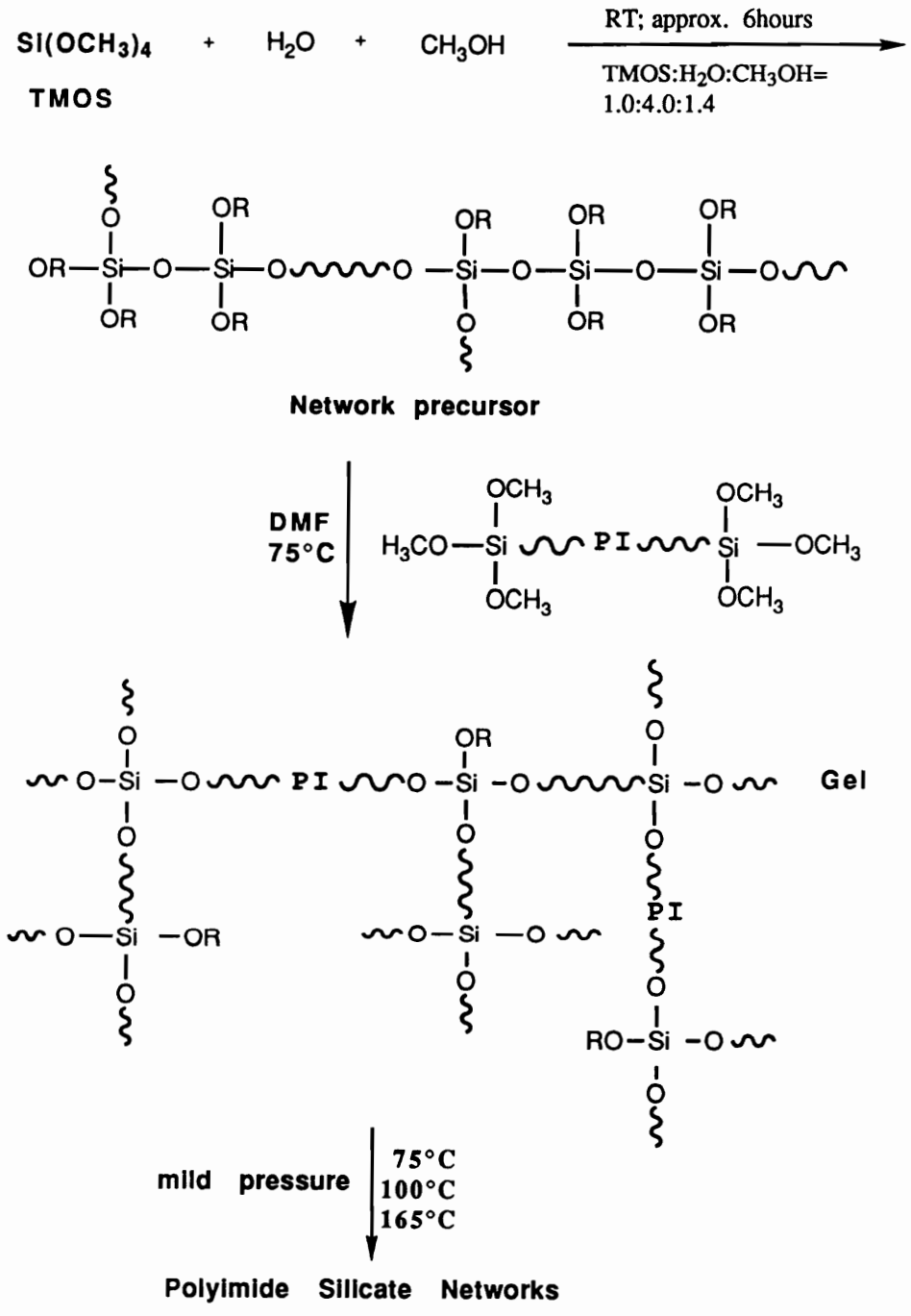

The compositions containing higher PI content required much longer gelation times, indicative of an inefficient crosslinking process of the polyimide component. (2) Polyimides with $<M_n>$ ranging from 1K to 9K were investigated. (3) DMF, NMP, and THF were investigated as the copolymerization solvents. In general, THF generated opaque hybrids due to the solvent loss at early stages of drying. NMP was found to be unsuitable for this process due to its degradation under the conditions employed for drying. DMF was selected as the reaction solvent and it was found to generate transparent hybrids over a relatively broad composition range (0 to ~ 50% PI). (4) A typical post-gelation treatment involved the use of a maximum temperature of 165°C, as shown in Scheme 1.25. However, additional drying up to 300°C was investigated for the PI/$SiO_2$ systems, according to the temperature vs time profile described in ***Figure 1.61***. This drying cycle was in addition to the regular post-gelation treatment which involved temperatures up to 165°C. The materials generated under the above described conditions, though transparent for lower PI compositions (<50%PI) and lower PI molecular weights (<9,000g/mole) were easily breakable, even more so than the unmodified $SiO_2$ materials. No improvement in the mechanical properties was observed for the samples reacted at 300°C (above the glass transition temperature of the polyimide component) for 12 hours.

### *4.2.2.3. Characterization of PI-Si02 networks*

High resolution scanning electron microscopy was employed to investigate phase separation in these systems. The micrographs were taken at magnifications of 50,000 and 100,000. ***Figure 1.62*** shows the fracture surface of the reference $SiO_2$ and one of the PI-$SiO_2$ hybrids which displayed phase separation. This particular sample was synthesized in an acid catalyzed reaction and such phase separation was not observed in any of the reactions which were carried out in the absence of catalyst. ***Figure 1.63*** shows a typical fracture surface for a PI-$SiO_2$ hybrid generated

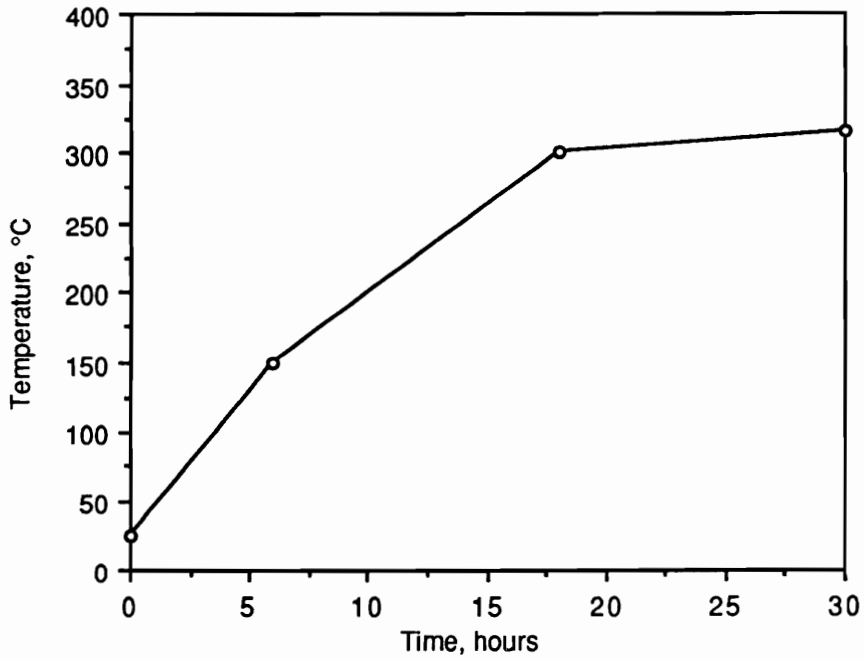


***Figure 1.61.*** Typical temperature-time profile for additional post-gelation treatment employed for PI/$SiO_2$ hybrids

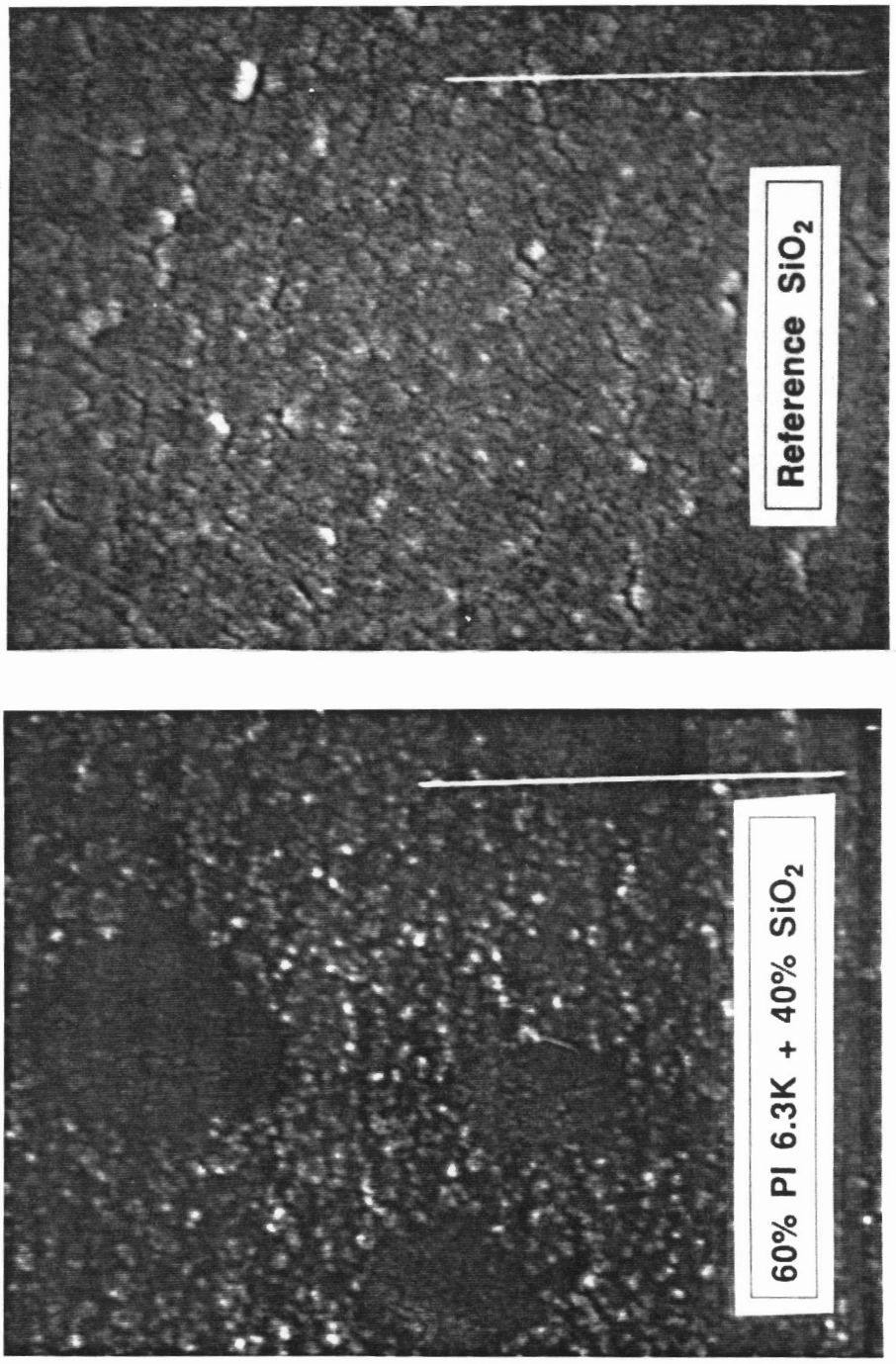


***Figure 1.62.*** Scanning electron micrographs of fracture surfaces at 100,000 magnification **(a)** Reference $SiO_2$, and **(b)** PI-$SiO_2$ hybrids synthesized by an acid catalyzed sol-gel reaction.

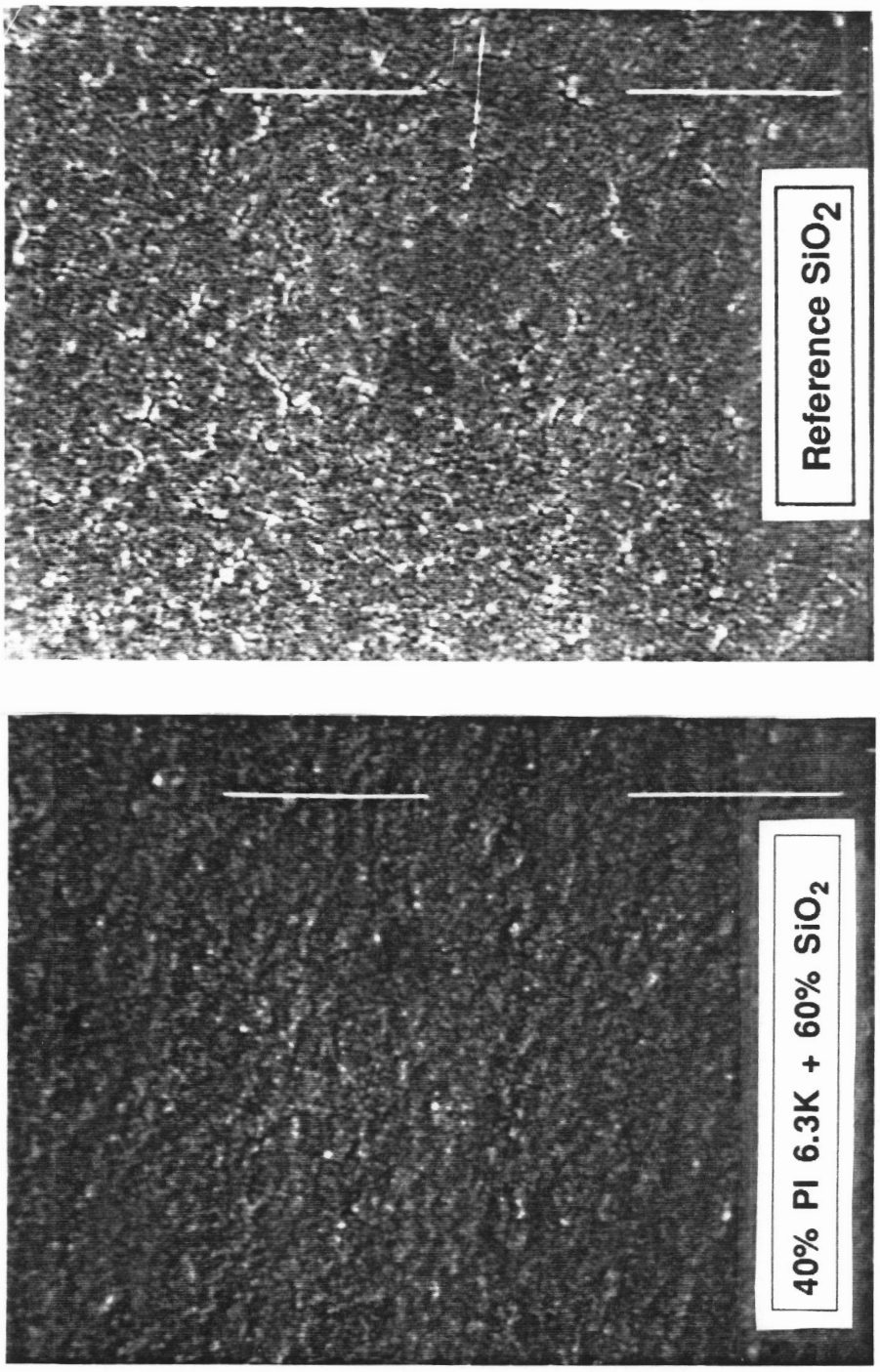


***Figure 1.63.*** Scanning electron micrographs of fracture surfaces at 100,000 magnification **(a)** Reference $SiO_2$, and **(b)** PI-$SiO_2$ hybrids synthesized by a catalyst-free sol-gel reaction

under catalyst-free conditions as well as the unmodified $SiO_2$ material for comparison. No phase separation was observed at this scale. Additionaly, it is worth noting that the fracture surface of the hybrid, as well as the unmodified glass is essentially featureless, indicative of a relatively brittle fracture. Therefore, the polyimide incorporation did not seem to contribute to the thermoplastic toughening of the inorganic glasses, or at least not in the oligomeric range of molecular weights employed in this study.

Even though consolidated polyimide-$SiO_2$ "composite" materials could not be generated under any of the conditions investigated in this work, the above materials were observed to possess enough integrity when prepared as thin films. Such materials may be suitable for protective coating applications. For example due to the low dielectric constant of the polyimide component, such hybrid materials may be of interest for dielectric coatings in electronic applications. Subsequently, a preliminary dielectric evaluation was performed on a limited number of PI-$SiO_2$ hybrids. Typical dielectric behavior in the KHz frequency region is shown in ***Figure 1.64*** for two of the hybrids, along with the reference $SiO_2$ and PI materials. The dielectric value of the $SiO_2$ inorganic networks is relatively high due to the residual OH and $OCH_3$ unreacted groups (as previously discussed), and due to residual solvent and reaction by-products retained within the microporous gels. A dramatic decrease in the dielectric values was observed above 200°C, at which temperature the loss of physically adsorbed solvent and reaction by-products was completed (as indicated by TGA-MS) and where vitrification of the network (which would result in loss of dipole mobility) may occur. However, the exaggerated decrease in the dielectric constant is most probably an artifact of physical changes accompaning the heating of the gels (e.g., change in the sample dimensions due to further shrinkage). The absolute values for the dielectric constant of these materials would have to be normalized for the change in the sample dimensions or for the microporosity of the samples which further contribute to an artificially low dielectric

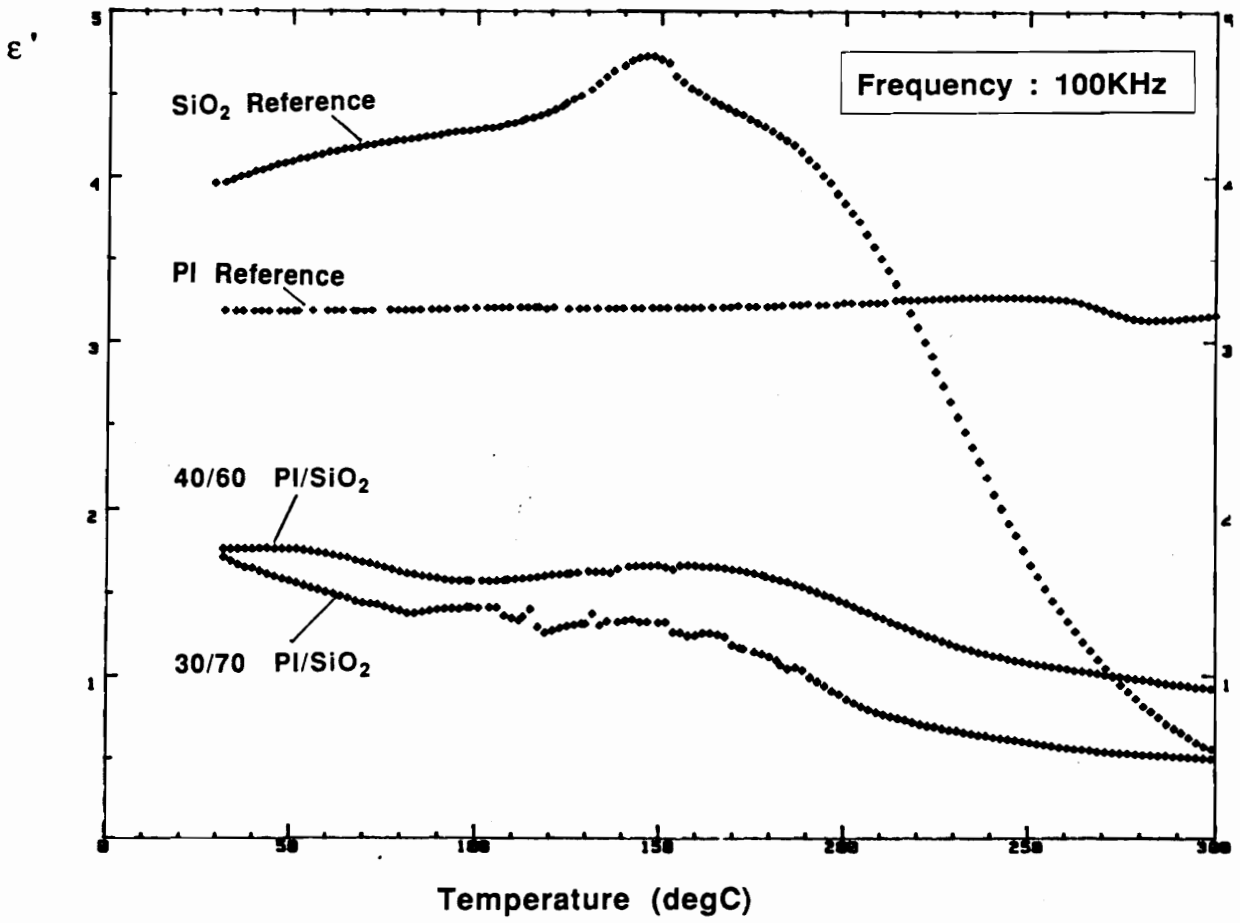


***Figure 1.64.*** DETA scans for PI-$SiO_2$ hybrid networks and for PI and $SiO_2$ References. Constant heating rate = 1deg/min; Frequency =100 kHz

constant value. The polyimide reference networks show a constant and relatively low dielectric value in the temperature range investigated. The dielectric behavior of two of the PI-$SiO_2$ materials is also shown in Figure 1.64. Both of the hybrid materials display an unusually low dielectric constant value, when compared to any of the references. These low values are most probably a combined effect of (1) decreased amount of residual OH and $OCH_3$ polar groups, as a result of lower percent of the glass component in the hybrid, (2) reduced network polarity as a result of incorporation of less polar polyimides, and (3) decrease in the amount of residual solvent as a result of reduced microporosity and polarity in the hybrid networks. It must be emphasized that the dielectric constant values shown in Figure 1.64 are relative to each other and indicate the trend obtained upon incorporation of 6F-Bis A polyimide into the $SiO_2$ gels. However, for absolute values, the numbers would have to be normalized for the inherent microporosity of these materials, and change in dimensions during the heating process.

*CHAPTER 5*

*CONCLUSIONS*----------

A catalyst-free route for the synthesis of $SiO_2$ networks via sol-gel reactions was established. This route involves the use of tetramethylorthosilicate (TMOS), the most reactive tetraalkoxide in the series, as the starting material. A catalyst-free reaction environment is highly desired for the incorporation of organic modifiers into the inorganic networks through these processes, since many organic components usually display a limited stability in the presence of acid or base catalysts generally employed for sol-gel reactions, especially at higher temperatures required for the drying of the gels. The reaction rate for the uncatalyzed sol-gel systems is highly dependent on the parameters in the initial reaction stages, such as the level of water in the initial hydrolysis step or the reaction concentration. Both hydrolysis and condensation reactions are faster at higher water levels and/or higher reaction concentrations. Consequently, the gelation times (defined visually at the point at which the reaction mixture would no longer flow) are also highly affected by these parameters. For example, the gelation time for a room temperature reaction was reduced 4 times, from 64 to 16 hours, when decreasing the solution concentration from a ratio of TMOS:$CH_3OH$ =1.0:**5.0** to a ratio of 1.0:**1.4**. Similarly, the gelation time was reduced by a factor of 2 when the water level utilized in the initial hydrolysis step was increased from a ratio of $H_2O$:TMOS = **2.5** to a ratio of **4.0**.

The growth mechanism under uncatalyzed reaction conditions and at medium water levels investigated is intermediate between an acid and a base-catalyzed reaction. Hydrolysis and condensation reactions occur simultaneously, at competitive rates, and condensation begins at early stages between incompletely hydrolyzed species, resulting in less highly crosslinked structures which more closely resemble the structures generated under acid-catalyzed

conditions. These data at the molecular level obtained from spectroscopic data ($^{1}H$ and $^{29}Si$ NMR) are in agreement with the macroscopic features of the resulting gels: the gels are always clear and have an intermediate density characteristic of less highly crosslinked networks. The gels generated at temperatures below the glass transition temperature of the $SiO_2$ glasses are characterized by a limited extent of conversion (aprox. 88%), as found from solid state MAS $^{29}Si$ NMR. The final extent of conversion at the end of a typical drying cycle is independent of the reaction parameters in the initial reaction stages, such as reaction concentration or the level of water. However, the final extent of conversion is dependent on the maximum post-gelation temperature. Higher conversions (approx. 93%) were achieved only when higher reaction temperatures ($T_{max.}$ =500°C) were employed. The incomplete extent of conversion which can be explained by the occurance of vitrification as the network build-up progresses, translates into residual OH and $OCH_3$ groups and result in a relatively high surface and bulk polarity, as indicated by the contact angle and the dielectric constant measurements.

The use of mild pressure during the drying of the gels was found to be a critical condition for the generation of monolithic dried gels. The role of pressure is probably complex and involves the effect on (a) the rate of solvent evaporation, (b) the surface tension of the solvent at the drying temperature, (c) as well as the extent of conversion when the drying of the gels begins, all important factors in determining the level of stresses associated with drying, and the ability of the developing networks to withstand such pressures.

Incorporation of oligomeric organic components into the inorganic networks was investigated as one possibility for improving the undesired features of the inorganic $SiO_2$ gels (highly polar, brittle networks), and/or tailor their properties by introducing new features into the system. It was expected that the use of relatively high molecular weight oligomeric modifiers, which may provide

a second phase within the glassy inorganic matrix, could more efficiently contribute to the network properties than the low molecular weight species, most often employed for this purpose. A simple approach for this incorporation was undertaken: the organic modifiers were functionalized with reactive groups capable to undergo hydrolysis and condensation reactions under the sol-gel conditions. Hence, the functionalized organic oligomers were copolymerized with soluble inorganic network precursors generated by prereacting the TMOS to a controlled extent of conversion.

The first organic component investigated as a network modifier, polydimethylsiloxane, is an elastomer. Methoxy functionalized polydimethylsiloxane oligomers were reacted at room temperature with inorganic soluble network precursors, in the absence of catalyst. Following gelation which occured within approximatelly 12 hours after the copolymerization was started, the PSX/$SiO_2$ hybrid networks were dried at a maximum temperature of 150°C, under similar conditions as the ones employed for drying of the inorganic $SiO_2$ gels. Under these conditions a very efficient incorporation of the PSX component was achieved, as demonstrated by the solid state MAS $^{29}Si$ NMR measurements, before and after extraction in boiling THF. A broad range of compositions resulted in transparent, homogeneous hybrids, with improved properties. (1) The PSX/$SiO_2$ hybrid networks posses a lower polarity and an increased resistance to water when compared to the inorganic networks, as demonstrated by the contact angle experiments. (2) The incorporation of flexible, elastomeric PSX chains resulted in an increase in the toughness of the otherwise brittle $SiO_2$ glasses, as suggested, qualitatively, by the SEM experiments. (3) The PSX/$SiO_2$ networks retain a relatively good thermal stability as shown by TGA measurements. The 5% weight loss in air does not occur until 375-400°C. This also demonstrates that no redistribution reactions of the polysiloxane chains occurs at elevated temperatures in the catalyst-free environment employed for these reactions. (4) Finally, the incorporation of a low glass

transition temperature oligomeric modifier was observed to affect the overall extent of conversion of the glass component in the hybrid, as demonstrated by the solid state $^{29}Si$ NMR measurements. For example, the effect on conversion achieved by the incorporation of 20 weight % PSX oligomer is equivalent to reacting the unmodified inorganic network at temperatures as high as 500°C. This feature may be critical when the sol-gels are to be applied as coatings on thermally sensitive substrates.

A similar approach to the synthesis of organic/inorganic hybrids was undertaken for the incorporation of a glassy components into the $SiO_2$ networks. Hence, polyimide oligomers were functionalized with silicon-methoxide groups capable, in principle, to undergo hydrolysis and condensation reactions under sol-gel conditions. The functionalized polyimides were reacted with soluble inorganic precursors at 75°C until an increase in viscosity indicating the approaching of gelation was observed. Even though the model study indicated that such functional groups were capable to undergo hydrolysis and subsequent condensation reactions under the sol-gel conditions, the functional polyimide oligomers did not show satisfactory extent of crosslinking at temperatures below their glass transition temperature. This behavior led to unsatisfactory polyimide incorporation, most probably due to the fact that the vitrification of the network occurs before the glass transition temperature of the polyimide component was reached. This resulted in materials without physical and mechanical integrity. Nevertheless, these materials showed enough integrity to allow for preliminary evaluation when generated as thin films, therefore they may still be of importance for coating applications. The PI/$SiO_2$ hybrids display a relatively low dielectric constant value which may be of interest for dielectric applications.

## *CHAPTER 6*

## *SUGGESTED FUTURE STUDIES*----------

The research presented here concerning the synthesis of organic-inorganic polymeric networks through a catalyst-free sol-gel process has at least laid the ground work for many future directions to be followed. These include:

### *I. Inorganic sol-gel systems.*

Study of the temperature effect on the reaction rate ($^{1}H$ NMR), growth mechanism ($^{29}Si$ NMR), and gel microstructure (density, porosity) on the catalyst-free hydrolysis-condensation of TMOS. These data would be important in order to establish the potential use of reaction temperature as an additional parameter for increasing the reaction rate in the system investigated. Preliminary studies indicated that the use of higher temperature (60°C) resulted in a considerable decrease in the gelation time, but also produced precipitation of the three-dimensional $SiO_2$ networks (section 4.1.1.4). This would be undesirable when monolithic materials are of interest.

### *II. Organic-inorganic hybrids.*

(1) The morphology of the two-component systems should be systematically explored. It is anticipated that both molecular weight of the organic polymer, and the hybrid chemical composition play an important role in determining the gel morphology (hence properties).

(2). The effect of incorporation of the organic component on the dimensional stability (Thermal Expansion Coefficient, TEC), modulus (DMTA), and hardness of the inorganic $SiO_2$ networks should be investigated. It is anticipated that the morphology of the two-component system plays a crucial role in preserving these outstanding features of the inorganic networks.

(3) The advantage of employing polymeric modifiers versus low molecular weight organic components should be documented. It has been speculated by the author, as well as by others (see Literature review, section 2.8.2) that the two type of systems would result in different morphologies: when low molecular weight organic components are used it is expected that such species are dispersed within a continuous glass matrix, while the use of polymeric modifiers may result in cocontinuous phases. The cocontinuous morphology would better preserve some of the highly desired features of the inorganic networks (such as dimensional stability, modulus and

hardness). A series of hybrids could be synthesized having identical compositions (i. g. same percentage of Si-$CH_3$ groups) generated by the use of two types of organic modifiers: poly(dimethylsiloxane) oligomers and methyltrimethoxysilane (MTMOS), respectively. Preliminary studies have already been carried out in this direction. For example it was determined that the hybrids derived from TMOS-MTMOS did not display a similar improvement in surface properties as observed for the PSX modified systems with an equivalent composition. A systematic study of the morphology of the two systems, at different hybrid compositions should help in understanding the fundamental difference between the two types of system design. TEM, SAXS, and DMTA measurements can be employed for elucidation of phase behavior in the two systems.

(4) The synthesis of polyimide modified hybrids was not quite succesfull, under the conditions employed. Development of a different functionalization route for polyimide oligomers, with less sterically hindered trimethoxysilyl end-groups should be the first step in improving this process. Synthesis of anhydride terminated polyimides and further capping with aminophenyltrimethoxysilane to provide trimethoxysilyl end-groups is a possible alternative:

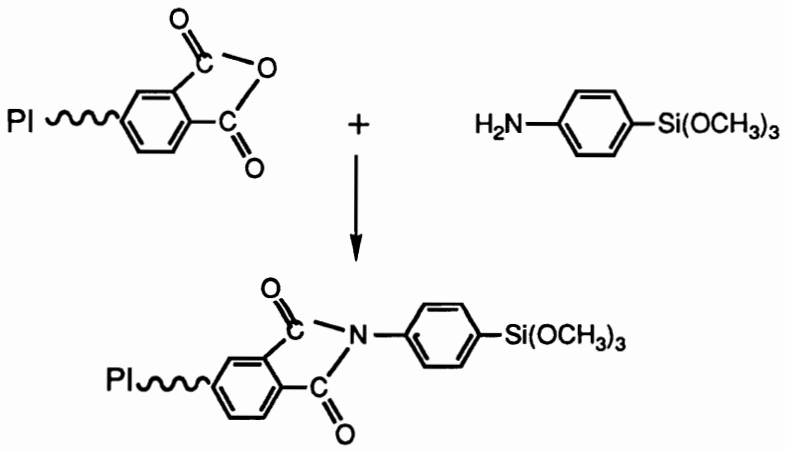


Preliminary work in this direction has been done in Prof. Wilkes' group. However, the direct Si-aryl linkages in these end-groups is highly susceptible to acid catalysts usually employed for TEOS based sol-gel reactions (ipso-substitution at the aromatic ring), hence a catalyst-free reaction environment would be very critical for this system. Replacing aminophenyltrimethoxysilane end-capper with aminopropyltrimethoxysilane would eliminate the susceptibility of the system towards acid-catalysts but would result in a decrease in the thermal stability of the end-groups.

# PART 2

# Synthesis of Poly(dimethylsiloxane) Oligomers with Pendant Amine Groups via Ring Opening Anionic co-Equilibration Reactions

*CHAPTER 1*

*INTRODUCTION*----------

Silicon compounds containing the siloxane bond (Si-O) occupy an important position in the chemistry of this element. The most important siloxane polymer is poly(dimethylsiloxane) (PDMS), $[-Si(CH_3)_2O-]_n$. The unprecedented inertness of this polymer under thermal, chemical, and biological environments, along with its unique physical behavior triggered intense interest from early days of its discovery. The unique properties of siloxane polymers led to a myriad of diversified applications, ranging from electrical insulation to biomaterials and to space research. Even though the polysiloxanes were discovered in the early 40's it was only relatively recently that the importance of these compounds as system modifiers for a variety of organic polymers, has been recognized. This realization resulted in an intensified effort for the development of reactive, organofunctionally terminated polysiloxanes to be used as intermediates for the synthesis of various block, segmented and graft copolymers or network structures for specialty applications.

Flexible polymerization chemistry of siloxanes provides an excellent route to the preparation of structurally well defined oligomers with controlled molecular weight and functionality [169,174,175,210-213]. Synthesis of telechelic siloxane oligomers is usually achieved by anionic or cationic ring opening polymerization of cyclic siloxane monomers such as octamethylcyclotetrasiloxane ($D_4$), in the presence of a disiloxane end-capper which provides the end-functional groups and the molecular weight control. Functionalization by this route is possible since the nearly covalent Si-C bond of the disiloxane end-blocker does not participate in redistribution reactions. In these linear functionalized oligomers, the content of the functional groups is dependent on the molecular weight of the oligomers and vice versa.

The present study describes a new molecular design for the synthesis of amine functionalized polysiloxane oligomers, via co-equilibration of octamethylcyclotetrasiloxane ($D_4$) with a new cyclic siloxane monomer containing aliphatic amine substituents on the silicon atoms. This allows for independent control of the molecular weight and the amine content of the resulting oligomers.

This section of the dissertation, Part 2, begins with a Literature Review for polysiloxanes. A large body of literature has accumulated, which has been extensively reviewed. The following chapter will not duplicate the already existing reviews, but rather highlight briefly the distinguishing features of the siloxane bond and the unique physical and chemical properties deriving from this. Special attention will be given to the effect of substituents on the flexibility of the polysiloxane chains, which plays an important role in determining the competition between the polymerization and cyclization during the entropically driven ring opening equilibration-polymerization processes. Computer modeling added a new dimension to understanding and predicting this behavior, and these aspects will be briefly discussed. Following the Literature Review, the details of the experimental investigations will be presented in Chapter 3. The research has followed two main paths. One involved a qualitative study of the competition between kinetic and thermodynamic factors during the ring opening co-equilibration of two cyclic siloxane monomers. The other involved a study of molecular weight and composition control of the copolymers synthesized by co-equilibration reactions. These will be detailed in Chapter 4, Results and Discussion, followed by some preliminary conclusions and a list of areas for future consideration.

# *CHAPTER 2*

# *LITERATURE REVIEW*----------

## *2.1. HISTORIC PROSPECTIVE*

The pioneering work on polyorganosilanes dates back to 1863-1871, to the studies of Friedel, Crafts, and Ladenburg [214-216]. However, it was only in the early 1900's when F. S. Kipping and his co-workers [217-219] demonstrated for the first time the polymeric nature of the siloxane structures. The word "*silicones*", first used by Kipping [219], has become a generic term for materials based on organosilicon chemistry and the poly(siloxane)s in general. *"Polyorganosilanes"* is a more precise term for these compounds than silicones. The name "siloxane" was based on the formulation of the Si-O-Si unit as *sil-oxane*, and this has found general acceptance in scientific nomenclature [169]. Silicones occupy an intermediate position between organic and inorganic compounds, and in particular between silicates and organic polymers. It is precisely this dual nature which gives this class of compounds its particular originality.

Over 20,000 publications all over the world stand proof of the increasing interest in this class of unique polymers. The history of publications in the field of organosilicon chemistry for each five year period over the last fifty years is given by Weyenberg in a recent review of the future directions for silicon-based polymers [220]. The curve takes on an exponential character, which coincides with the first commercialization of silicones in 1940s. The 45 years commercial history of silicones is easily divided into several eras. The period from 1943 to 1960 was dominated by the classical silicones, poly(dimethylsiloxane)s being the backbone for all the developments. Second generation of silicones, between 1960 and 1980 included the development of fluorosilicones, silicone-polyether surfactants, and silanes with organic functional groups. The dominant direction

for this period has been and continues to be the development of more specialized materials [220]. The present trend is towards the synthesis of systems with increasing sophistication, the system synthesis being recognized as one of the key challenges in chemistry [221].

The siloxane literature has been extensivelly reviewed. The reviews by Wright [222], Sigwalt [223], Kendrick et al. [224], and Yilgor and McGrath [171] are relatively recent whereas that by Voronkov et al. [225] covers the earlier literature. Additionally, extensive reviews on polysiloxane synthesis, with emphasis on the synthesis of telechelic polysiloxane oligomers with different end group functionalities have been given in our own group [133,138,139,172-176,226]. Therefore, the reader will be referred to these previous reviews for general aspects related to polysiloxane synthesis. The present Literature review will focus on the unique properties of Si-O bond, responsible for the physical and chemical behavior of this class of polymers. Predicting the behavior of siloxanes containing different substituents on the silicon atom is one aspect of interest for synthesis of new polymers. Computer modeling will play an important role in understanding this relationship between structure and properties. Hence these aspects will be briefly reviewed. Additionally, the use of copolymerization as a tool for system design will also be discussed.

## *2.2. PROPERTIES OF POLYSILOXANES*

Semiinorganic polymers typically have inorganic elements making up at least part of the chain backbone, with organic groups as side chains [227]. Silicon containing polymers are the most important in this class. In these polymers silicon atoms contribute the inorganic character and are present in the backbone either alone (silanes), or with atoms of oxygen (siloxanes), carbon (silalkylenes), or nitrogen (silazanes). The siloxanes or silicones have been studied the most and are also of the greatest commercial importance. The silicon in polyorganosiloxanes can be

combined with one, two, or three organic groups, the remaining valences being satisfied by oxygen. Accordingly, there are three groups containing silicon, oxygen, and organic radicals which can be considered *siloxane units* of the polymers [169]:

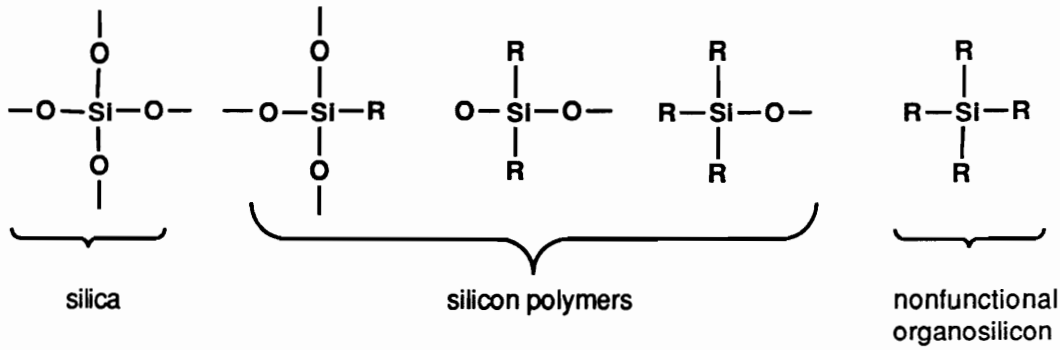


The ($SiO_4$) is the structural unit from which the three-dimensional networks of silica and the silicates are formed. These type of structures have been discussed in Part 1 of this dissertation. At the other end of the scale $R_4Si$ represents a nonfunctional organosilicon compound. The structural unit of the silicon polymers lies between these extremes, and here the dual nature of the polyorganosiloxanes as a link between silicate chemistry and organic chemistry is made evident.

PDMS, composed of pendant organic methyl groups along the siloxane backbone is the simplest and the most representative component in the polysiloxane series. It also represents the starting point for new materials which can be developed with modifications made to enhance desirable attributes and to minimize the undesirable ones. The most important features of the polysiloxanes are listed below [228]:

- low surface tension and moderate interfacial tension against water;
- high water repellency;
- large free volume;

- low apparent energy of activation for viscous flow;
- low glass transition temperature;
- free rotation about bonds;
- high compressibility and dampening action;
- liquid nature to high molecular weight;
- low boiling and freezing points;
- small temperature variation of physical constants;
- high dielectric strength, gas permeability, and resistance to shear;
- high thermal and oxidative resistance;
- low reactivity, toxicity, and combustibility;
- low environmental hazard.

Four structural characteristics of polysiloxanes account for the above features and constitute the link between the structure, properties, and uses of most polysiloxane materials [228]:

1. low intermolecular forces between alkyl radicals,
2. unique flexibility of siloxane backbone,
3. high energy of siloxane bond, and
4. partial ionic nature of siloxane bond.

### *2.2.1. Low intermolecular forces*

The energy ranges of intermolecular forces across an interface are shown in ***Table 2.1*** [229]. The lowest of the London dispersion forces are the weakest intermolecular interactions. For pendant groups in polymers, these interactions are associated with aliphatic hydrocarbon and fluorocarbon groups. The weak intermolecular

***Table 2.1***. Types of interactions at interfaces [229].

| Interaction type | Bond energy range (kJ/mol) | Interaction class | Adsorption nature |
|---|---|---|---|
| Ionic | 600-1000 | Primary bond | Chemisorption |
| Covalent | 60-700 | Primary bond | Chemisorption |
| Metallic | 100-350 | Primary bond | Chemisorption |
| Strong H bonds (involving F) | up to 40 | Permanent dipole | Physical adsorption |
| Other H bonds | 10-25 | Permanent dipole | Physical adsorption |
| Other dipole-dipole interactions | 4-20 | Permanent dipole | Physical adsorption |
| Dipole-induced dipole interactions | 1-2 | van der Waals forces | Physical adsorption |
| London dispersion forces | 0.1-40 | van der Waals forces | Physical adsorption |

interactions between these groups are reflected in Zisman's critical surface tension of wetting [230]. Among hydrocarbons, surfaces comprising closely packed methyl groups have the lowest surface tensions. Since essentially both PDMS and paraffin wax have all methyl surfaces, they have similar surface tension, despite the difference in their molecular architecture. Likewise, the viscosity of low-molecular weight linear and cyclic polydiorganosiloxanes is considerably lower than that of hydrocarbons with a comparative molecular weight [231]. The activation energy of the viscous flow of siloxanes is also smaller than that of the hydrocarbons. For poly(dimethylsiloxane)s it is equal to 15.9 kJ/mole (3.8 kcal/mole) [232] and for saturated hydrocarbons it is 25.1-29.3 kJ/mole (6-7 kcal/mole) [233]. The activation energy of viscous flow increases when the methyl groups in a poly(dimethylsiloxane) are replaced by polar or bulky groups: for poly(methylpropylsiloxane) it is equal to 4.3 kcal/mole (18 kJ/mole), for poly(methyl-3,3,3-trifluoropropylsiloxane) it is 33 kJ/mole (7.9 kcal/mole), and for poly(methylphenylsiloxane) it is 49.8 kJ/mole (11.9 kcal/mole) [234].

The low intermolecular forces can explain certain other physical properties of methylpolysiloxanes, for all the following characteristics imply or are consistent with weak intermolecular forces: (i) the low boiling points and heat of vaporization of liquid PDMS materials when compared with those of organic materials with similar molecular weight [167]; (ii) the low surface tension; (iii) the large molar volumes and remarkably high compresibilities of the silicone fluids; (Methyl silicone fluids of high molecular weight do not crystallize even at pressures greater than 500,000 $lb/in^2$ [235]); (iv) the low dielectric constant of liquid and solid polymers; (v) the poor tensile strength of elastomeric polymers and the moderate adhesion and strength of methyl silicone resins; (vi) the retention of flexibility of silicone rubber down to very low temperatures.

### *2.2.2. Unique flexibility of siloxane backbone*

The molecular motions in a single polymer chain are controlled by three major factors [236]: (i) the external resistance to motion exerted by the environmental frictional forces; (ii) the internal resistance associated with barriers to conformational transitions; (iii) the chain connectivity. The first two factors are common to both small molecules and macromolecules. The third is an inherent property of macromolecules uniquely, and distinguishes them from small molecules. Theoretical models have been developed to calculate the extent of chain flexibility in polymers. The result of such calculations indicate that for a sufficiently long sequence (~20 bonds) a large number (~4 x $10^6$) of conformational transitions induced by single-bond rotations are possible without appreciably moving the ends of the mobile sequence. The implication is that highly flexible polymer chains can exist in a high number of conformations (high entropy of the system). This observation will become important later in the discussion.

The various properties of PDMS previously discussed are the result not only of low intermolecular interactions but also of the extreme flexibility of the siloxane backbone. This flexibility is unique and it is determined by a number of structural features of the siloxane bond.

(i) Rotation about siloxane bonds in PDMS is virtually free, the energy being almost zero, compared with 14 kJ/mole (3.3 kcal/mol) for rotation about carbon-carbon bonds in polyethylene and >20 kJ/mole (> 4.8 kcal/mol) for poly(tetrafluoroethylene) [237]. This free rotation is reflected in the low glass transition temperature of polysiloxanes. ***Table 2.2*** [228] gives the $T_g$s of a variety of polyorganosiloxanes along with all polymers with $T_g$ < 160°K (-113°C). In general, the mobility of the units of a polymer chain is determined by two factors [225]: steric (volume of the substituents) and the energy of interaction between the atoms of the same and neighboring chains. Increase in the volume of the substituents determines a fall in segmental mobility.

***Table 2.2.*** $T_g$s of siloxanes and low $T_g$ polymers [228].

| Polymer | Tg (°K) | Tg (°C) | Ref. |
|---|---|---|---|
| Poly(hydrogen methylsiloxane) | 135 | -138 | 238 |
| Poly(ethylmethylsiloxane) | 138 | -135 | 239 |
| PDMS | 146 | -127 | 240 |
| Polyethylene | 148 | -125 | 240 |
| Poly(propylmethylsiloxane) | 153 | -120 | 239 |
| Poly(thiodifluoromethylene) | 155 | -118 | 240 |
| Poly(oxytetramethyleneoxyadipoyl) | 155 | -118 | 240 |
| Poly(cis-1-pentenylene) | 159 | -114 | 240 |
| Poly(phenylmethylsiloxane) | 187 | - 86 | 240 |
| Poly(trifluoropropylmethylsiloxane) | 203 | -70 | 239 |
| Poly(diethylsiloxane) | 201 | -68 | 240 |

Therefore, when methyl groups on silicon atoms in PDMS are replaced by other organic radicals, the properties described above are usually affected to a certain degree. The most dramatic influence of the substituents is the chain mobility. The mobility of polysiloxane molecules decreases [225] in the series $[H(CH_3)SiO]_n$ > $[(CH_3)_2SiO]_n$ > $[CH_2=CH(CH_3)SiO]$ > $[CH_3CH_2CH_2(CH_3)SiO]_n$ > $[(CH_3)(C_6H_5)SiO]_n$ > $[(C_6H_5)_2SiO]_n$. An exception is polydiethylsiloxane. Despite the fact that the volume of the substituents is greater than PMS and PDMS, polydiethylsiloxane possesses greater segmental mobility than PDMS below ~ 170°K, and greater than PMS below ~155°K. This behavior can be attributed to lower intermolecular interactions in polydiethylsiloxanes when compared with PMS and PDMS [228].

(ii) Additionally, compared with carbon-carbon and carbon-oxygen backbones, the siloxane backbone has the widest bond angle and the longest bond [241]. The wide variability of the Si-O-Si bond angle compared with the tetrahedral angle of the carbon system may also contribute to the backbone flexibility. The flexibility of this bond angle was previously discussed in both a theoretical [242-244] and an experimental framework [245]. The energy variation is insignificant for small deviations of bond angle from its equilibrium value. Experimentally it was determined that in different compounds this bond angle may have values between 128-155° [246] and may even become linear, the linearization barrier being only 1.2 kJ/mol (0.3 kcal/mol) [245]. Values from 105° to 180° have also been quoted [225].

(iii) The ionic character of the Si-O bond which will be discussed next also suggests another way of explaining the flexibility of the siloxane backbone, since a purely covalent bond is completely directional in space, whereas a purely ionic bond has no direction [228].

### *2.2.3. High bond energy and partially ionic character of the siloxane bond.*

The high bond energy and the partially ionic character of the siloxane bond, which impart a hybrid organic-inorganic nature to the polysiloxanes, are responsible for most of specific chemical behavior of these polymers. The Si-O bond energy of 445 kJ/mol (106.3 kcal/mol) [247] is higher than the general value for carbon-carbon (346 kJ/mol or 82.7 kcal/mol) and carbon-oxygen (358 kJ/mol or 85.6 kcal/mol) bonds [248]. The silicon-carbon bond energy of 306 kJ/mol (73.1 kcal/mol) [249] is less than the Si-O, C-C, and C-O bond energies. However, a methyl group on silicon has a higher thermal and oxidative stability compared with a methyl group that is part of a hydrocarbon chain. This stability is due to the partially ionic or polar nature of the siloxane backbone. The positively polarized silicon atom acts as an electron drain, polarizing the methyl groups and rendering them less susceptible to thermal and oxidative degradation [228].

The value of the Si-O bond length is equal to 1.64 ±0.03Å [238], substantially smaller than that of Si-O bond length calculated from the additivity of atomic radii (1.83Å). This discrepancy has been attributed to a resonance-type bond having both polar and covalent bond components. This bond type is the result of the relatively large difference in the electronegativities of silicon and oxygen (1.7) [228]. According to Pauling [250], this difference gives a polar- or ionic-bond contribution of 41%. The electronic charge density for a Si-O-Si unit can be calculated using molecular modeling. The plot of electronic charge density differences is shown in ***Figure 2.1*** [251] for a simple molecule containing the Si-O-Si unit ($H_3Si$-O-$SiH_3$). The blue regions indicate a deficit of electronic charge and the yellow regions show a surplus of electronic charge. The figure indicates that the electronic charge localized at lone pairs on oxygen is transfered to the covalent bonding region between Si and O. The lone pairs at oxygen are diminished, and the $sp^3$ hybridization geometry is altered. The consequence is a wider Si-O-Si bond angle. Therefore, charge transfer has two major effects: (1) the additional charge transferred to the covalent region

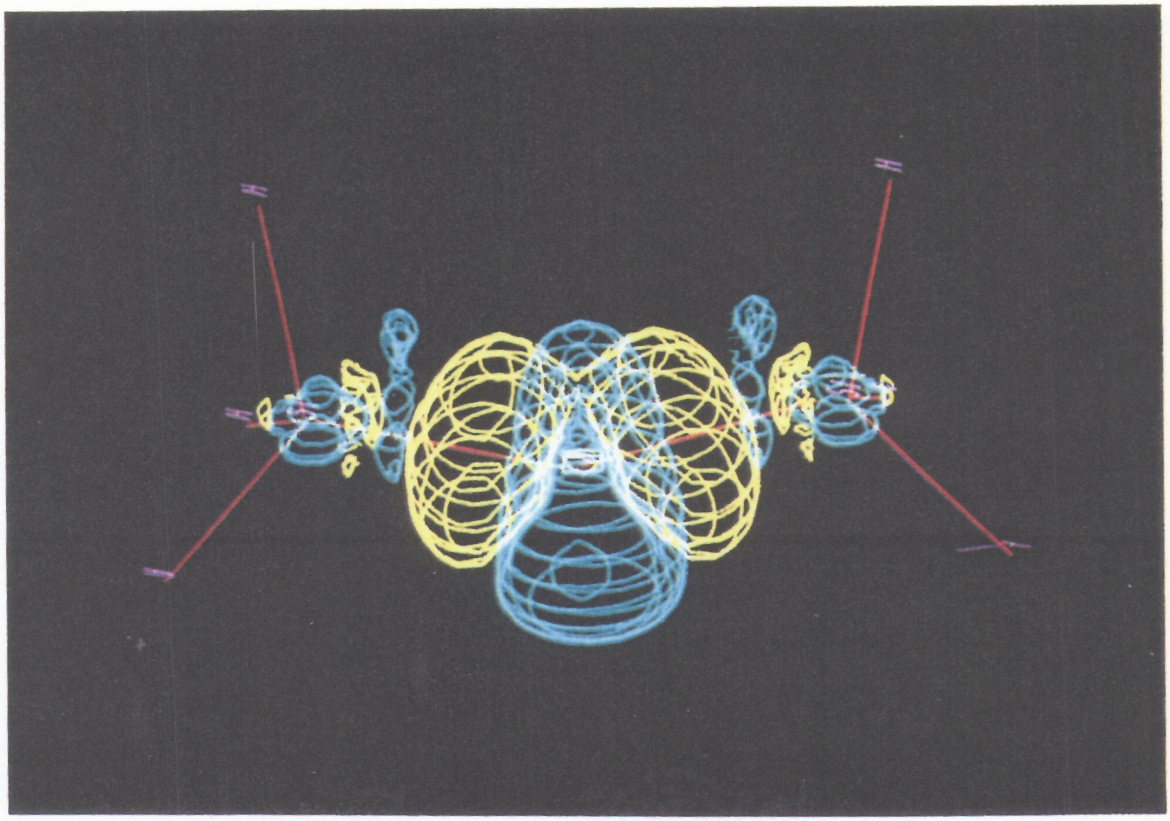

***Figure 2.1.*** Electronic charge density for a Si-O-Si unit. The blue regions indicate a deficit of electronic charge and the yellow regions show a surplus of electronic charge [251].

between Si and O shortens the bond length, and (2) the Si-O-Si bond angle widens. Some relevant numerical data for the most representative polymer of this class, PDMS, are given in ***Table 2.3*** [228].

The above structural features dominate the chemical behavior of siloxanes. While exceedingly resistant to homolytic cleavage, the electronegativity difference between Si and O in the siloxane backbone renders polysiloxanes highly sensitive to electrophilic and nucleophilic cleavage. This feature can be used to an advantage in the synthesis of polysiloxanes, as will be discussed later, but it can also affects the otherwise good thermal and hydrolytic stability of such polymers if residual amounts of catalysts or impurities which can facilitate an electrophilic or nucleophilic attack are present. This combination of higher thermal stability (when compared with the carbon-carbon chain polymers) and susceptibility to electrophilic or nucleophilic attack is shared by virtually all inorganic polymers [259].

## *2.3. SYNTHESIS OF POLYSILOXANES*

Since the siloxane bond is resistant to homolytic cleavage, free radical initiators can not be efficiently used for the polymerization of cyclosiloxanes and these reactions are carried out under the influence of electrophilic or nucleophilic initiators. During the polymerization the active centers attack the Si-O bonds in both the cyclosiloxanes and the linear polymer. Ring-opening polymerization of siloxane cyclics can be represented generically by the equation:

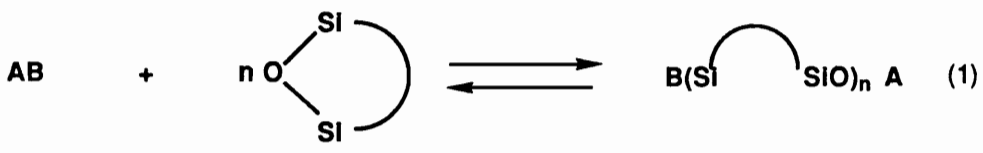


in which the species AB is an acidic or basic initiator. The reaction above is represented as reversible, but conditions can be adjusted so that the reversibility can be greatly supressed with

***Table 2.3.*** Selected properties of PDMS [228]

| Property | Value | Unit | Temp. | Comments | Ref. |
|---|---|---|---|---|---|
| **Surface properties** | | | | | |
| Surface tension | 20.3 | mN/m | 20°C | 70mm2/s(cs) fluid | 249 |
| Interfacial tension (against water) | 44.3 | mN/m | 20°C | 100mm2/s (cs) fluid | 252 |
| Critical surface tension of wetting | 24 | mN/m | 20°C | Elastomer | 253 |
| Polar component of surface tension | 1.1 | mN/m | | | |
| Dispersion force component of surface tension | 21.7 | mN/m | 20°C | Fluid baked on glass at 300°C | 254 |
| Water contact angle | 110 | deg. | RT | Fluid baked on glass at 300°C | 254 |
| Surface viscosity | <110 | ug/s | 20°C | High molec. wt. fluid ($10^7$) | 255 |
| **Structural properties** | | | | | |
| Si-O bond length | 0.165 | nm | | | |
| Si-C bond length | 0.192 | nm | | | |
| Si-O-Si bond angle | 142.5 | deg. | | Cyclic tetramer | 169 |
| O-Si-O bond angle | 109 | deg. | | | |
| Si-O bond energy | 445 | kJ/mol | | Hexamethyldisiloxane | 247 |
| Si-C bond energy | 306 | kJ/mol | | Trimethylchlorosilane | 247 |
| Tg | -123 | °C | | Elastomer | 256 |
| Energy of rotation | 0 | kJ/mol | | Elastomer | 237 |
| Activation energy of viscous flow | 14.7 | kJ/mol | | $100mm^2/s$ (cs) fluid | 257 |
| Si-O bond polar character | 41 | % | | Pauling calculation | 250 |
| Si-O bond dipole moment | $9.8x10^{-30}$ | cm | | Calculated from hexamethyldisiloxane molecular dipole moment | 258 |

* cs is centistokes, the usual unit for viscosity.

the proper choice of monomer, initiator, solvent and temperature. The nearly planar cyclic trimer, $D_3$, is known to be somewhat strained and to polymerize with a significant exothermic enthalpy. If initiation is comparable to propagation, a living polymerization mechanism operates in this system producing polydimethylsiloxane chains with narrow molecular weight distribution. The ring strain in the $D_3$ cyclic, the use of organolithium initiators and the polar solvent THF are all necessary conditions for this living polymerization mechanism [260].

While the Si-O bonds in the strained $D_3$ ring are much less flexible, the flexibility of the siloxane bonds is considerably higher in the relatively unstrained $D_4$ ring and it is close to their flexibility in the linear polydimethylsiloxanes [261]. This eight membered ring molecule can exist in a large number of conformations. Using computer modeling approximately 50 different conformations have been generated for the $D_4$ molecule [262]. The most stable forms and their relative energies are shown in ***Figure 2.2*** [251]. The most stable conformation is one corresponding to the $S_4$ form and this in agreement with the gas phase electron diffraction data [246]. It is important to notice that other symmetrical forms have their energies quite close to the most stable conformation, $S_4$. The experimental valence geometry and theoretical data obtained by optimizing the geometry for the eight-membered ring are compared in ***Figure 2.3*** [251]. The larger calculated values for Si-O-Si angles compensate for the smaller O-Si-O, when compared with assigned experimental values. The calculated torsional angles along the ring are very close to the experimental values. Thus, overall, the structures are similar.

The interconversion between stable conformers is impeded by the steric repulsion between the methyl groups in cis position on opposite silicons. The boat-boat form has a total energy 20kcal/mol (83.7 kj/mol), higher than the most stable $S_4$ form. The common feature of the most stable conformations is the relative position of the methyl groups. The planes generated by

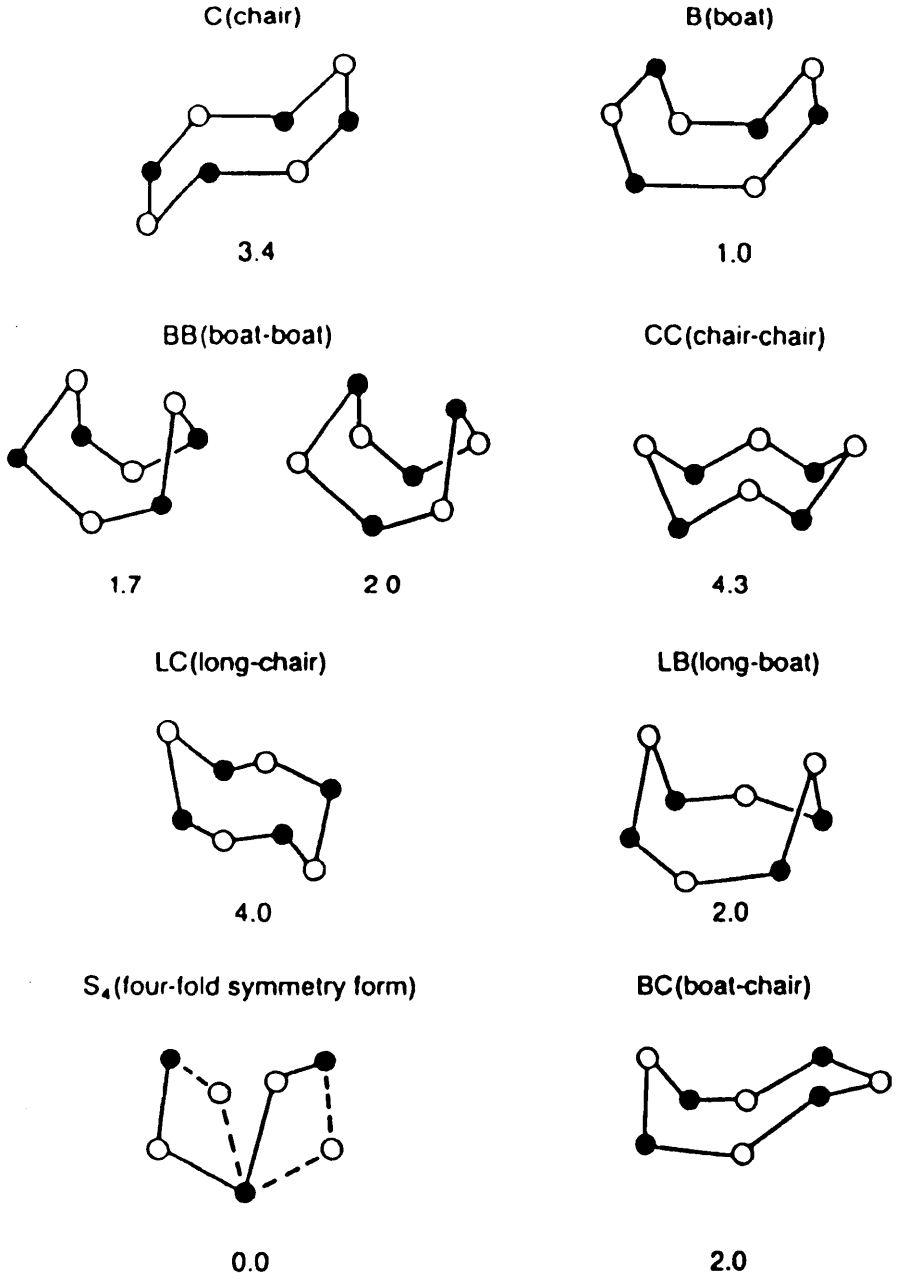


***Figure 2.2.*** Canonical symmetric forms of $D_4$ and their relative energy (kcal/mol) calculated from molecular mechanics potentials [251].

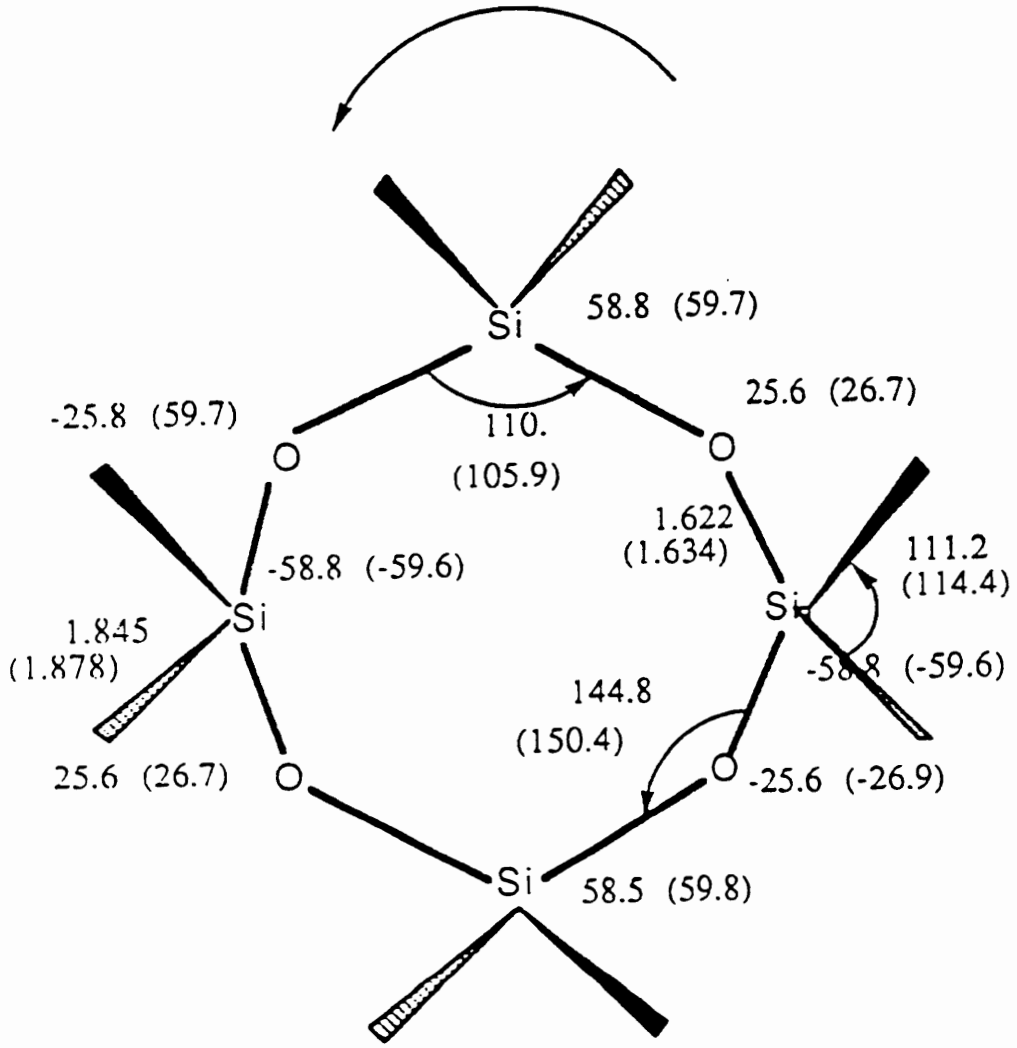


***Figure 2.3.*** Comparison of the optimized geometry with experimental values (shown in parantheses) for $D_4$ in $S_4$ conformation [251].

The arrow in the top of the figure indicates the sense considered for torsional angles. Bond lengths are in angstroms while bond angles are in degrees. Experimental data are from reference [246].

vicinal methyl groups form a dihedral angle of 20-40° with the methyl groups at the opposite Si atom in the ring. Thus, the distance between methyl groups is maximized, and the steric repulsion is reduced. The orientation of the methyl groups is illustrated in ***Figure 2.4*** [251]. The conclusions from this analysis are two fold: firstly, the eight membered ring can adopt a geometry in which the ring strain is almost zero; secondly, the stability of these rings is dependent on the position of methyl groups in cis position on opposite silicons: the steric repulsion is reduced by maximizing the distance between these methyl groups. This means that replacing the methyl groups with bulky substituents can highly affect the stability of the ring and hence its reactivity during ring opening polymerization processes.

In the polymerization of unstrained cyclosiloxanes, where the energy of the siloxane bond is close to the energy of the bond in the polymer, the active centers cleave the Si-O bonds in both the rings and the linear macromolecules. Such reactions are known as "equilibration" or "redistribution" reactions. Under these conditions, the system is described by two equilibria [263]:

$$\sim D^*_n + D_x \underset{}{\overset{K_2}{\rightleftharpoons}} \sim D^*_{(n+x)} \qquad (2)$$

and

$$\sim D_n \sim + \sim D_m \sim \overset{K_3}{\rightleftharpoons} \sim D_{(n+y)} \sim + \sim D_{(m-y)} \sim \qquad (3)$$

Both processes are siloxane redistributions. Reaction 2 contributes to chain growth by x units [264-267], whereas reaction 3, which does not give a net change in number average molecular weight, results in an exchange of y repeat units between the chains [264-266]. The redistribution in reaction 3 begins early in the process [267] and when both equilibria are finally reached, a Gaussian distribution of molecular sizes results [264,265]. Therefore, each D unit, whether located in a ring or chain, is subject to redistribution and participates in both equilibria. Knowledge

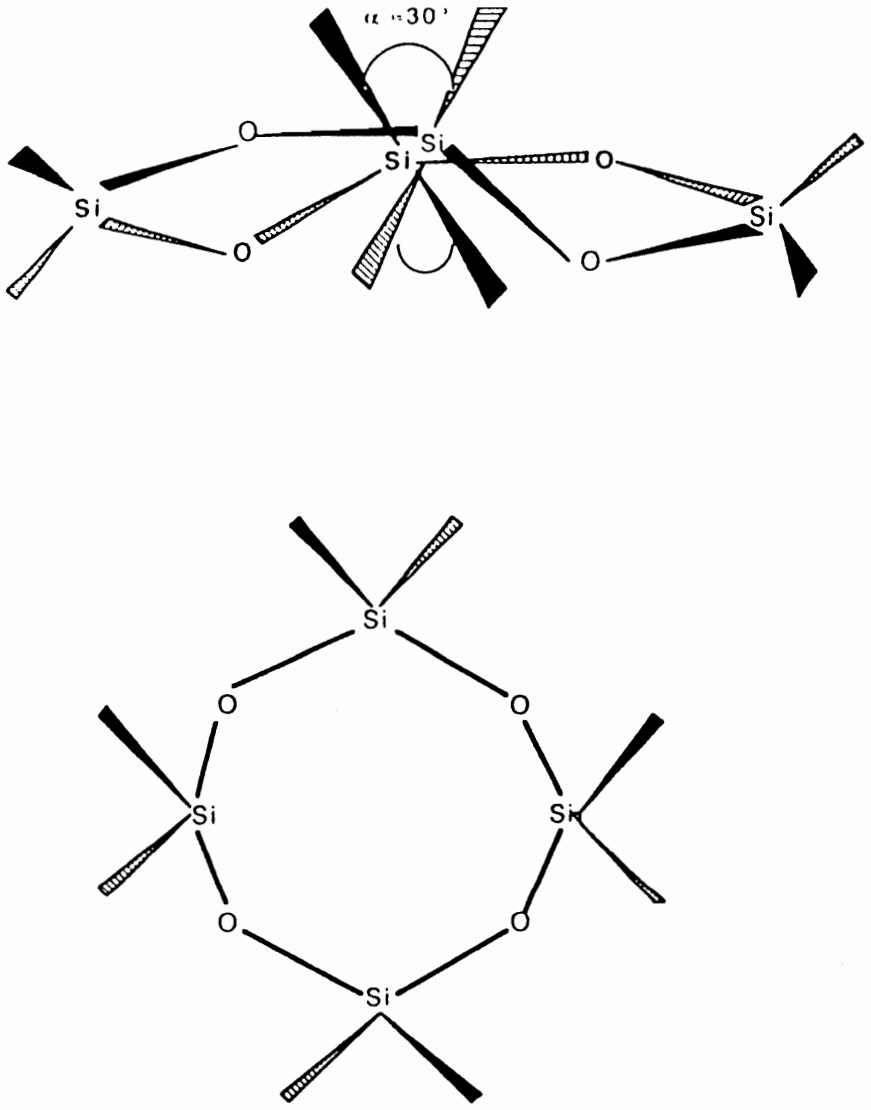


***Figure 2.4.*** The most stable conformation of $D_4$. Notice the relative orientation of methyl groups forming an angle between the planes defined by two adjacent groups [251].

of the relative amounts of rings and chains at equilibrium permits an approximation of thermodynamics of reaction 2 through equation 4 [268]:

$$\ln (1 - w_p) = \frac{\Delta H_2}{RT} - \left( \frac{\Delta S_2}{R} + \ln D_0 \right) \quad (4)$$

where $w_p$ is the weight fraction of linear chains, $\Delta H_2$ and $\Delta S_2$ are the enthalpy and entropy for equilibrium 2, respectively, $D_0$ is the total molar fraction of D units in cyclics and linear species, and R and T are the gas constant and temperature respectively. In the absence of ring strain or special group interactions, the amount of cyclics at equilibrium, $(1 - w_p)$ was reported to be independent of temperature [269-271] and therefore no net change in enthalpy can occur and $\Delta H_2 = 0$. Hence, for unstrained rings, the process is driven by entropy. According to Jacobson-Stockmayer theory [272] which postulates an equilibrium molecular weight distribution of the linear and cyclic compounds, a critical concentration exists in an inert solvent below which only cyclic compounds are found at equilibrium. The critical conditions of temperature and dilution at equilibrium for polymer formation can be defined by setting $w_p$ to zero in equation 4. With $\Delta H_2 = 0$, equation 4 becomes [263]:

$$\ln (1 - w_p) = - \left( \frac{\Delta S_2}{R} + \ln D_0 \right) \quad (5)$$

and at critical conditions,

$$- \frac{\Delta S_2}{R} = \ln [D_0]_{crit} \quad (6)$$

in which $[D_0]_{crit}$ is the critical molar fraction of D units below which no polymer is present. Therefore, unlike many other polymers at equilibrium with their monomers , poly(dimethylsiloxane) has no "unzipping temperature" (ceiling temperature) [260], but it has an "unzipping dilution". For poly(dimethylsiloxane)s this critical dilution is roughly 30 vol % siloxane at equilibrium [263].

The yield of polymer, $w_p$, is highly dependent on the size of the substituent groups in the siloxane system [273,274]. In the series $CH_3RSiO$, $w_p$ decreases in the order R = H > $CH_3$ > $C_2H_5$ > $C_3H_7$ > $CF_3CH_2CH_2$. This order corresponds, in general, to the order of decreasing mobility of polysiloxane chains and it is not altered by dilution. The application of Jacobson-Stockmayer theory to the prediction of individual concentrations of rings at equilibrium were successful only when ring sizes excedeed 15-20 units. Details are available in the original work [271,273] as well as in a more recent review [222].

The molecular weight of the linear polymer at equilibrium is controlled by the incorporation of a disiloxane (end-capper). When the disiloxane is also functionalized it provides additionally the functional end-groups in the resulting polymer. Functionalization by this route is possible since the nearly covalent Si-C bond of the disiloxane (end-capper) does not participate in redistribution reactions. A general reaction scheme for the synthesis of controlled molecular weight, functionalized polysiloxanes was given in Part 1 (Scheme 1.13, page 170). Detailed procedures for these syntheses have been given in the literature [174,222,275-278]. Extensive work on the synthesis of controlled molecular weight, functionalized polysiloxane oligomers and their subsequent use for the synthesis of segmented copolymers has been carried out in our laboratories [133,138,139,226]. A survey of the recent development in the synthesis of functionalized polysiloxanes and their further use for the synthesis of segmented copolymers or as network modifiers has been published by Yilgor and McGrath [171].

*2.4. MECHANISM OF RING OPENING POLYMERIZATION.*

The ionic character of the Si-O bond and its susceptibility to electrophilic and nucleophilic attack can be used to an advantage for the synthesis of polysiloxane oligomers. Such reactions can be carried out under both acid and base catalysts.

***Base-catalyzed polymerization.*** The mechanism of the reaction of siloxanes with bases was postulated by Hurd, Osthoff, and Corrin [279]. These authors proposed that the attack of a base on a siloxane takes place at the silicon atom with a displacement of the siloxanyl bond, thus

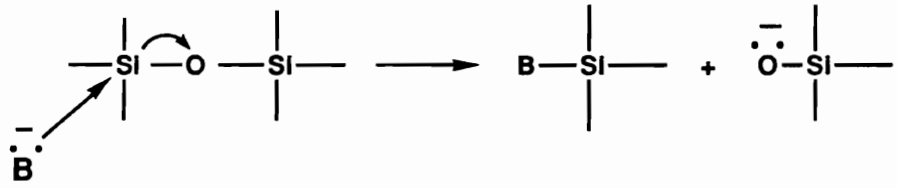


(7)

This reaction was once thought to proceed via free ionic intermediates [280]; however, little evidence supported this mechanism. Most workers now agree that reactive intermediates consist of ion pairs or charge-separated ion-pairs [223,224]. The reaction rates in ring opening polymerization of cyclic siloxanes catalyzed by alkali metals are typically proportional to a fractional order of the catalyst and close to first order in cyclosiloxane:

$$Rp = [B]^{1/n}[D_X] \qquad (8)$$

In the absence of polar solvents, n=2 is commonly reported for potassium silanolate initiators [281,282]. The fractional order is attributed to strongly associated ion pairs at the chain ends. These ion pairs must dissociate to provide a low concentration of unassociated ion pairs prior to propagation. Hence, one expects that the formation of free ions should depend on the polar nature and the spatial requirements of the counter-cation. A large effective cation size should supress the cation-siloxane coordination, favor the free ion pair species, and enhance charge separation, hence reaction rates. Evidence that these effects were achieved were obtained in

our own laboratories [133,176,212]. It was found for example, that the tetramethylammonium and tetrabutylphosphonium siloxanolate catalysts were much more efficient than the potassium catalyst. Different aspects of base-catalyzed equilibration reactions have been reviewed in more detail by Dr.C. Elsbernd in her dissertation [133] and the reader is referred to this source for more information.

***Acid-catalyzed polymerization.*** Although the first high-molecular weight polymethylsiloxane was obtained through an acid-catalyzed reaction [283], the acid-catalyzed polymerization of cyclosiloxanes has not received nearly as much attention in the published literature, despite a long history of continued applications. Consequently, the uncertainty and controversy over the mechanism is greater than that for base-catalyzed polymerizations. A recent paper by Sigwalt [284] reviews the more current activity on this subject.

Acid-catalyzed polymerization resembles the base-catalyzed process in terms of yields of polymer and other products formed at equilibrium. The pathway to the final product, however, is quite different, because the overall rate equation and relative reactivities of the monomers differ considerably from those of the base-catalyzed process. The polymerization of $D_4$ when catalyzed by either sulfuric acid [285] or trifluoromethanesulfonic acid [286] proceed as a step growth polymerization as evidenced by traces of the molecular weight distribution as monomer is converted [140]. After an initial induction period, the molecular weight of the polymer fraction increases, whereas the molecular weight distribution steadily broadens until it fits the distribution expected for a step-growth polymer [285]. Low molecular weight oligomers, and cyclosiloxanes other than $D_4$ ($D_5$-$D_9$), on the other hand, appear quickly and then remain invariant throughout the polymerization [286].

## *2.5. COPOLYMERIZATION OF CYCLOSILOXANES*

The use of copolymerization techniques for the synthesis of polysiloxanes through equilibrium polymerization is of high practical importance. Polymerization of mixtures of monomers, such as $(SiR_2O)_x$ with $(SiR_2'O)_y$ , can be used to obtain random copolymers. Sequence distribution of repeat units in copolymers, which is crucial in determining both their properties and applications, can be derived from an understanding of the kinetic copolymerization parameters that are typically arrived at from the Mayo-Lewis model which presumes an irreversible process [287,288]. For siloxane copolymerizations the reversibility can be established quickly, and rapid redistribution of monomer units between rings and chains via equilibria 2 and 3 will confound any study of comonomer reactivity ratios. Although copolymerizations of cyclosiloxanes are reversible, previous studies either ignored this or sought to circumvent the difficulty by limiting the copolymerization to low conversions [289,290] or by selecting strained ring monomers and mild catalysts which do not readily induce siloxane redistributions [291,292]. Therefore, all early studies of copolymerizations must be examined critically when the ring size of any of the comonomers exceeds three.

The lack of reliable information on kinetic parameters for the copolymerization of important cyclosiloxanes with ring sizes exceeding three is a serious deficiency. Industrial and routine laboratory syntheses rely almost entirely on such monomers, and in many cases, the processes involve copolymerizations. An understanding of these constants would give valuable information on copolymer microstructure and its control. Unambiguous studies of such copolymerizations have been impeded by reversibility until recently, when alternatives to the Mayo-Lewis model have been developed to take into account reversibility, predict microstructure at various stages of conversion, and determine how microstructure is influenced by kinetic factors [293-295].

Copolymerization at equilibrium appears to be an entirely random process, according to three separate studies of KOH-initiated copolymerizations of $D_4$ with $[CH_2=CH(CH_3)SiO]_4$ [296], and $[(C_6H_5)_2SiO]_4$ [297,298]. The conclusions in each case were based on the analysis of signal intensities of pentad and triad sequences in high resolution $^{29}Si$ NMR of the copolymers at equilibrium. The random sequence distribution persisted over a broad composition range [296,298] and this result was unaffected by temperature [296]. The findings indicated that, as with homopolymerization, there was no enthalpic driving force. The study also indicated that the composition of the cyclosiloxanes at equilibrium and the sequencing of their comonomer units matched exactly those of the copolymer chains.

The random nature of the copolymerization was interpreted as a consequence of two concurrent entropically driven equilibria similar to reactions described by equations 2 and 3 [263]. These copolymerization equilibria, however, would involve the comonomers interacting reversibly with two different chain ends and the reversible transfer of the different comonomer units between chains. It is possible to construct a model for cyclosiloxane copolymerization <u>at equilibrium</u> which resembles the Mayo-Lewis scheme but where the competing rate constants are replaced by equilibrium constants and where comonomer concentrations represent <u>total</u> concentrations of each comonomer unit regardless of their locations in the rings or chains [296]:

$$
\begin{aligned}
\sim M_1^* + M_1 &\overset{K_{11}}{\rightleftharpoons} \sim M_1M_1^* \\
\sim M_1^* + M_2 &\overset{K_{12}}{\rightleftharpoons} \sim M_1M_2^* \\
\sim M_2^* + M_2 &\overset{K_{22}}{\rightleftharpoons} \sim M_2M_2^* \\
\sim M_2^* + M_1 &\overset{K_{21}}{\rightleftharpoons} \sim M_2M_1^*
\end{aligned}
\qquad (8)
$$

where units with an asterisk represent an active end and $M_1$ and $M_2$ represent comonomer units anywhere in the rings or chains. This scheme combined with the same type of equilibria described in equations 2 and 3 provides a pathway that allows comonomer units to distribute throughout the entire system and give essentially the same composition of comonomer units in the rings as well as in the copolymer chains.

The equilibrium constant for homopolymerization of $D_4$ has been shown by several investigators to be independent of temperature and hence driven only by entropy [269-271] but in copolymerization the possibility of enthalpic contributions from the second monomer units in $K_{12}$, $K_{22}$, and $K_{21}$ is possible. When the second monomer was the methylvinylsiloxane unit, the lack of selectivity and the absence of a temperature effect was interpreted as a lack of such contributions [296]. Experimental data indicated that even though the process is initially specific, the system quickly randomizes and the composition of the ring and chains roughly match as this occur. However, this observation may not be general when bulkier or more polar substituents are introduced on the silicon atoms.

# *CHAPTER 3*

# *EXPERIMENTAL TECHNIQUES*----------

This section describes in detail the experimental techniques specific for the work discussed in Part 2 of the dissertation. Many analytical techniques and general experimental procedures have already been discussed in the first part of this dissertation. Consequently, these techniques will not be repeated and, when necessary, the reader will be reffered to this part for more details.

## *3.1. PURIFICATION OF REAGENTS*

### *3.1.1. Solvent purification*

All equilibration reactions were carried out in bulk, therefore no solvents were required for the reaction stage. Solvents were used for derivatization reactions, for titration, or to carry out chromatographic analysis. The THF solvent utilized for derivatization reactions, which will be discussed later in this section, was distilled from Na dispersion in paraffin, using benzophenone as indicator, as described in Part 1. THF and toluene, HPLC grade, were used for GPC analysis. HPLC grade acetonitrile and acetone were employed for HPLC analysis. Certified grade isopropyl alcohol (IPA) was used for potentiometric titrations without further purification. Chloroform-d (Aldrich, 99.8 atom % D) was used as received for routine NMR analysis.

### *3.1.2. Purification of monomers and general reagents*

Octamethylcyclotetrasiloxane ($D_4$) obtained from Union Carbide was dried over calcium hydride and distilled under reduced pressure. Hexamethyldisiloxane end-capper purchased from Petrarch Inc. was distilled under vacuum. The new cyclic siloxane monomer, cyclic **2** below, was generously supplied by Dow Corning and it was used without further purification.

Tetramethylammonium hydroxide pentahydrate ($TMAH{\cdot}5H_2O$), used for the preparation of tetramethylammonium silanolate catalyst, was obtained from Aldrich and it was used as received.

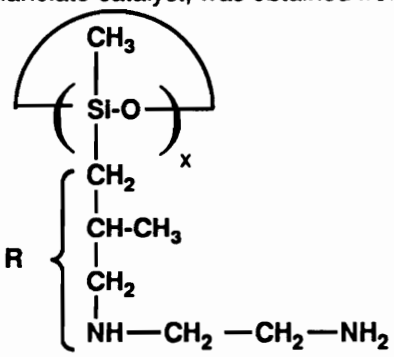

Cyclic 2
~

Phenyl isocyanate utilized for the derivatization of both primary and secondary amines in the R groups was purchased from Petrarch and it was fractionally distilled under reduced pressure, before use. The distilled phenyl isocyanate was stored under nitrogen pressure in the desiccator.

### *3.2. CATALYST SYNTHESIS*

The equilibration reactions were carried out under basic conditions using tetramethylammonium silanolate as a transient catalyst. The silanolate catalyst was prepared according to ***Scheme 2.1***. Details on the silanolate catalyst synthesis can be found in C.S. Elsbernd's dissertation [133] and the reader is refered to this source for more information.

### *3.3. CO-EQUILIBRATION REACTIONS*

All co-equilibration reactions were carried out in bulk, isothermally (at 80°C), under a dry nitrogen atmosphere. A catalyst concentration of 0.025 mole percent based on siloxane units (Si-O bonds) was used. The desired amount of $D_4$ and cyclic siloxane monomer 2 along with a calculated amount of hexamethyldisiloxane (end-blocker) was charged to a four-necked flask equipped with mechanical stirrer, nitrogen inlet, reflux condenser, and a rubber septum for the removal of samples via syringe or disposable pipet (for more viscous, higher molecular weight

***Scheme 2.1.*** Synthesis of tetramethylammonium silanolate - transient catalyst for siloxane equilibration.

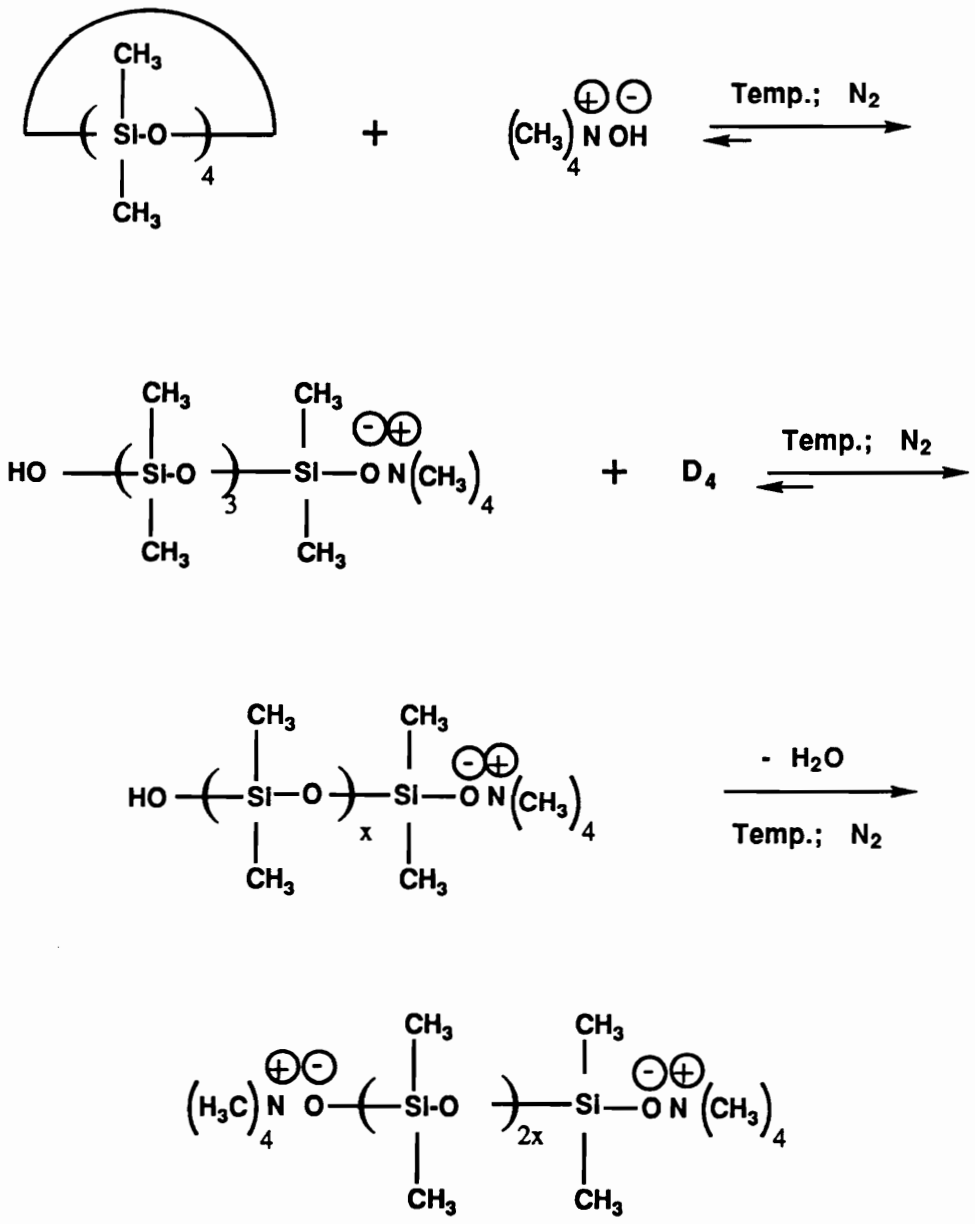

oligomers). The corresponding amount of catalyst was added after the reaction mixture reached thermal equilibrium at 80°C. The initial reaction mixtures were heterogeneous; however, as the equilibration proceeded the reactions became clear, viscous and homogeneous. Samples were removed at desired time intervals during the equilibration, quenched in a dry ice/acetone bath and refrigerated until analysis. All reactions were allowed to equilibrate for at least 24 hours, or until the thermodynamic equilibrium was reached. The thermodynamic equilibrium was considered to be reached when no further change was observed in the apparent molecular weight, apparent molecular weight distribution, and reaction composition as determined by GPC. At the end of equilibration the reaction mixture was heated for 30 minutes at 140°C under fast nitrogen flow , in order to decompose the transient silanolate catalyst. The equilibrium mixture consisted of 15 to 29 weight percent cyclic species, as determined from GPC, depending upon the reaction chemical composition. The cyclics were removed from the reaction mixture by vacuum distillation (approximatelly 200mtorr and 200°C). Complete removal of cyclics was achieved under the above conditions.

### *3.4. CONTROL EQUILIBRATION REACTIONS*

For comparison purposes, two control reactions were carried out. The first control reaction was the equilibration of $D_4$ $\{[(CH_3)_2SiO]_4\}$ in the presence of hexamethyldisiloxane as the end capper. The reaction was carried out under similar conditions described above for the co-equilibration reactions with the exception that $D_4$ was the only cyclic siloxane monomer employed in the polymerization. The second control reaction consisted in an equilibration reaction in which the cyclic 2, $\{[(CH_3)RSiO]_x\}$ was used exclusively as the siloxane monomer. The reaction was carried out using hexamethyldisiloxane as the end-capper, and under identical conditions (catalyst concentration, time, temperature, etc.) as the ones employed for the co-equilibration

reactions. Both control reactions were also continuously monitored as a function of equilibration time.

*3.5. CHARACTERIZATION TECHNIQUES*

***3.5.1. Magnetic Resonance Spectroscopy.*** $^{1}H$ NMR data were obtained at room temperature on a Bruker WP-270 high resolution spectrometer operating at 270 MHz. $CDCl_3$ used as a solvent also provided the signal for the $^{2}H$ NMR internal lock and served as an internal reference. $^{29}Si$ NMR spectra were obtained at room temperature on a Bruker WP 200 spectrometer operating at 39.759 MHz or on a Varian Unity-400 operating at 79.459 MHz. For quantitative measurements, an inverse-gated pulse program was employed to decouple the protons and eliminate the nuclear overhauser effect (NOE). A relaxation agent, 0.04 M chromium (III) acetylacetonate [$Cr(acac)_3$] solution in $CDCl_3$ was employed to shorten the relaxation time ($T_1$) as well as help supress (NOE). Tetramethylsilane (TMS) was used as an internal standard and all chemical shifts were reported with respect to TMS (0.00ppm), positive shifts being downfield.

***3.5.2. Potentiometric titrations.*** The amine content was required in order to evaluate the initial cyclic 2, to determine the composition of different fractions at equilibrium (e.g. cyclics and linear species), or in order to determine the amount of phenyl isocyanate necessary to quantitatively derivatize the samples for chromatographic analysis. Both primary and secondary amines on the pendant R groups were titrated with 0.1N alcoholic HCl using a MCI GT-05 (COSA Instruments Corporation) automatic potentiometric titrator or using bromophenol blue as indicator. The detailed procedure for potentiometric titration was described in Part 1 of this dissertation. Certified grade isopropyl alcohol was used as the solvent. When bromophenol blue was used as indicator, the end point was determined by the change in color from light blue under basic conditions to light yellow. The results for the two titration methods were in good agreement.

However, the potentiometric titration was prefered when possible. The silanolate catalyst was also titrated using 0.1 N alcoholic HCl and the automatic potentiometric titration. The results were typically the average of three samples.

***3.5.3. Chromatographic analyses.*** Gel permeation chromatography was carried out at 30°C on a Waters 150-C17 GPC equipped with micro-styragel columns. Two sets of conditions were used corresponding to two different type of samples. (1) GPC samples containing $[(CH_3)RSiO]$ units (from co-equilibration reactions or from equilibration of cyclic 2) were derivatized prior to GPC analysis in order to avoid column adsorption. The derivatization described in ***Scheme 2.2***. consisted in reacting both primary and secondary amines in the pendant groups R with phenyl isocyanate, at room temperature, in THF solvent. The amine content of the individual samples were titrated as described above, in order to determine the amount of phenyl isocyanate required to completely derivatize the amine functionalities. The derivatized samples were then retitrated to ensure that complete derivatization had taken place, and analyzed by IR for excess isocyanate (2275 $cm^{-1}$) before the GPC analysis was conducted. The conditions employed for the analysis of derivatized samples included: a set of four columns with porosities 500, $10^2$, $10^4$, $10^5$ Å, spectrograde tetrahydrofuran (THF) as the eluent, 1 ml/min. flow rate, and a Waters 490 programmable wavelength UV detector set at 254 nm in conjunction with a differential refractive index detector (DRI). (2) GPC samples containing only $[(CH_3)_2SiO]$ units (from equilibration of $D_4$) were analyzed using a second set of three columns (porosities 100, 500, $10^3$Å) in spectrograde toluene as the eluent, 1ml/min flow rate and a differential refractive index detector(DRI).

High Performance Liquid Chromatography (HPLC) data were obtained on a Varian 5500 series liquid chromatograph using reverse phase chromatography (C18 column) and a UV detector set

***Scheme 2.2.*** Derivatization of amine containing siloxane oligomers for GPC analysis

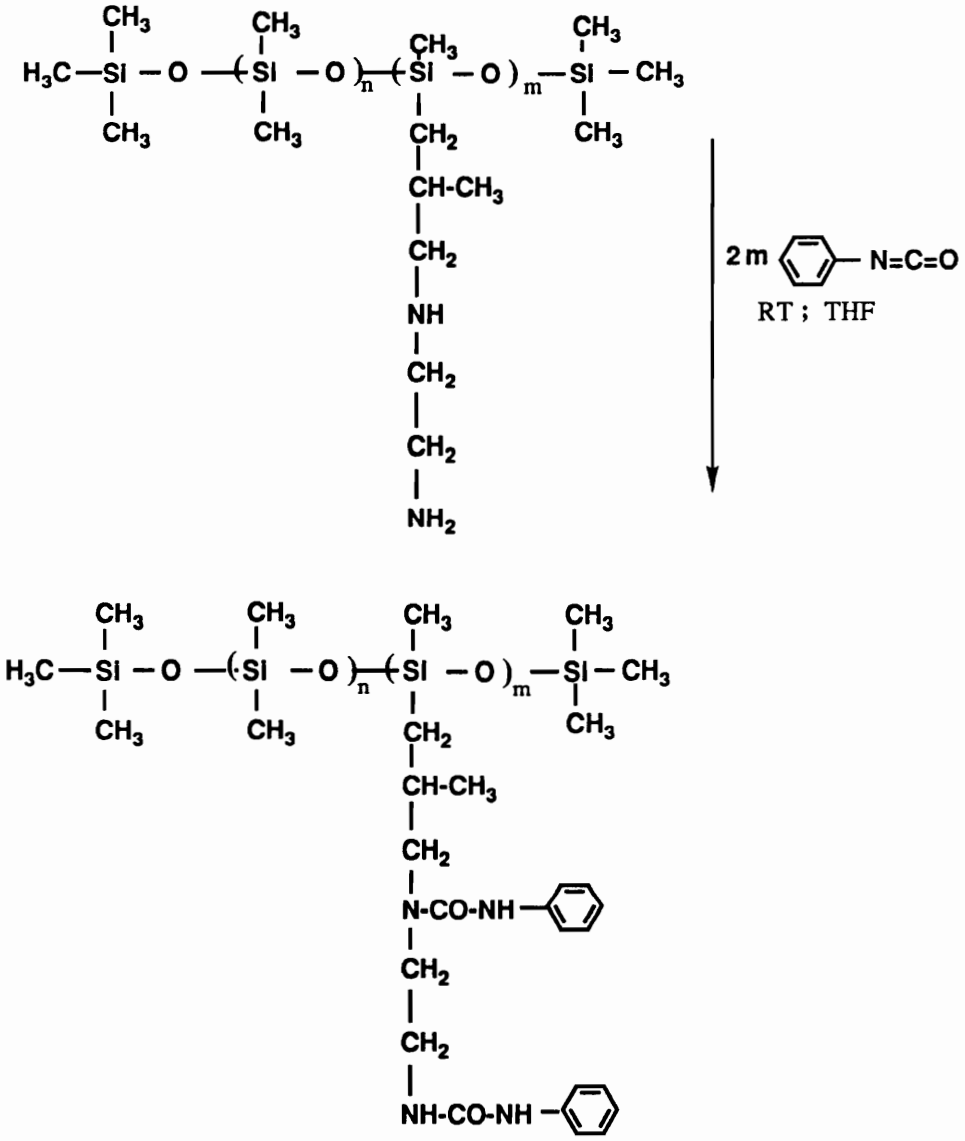

at 254 nm. The mobile phase was a 90:10 mixture of acetonitrile:acetone at a flow rate of 0.8 ml/min. The HPLC samples were similarly derivatized to avoid column adsorption.

***3.5.4. Mass spectroscopy.*** Low resolution mass spectral data and parent peak matches were obtained at 70 eV by using a VG 770E mass spectrometer. A temperature source of 200°C and desorption chemical ionization (DCI) techniques were employed.

# *CHAPTER 4*

# *RESULTS AND DISCUSSION*----------

## *4.1. AMINE CONTAINING POLYSILOXANE OLIGOMERS. TERMINAL VS PENDANT AMINE GROUPS.*

Traditionally, functionally terminated siloxane oligomers with controlled structures are synthesized by the ring opening of the cyclic siloxane tetramer, octamethylcyclotetrasiloxane ($D_4$), in the presence of α,ω-difunctional disiloxanes {$R(CH_3)_2Si\text{-}O\text{-}Si(CH_3)_2R$}, as shown in Scheme 1.13, page 170. During these reactions the disiloxanes are used as chain transfer agents or "end-blockers" and they play a double role: they control the type of the functional endgroup (through the nature of R), and regulate the number average molecular weight by the initial ratio of the cyclic tetramer to the dimer. The above control is possible due to the fact that under the acid or base catalyzed equilibration conditions, the Si-O bonds are easily broken and redistributed, whereas the Si-C bonds and other less polar organic bonds (C-C, C-O, C-N) are stable. A large number of functionalities can be imparted to the siloxane oligomers by a proper choice of disiloxane and reaction conditions [167-173]. One of the most important uses of end-functionalized polymers is in the preparation of block copolymers. The use of functionally terminated oligomers for the synthesis of well-defined block copolymer or for network modifications was extensively investigated in our own group [133,138,139,226].

Amine functionalized polysiloxanes are generally synthesized using aminopropyldisiloxane as the end-capper, as indicated in ***Scheme 2.3***. In these linear functionalized oligomers, the content of the functional groups is dependent on the oligomer molecular weight and vice versa. The present study describes a new molecular design for the synthesis of amine containing polysiloxane oligomers. This was accomplished by copolymerization of octamethylcyclotetra-siloxane ($D_4$) with a new cyclic siloxane monomer (2) containing aliphatic amine substituents on

***Scheme 2.3.*** General reaction scheme for the synthesis of aminopropyl terminated poly(dimethylsiloxane) oligomers by anionic ring opening equilibration reaction.

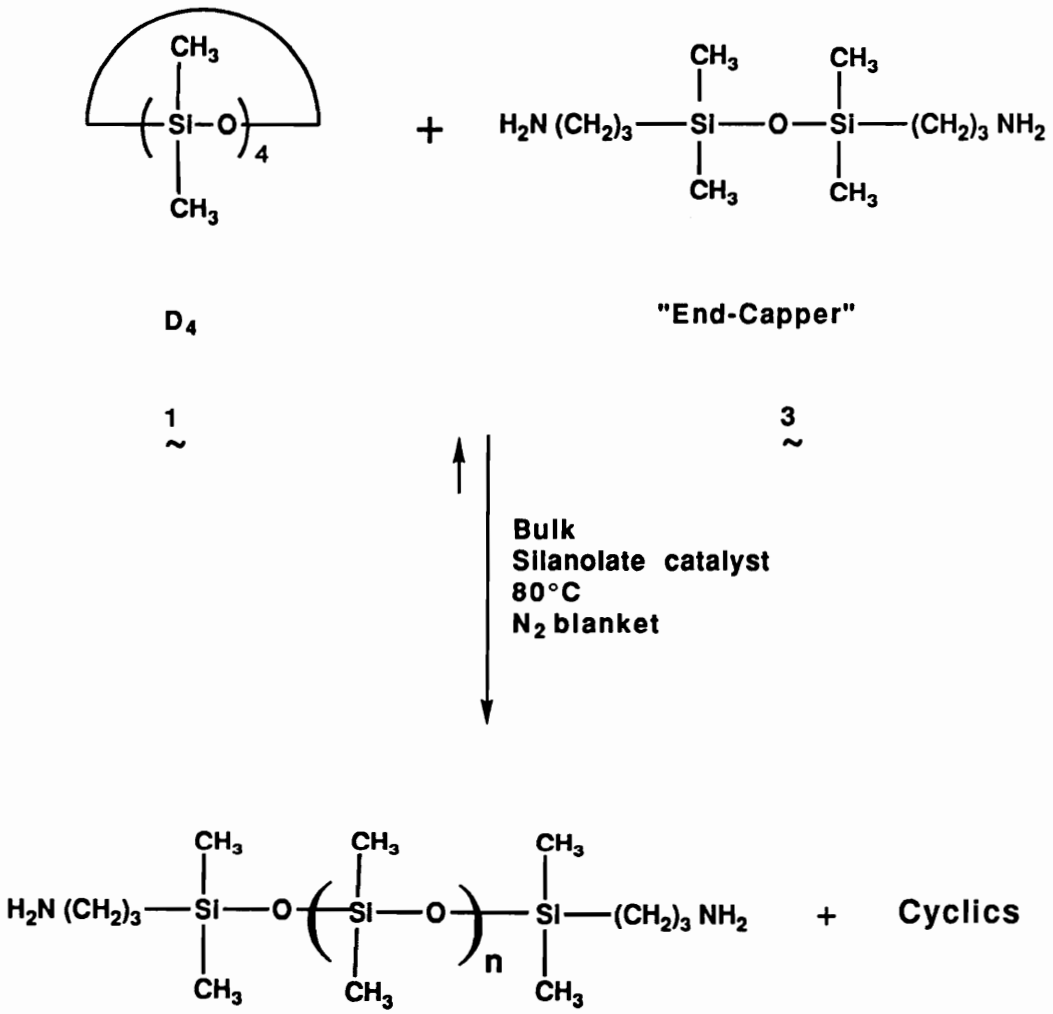

the silicon atom, via co-equilibration reactions, as described in ***Scheme 2.4.*** In the resulting copolymer, 4, the amine content is controlled by the relative ratio of the cyclic siloxane monomers (1 vs 2) whereas the molecular weight of the oligomer is determined by the ratio of the cyclic monomers (1 + 2) to the dimer or end-capper, (3). In such systems, the amine content and the molecular weights can therefore be independently controlled. The main features of the two types of molecular design for amine functional poly(dimethylsiloxane) oligomers (terminal vs. pendant amine functionalities) are summarized in ***Figure 2.5.*** Decoupling of the molecular weight and the amine content of the oligomers may be desired for certain polysiloxane applications such as encapsulates, crosslinked membranes or in system modifications for the development of toughened networks from epoxy or maleimide materials.

Two main aspects of co-equilibration were investigated during the present study. (1) The competition between kinetic and thermodynamic factors during the co-equilibration of the two cyclic siloxanes, and (2) The extent of control of the molecular weight and chemical composition in the system investigated, for the synthesis of polysiloxane copolymers of controlled structure. It was anticipated that the siloxane cyclics containing the bulky substituents R on the silicon atoms would contain a higher degree of ring strain, therefore would favor ring opening (kinetic reasons). In the meantime, the resulting polysiloxane chains, containing [$(CH_3)RSiO$] units with the bulky substituents R, would possess a much lower chain flexibility, when compared to the poly(dimethylsilixane) chains. The decreased chain flexibility would result in a lower propensity for linear chain formation (thermodynamic reasons). The competition of the two opposite contributions and the chemical structure of the linear and cyclic species at the thermodynamic equilibrium were analyzed.

***Scheme 2.4.*** General reaction scheme for the synthesis of poly(dimethylsiloxane) oligomers with pendant amine groups by anionic ring opening co-equilibration reaction.

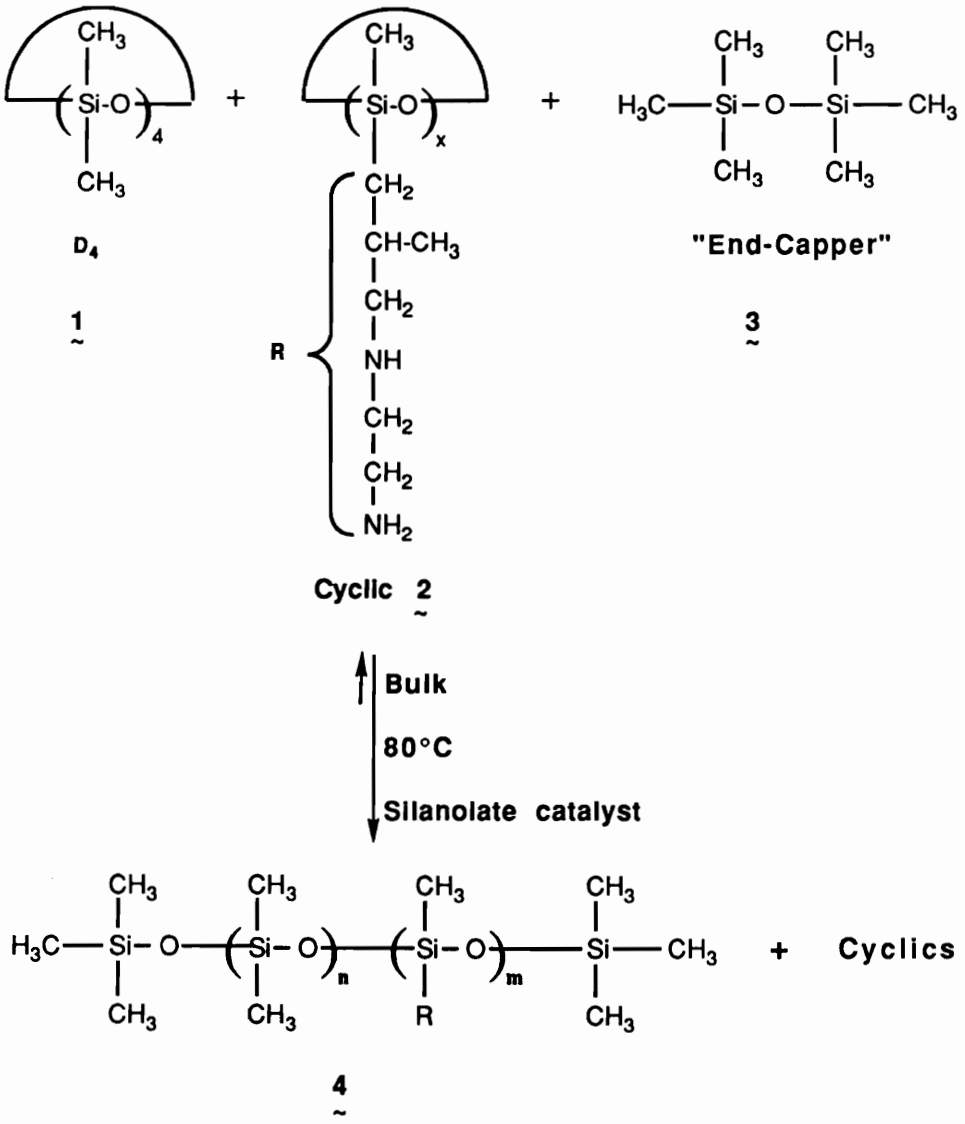

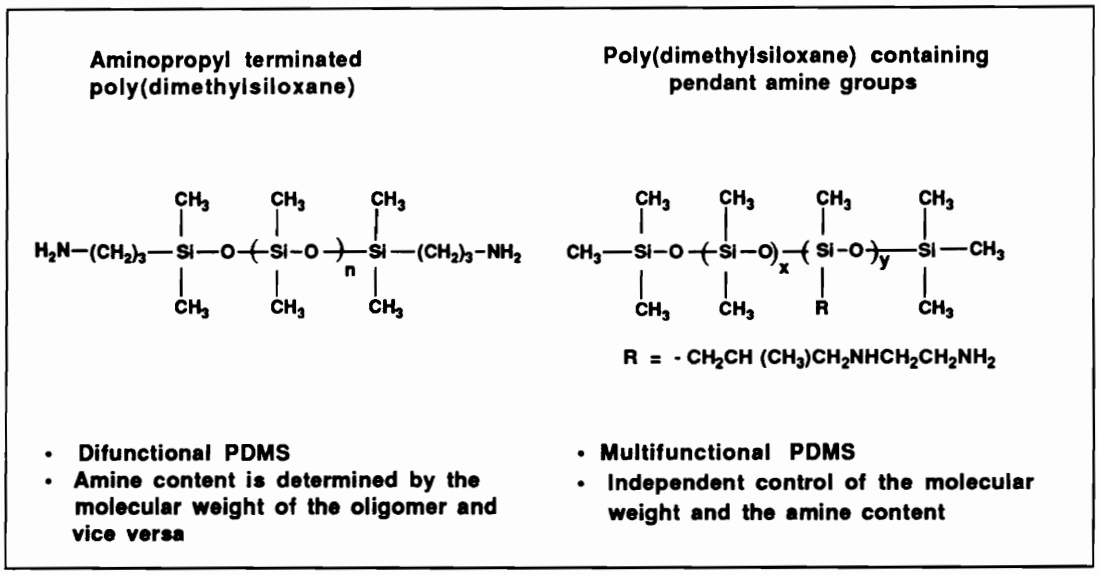


***Figure 2.5.*** Poly(dimethylsiloxane) oligomers with terminal vs pendant amine functionalities-general features.

*4.2. CHARACTERIZATION OF THE CYCLIC MONOMER 2.*

The structure of the cyclic siloxane monomer 2 in which one methyl group on each silicon atom was replaced by the bulky and polar substituent R is given below:

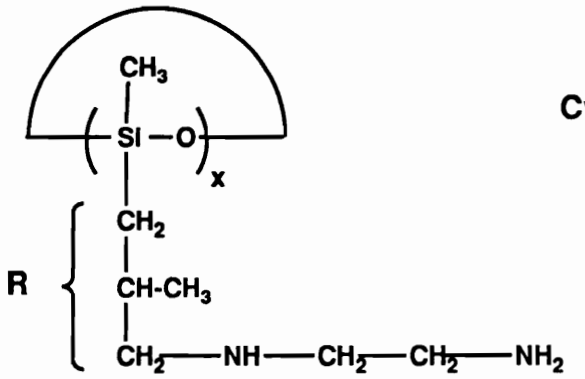


**Cyclic 2**

This siloxane monomer was provided by Dow Corning. The cyclic was synthesized by controlled hydrolysis of the corresponding dimethoxy-organosilane compound $[(OCH_3)_2Si(R)(CH_3)]$. The controlled hydrolysis usually results in a mixture of linear diols and cyclic structures. The cyclics were provided after their separation from the linear species. The size of the cyclic (the value of x) was not initially known. Titration of both primary and secondary amines in the pendant group R resulted in a molecular weight of approximately 174 grams/$[(CH_3)RSiO]$ unit, confirming the above structure. The $^1H$ NMR spectrum in ***Figure 2.6.*** was also consistent with this structure. The $^{29}Si$ NMR spectrum (***Figure 2.7***) contains three main resonances corresponding to three type of Si nuclei, in the following approximate ratio:5% (-15.8 to -16.6ppm), 33% (-20.0 to -20.8 ppm), and 62% (-22.5 to -23.6 ppm). The molecular ions corresponding to x=3, 4, and 5 (six, eight, and ten membered rings, respectively) could be identified in the mass spectra ***(Figure 2.8).*** The combination of the above techniques suggested that the cyclic siloxane monomer 2 corresponded to a mixture of six, eight, and ten member rings, in the approximate molar ratio of 5%, 33%, and 62% respectively.

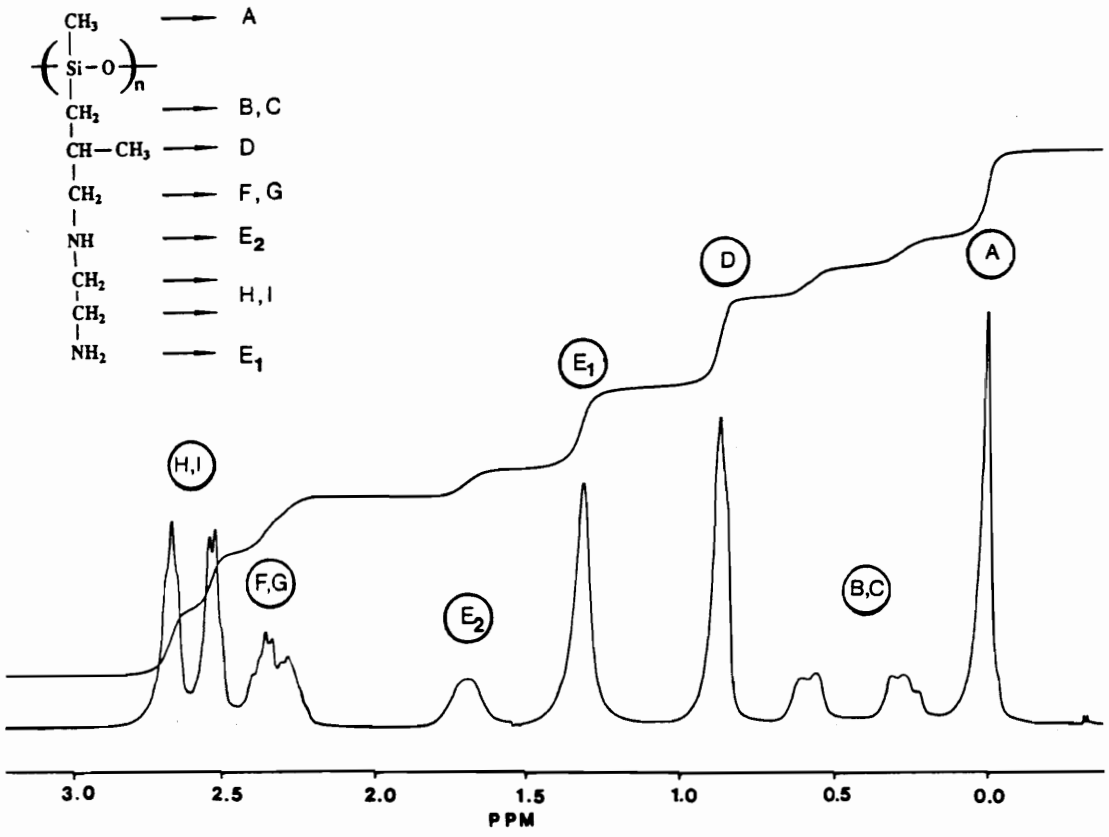


***Figure 2.6.*** $^{1}H$ NMR of the cyclic siloxane monomer (2) with pendant amine groups on silicon.

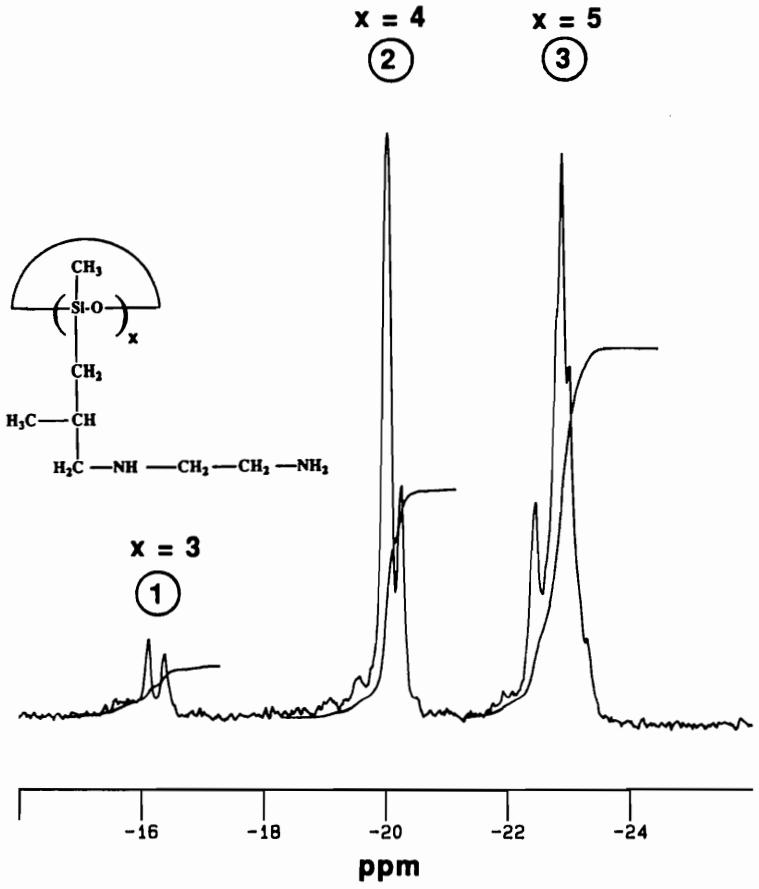


***Figure 2.7.*** $^{29}Si$ NMR of the cyclic siloxane monomer (2) with pendant amine groups on silicon.

| | x = 3<br>6 member ring | x = 4<br>8 member ring | x = 5<br>10 member ring |
|---|---|---|---|
| M | 522 | 696 | 870 |
| M +1 | 523 | 697 | 871 |
| M - 1 | 521 | 695 | 869 |

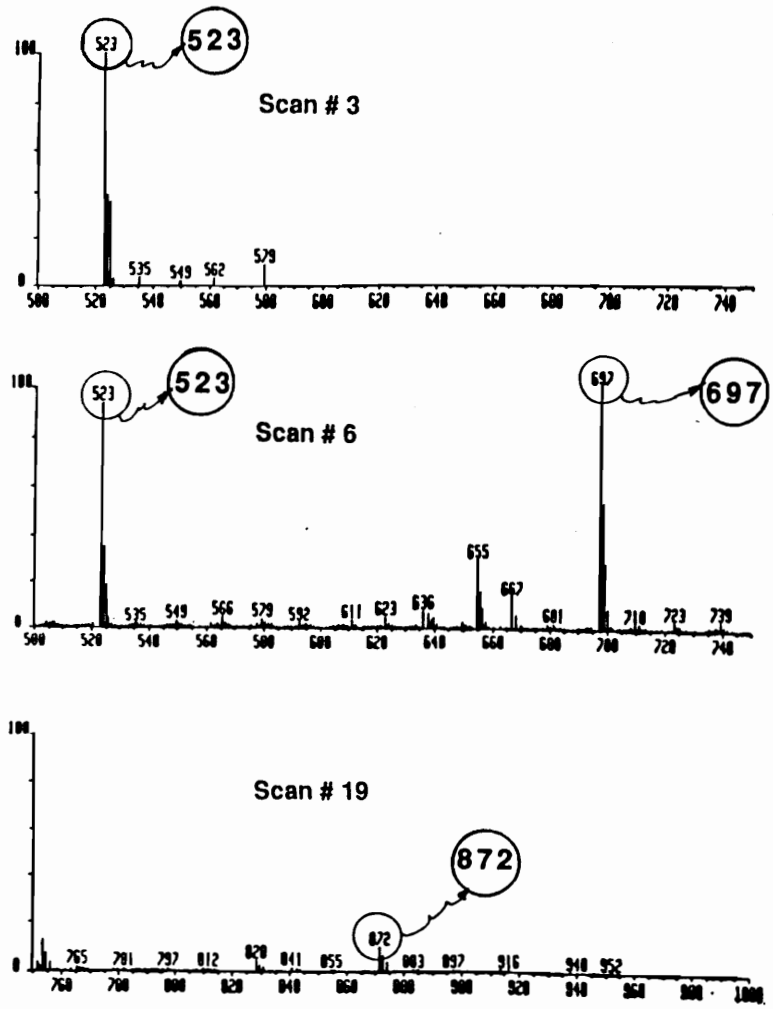


***Figure 2.8.*** Mass spectra of the cyclic siloxane monomer (2) with pendant amine groups on silicon.

*4.3. THERMODYNAMIC VS KINETIC FORCES IN EQUILIBRATION REACTIONS*

A range of number average molecular weights from 3,000 to 10,000 grams/mole was investigated. In this molecular weight range, copolymers with different chemical compositions were synthesized: from low concentrations of $[(CH_3)RSiO]$ units (2 and 3 siloxane units of the type $[(CH_3)RSiO]$ per polydimethylsiloxane chain) to higher concentrations (up to 22 mole percent $[(CH_3)RSiO]$ units).

Two control reactions were also performed, using the same reaction conditions employed for the copolymerization, as described in Chapter 3, Experimental techniques. The first control reaction corresponds to the control equilibration of $D_4$. Upon ring opening of $D_4$ tetramer, highly flexible poly(dimethylsiloxane) chains are generated. The second control reaction corresponds to the equilibration of the new siloxane cyclic, $[(CH_3)RSiO]_x$, under similar conditions. Upon ring opening of the cyclic 2, polysiloxane chains containing the bulky and polar substituent R on each siloxane unit, would be generated.

All of the above equilibration and co-equilibration reactions were continuously monitored by GPC and allowed to proceed until the most probable distribution was achieved, at the thermodynamic equilibrium. The equilibrium was considered to be reached when no further change was observed in the apparent molecular weight, apparent molecular weight distribution, and distribution of species (e.g. linear and cyclic species), as determined by GPC analyses. The range of polysiloxane molecular weights and chemical compositions investigated are summarized in ***Table 2.4,*** along with the corresponding distribution of linear and cyclic species at the thermodynamic equilibrium. The weight percent of the linear and cyclic species at the thermodynamic equilibrium were calculated from GPC traces.

***Table 2.4.*** Distribution of molecular species at thermodynamic equilibrium in base-catalyzed equilibration reactions as a function of molecular weight and chemical composition

| Rxn. No. | Theor. $\langle M_n \rangle$ | Theoretical chemical composition, % $[(CH_3)RSiO]$ units | | Equilibrium distribution, [ weight %] | |
|---|---|---|---|---|---|
| | [g/mol] | Weight % | Mole % | Cyclic species | Linear species |
| **1.** | **5,000** | **0** | **0** | **10** | **90** |
| 2. | 3,000 | 11.6 | 5.3 | 16 | 84 |
| 3. | 5,000 | 7.2 | 3.2 | 16 | 84 |
| 4. | 10,000 | 3.5 | 1.5 | 15 | 85 |
| 5. | 3,000 | 17.4 | 8.2 | 29 | 71 |
| 6. | 5,000 | 10.3 | 4.8 | — | — |
| 7. | 10,000 | 5.2 | 2.3 | 18 | 82 |
| 8. | 3,000 | 40.0 | 22.0 | >95 | <5 |
| 9. | 10,000 | 40.0 | 22.0 | >95 | <5 |
| **10.** | **5,000** | **100** | **100** | **~100** | **~0** |

a). Reaction # 1 is the control equilibration of $D_4$;
b). Reaction # 10 is the control equilibration of the cyclic 2, $[(CH_3)RSiO]_x$;
c). Reactions 2-4 were designed such that the oligomers contain two $[(CH_3)RSiO]$ units per poly(dimethylsiloxane) chain;
d). Reactions 5-7 were designed such that the oligomers contain three $[(CH_3)RSiO]$ units per poly(dimethylsiloxane) chain;

A series of trends for the ratio between the cyclic and the linear species present at the thermodynamic equilibrium, become noticeable. Firstly, it is observed that at thermodynamic equilibrium all co-equilibration reactions (Reactions 2 through 9 ) resulted in a higher concentration of cyclic species, when compared to the control equilibration of the $D_4$ cyclic (Reaction 1). Secondly, at low concentration of $[(CH_3)RSiO]$ units the equilibrium composition was independent of the reaction chemical composition (compare reactions 2,3, and 4) suggesting that random statistics govern the copolymerization process. However, for similar molecular weights, the increase in the concentration of $[(CH_3)RSiO]$ units resulted in a higher percentage of cyclic species at the thermodynamic equilibrium (e.g. reaction 2 vs 5). Thirdly, reaction compositions corresponding to a high concentration of the $[(CH_3)RSiO]$ units with the bulky and polar substituents R on the silicon atom (reactions 8 and 9) resulted in an equilibrium composition in which the cyclic species are highly favored, representing more than 95%, while linear species represent less than 5%. Finally, no ring-chain equilibration was observed to be taking place during the control equilibration of the cyclic 2, $[(CH_3)RSiO]_x$,(reaction no. 10). Instead, a ring-ring redistribution accompanied the equilibration process. This redistribution is depicted in ***Figure 2.9*** which shows the $^{29}Si$ NMR spectra of the cyclic 2 before and after equilibration. The redistribution resulted in a complete disappearance of the highly stressed 6-membered rings (-15.8 to -16.6 ppm), along with an increase in the concentration of the 8-membered rings (-20.2 to -20.8ppm) at the expense of the 10-membered rings (-22.5 to -23.6 ppm). No ring-ring redistribution occured in the absence of equilibration catalyst, as observed by $^{29}Si$ NMR.

All of the above observations indicate that the siloxane units with larger side-groups, $[(CH_3)RSiO]$, show a much higher propensity for cyclization than the dimethyl substituted units, $[(CH_3)_2SiO]$. Such tendency has been reported previously for other systems. For example the weight percent cyclics in high molecular weight equilibrates of cyclosiloxane tetramers with the structure

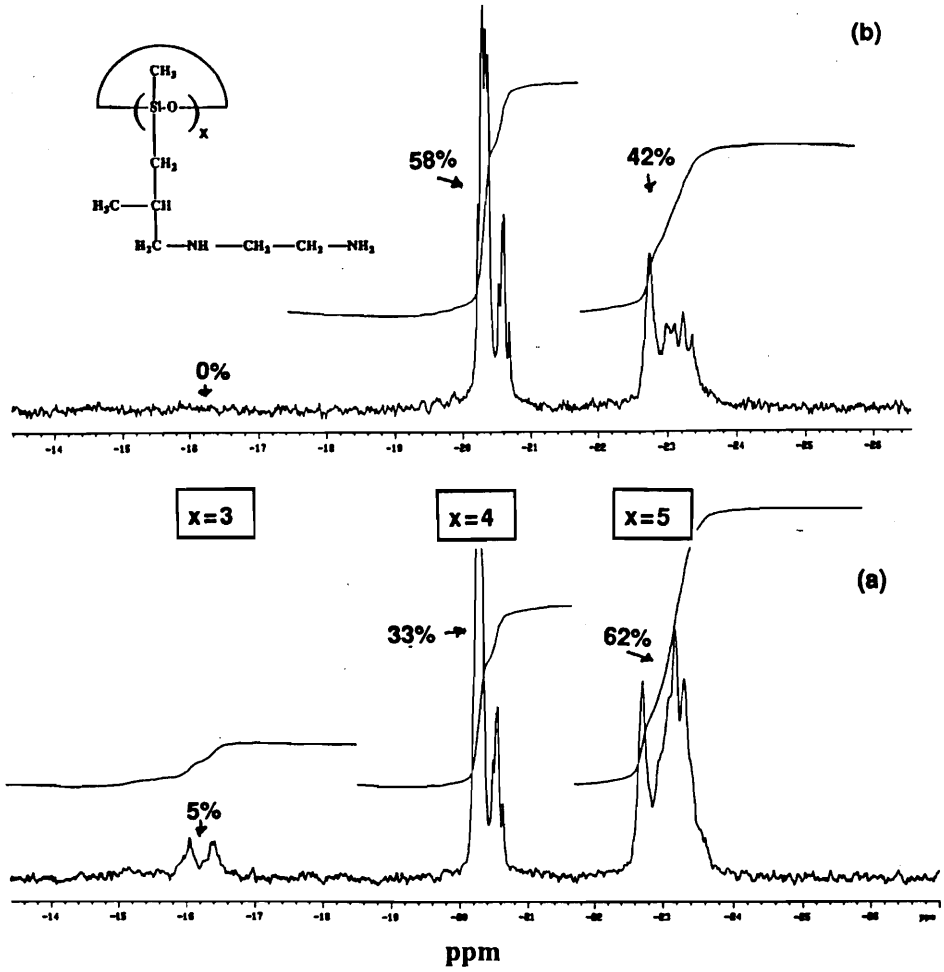


***Figure 2.9.*** $^{29}Si$ NMR spectra of the cyclic siloxane monomer 2, (a) before, and (b) after equilibration (in the presence of silanolate catalyst).

$[R(CH_3)SiO]_4$, was reported to be 12.5, 18.3, 25.8, and 82.7 for R= H, $CH_3$, $CH_3CH_2$, and $CF_3CH_2CH_2$ respectively [273]. The observed dependence of the equilibrium distribution of species on the chemical composition of the oligomers can be attributed to the complex contribution of both kinetic and thermodynamic factors. The Gibbs equation:

$$\Delta G = \Delta H - T\Delta S \qquad (9)$$

must yield a negative free energy change for the general transformation of a cyclic ring to a linear macromolecular chain-like molecule, if the polymerization is to be favored. This change is made up of enthalpy and entropy contributions which along with the reaction temperature determine the sign and magnitude of the free energy [260]. It becomes obvious that the chemical structure of the cyclic ring will affect the free energy of polymerization. Factors such as the size and ring strain associated with the monomer, the type of substituents on the cyclic ring, the geometrical and stereochemical chain isomerism, etc. are important in these processes.

The increase in the ring strain when the methyl groups in cyclosiloxanes are replaced with bulkier substituents R, is expected to favor the ring opening and formation of linear chains. The exothermic enthalpy in this case ($\Delta H<0$) should therefore favor the polymerization process. The experimentally observed shift in thermodynamic equilibrium in favor of cyclics, as the amount of $[(CH_3)RSiO]$ units is increased, is evidently associated with entropic factors.

(1) A first factor favoring cyclization arrives from the decrease in the entropy of linear polysiloxane chains when the methyl groups are replaced with bulkier substituents R. This decrease in entropy can be attributed to the reduced mobility of the segments of the polymer chains [225]. The effect of substituents on the mobility of polysiloxane chains has been investigated in the past by different methods. One way of measuring the degree of mobility of polymer chains is by comparing the unperturbed molecular dimensions with those calculated from free rotation. Such

experiments have been conducted by Lee et al. [299] for polysiloxanes with different substituents. They found that poly(dipropylsiloxane)s have a lower degree of flexibility than poly(dimethylsiloxane)s, and they attributed this decrease in chain mobility to the short range steric interactions between near neighboring units of the chain. These results also fit in with the interpretation given by Flory and co-workers [300,301]. Another way to characterize the flexibility of the polymer chains is to determine the line width vs. temperature dependence in NMR. Lee and co-workers [238] found that the temperature at which line narrowing commences or at which narrow line is attained increases as one of the pendant groups on the polysiloxane chain is changed from H to $CH_3$ to $C_6H_5$. These experimental data indicate that the molecular mobility is dependent on steric effects of the pendant groups and that the mobility decreases in the order $H>CH_3>C_6H_5$. It can be argued, therefore, that the introduction of $[(CH_3)RSiO]$ units containing the bulky substituent R into the poly(dimethylsiloxane) chains would similarly restrict the chain mobility and hence contribute to the decrease in the configurational entropy of the polysiloxane linear chains (decrease of $\Delta S$ term in equation 8). The result would be an increased tendency towards cyclization, at the expense of linear species, which was in fact experimentally observed.

(2) In co-equilibration reactions there is a second contributing factor to the shift of thermodynamic equilibrium in favor of cyclics and this is the increase in the entropy of the cyclic species as the equilibration proceeds. ***Figure 2.10*** contains typical HPLC traces for an initial and an equilibrated reaction mixture (top trace and bottom trace, respectivelly) for a co-equilibration reaction in which the cyclic species were favored at thermodynamic equilibrium. The HPLC traces reveal that a high variety of cyclic species are generated during these co-equilibration reactions, resulting in an increase in the entropy of the cyclics. This contributes to a further decrease in the $\Delta S$ term in equation 8, and a shift of the thermodynamic equilibrium in favor of cyclics.

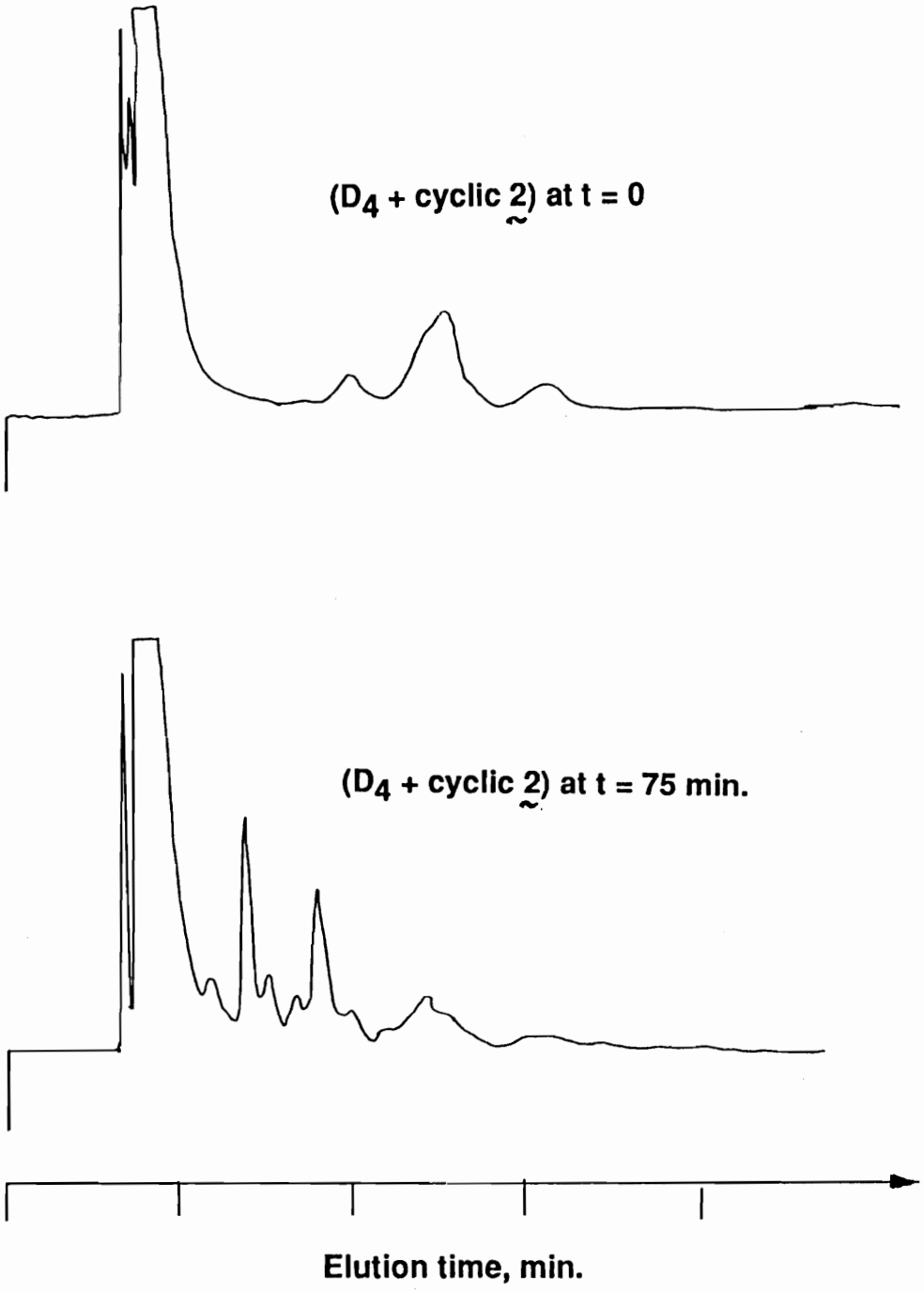


***Figure 2.10.*** HPLC traces for a co-equilibration reaction mixture, before and after equilibration (chemical composition favoring cyclic species at thermodynamic equilibrium).

GPC analysis provided an insight into the competition between kinetic and thermodynamic contributions during equilibration polymerization reactions. ***Figure 2.11***. and ***Figure 2.12***. show GPC traces as a function of equilibration time for a typical thermodinamically favored co-equilibration and a control equilibration of $D_4$, respectively. In both cases a continuous redistribution between cyclic and linear species was observed throughout the equilibration process, until a thermodynamic equilibrium was reached, at which the linear species predominate. This behavior was characteristic for the equilibration of $D_4$, and for all co-equilibration reactions containing up to 8.2 mole percent [$(CH_3)RSiO$] units (reactions 2 through 7, Table 2.4). For these compositions the increase in the entropy of the system was provided by the formation of linear polysiloxane chains with high mobility (high configurational entropy) which represent the favored species at thermodynamic equilibrium.

***Figure 2.13***, on the other hand, shows GPC traces as a function of reaction time for a co-equilibration reaction in which cyclic species were favored at thermodynamic equilibrium. These traces indicate that in the early stages of the reaction high molecular weight linear species were produced. However, as the equilibration proceeded, the initial kinetic control that promoted polymerization of the siloxane cyclics was negated, and the thermodynamic driving force became predominant. In these systems, the driving force was provided by the increase in the entropy of the cyclic species, as a result of formation of a wide variety of cyclics of different size, chemical composition, and stereochemistry. For these compositions the cyclic species were therefore favored at the thermodynamic equilibrium. This behavior was characteristic for the co-equilibration reactions in which up to 22 mole percent [$(CH_3)RSiO$] units were incorporated (reactions 8 and 9).

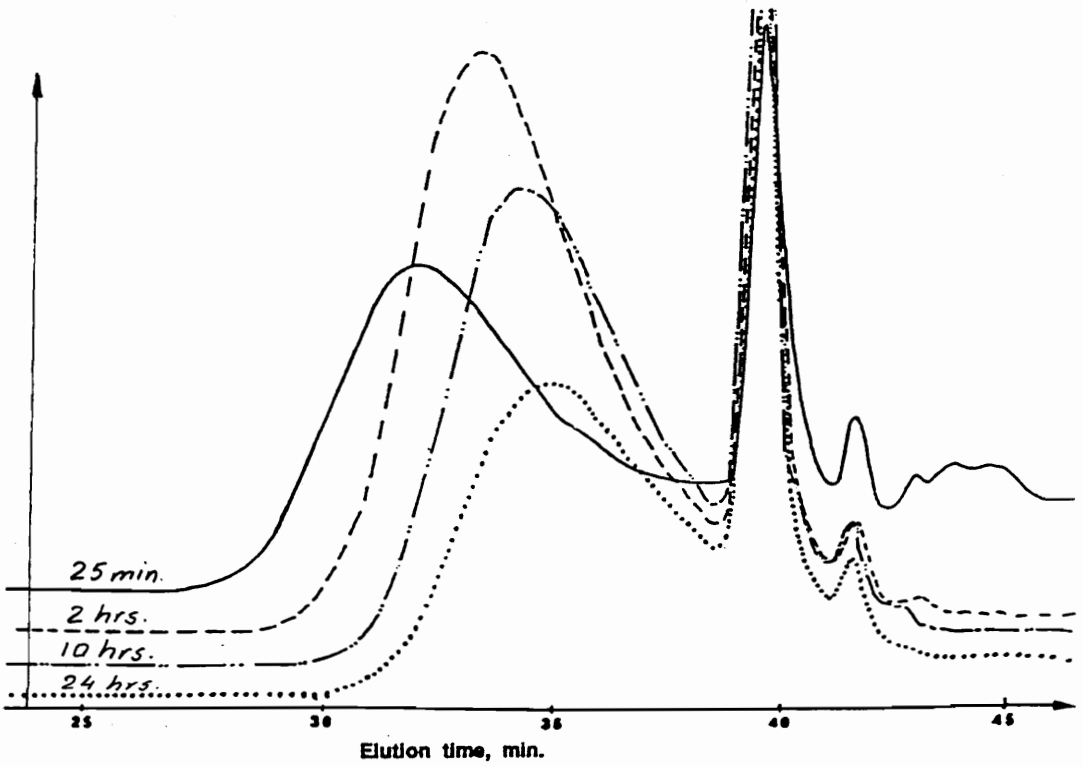


***Figure 2.11.*** GPC traces as a function of time for a co-equilibration reaction in which linear species are favored at thermodynamic equilibrium.

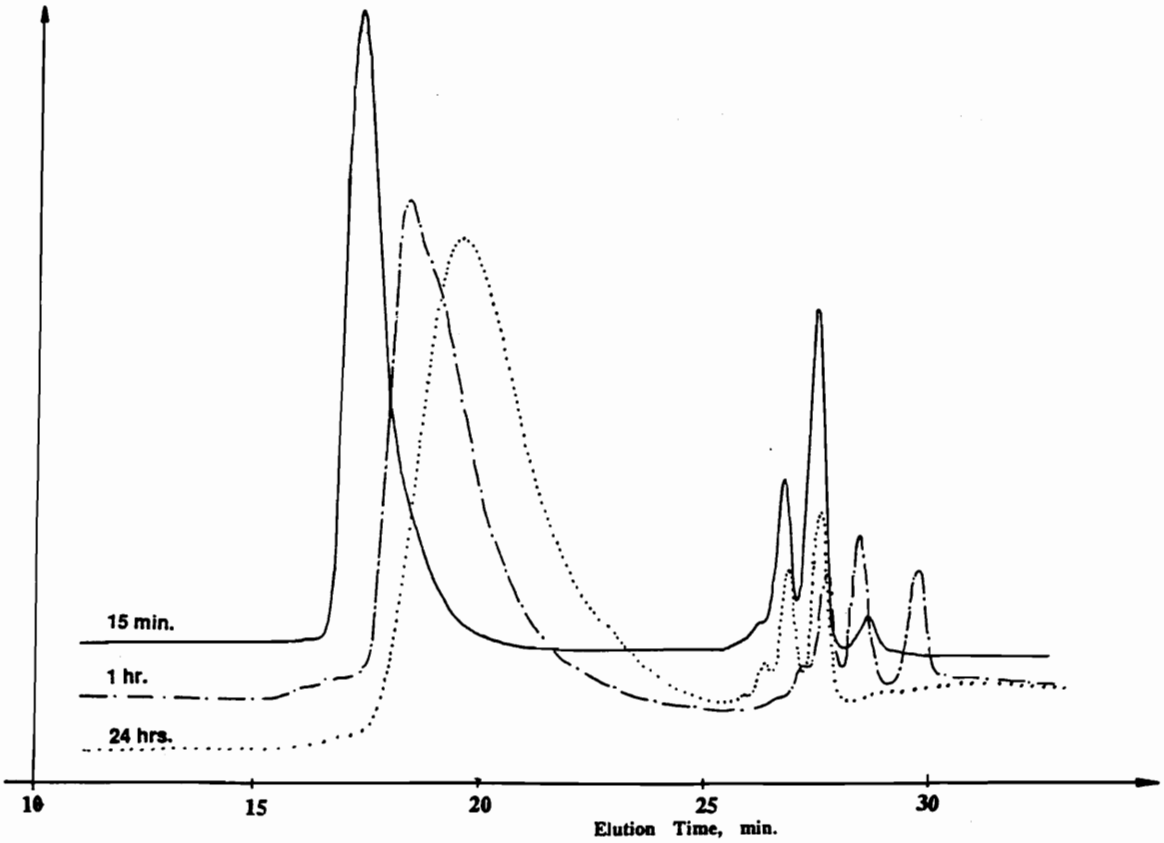


***Figure 2.12.*** GPC traces as a function of time for a control equilibration of $D_4$.

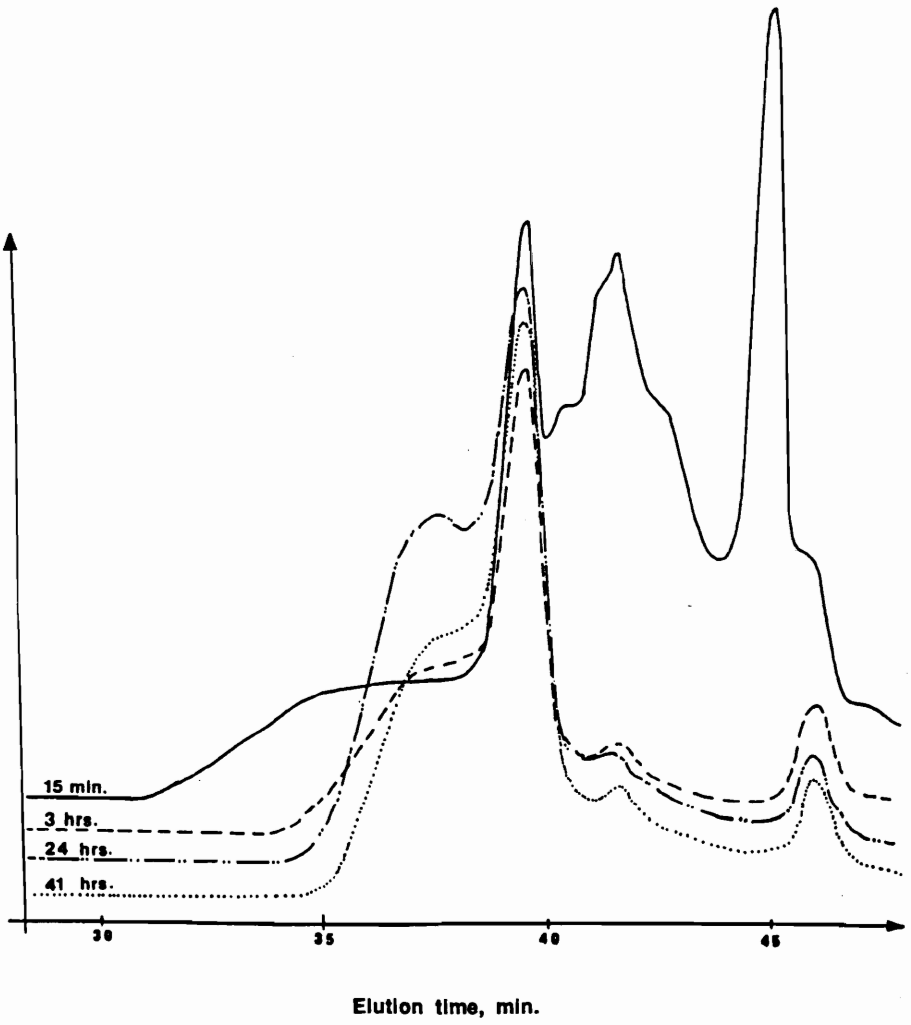


***Figure 2.13.*** GPC traces as a function of time for a co-equilibration reaction in which cyclic species are favored at thermodynamic equilibrium.

*4.4. CONTROL OF MOLECULAR WEIGHT AND CHEMICAL COMPOSITION*

For co-equilibration reactions in which the linear species were thermodinamically favored, it was possible to obtain a stable poly(dimethylsiloxane) oligomer with pendant amine groups on the silicon atoms, free of cyclics. The oligomers resulted in a Gaussian distribution of molecular sizes, as shown by the GPC traces in ***Figure 2.14***. The number average molecular weight , $<M_n>$, of the polysiloxane oligomers was determined by $^{29}Si$ NMR from the ratio of the terminal to the internal silicon atoms, as shown in ***Figure 2.15*** These results are summarized in ***Table 2.5.*** The molecular weight control was satisfactory in these systems, according to the $^{29}Si$ NMR measurements. However, this is not a very sensitive technique, especially at higher molecular weights, and other techniques are required in order to address the question of molecular weight control in more detail.

GPC was investigated as an alternative method for measurement of the molecular weight. Poly(dimethylsiloxane)s (PDMS) with narrow molecular weight distributions (prepared by living polymerization of $D_3$, [5]) were used as the GPC standards. However, according to PDMS standards, the molecular weight of the copolymers $[(CH_3)_2SiO]_x[(CH_3)RSiO]_y$ was consistently and considerably higher than the theoretical molecular weight, or the molecular weight measured by $^{29}Si$ NMR. This is shown in ***Figure 2.16*** in which two GPC calibration curves were constructed using the PDMS standards and the siloxane copolymers synthesized above. In order to construct the second curve, the elution volume in ml for each of the copolymer was measured at the peak maxima and considered to correspond to the number average molecular weight determined by $^{29}Si$ NMR. It can be clearly seen that in general the siloxane copolymers give a lower retention time when compared to poly(dimethylsiloxane) oligomers at the equivalent degree of polymerization. Similar data were published by Lee and Emerson for poly(dipropylsiloxane) vs poly(dimethylsiloxane), as indicated in ***Figure 2.17*** reproduced from reference 299.

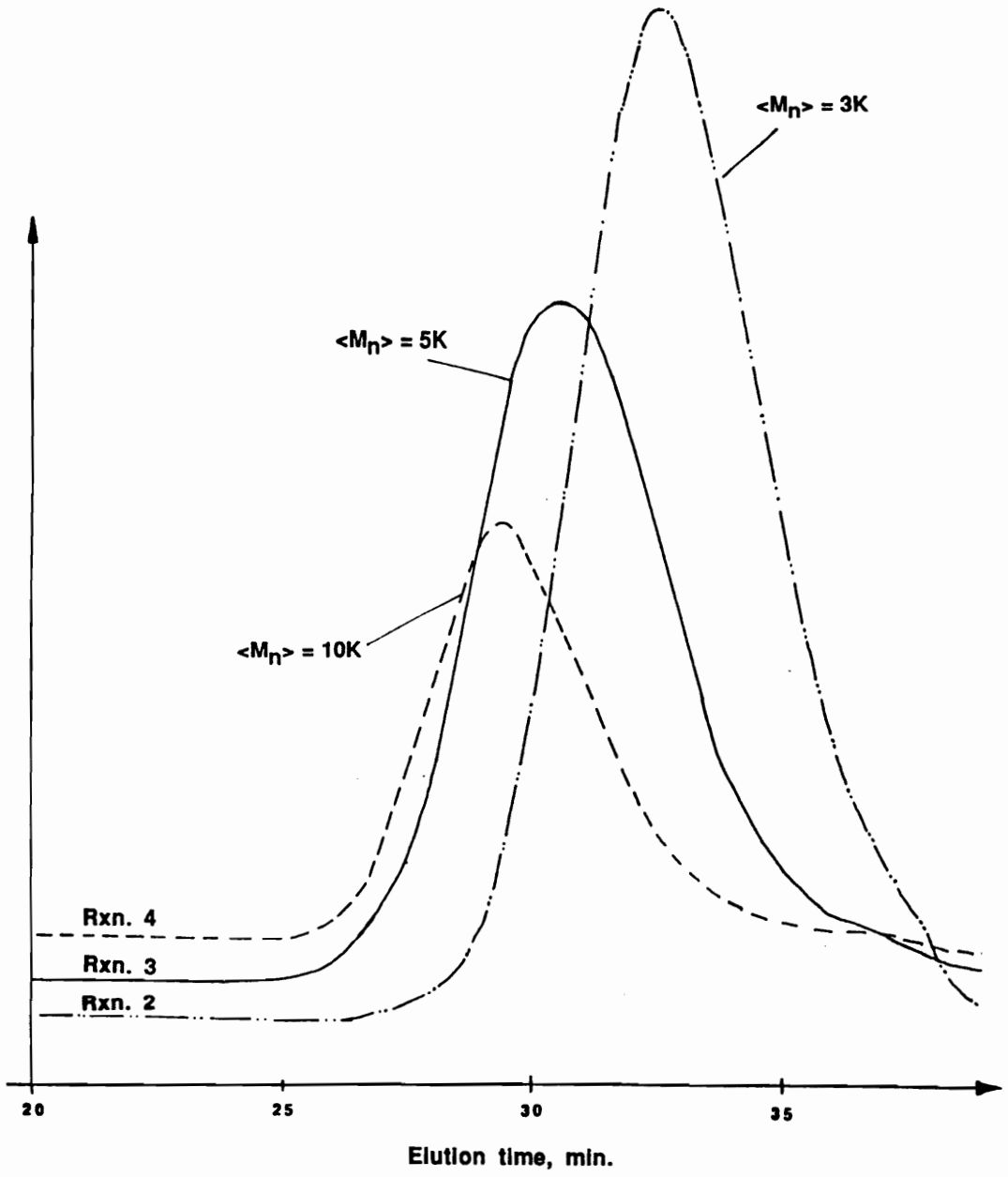


***Figure 2.14*** Typical GPC traces for $[(CH_3)_2SiO]_x[(CH_3)RSiO]_y$ copolymers, after vacuum stripping.

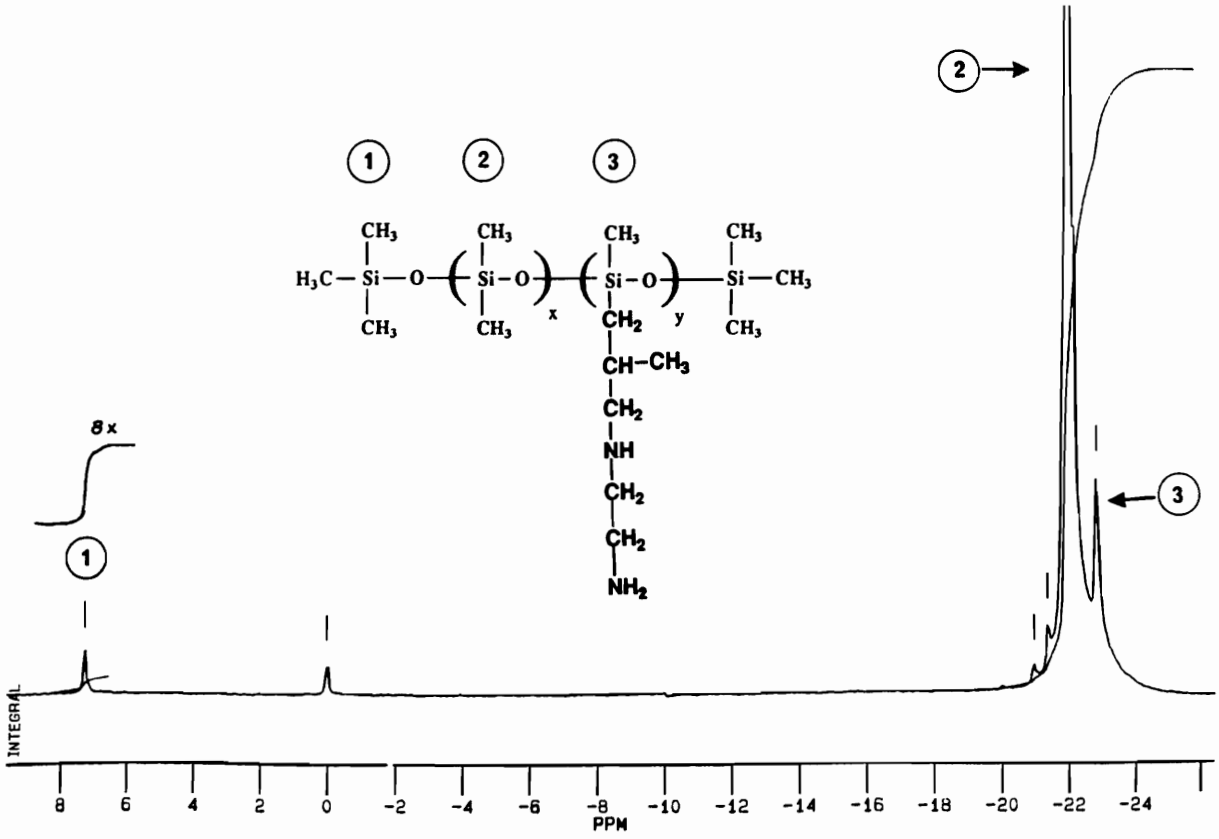


***Figure 2.15.*** Typical $^{29}Si$ NMR spectrum for a $[(CH_3)_2SiO]_x[(CH_3)RSiO]_y$ copolymer, after vacuum stripping.

***Table 2.5***. Theoretical vs experimental number average molecular weight $<M_n>$ for polysiloxane oligomers.

| Rxn. No. | Number average molecular weight, $<M_n>$, [g/mole] | |
|---|---|---|
| | Theoretical | Experimental (from $^{29}Si$ NMR) |
| 1. | 5,000 | – |
| 2. | 3,000 | 4,300 |
| 3. | 5,000 | 6,600 |
| 4. | 10,000 | 8,800 |
| 5. | 3,000 | 4,400 |
| 6. | 5,000 | – |
| 7. | 10,000 | 9,700 |
| 8. | 3,000 | >95% cyclics |
| 9. | 10,000 | >95% cyclics |
| 10. | 5,000 | no linear species |

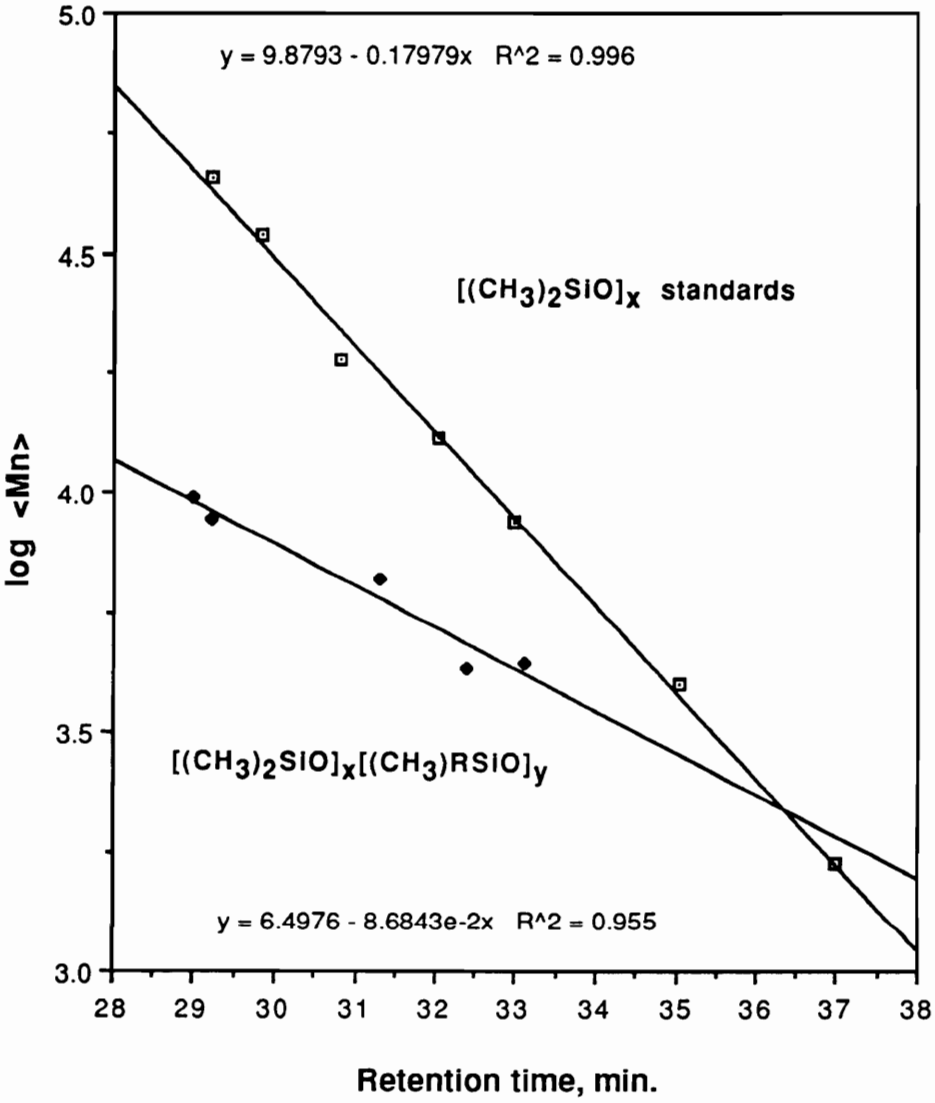


***Figure 2.16.*** GPC calibration curves constructed with: (1) $[(CH_3)_2SiO]_x$ PDMS with narrow molecular weight distribution; (2) $[(CH_3)_2SiO]_x[(CH_3)RSiO]_y$ copolymers containing 1.5 to 8.2 mole percent $[(CH_3)RSiO]$ units (Reactions 2-7).

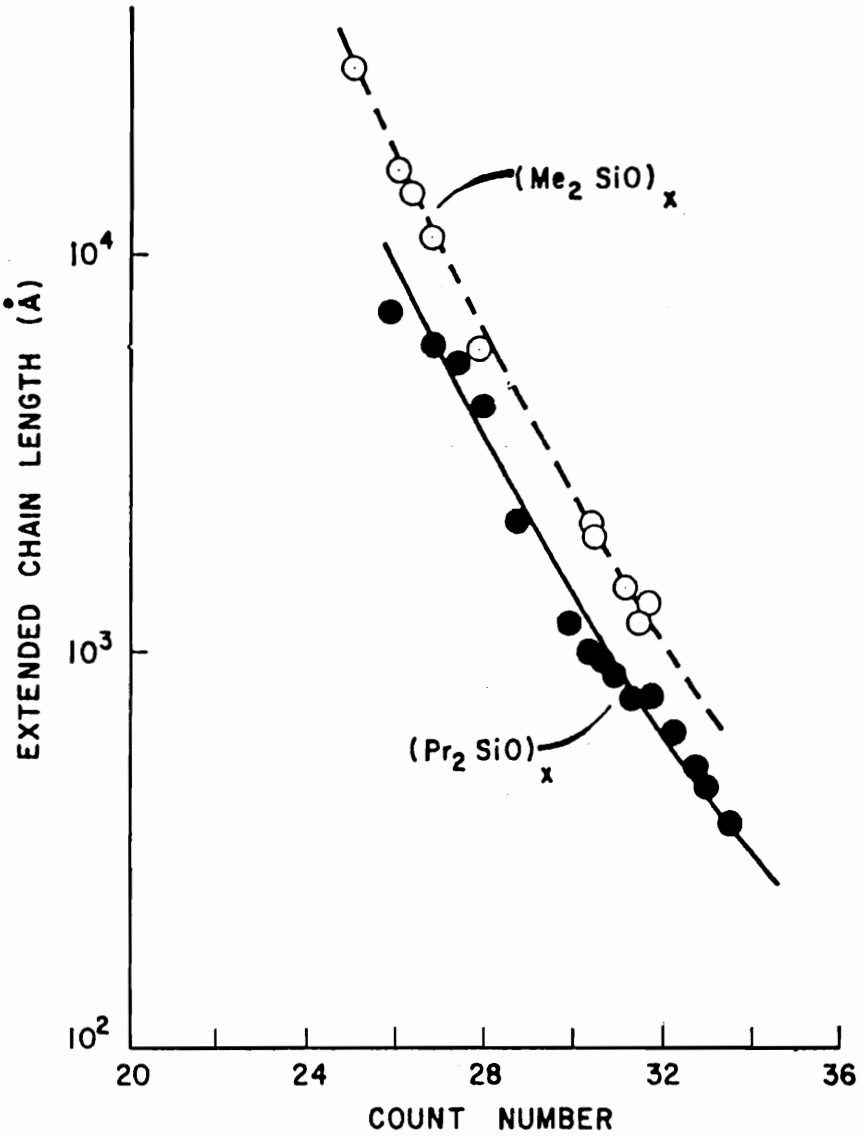


***Figure 2.17.*** GPC calibration curves for poly(dipropylsiloxane) and poly(dimethylsiloxane) [299].

The data in Figure 2.16 were interpreted by Lee and Emerson as an indication that the molecular dimensions (hydrodynamic volume) of poly(dipropylsiloxane) are greater than those of poly(dimethylsiloxane). Similarly, it can be argued that the copolymers containing the [$(CH_3)$RSiO] units have a higher hydrodynamic volume than the poly(dimethylsiloxane) with comparable degree of polymerization, indicating that the extension of the copolymer chains is appreciably larger than that of poly(dimethylsiloxane). This, again, is in agreement with the lower degree of flexibility resulting from the steric factors mentioned previously for copolymers containing the [$(CH_3)$RSiO] units. This is also in agreement with the increased propensity for cyclization, which was experimentally observed for these siloxane units.

The efficiency of incorporation of [$(CH_3)$RSiO] units into the poly(dimethylsiloxane) chains was determined by comparing the experimental chemical compositions for both cyclic and linear species at thermodynamic equilibrium with the theoretical composition. The chemical composition was determined from $^{29}$Si NMR or, more accurately, by titrating the amine content, and the results are summarized in ***Table 2.6.*** A relatively good agreement between the theoretical and experimental compositions was observed for both cyclic and linear species, in the range of molecular weights and chemical compositions investigated by reactions 2 through 7 (low level of [$(CH_3)$RSiO] units). These observations indicate that in the above mentioned composition range the redistribution via equilibration reactions is mainly based on random statistics. However, slightly higher concentrations of [$(CH_3)$RSiO] units were consistenly observed for the cyclic species, indicating an increased preference of these units for cyclization.

***Table 2.6.*** Theoretical vs experimental chemical compositions for siloxane copolymers $[(CH_3)_2SiO]_x[(CH_3)RSiO]_y$.

| Rxn. No. | Chemical composition, mole % $[(CH_3)RSiO]$ units | | | |
|---|---|---|---|---|
| | Theoretical[a] | Experimental | | |
| | | Linear species | | Cyclic species |
| | | $^{29}Si$ NMR | Titration | Titration |
| 1. | 0 | – | – | – |
| 2. | 5.3 | 5.6 | 5.2 | 6.1 |
| 3. | 3.2 | 5.9 | 3.5 | 4.0 |
| 4. | 1.5 | 2.4 | 1.4 | 1.7 |
| 5. | 8.2 | 9.3 | 7.8 | 10.5 |
| 6. | 4.8 | 5.2 | 5.1 | 6.8 |
| 7. | 2.3 | 3.3 | 2.3 | 2.7 |
| 8. | 22.0 | b | b | c |
| 9. | 22.0 | b | b | c |
| 10. | 100 | No linear species were formed | | |

a). Calculated from the charged components

b). <5% linear species

c). > 95% cyclic species

*CHAPTER 5*

# *CONCLUSIONS*

Base-catalyzed co-equilibrations of $D_4$ with a new cyclic siloxane monomer containing aliphatic amine substituents on silicon atoms have been conducted for a relatively broad range of molecular weights and chemical compositions. The equilibrium distribution of the molecular species proved to be independent of molecular weight, in the range investigated (3,000 to 10,000 g/mole) and at low concentrations of $[(CH_3)RSiO]$ units (lower than 8.2 mole percent). However, the equilibrium distribution was highly dependent on the concentration of the siloxane units with bulky substituents on the silicon atoms. The increase in the concentration of such units resulted in a much higher level of cyclic species at thermodynamic equilibrium. For example when the siloxane units containing the bulky substituents R represented 22 mole percent, excessively high concentration of cyclic species (>95%) were obtained at the thermodynamic equilibrium for all the molecular weights investigated. This demonstrated an increased propensity for cyclization of the $[(CH_3)RSiO]$ units when compared to $[(CH_3)_2SiO]$ units.

Furthermore, no ring-chain redistribution was observed during the equilibration reaction of the cyclic 2, $[(CH_3)RSiO]_x$,indicating that the formation of linear polysiloxane chains in which each siloxane unit would contain the bulky substituent R is highly unfavorable, due to reduced chain flexibility as a result of increased steric interactions between near neighboring groups. However, under base-catalyzed conditions, a ring-ring redistribution was observed during which the strained 6-membered rings completely disappeared while the concentration of the 8-membered rings increased at the expense of the 10-membered rings. Under these conditions, the 8-membered rings became predominant (58% 8-membered rings and 42% 10-membere rings

respectively). This ring-ring redistribution was not observed at the equilibration temperature (80°C) in the absence of equilibration catalysts, even after relatively long times (>24hours).

The replacement of a methyl group on the silicon atom with the bulky substituent R is expected to increase the ring strain, therefore to favor polymerization. The experimentally observed propensity for cyclization for the co-equilibration reactions, as the percentage of such units was increased is, most probably, associated with entropic factors.

In the favorable range of chemical compositions (up to 8.2 mole percent [$(CH_3)RSiO$] units) polysiloxane oligomers of controlled molecular weight and chemical compositions, containing pendant amine groups, have been synthesized. In these oligomers, the amine content and the molecular weights were independently controlled. The amine content was determined by the relative ratio of the two cyclics in the co-equilibration reactions.whereas the molecular weight was controlled by the ratio of the cyclic monomers to the siloxane dimer or endcapper. Multifunctional poly(dimethylsiloxane) oligomers containing amine functionalities, in which the amine content and the molecular weights can be independently controlled, could be of interest for polysiloxanes used in crosslinked membranes or in system modifications such as the development of toughened networks.

*CHAPTER 6*

*SUGGESTED FUTURE STUDIES*----------

During the course of this research, the effect of the substituents at silicon atoms in cyclic siloxane monomers on the thermodynamic equilibrium in ring opening equilibration reactions has been explored. However, many fundamental aspects merit further investigation. These include:

(1) A study of the equilibrium distribution of species as a function of temperature, for established chemical compositions; This would allow to determine if the enthalpic factors are important at the equilibrium stage (It is believed that enthalpic factors play a role in the initial stage of the reaction).

(2) Determine the composition and microstructure of cyclic and linear species at different equilibration times, using quantitative $^{29}Si$ NMR. This would allow to determine how kinetic factors affect microstructure in the system investigated; it may also provide information on the possibility to control the chemical composition and microstructure of the linear chains through kinetic factors.

(3). The flexibility of the siloxane units containing the bulky substituent on the silicon atom [$(CH_3)RSiO$] can be determined by a temperature-dependent NMR study [238]. This study would help in understanding the extent to which such bulky substituents hinder the free rotation about siloxane bond, by comparison to dimethylsubstituted siloxane units [$(CH_3)_2SiO$] for which literature data are available [238].

# *APPENDIX 1.1*

A typical work-sheet from the deconvolution of the glass peak in $^{29}Si$ NMR of the $SiO_2$ gels listed in Table 1.10 is shown below. For the five samples listed in this table the RMS Error of the normalized integral areas ranged from 2.5 to 4.0 %.

RMS ERROR = 3.92 %

SUMMARY OF CALCULATED LINES

| LINE NUMBER | SHIFT (PPM) | POSITION (HZ) | WIDTH (HZ) | NORMALIZED HEIGHT | NORMALIZED INTEGRAL | TYPE |
|---|---|---|---|---|---|---|
| $Q^2-1$ | 414.04 | 10923.00 | 476.39 | 17.25 | 14.87 | GAUSS |
| $Q^3-2$ | 405.37 | 10406.49 | 401.44 | 71.57 | 51.99 | GAUSS |
| $Q^4-3$ | 396.61 | 9884.64 | 552.61 | 100.00 | 100.00 | GAUSS |

RMS ERROR = 3.99 %

SUMMARY OF CALCULATED LINES

| LINE NUMBER | SHIFT (PPM) | POSITION (HZ) | WIDTH (HZ) | NORMALIZED HEIGHT | NORMALIZED INTEGRAL | TYPE |
|---|---|---|---|---|---|---|
| $Q^2-1$ | 414.11 | 10927.58 | 476.39 | 15.57 | 14.14 | GAUSS |
| $Q^3-2$ | 405.37 | 10406.49 | 438.28 | 67.13 | 56.08 | GAUSS |
| $Q^4-3$ | 396.32 | 9867.10 | 524.67 | 100.00 | 100.00 | GAUSS |

RMS ERROR = 2.64 %

SUMMARY OF CALCULATED LINES

| LINE NUMBER | SHIFT (PPM) | POSITION (HZ) | WIDTH (HZ) | NORMALIZED HEIGHT | NORMALIZED INTEGRAL | TYPE |
|---|---|---|---|---|---|---|
| $Q^2-1$ | 413.77 | 10906.98 | 431.93 | 14.77 | 12.10 | GAUSS |
| $Q^3-2$ | 404.99 | 10383.61 | 429.39 | 67.46 | 54.94 | GAUSS |
| $Q^4-3$ | 396.04 | 9850.31 | 527.21 | 100.00 | 100.00 | GAUSS |

RMS ERROR = 3.92 %

SUMMARY OF CALCULATED LINES

| LINE NUMBER | SHIFT (PPM) | POSITION (HZ) | WIDTH (HZ) | NORMALIZED HEIGHT | NORMALIZED INTEGRAL | TYPE |
|---|---|---|---|---|---|---|
| $Q^2-1$ | 414.04 | 10923.00 | 476.39 | 17.25 | 14.87 | GAUSS |
| $Q^3-2$ | 405.37 | 10406.49 | 401.44 | 71.57 | 51.99 | GAUSS |
| $Q^4-3$ | 396.61 | 9884.64 | 552.61 | 100.00 | 100.00 | GAUSS |

RMS ERROR = 2.47 %

SUMMARY OF CALCULATED LINES

| LINE NUMBER | SHIFT (PPM) | POSITION (HZ) | WIDTH (HZ) | NORMALIZED HEIGHT | NORMALIZED INTEGRAL | TYPE |
|---|---|---|---|---|---|---|
| $Q^2-1$ | 413.79 | 10908.51 | 444.63 | 9.38 | 6.62 | GAUSS |
| $Q^3-2$ | 405.83 | 10433.96 | 397.63 | 40.40 | 25.49 | GAUSS |
| $Q^4-3$ | 396.99 | 9906.77 | 630.11 | 100.00 | 100.00 | GAUSS |

The effect of this error on the calculated conversion values is highest when it affects the measurement of the area associated with $Q^4$ species, since these species represent the major component (>50%) and have the highest contribution to the extent of conversion. A sample calculation to determine the maximum effect of this error on the calculated extent of conversion will be given for three situations:

**RMS ERROR = 4%** (use data from line 2 in the above work-sheet)

**1). No error was associated with the estimation of the integral area:**

| | Area (measured) | Area +0 %error | % $Q^i$ | $^*N_r$ |
|---|---|---|---|---|
| $Q^2$ | 14.14 | 14.14 + 0% | 8.3 | 16.6 |
| $Q^3$ | 56.08 | 56.08 + 0% | 33.0 | 99.0 |
| $Q^4$ | 100.0 | 100.0 + 0% | 58.7 | 234.6 |
| Total | | 170.48 | | 350.2 |

**% Conversion = 350.2/400 • 100 = 87.5%**

**2). The area corresponding to the integral associated with $Q^4$ species was overestimated by 4%:**

| | Area (measured) | Area + 4%error | % $Q^i$ | $^*N_r$ |
|---|---|---|---|---|
| $Q^2$ | 14.14 | 14.14 + 0% | 8.2 | 16.2 |
| $Q^3$ | 56.08 | 56.08 + 0% | 32.2 | 96.6 |
| $Q^4$ | 100.0 | 100.0 + 4% | 59.7 | 238.8 |
| Total | | 174.22 | | 351.6 |

**% Conversion = 351.6/400 • 100 = 87.9%**

3). **The area corresponding to the integral associated with $Q^4$ species was underestimated by 4%**

| | Area (measured) | Area - 4%error | $\%Q^i$ | $^*N_r$ |
|---|---|---|---|---|
| $Q^2$ | 14.14 | 14.14 - 0% | 8.5 | 17.0 |
| $Q^3$ | 56.08 | 56.08 - 0% | 33.7 | 96.6 |
| $Q^4$ | 100.0 | 100.0 - 4% | 57.8 | 231.2 |
| Total | | 166.22 | | 344.8 |

**% Conversion = 344.8/400 • 100 = 86.2%**

$^*N_r$ in the above calculations represents the number of reacted functional groups in 100 repeat units, as defined in Chapter 4, Section 4.1.3.1. The maximum reacted functional groups per 100 units is 400 (four functional groups per repeat unit).

**The maximum error associated with in the calculated conversion values is:**

**87.9-86.2=1.7 (±0.9%)**

## *APPENDIX 1.2*

A sample calculation for the initial and final composition of a PSX-$SiO_2$ hybrid is given below. The way the molecular weight was defined for each component, for the initial and final composition is also explained. The calculations are demonstrated for 100 g initial weight and an initial chemical composition of 50:50 weight percent PSX:TMOS. The values may be scaled accordingly for any initial reaction size and/or chemical composition.

***Initial composition:***

| Material | Molec. weight* [grams/mole] | Weight, g. (Charged) | No. Moles | Weight% **(Initial)** | Mole% |
|---|---|---|---|---|---|
| TMOS | 152.2 | 50.0 | 0.3285 | **50** | 32.7 |
| PSX | 74 | 50.0 | 0.6756 | **50** | 67.3 |
| Total | | 100.0 | 1.0041 | | |

* For the alkoxide component the molecular weight is defined as the molar mass of the TMOS (before reaction); For the PSX component, the molecular weight is defined as the molar mass of the repeat unit as shown below:

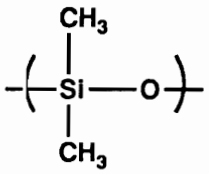

**M.W.=74 g/mole repeat unit**

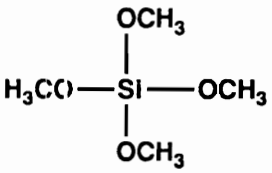

**M.W.=152.2 g/mole**

***Final composition:***

| Material | M W ** | Weight, grams | | No. Moles | Weight% | |
|---|---|---|---|---|---|---|
| Mole% | | | | | | |
| | [g/mole] | Charged | Final | | **(Final)** | |
| $SiO_2$ | 152.2 (60) | 50.0 | 19.7 | 0.3285 | **28.3** | 32.7 |
| PSX | 74 | 50.0 | 50.0 | 0.6756 | **71.7** | 67.3 |
| Total | | 100.0 | 69.7 | 1.0041 | | |

** For the alkoxide component two molecular weights were defined for the calculation of the initial and final compositions:

(1) The molar mass of the TMOS (152.2 g/mole) was used to calculate the number of units of alkoxide component in the hybrid; The number of moles does not change upon reaction. What changes is the molar mass of the repeat unit of the alkoxide component due to the elimination of 4 moles of $CH_3OH$ per TMOS molecule during the condensation reactions. Therefore, a new molar mass was defined for the building unit in the reacted (final) hybrid,

(2) The molecular weight of the ($SiO_2$) building block (60 g/mole) was used to calculate the final weight of the TMOS component in the reacted hybrid.:

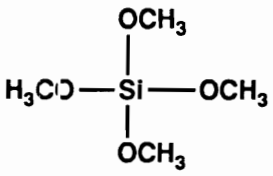

**M.W.=152.2 g/mole**

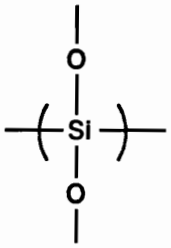

**M.W.= 60 g/mole building unit**

For the PSX component, the molecular weight is defined as the molar mass of the repeat unit, as explained for the calculation of the initial composition.

According to the above sample calculation, a reaction mixture containing initially 50% TMOS by weight will result in a hybrid with approximatelly 33 % of the glass component ($SiO_2$) in the fully reacted sample. Therefore, the use of final composition more suggestively describes the nature of the hybrid.

# *APPENDIX 1.3*

A typical work-sheet from the integration of the $^{29}Si$ NMR spectrum of a PSX-$SiO_2$ gel (as the spectrum shown in Figure 1.44) is attached below. The two values (100.532 and 389.802) correspond to the integral area of the PSX peak (at approximatelly -21ppm) and glass peak (-90 to -120ppm), respectively.

```
 -1.2202  -36.1407 AREA =    100.532 ⟶ PSX
-77.0008 -139.2638 AREA =    389.802 ⟶ SiO2
```

The error in the measured integral for the two peaks is assumed to be approximatelly 5%. A sample calculation to determine the maximum effect of this error on the calculated chemical composition is shown for four situations:

**1). No error was associated with the estimation of the integral areas:**

| | Area (measured) | Area +0 %error | Composition,mole % |
|---|---|---|---|
| PSX | 100.5 | 100.5 + 0% | **20.5** |
| $SiO_2$ | 389.8 | 389.8 + 0% | **79.5** |
| **Total** | | **490.3** | |

**2). The area corresponding to the PSX species was overestimated by 5%:**

| | Area (measured) | Area +5 %error | Composition,mole % |
|---|---|---|---|
| PSX | 100.5 | 100.5 + 5% = 105.5 | **21.3** |
| $SiO_2$ | 389.8 | 389.8 + 0% = 389.8 | **78.7** |
| **Total** | | **495.3** | |

**3). The area corresponding to the PSX species was underestimated by 5%:**

| | Area (measured) | Area +5 %error | Composition,mole % |
|---|---|---|---|
| PSX | 100.5 | 100.5 - 5% = 95.5 | **19.7** |
| $SiO_2$ | 389.8 | 389.8 - 0% = 389.8 | **80.3** |
| **Total** | | **485.3** | |

**4). The area corresponding to the $SiO_2$ species was overestimated by 5%:**

| | Area (measured) | Area +5 %error | Composition,mole % |
|---|---|---|---|
| PSX | 100.5 | 100.5 + 0% = 100.5 | **19.7** |
| $SiO_2$ | 389.8 | 389.8 + 5% = 409.3 | **80.3** |
| **Total** | | **509.8** | |

**5). The area corresponding to the $SiO_2$ species was underestimated by 5%:**

| | Area (measured) | Area +5 %error | Composition,mole % |
|---|---|---|---|
| PSX | 100.5 | 100.5 - 0% = 100.5 | **21.3** |
| $SiO_2$ | 389.8 | 389.8 - 5% = 370.3 | **78.7** |
| **Total** | | **470.8** | |

The maximum error associated with the above calculations of chemical composition is:

**21.3 - 19.7 = 1.6 % (±0.8%)**

## *References*


1. Ulrich, D. R., *Chemtech*, **1988**, 242.

2. Ebelmen, *Ann ales de Chimie et de Physique,* **1846**, 57, 319.

3. Geffcken, W.; Berger, E. *GDR Patent* 736 411, assigned to Jenaer Glaswerk Schott & Gen., Jena, GDR, May 6, **1939**.

4. Dislich, H.; Hinz, P.; Kaufmann, R. *FRG Patent* 19 41 191, assigned to Jenaer Glaswerk Schott & Gen., Mainz, FRG, Aug. 13, **1969**.

5. Dislich, H. *Angew. Chem. Int. Ed. Engl.* **1971**, 10(6), 363.

6. Yoldas, B. E. *Ceramic Bull.* **1975**, 54(3),286.

7. Dislich, H. *J. Non-Cryst. Solids,* **1983**, 57, 371.

8. Muckerje, S. P. *J. Non-Cryst. Solids,* **1984**, 63, 375.

9. Yoldas, B. E. *J. Mate. Sci.* **1977**, 12, 1203.

10. Yoldas, B. E. *J. Mate. Sci.* **1979**, 14, 1843.

11. Sommer, L. H.; Frye, C. L. *J. Am. Chem. Soc.* **1960**, 82, 3796.

12. Voronkov, M. G.; Mileshkevich, V. P.; Yuzhelevski, Y. A. in *The Siloxane Bond*, Plenum Press, New York, **1978**.

13. McNeil, K. J. ; DiCaprio, J. A.; Walsh, O. A.; Pratt, R. F. *J. Am. Chem. Soc.* **1980**, 102, 1859.

14. Taft, R. W. in *Steric Effects in Organic Chemistry*; Newman, M. S. Ed.; Wiley, New York, **1956**, Ch. 13.

15. Pohl, E. R., *38th Annual Conference, Reinforced Plastics/Composites Institute, The Society of Plastics Industry, Inc.*, **1983,** Session 4-B, p1.

16. DeTar, D. F. *J. Org. Chem.* **1980**, 45, 5166.

17. Stevenson, W. H.; Martin, J. C. *J. Am. Chem. Soc.* **1985**, 107, 6352.

18. Swain, C. G.; Esteve, Jr. R. M.; Jones, R. H. *J. Am. Chem. Soc.* **1949**, 71, 965.

19. Sommer, L. H.; Frye, C. L.; Muslof, M. C.; Parker, G. A.; Rodewald, P. G.; Michael, K. W.; Okaya, Y.; Pepinski, P. *J. Am. Chem. Soc.* **1961**, 83, 2210.

20. Sommer, L. H.; Frye, C. L. *J. Am. Chem. Soc.* **1960**, 82, 3796.

21. Swain, C. G.; Esteve, R. M. Jr.; Jones, R. H. *J. Am. Chem. Soc.* **1949**, 11, 965.

22. Boonstra, A. H.; Bernards, T. N. M.; Smiths, J. J. T. *J. Non-Cryst. Solids*, **1989**, 109, 141.

23. Aelion, R.; Loebel, A.; Eirich, F. *J. Am. Chem. Soc.* **1950**, 72, 5705.

24. Leyden, D. E.; Shreedhara Murthy, R. S.; Atwater, J. B.; Blitz, J. P. *Analytica Chimica Acta* **1987**, 200, 459.

25. Tiller, H. J.; Gobel, R.; Hartung, U. *J. Non-Cryst. Solids*, **1988**, 105, 162.

26. Grubb, W. T. *J. Am. Chem. Soc.* **1954**, 76, 3408.

27. Iler, R. K. in *The Chemistry of Silica*, John Wiley & Sons, New York, **1979**.

28. Kay, B. D.; Assink, R. A., 104., *J. Non-Cryst. Solids* **1988**, 104, 112.

29. Pohl, E. R.; Osterholtz, F. D. in *Molecular Characterization of Composite Interfaces*, H. Ishida and G. Kumar Eds., Plenum Publishing Corp., **1985**.

30. Martyakova, N. I.; Dolgoplosk, C. B.; Kagan, E. G.; Mileshkevich, V. P. *Vysokomol. Soedin,* **1971**, 13B, 579.

31. Dolgoplosk, S. B.; Kagan, E. G.; Aklanova, L. D.; Klebanskii, A. L.; Martyakova, N. I.; Paper, E. Sh. *Vysokomol. Soedin,* **1970**, 12A, 223.

32. Falcone, J. S., Jr. in *Soluble Silicates, ACS Symp. Ser. 194,* J. S. Falcone, Jr. Ed., **1982**, p133

33. Kelts, L. W.; Effinger, N. J.; Melpolder, S. M. *J. Non-Cryst. Solids* **1988**, 105, 162.

34. Barrer, R. M., in *Hydrothermal Chemistry of Zeolites*, Acad. Press, London, **1982**.

35. McCormick, A. V.; Bell, A. T.; Radke, C. J., *Mater. Res. Soc. Symp. Proc.* **1988**, 121, 67.

36. Davis, L. P.; Burggraf, L. W. in *Ultrastructure Processing of Advanced Ceramics*, Mackenzie, J D, and Ulrich, D. R., Eds., John Wiley&Sons, **1988**, p367.

37. Strelko, V. V., *Kolloidn. Zh.* **1970**, 32(3), 430.

38. Okkerse, C. in *Physical and Chemical Aspects of Adsorbents and Catalysts*, Linsen, B. G. Ed., Academic, New York, **1970**.

39. Ro, J. C.; Chung, I. J. *J. Non-Cryst. Solids*, **1989**, 110, 26.

40. Brinker, C. J.; Keefer, K. D.; Schaefer, D. W.; Ashley, C. S. *J. Non-Cryst. Solids*, **1982**, 48, 47.

41. Strawbridge, I.; Craievich, A. F.; James, P. F. *J. Non-Cryst. Solids*, **1986**, 72, 139.

42. Yamane, M.; Inoue, S.; Yasumari, A. *J. Non-Cryst. Solids*, **1984**, 63, 13.

43. Brinker, C. J.; Keefer, K. D.; Schaefer, D. W.; Assink, T. A.; Kay, B. D.; Ashley, C. S. *J. Non-Cryst. Solids*, **1984**, 63, 45.

44. Sakka, S.; Kozuka, H.; Kim, S. H. in *Ultrastructure Processing of Advanced Ceramics*, Mackenzie, J. D, and Ulrich, D. R., Eds., John Wiley&Sons, **1988**, p159.

45. Keefer, K. D in *Better Ceramics Through Chemistry*, Brinker, C. J.; Clark, D. E.; Ulrich D. R. Eds., Elsevier, New-York, **1984**, p15.

46. Pope, E. J. A.; Mackenzie, J. D. *J. Non-Cryst. Solids*, **1986**, 87, 185.

47. Winter, R.; Chan, J. B.; Frattini, R.; Jonas, J. *J. Non-Cryst. Solids*, **1988**, 105, 214.

48. Klein, L. C.; Garvey, G. J., *Mater. Res. Soc. Symp. Proc.* **1984**, 32,

49. Colby, M. W.; Osaka, A.; Mackenzie, J. D. *J. Non-Cryst. Solids*, **1986**, 82, 37.

50. Noll, W. in *Chemistry and Technology of Silicones*, Academic Press, **1968**, Chapter 11.

51. Schmidt, H.; Scholze, H.; Kaiser, A. *J. Non-Cryst. Solids*, **1984**, 63, 1.

52. Mackenzie, J. D. in *Science of Ceramic Chemical Processing*, L. L. Hench and D. R. Ulrich Eds., John Wiley & Sons, New York, **1986**.

53. Strawbridge, I.; Craievich, A. F.; James, P. F. *J. Non-Cryst. Solids*, **1985**, 72, 139.

54. Keefer, K. D. *Mate. Res. Soc. Symp. Proc.* **1984**, 32, 15.

55. Klein, L. C.; Garvey, G. J. *Mate. Res. Soc. Symp. Proc.* **1984**, 32, 33.

56. Yoldas, B. E. *J. Non-Cryst. Solids*, **1982**, 51, 105.

57. Yamane, M. in *Sol gel Technology for thin films, Fibers, Preforms, Electronics and Specialty Shapes*, L. C. Klein Ed., Noyes Publications, **1988**, 200

58. Bechtold, M. F.; Mahler, W.; Schunn, R. A. *J. Polym. Sci. Polym. Chem. Ed.*, **1980**, 18, 2823.

59. Yamane, M.; Okano, S. *Yogyo- Kyakai- Shi* **1979**, 87, 434.

60. Veklov, V. A.; Dudnik, E. P.; Ramyantseva, E. I. *J. Inorg. Chem.* **1965**, 10, 1281.

61. Hurd, C. B.; Marotta, A. J. *J. Am. Chem. Soc.* **1940**, 62, 2767.

62. Hurd, C. B.; Barclay, R. W. *J. Phys. Chem.* **1940**, 44, 847.

63. Brady, A. P.; Brown, A. G.; Huff, H. *J. Colloid Sci.* **1953**, 8, 252.

64. Artaki, I.; Zerda, T. W.; Jones, J. *J. Non-Cryst. Solids*, **1986**, 81, 381.

65. Carey, F. A.; Sundberg, R. J. in *Advanced Organic Chemistry*, Academic Press, New York, **1970**, p. 213.

66. Artaki, I.; Bradley, M.; Zerda, T. W.; Jonas, J., *J. Phys. Chem.* **1985**, 89, 4404.

67. Orcel, G.; Hench, L. L. *Mater. Res. Soc. Symp. Proc.* **1984**, 32, 79.

68. Avnir, D.; Kaufman, V. R. *J. Non-Cryst. Solids*, **1987**, 192, 180.

69. Artaki, I.; Sinha, S.; Irwin, A. D.; Jonas, J. *J. Non-Cryst. Solids*, **1985**, 72, 391.

70. Zerda, T. W. Hoang, G. *J. Non-Cryst. Solids*, **1989**, 109, 9.

71. Flory, P. J. in *Principles of Polymer Chemistry*, Cornell University Press, Ithaca, New York, **1953**.

72. Schaefer, D. W.; Keefer, K. D. *Mate. Res. Soc. Symp. Proc.* **1984**, 32, 1.

73. Porod, G. *Kolloid Z.* **1951**, 124, 83.

74. Schaefer, D. W.; Keefer, K. D.; Brinker, C. J. *Polym. Prepr. (Am. Chem. Soc. Div. Polym. Chem.)* **1983**, 24, 239.

75. Mandelbrot, B. B. in *Fractals, Form, Chance and Dimension*, Freeman, San Francisco, **1977**.

76. Schaefer, D. W.; Keefer, K. D. *Mate. Res. Soc. Symp. Proc.* **1986**, 73, 277.

77. Schaefer, D. W.; Wilcoxon, J. P.; Keefer, C. D.; Bunker, B. C.; Pearson, R. K.; Thomas, I. M.; Miller, D. E. in *Physics and Chemistry of Porous Media*, **1987**.

78. Dubois, M.; Cabane, B. *Macromolecules* **1989**, 22, 2526.

79. Zarzycki, J. in *Science of Ceramic Chemical Processing*, Hench, L. L. and Ulrich, D. R. Eds, Wiley, New York, **1986**, p.21.

80. Yoldas, B. E *J. Non-Cryst. Solids*, **1986**, 83, 375.

81. Martin, J. E. *J. Appl. Crystall.* **1986**, 19, 25.

82. Brinker, C. J.; Scherer, G. W. *J. Non-Cryst. Solids*, **1985**, 70, 301.

83. Hench, L. L.; Orcel, G. in *Better Ceramics Through Chemistry II*, C. J. Brinker, D. E. Clark and D. R. Ulrich Eds., **1986**, 73, 35.

84. Orcel, G.; Gould, R. W.; Hench, L. L. in *Better Ceramics Through Chemistry II*, C. J. Brinker, D. E. Clark and D. R. Ulrich Eds., **1986**, 73, 289.

85. Nogami, M.; Moriya, Y. *J. Non-Cryst. Solids*, **1980**, 37, 191.

86. Sakka, S. in *Better Ceramics Through Chemistry, Mate. Res. Soc. Symp. Proc.* **1984**, 33, 91.

87. Bailey, J. K.; Nagase, T.; Broberg, S. M.; Mecartney, M. L. *J. Non-Cryst. Solids*, **1989**, 109, 198.

88. Himmel, B; Gerber, Th.; Burger, H. *J. Non-Cryst. Solids*, **1987**, 91, 122.

89. Zarzycki, Z.; Prassas, M.; Phalippou, J. *J. Mate. Sci.* **1982**, 17, 3371.

90. Bertoluzza, A.; Fagnano, C.; Morelli, M. A.; Gottardi, V.; Guglielmi, M. *J. Non-Cryst. Solids*, **1982**, 48, 117.

91. Kawaguchi, T.; Iura, J.; Taneda, N.; Hishikura, H.; Kokubu, Y. *J. Non-Cryst. Solids*, **1986**, 82, 50.

92. Brinker, C. J.; Scherer, G. W.; Roth, E. P. *J. Non-Cryst. Solids*, **1985**, 72, 345.

93. Shaefer, M. W.; Awschalom, D. D.; Warnock, J.; Ruben, G. *J. Appl. Phys.* **1987**, 61(12), 5438.

94. Scherer, G. W.; Brinker, C. J.; Roth, E. P. *J. Non-Cryst. Solids*, **1985**, 72, 345.

95. Lieban, F. in *Structural Chemistry of Silicates*, Springer, New York, **1985**.

96. Elkins, P. B.; Shull, C. G.; Roess, L. C. *Ind. Eng. Chem.*, **1945**, 37, 327.

97. Shapiro, I.; Kolthoff, I. M. *J. Am. Chem. Soc.* **1950**, 72, 776.

98. Schmidt, H. *J. Non-Cryst. Solids*, **1985**, 73, 681.

99. Gulledge, H. C. *US Patent* 2512 058, **1950**.

100. Andrianov, K. A. in *Organic Silicon Compounds*, Moscow, **1955**.

101. Andrianov, K. A.; Zhdanov, A. A. *J. Polym. Sci.* **1958**, 513.

102. Schmidt, H. *Mate. Res. Soc. Symp. Proc.* **1984**, 32, 327.

103. Schmidt, H.; Tunker, G.; Scholze, H. *DP* 30 11 761, **1980**.

104. Kaiser, A.; Schmidt, H. *J. Non-Cryst. Solids*, **1984**, 63, 261.

105. Shea, K. J.; Loy, D. A.; Webster, O. W. *Chemistry of Materials*, **1989**, 1, 572.

106. Wilkes, G. L.; Orler, B.; Huang, H. *Polym. Prepr. (Am. Chem. Soc. Div. Polym. Chem.)* **1985**, 26(2), 300.

107. Huang, H. H; Orler, B.; Wilkes, G. I. *Polym. Bull.* **1985**, 14(6), 557.

108. Huang, H. H.; Orler, B.; Wilkes, G. L. *Macromolecules*, **1987**, 20(6), 1322.

109. Huang, H. H.; Glaser, R. H.; Wilkes, G. L. *ACS Symposium Series No. 360; American Chemical Society:* Washington D. C., **1988**, p 354.

110. Huang, H. H., PhD Dissertation, Virginia polytechnic Institute and State University, **1987**.

111. Huang, H. H.; Wilkes, G. L. *Pol. Bull.* **1987**, 18, 455.

112. Phillip, G.; Schmidt, H., *J. Non-Cryst. Solids*, **1984**, 63, 283.

113. Phillip, G.; Schmidt, H., *J. Non-Cryst. Solids*, **1986**, 82, 31.

114. Schmidt, H.; Scholze, H.; Tunker, G., *J. Non-Cryst. Solids*, **1986**, 80, 557.

115. Jiang, C. Y.; Mark, J. E., *Makromol. Chem.* **1984**, 185, 2609.

116. Mark, J. E.; Jiang, C. Y.; Tang, M. Y. *Macromolecules*, **1984**, 17, 2613.

117. Sur, G. S.; Mark, J. E. *Eur. Polym. J.* **1985**, 21, 1051.

118. Mark, j. E.; Pan, S. J. *Makromol. Chem. Rapid Commun.* **1982**, 3, 681.

119. Noell, J. L. W.; Wilkes, G. L.; Mohanty, D. K.; McGrath, J. E., J. Appl. Polym. Sci., **1990**, 40, 1177.

120. Sakka, S. *J. Non-Cryst. Solids*, **1985**, 73, 651.

121. Okazaki, H.; Kitagawa, T.; Shibata, S.; Kimura, T. *J. Non-Cryst. Solids*, **1990**, 116, 87.

122. Rabinovitch, E. M.; Johnson Jr., D. W.; MacChesney, J. B.; Vogel, E. M. *J. Non-Cryst. Solids*, **1982**, 47, 435.

123. Sakka, S.; Kamiya, K.; Yamamoto, Y, *J. Non-Cryst. Solids*, **1984**, 63, 223.

124. Schroeder, H. in *Physics of Thin Films*, Vol 5, Academic Press, New York, **1969**, p. 87.

125. Geotti - Bianchini, F.; Guglielmi, M.; Palato, P.; Soraru, G. D. *J. Non-Cryst. Solids*, **1984**, 63, 251.

126. Arfsten, J. J. *J. Non-Cryst. Solids*, **1984**, 63, 243.

127. Mukherjee, S. P.; Lowdermilk, W. H. *Appl. Optics*, **1982**, 21, 293; *J. Non-Cryst. Solids*, **1982**, 48, 177.

128. Dislich, H. *J. Non-Cryst. Solids*, **1985**, 73, 599.

129. Hubert - Pfalzgraf, L. G. *New Journal of Chemistry* **1987**, 11, 663.

130. Klein, L. C. *Ann. Rev. Mater. Sci.* **1985**, 15, 227.

131. Philipp, G.; Schmidt, H. *J. Non-Cryst. Solids*, **1984**, 63, 283.

132. Szwarc, M. in *Carbanions, Living Polymers and Electron Transfer Processes* Interscience: New York, **1968**, p12.

133. Elsbernd, C. S., Ph. D. Dissertation, Virginia Polytechnic Institute and State University, Blacksburg, Virginia 24061, **1988**.

134. Kirk, N., *U. S. Patent* 2,883,272, assigned to General Electric Company, **1959**.

135. Gilbert, A. R., Kantor, S. W., *J. Polym. Sci.*, **1959**, 40, 35.

136. Laita, Z., Hlozek, P., Bucek, B., Jelinek, M., *J. Polym. Sci.* **1967**, C16, 669.

137. Speier, J. L. *Advances in Organometallic Chemistry*, **1979**, 17, 407.

138. Arnold, C. A. Ph. D. Dissertation, Virginia Polytechnic Institute and State University, Blacksburg, Virginia 24061, **1989**.

139. Summers, J. D., Ph. D. Dissertation, Virginia Polytechnic Institute and State University, Blacksburg, Virginia 24061, **1988**.

140. Odian, G., *Principles of polymerization*, 2nd ed., Wiley, New York, **1981**.

141. A. Rudin, *The Elements of Polymer Science and Engineering*, Academic Press, Orlando, **1982**.

142. Hiemenz, P. C., *Polymer Chemistry-The Basic Concepts*, M. Dekker, Inc. New York **1984**.

143. Lewis, L. N., and Lewis, N., *J. Am. Chem. Soc.* **1986**, 108, 7228.

144. Maciel, G. E., Sindorf, D. W., *J. Am. Chem. Soc.* **1980**, 102, 7606.

145. Engelhardt, G., Jancke, H., Lippmaa, E., and Samoson, A., *J. Organomet. Chem.* **1981**, 210, 295.

146. DeSimone, J. Ph. D. Dissertation, Virginia Polytechnic Institute and State University, Blacksburg, Virginia 24061, **1990**.

147. Yoldas, B. E., *J. Polym. Sci: Part A:Polymer Chemistry* **1986**, 24, 3475.

148. Kelts, L. W., Effinger, N. J., and Melpolder, S. M., *J. Non-Cryst. Solids*, **1986**, 83, 353.

149. Engelhardt, G., Zeigan, D., Jancke, H., Hoebbel, D., and Wieker, W., *Z. Anorg. Allg. Chem.* **1975**, 418, 17.

150. Engelhardt, G., Alternburg, W., Hoebbel, D., and Wieker, W., *Z. Anorg. Allg. Chem.* **1977**, 428, 43.

151. Harris, R. K., and Knight< C. T. G., *J. Chem. Soc. Faraday Trans.* **1983**, 79, 1525.

152. Harris, R. K., Knight, C. T. G., and Smith, D. N., *J. Chem. Soc. Chem. Commun.* **1980**, 726.

153. Harris, R. K., and Knight, C. T. G., *J. Chem. Soc. Faraday Trans.* **1983**, 79, 1539.

154. Hoebbel, D., Garzo, G., Engelhardt, G., and Till, A., *Z. Anorg. Allg. Chem.* **1979**, 450, 5.

155. Kelts, L. W., Armstrong, N. J., *J. Mater. Res.* **1989**, 4(2), 423.

156. Artaki, I., Bradley, M., Zerda, T. W., and Jonas, J., *J. Phys. Chem.* **1985**, 89, 4399.

157. Zerda, T. W., Artaki, I., and Jonas, J., *J. Non-Cryst. Solids*, **1986**, 81, 365.

158. Orcel, G., Hench, L., *J. Non-Cryst. Solids*, **1986**, 79, 177.

159. Pouxviel, J. C., Boilot, J. P., Beloeil, J. C., and Lallemand, J. Y., *J. Non-Cryst. Solids*, **1987**, 89, 345.

160. Pouxviel, J. C., and Boilot, J. P., *J. Non-Cryst. Solids*, **1987**, 94, 374.

161. Assink, R. A., and Kay, B. D., *J. Non-Cryst. Solids*, **1988**, 99, 359.

162. Hartman, J. S., Millard, R. L., and Vance, E. R., *J. Non-Cryst. Solids*, **1989**, 108, 49.

163. Gillham, J. K., *Polym. Eng. Sci.*, **1979**, 19, 676.

164. Prassas, M. Phalippou, J., and Zarzycki, J., *J. Mater. Sci.* **1984**, 19, 1656.

165. Scherer, G. W., *J. Non-Cryst. Solids*, **1987**, 89, 217.

166. Yamane, M., Aso, S., and Sakaino, T., *J. Mater. Sci.* **1978**, 13, 865.

167. Eaborn, C., in *Organosilicon Compounds*, Butterworth Scientific Publications, London, **1960**.

168. Kantor, S. W., Grubb, W. T., Osthoff, R. C., *J. Am. Chem. Soc.*, **1954**, 76, 5190.

169. Noll, W., in *Chemistry and Technology of Silicones* , Academic Press, New York, **1968**.

170. Stark, F. O., Falender, J. R., Wright, A. P., in *Comprehensive Organometallic Chemistry,* Vol. 2, Pergamon Press, New York, **1982**.

171. Yilgor, I., and McGrath, J. E., in *Polysiloxane Containing Copolymers: A Survey of Recent Developments*, D. Olive Ed., **1987**, p 3.

172. McGrath, J. E., Riffle, J. S., Banthia, A. K., Yilgor, I., and Wilkes, G. L., *ACS Symp. Ser. No. 212,* Washington D.C., **1988**, pag. 180.

173. Summers, J. D., Elsbernd, C. S., Sormani, P. M., Brandt, P. J., Arnold, C. A., Yilgor, I., Riffle, J. S., Kilic, S., and McGrath, J. E. in *Inorganic and organometallic polymers, ACS Symp. Ser. No. 360*, Zeldin, M., Wynne, K. J., and Allcock, H. R., Eds., Washington DC **1988**, 180.

174. Riffle, J. S., Yilgor, I., Tran, C., Wilkes, G. L., McGrath. J. E., Banthia, A. K., in *Epoxy resin chemistry II, ACS Symp. Ser. No. 221,* Bauer, R. S. Ed., Washington D.C., **1983**, Chapter 2.

175. Yilgor, I., Riffle, J. S., McGrath, J. E., in *Reactive oligomers, ACS Symp. Ser. No. 282,* Harris, F. W., Spinelli, H., Eds., J.,Washington D.C., **1985**, pag. Chapter 14

176. Elsbernd, C. S., Spinu, M., Kilic, S., and McGrath, J. E., *Polym. Prepr. (Am. Chem. Soc. Div. Polym. Chem.)* **1988**, 29(1), 355.

177. Miller, H. C., and Schreiber, R. S., *U. S. Patent* 2,379,821, **1945.**

178. Sommer, L. H., Pietrusza, E. W., and Whitmore, F. C., *J. Am. Chem. Soc.*, **1947**, 69, 188.

179. McKenzie, C. A., Spialter, L., and Schoffman, M, *French Patent* 961,878, **1949.**

180. Barry, A. J., and Hook, D. E., *U. S. Patent* 2,626,271, **1953.**

181. Wagner, G. H., and Strother, C. O. *U. S. Patent* 2,632,013, **1953.**

182. Sommer, L. H., Pietrusza, E. W., and Whitmore, F. C., *J. Am. Chem. Soc.*, **1957**, 79, 4560.

183. Pietrusza, E. W., Sommer, L. H., and Whitmore, F. C., *J. Am. Chem. Soc.*, **1948**, 70, 484.

184. Kadonaga, M., and Jino, K., *Jap. Patent* 5645, **1954**.

185. Shchukovskaya, L. L., Petrov, A. D., and Egorov, Y. P., *Zhur. Obshchei Khim.*, **1956**, 26, 3338.

186. Lipscomb, R. D., *U. S. Patent* 2,570642, **1951**.

187. Speier, J. L., and Webster, J. A., *J. Org. Chem.*, **1956**, 21, 1044.

188. Topchiev, A. V., Nametkin, N. S., and Solovova, O. P., *Doklady Akad. Nauk SSSR*, **1952**, 86, 965.

189. El-Abbady, and Anderson, L. C., *J. Am. Chem. Soc.*, **1958**, 80, 1737.

190. Wagner, G. H., and Strother, C. O., *British Pattent* 670,617, **1952**.

191. Wagner, G. H., *U. S. Pattent* 2,637,738, **1953**.

192. Wagner, G. H., and Whitehead, Jr. W. G., *U.S. Pattent* 2,851,473, **1958**.

193. Ponomarenko, V. A., Sokolov, B. A., Minachev, Kh. M., and Petrov, A. D., *Doklady Akad. Nauk SSSR*, **1956**, 76, 106.

194. Petrov, A. D., Ponomarenko, V. A., Sokolov, B. A., and Odabashyan, G. V., *Izvest. Akad. Nauk SSSR, Otdel. Khim. Nauk*, **1957**, 1206.

195. Petrov, A. D., Minachev, Kh. M., Ponomarenko, V. A., Sokolov, B. A., and Odabashyan, G. V., *Doklady Akad. Nauk SSSR*, **1957**, 112, 273.

196. Shostakovskii, M. F., and Kochkin, D. A., *Izvest. Akad. Nauk SSSR, Otdel. Khim. Nauk*, **1956**, 1150.

197. Petrov, A. D., Mironov, V. F., Vdovin, V. M., and Sadykh-Zade, *Izvest. Akad. Nauk SSSR, Otdel. Khim. Nauk*, **1956**, 256.

198. Nitzsche, S., *Fed. Germ. Rep. Pat.* 916,529, **1954**.

199. Speier, J. L., Webster, J. A., and Barnes, G. H., *J. Am. Chem. Soc.*, **1957**, 79, 974.

200. Schlenk, W., *Fed. Germ. Rep. Pat.* 899,500, **1953**.

201. Ponomarenko, V. A., Cherkaev, V. G., Petrov, A. D., and Zadorozhnyi, N. A., *Izvest. Akad. Nauk SSSR, Otdel. Khim. Nauk*, **1958**, 247.

202. Topchiev, A. V., Nametkin, N. S., Durgaryan, S. T., and Dyankov, S. S., in *Chemistry and Practical Use of Organosilicon Compounds*, Leningrad, Izd. **1958**, p118.

203. Meals, R. N., *Pure Appl. Chem.*, **1966**, 13 (1-2), 141.

204. Prober, M, *French Patent*, 1,118,500 **1956**.

205. He, X., Lapp, A., Herz, J., *Makromol. Chem.* **1988**, 189, 1061.

206. Engel, L., Klingele, H., Ehrenstein, G. W., Schaper, H., in *An Atlas of Polymer Damage*, Prentice-Hall Inc., Engeewood Cliffs, New Jersey, **1981**, p170.

210. Yilgor, I., and McGrath, J. E., *Adv. Polym. Sci.* **1988**, 88,1.

211. Kojima, K., Gore, C. R., Marvel, C. S., *J. Polym. Sci. A-1*, **1966**, 4(9), 2325.

212. Elsbernd, C. S., Spinu, M., Krukonis, V. J., Gallagher, P. M., Mohanty, D. K., and McGrath, J. E., in *Silicon -Based Polymer Science; Advances in Chemistry Series 224,* Washington D.C., Ziegler, J. and Fearon, G. Eds., **1990**, p145.

213. McGrath, J. E., Sormani, P. M., Elsbernd, C. S., *Makromol. Chem. Macromol. Symp.* **1986**, 6, 67.

214. Friedel, C., Crafts, J. M., *Liebigs Ann. Chem.*, **1863**, 127, 31.

215. Friedel, C. Crafts, J. M., *Ann. Chem. Phys.* **1870**, 19(5), 334.

216. Friedel, C., Ladenburg, A., *Liebigs Ann. Chem.*, **1871**, 159, 259.

217. Kipping, F. S., Lloyd, L., *J. Chem. Soc.*, **1901**, 79, 449.

218. Kipping, F. S., , *J. Chem. Soc.*, **1907**, 91,209.

219. Robison, R., Kipping, F. S., *J. Chem. Soc.*, **1914**, 105,40.

220. Weyenberg, D. R., Lane, T. H., in *Silicon-Based Polymer Science; Advances in Chemistry Series 224*, Washington DC, Ziegler, J., and Fearon, G. Eds., **1990**, p. 753.

221. Wrington, M. S. *Comments Inorg. Chem.* **1985**, 4(5), 269.

222. Wright, P. V., in *Ring Opening Polymerization*, Ivin, K. J., and Saegusa, T., Eds., Elsevier, **1984**, Ch. 14.

223. Sigwalt, P., *Actual. Chim.*, **1986**, 3, 45.

224. Kendrick, T. C., White, J. W., Parbhoo, B., in *Comprehensive Polymer Science*, Eastmond, G. C., Ledwith, A., Russo, S., Sigwalt, P., Eds., Pergamon: New York, **1989**, Vol. 4(II), p 459.

225. Voronkov, M. G., Mileshkevich, V. P., Yuzhelevskii, Yu. A., in *The Siloxane Bond*, Consultants Bureau: New York, **1978.**

226. Sormani, P. M. Ph. D. Dissertation, Virginia Polytechnic Institute and State University, Blacksburg, Virginia 24061, **1985**.

227. Zeldin, M., in *Inorganic and organometallic polymers*, Zeldin, M., Wynne, K. J., and Allcock, H. R., Eds., *ACS Symp. Ser. No. 360*, Washington DC **1988**, 180.

228. Owen, M. J., in *Silicon-Based Polymer Science; Advances in Chemistry Series 224*, Washington DC, Ziegler, J., and Fearon, G. Eds., **1990**, p 705.

229. Good, R. J., in *Treatise on Adhesion and Adhesives*, Patrick, R. L., Ed., Marcel Dekker: New York, **1967**, p 15.

230. Zisman, W. A., *Contact Angle, Wettability, and Adhesion; Advances in Chemistry Series 43* , Washington DC, **1964**, p 1.

231. Hunter, M. J., Hyde, J. F., Warrick, E. L., and Fletcher, H. J., *J. Am. Chem. Soc.* **1946**, 68, 667.

232. Wilcock, D. F. *J. Am. Chem. Soc.* **1946**, 68, 691.

233. Engelhardt, G., and Janeke, H. *Z. Chem.*, **1974**, 14, 206.

234. Polmanteer, K. E., *J. Elastoplastics*, **1970**, 2, 165.

235. Bridgmann, P. W., *Proc. Amer. Acad. Arts Sci.* **1949**, 77, 115.

236. Bahar, I., Erman, B., and Monnerie, L., *Macromolecules*, **1990**, 23, 1174.

237. Tobolski, A. V., in *Properties and Structures of Polymers*, Wiley: New York, **1960**, p 67.

238. Lee, C. L., Haberland, G. G., *Polym. Lett.*, **1965**, 3, 883.

239. Stern, S. A., Shah, V. M., and Hardy, B. J., *J. Polym. Sci., Part B,* **1987**, 25, 1263.

240. Lee, W. A., Rutherford, R. A., in *Polymer Handbook*, Brandrupi, J., and Immergut, E. H. Eds., Wiley: New York, **1975**, pIII-139.

241. Owen, M. J., *Ind. Eng. Chem. Prod. Res. Dev.*, **1980**, 19, 97.

242. Grigoras, S., and Lane, T. H., *J. Comput. Chem.* **1987**, 8, 84.

243. Ernst, C. A., Allred, A. L., Ratner, M. A., Newton, M. D., Gibbs, G. V., Moskowitz, J. W., and Topiol, S., *Chem. Phys. Lett.*, **1981**, 81, 424.

244. Oberhammer, H., and Boggs, J. E., *J. Am. Chem. Soc.*, **1980**, 102, 7241.

245. Durig, J. R., Flanagen, M. J., and Kalasinsky, V. F., *J. Chem. Phys.* **1977**, 66, 2775.

246. Oberhammer, H., Zeil, W., and Fogarasi, G. *J. Mol. Struct.* **1973**, 18, 309.

247. Beezer, A. E., and Mortimer, C. T., *J. Chem. Soc.* , **1966**, 514.

248. Ebsworth, E. A. V., in *The Bond to Carbon*, Mac Diarmid, A. G. Ed., Marcel Dekker: New York, **1968**, p 46.

249. Fox, H. W., Taylor, P. W., Zisman, W. A., *Ind. Eng. Chem.* **1947**, 39, 1401.

250. Pauling, L. J., *J. Phys. Chem.* **1952**, 56, 361.

251. Grigoras, S., and Lane, T. H., *J. Comput. Chem.* **1988**, 9(1), 25.

252. Siow, K. S., and Patterson, D. J., *J. Phys. Chem.* **1973**, 77, 356.

253. Lee, L. H. *J. Adhes.* **1972**, 4, 39.

254. Hunter, M. J., Gordon, M. S., Barry, A. J., Hyde, J. F., and Heidenreich, R. D., *Ind. Eng. Chem.* **1947**, 39, 1389.

255. Hard, S., and Neuman, R. D., *J. Colloid, Interface Sci.*, **1987**, 120, 15.

256. Polmanteer, K. E., and Hunter, M. J., *J. Appl. Polym. Sci.* **1959**, 1, 3.

257. Kataoka, T., and Ueda, S., *J. Polym. Sci., Part B* **1966**, 4, 317.

258. Sauer, R. O., and Mead, D. J. *J. Am. Chem. Soc.* **1946**, 68, 1794.

259. Critchley, J. P., Knight, G. J., and Wright, W. W., in *Heat Resistant Polymers*, Plenum: New York, **1983**, p 441.

260. McGrath, J. E., in *Ring Opening Polymerization, ACS Symp. Ser. 286*, McGrath, J. E. Ed. **1985**, p 1.

261. Holland, R. S., and Smith, C. P., *J. Am. Chem. Soc.* **1955**, 77, 268.

262. Go, N., and Scheraga, H. A. *Macromolecules*, **1970**, 3, 178.

263. Saam, J. C., in *Silicon-Based Polymer Science; Advances in Chemistry Series 224*, Washington DC, Ziegler, J., and Fearon, G. Eds., **1990**, p. 71.

264. Carmichael, J. B., and Heffel, J. *J. Phys. Chem.* **1965**, 69, 2213.

265. Carmichael, J. B., and Heffel, J. *J. Phys. Chem.* **1965**, 69, 2218.

266. Brown, J. F., and Slusarczuk, G. M., *J. Am. Chem. Soc.* **1965**, 87, 931.

267. Chojnowski, J, Kazmerski, K., Rubinszstein, S., and Stanczyk, W., *Macromol. Chem.* **1986**, 187, 2039.

268. Gee, G. in *Inorganic Polymers, an International Symposium, Special Publication No. 15*, Sidney: London, **1961**, p 67.

269. Tanaka, T. *Bull. Chem. Soc. Jpn.* **1960**, 33, 282.

270. Lee, C. L., and Johannson, O. K. *J. Polym. Sci., Part A-1* **1966**, 4, 3013.

271. Semlyen, J. A., and Wright, P. V. *Polymer* **1969**, 10, 543.

272. Jacobson, H., and Stockmayer, W. H. *J. Chem. Phys.* **1950**, 18, 1600.

273. Wright, P. V., and Semlyen, J. A. *Polymer* **1970**, 11, 462.

274. Semlyen, J. A. *Adv. Polym. Sci.* **1976**, 41, 21.

275. Litvinov, V. M., Lavrukhin, B. D., and Zhdanov, A. A. *Polymer Science USSR* **1985**, 27, 2777.

276. Sormani, P. M., Minton, R. J., and McGrath, J. E., in *Ring Opening Polymerization, ACS Symp. Ser. 286*, McGrath, J. E. Ed., Washington DC **1985**, Ch. 11.

277. Yilgor, I., and McGrath, J. E., *Adv. Polym. Sci.* **1988**, 86.

278. McGrath, J. E., Sormani, P. M., Elsbernd, C. S.,and Kilic, S. *Makromol. Chem, Makromol. Symp.* **1986**, 6, 67.

279. Hurd, D. T. Osthoff, R. C., and Corrin, M. I. *J. Am. Chem. Soc.* **1954**, 76, 240.

280. Laita, Z.,and Jelinek, M. *Polym. Sci. USSR, Engl. Transl.* **1965**, 4, 535.

281. Grubb, W. T., and Osthoff, R. C., *J. Am. Chem. Soc.* **1955**, 77, 1405.

282. Mazurek, M. scibiorek, M. Chojnowski, J. Zavin, B. G., and Zdanov, A. A. *Eur. Polym. J.* **1980**, 66(1), 67.

283. Patnode, W. S., and Wilcock, D. F. *J. Am. Chem. Soc.* **1946**, 68, 358.

284. Sigwalt, P. *Polym. J.* **1987**, 19, 567.

285. Kojima, K., Tarumi, J., and Wakatsuki, Y., *Nippon Kagaru Zasshi* **1956**, 77(12), 1755.

286. Sauvet, G., Lebrun, J. J.,and Sigwalt, P. in *Cationic Polymerization and Related Processes,* Goethals, E. J. Ed., Academic: New York, **1984**, p 237.

287. Mayo, F. R., and Lewis, F. M., *J. Am. Chem. Soc.* **1944**, 66, 1594.

288. Koening, J. L. in *Chemical Microstructure of Polymer Chains*, Wiley: New York **1980**.

289. Laita, Z., and Jelinek, M. *Vyskomol. Soedin* **1963**, 5, 1268.

290. Reiksfeld, V. O., and Ivanova, A. G. *Vyskomol. Soedin* **1962**, 4, 30.

291. Lee, C. L., and Marko, O. W. *Polym. Prepr. (Am. Chem. Soc., Div. Polym. Chem.)* **1978**, 16, 250.

292. Baratova, T. N., Mileshkevich, V. P., Gulari, V. E. *Polym. Sci. USSR (Engl. Transl.)* **1983**, 12, 2899.

293. Szwarc, M., and Perrin, C. L. *Macromolecules* **1985**, 18, 528.

294. Jensen, P. J., and Bennemann, K. H. *J. Chem. Phys.* **1985**, 83, 6457.

295. Cai, G., and Yan, D., *J. Macromol. Sci., Chem.* **1987**, A24(8), 869.

296. Ziemelis, M. J. and Saam, J. C. *Macromolecules* **1989**, 22, 2111.

297. Brandt, A., Subramarian, R., Sormani, P. M., Ward, T. C.,and McGrath, J. E. *Polym. Prepr. (Am. Chem. Soc., Div. Polym. Chem.)* **1985**, 26(2), 213.

298. Babu, G. N., Christopher, S. S. and Newmark, R. A. *Macromolecules*, **1987**, 20, 2654.

299. Lee, C. L., and Emerson, F. A. *J. Polym. Sci., Part A-2*, **1967**, 5, 829.

300. Flory, P. J., Mandelkern, L., Kisinger, J. B., and Schultz, W. H., *J. Am. Chem. Soc.* **1952**, 74, 3364.

301. Flory, P. J., Crescenti, V., and Mark, J. E. *J. Am. Chem. Soc.* **1964**, 86, 146.

# VITA

Maria Ghimpu (Spinu) was born November 19, 1950, in Beresti-Galatzi, Romania. She graduated from Tecuci High School, Romania, in June 1969. She enrolled at Jassy Polytechnical Institute in the fall of 1969 from which she received a M.S. Degree in Technology of Macromolecular Compounds in June 1974. She married Ionel Spinu in march 1974 and in January 1975 their first and only child, Ioana Monica, was born. After graduation she worked at Jilava Rubber and Plastics Inc., Bucharest, Romania as a chemical engineer between 1974-1978, and at the Institute for Engineering and Design for Chemical Industry, Bucharest, Romania as a design engineer between 1978-1982.

In 1982 she and her family (husband and daughter) left Romania in search of political and economical freedom. She arrived in the United States in July 1982 where she received the status of political refugee, and enjoyed the freedom and kindness of this land and its people ever since. In february 1983 she began working at Thoratec Inc. in Berkeley, California, first as a fabrication technician, later as an associate scientist. During her years at Thoratec she worked with Dr. Judy Riffle, a former graduate of VPI, and met Prof. James McGrath who later became her research advisor at Virginia Tech. It was the encouragement of both Dr. Judy Riffle and Prof. James E. McGrath which fueled her determination to drive cross country to join Virginia Polytechnic Institute and State University in September, 1986. Her graduate research efforts were broadly defined but centered around synthesis of silicon containing organic and inorganic polymers.

She became an american citizen in may of 1988. She received her doctorate degree in chemistry in October 1990. At the end of October she joined the Central Research and Development Department at DuPont in Wilmington, Delaware.